An investigation into the role of *Arabidosis thaliana* NAD metabolising enzymes in plant cellular stress responses

by

Sarah L Henry

Thesis submitted for the degree of Doctor of Philosophy.

Division of Biochemistry and Molecular Biology

Institute of Biomedical and Life Sciences

University of Glasgow

September 2008

Abstract

Adverse growing conditions resulting from abiotic stresses e.g. pathogen attack results in large losses in crop yields. Understanding and improving plants tolerance to an unfavourable environment remains one of the objectives in the study of plant biotechnology.

One growing theory for reducing plant susceptibility to a broad range of stresses is modulation of cellular energy homeostasis.

NAD^+ (along with ATP) is the most important of cellular energy transducers in the form of a hydrogen ion donor and acceptor. However, a bigger picture is emerging as its role broadens to include a coenzyme, precursor for secondary messengers and a substrate for protein modifications.

Three groups of proteins use NAD^+ as a substrate, the NAD^+ protein deacetylases, poly ADP polymerases and ADP ribose cyclases. Work on these groups of proteins in model organisms have identified their involvement in many biological roles including DNA repair, increasing longevity, initiating apoptosis and regulation of transcription. However, their role in plants is largely unknown.

The aim of this study has been to identify the genes involved which use NAD^+ and to further characterise their role in plant stress responses. A summary of the main results follows,

a) AtPARG2 and sirtuin At5g55760 null lines were more sensitive to DNA damaging agents.
b) AtPARG2 lines showed a disruption in circadian rhythm resulting in early flowering.
c) Sirtuin At5g09230 null lines were more sensitive to UV-B exposure
d) AtPARP3 was highly upregulated with exogenous Abscisic acid application.

List of Abreviations.

0-AADPR	0-Acetyl adenosine diphosphate ribose
ABA	Abscisic acid
ADP	Adenosine diphosphate
AIF	Apoptosis inducing factor
ATP	Adenosine triphosphate
BER	Base Excision Repair
cADPr	Cyclic Adenosine diphosphate ribose
CHS	Chalcone synthase
DNA	Deoxyribonucleic acid
EDTA	Ethylenediaminetetraacetic acid
HPLC	High pressure liquid chromatography
HR	Homologous recombination
IPTG	Isopropyl β-D-1-thiogalactopyranoside
LPS	Lipopolysaccharide
MMS	Methyl methane sulphonate
MS	Murishige and Skoog
NAA	1-naphthaleneacetic acid
NaAD	Nicotinic acid adenyl dinucleotide
NAD^+	Nicotinamide adenine dinucleotide
$NADP^+$	Nicotinamide adenine dinucleotide phosphate
NAMase	Nicotinamidase
NaMNAT	Nicotinic acid mononucleotide adenylyltransferase
NAPRT	Nicotinic acid phosphoribosyl transferase
NER	Nucleotide excision repair
NHEJ	Non-homologous end joining
NMN	Nicotinamide mononucleotide
NMNAT	Nicotinic acid mononucleotide adenylyltransferase
OKA	Okadaic acid
PAR	Poly ADP ribose
PARG	Poly ADP ribose glycohydrolase
PARP	Poly ADP ribose polymerase
PCR	Polymerase chain reaction
qPCR	Quantitative polymerase chain reaction
SIRT	Sirtuin
SQRT-PCR	Semi-quantitative reverse transcriptional polymerase chain reaction
STA	Staurosporin
T-DNA	Transfer DNA

Table of Contents

List of Figures

List of Tables

Acknowledgements.

Big thanks to my supervisor Dr Susan Rosser for all her help. Her support, encouragement and knowledge of all things scientific have been as important as her patience and enthusiasm. And the serious assurance that if I didn't finish this thesis she would hunt me down and beat me up.

Similar gratitude is owed to Dr Emma Travis and Dr Jillian Price. Their on hand lab experience and friendship has been invaluable, not to mention the walking trips, board games and late night excursions into deepest Fife.

Many thanks to Prof Gareth Jenkins and his lab for their help on the work with UV-B and to Prof Richard Cogdell for his advice on protein purification.

Also thanks to all members of the Arnott lab past and present for all the assistance over the years and making the dirge of lab work interesting and fun.

Many thanks to those who have endured my daily rants and frustrations and helped me forget about work, Anna, John, Vic, Innes, Andreas and Colin. The food, beer and laughter have kept me sane.

Finally, huge thanks to my long-suffering parents and brothers for their love and their belief in me that I could do this.

Chapter 1 Introduction

1.1 Introduction to NAD and its biosynthesis.

For anyone interested in biological science the importance of NAD^+, a coenzyme found in all living organisms, cannot be avoided. NAD^+ mediates hundreds of redox reactions and therefore impacts on the majority of metabolic pathways in the cell. NAD^+ was first discovered in the early 20th century by Arthur Harden, who showed that boiled and filtered yeast extracts greatly accelerated alcoholic yeast fermentation in unboiled yeast extracts. (Harden et al 1913). This as yet unidentified fraction of yeast extract was termed co-ferment but it was not characterised until 1929 when Hans von Euler-Chelpin determined it as a heat stable nucleotide sugar phosphate, work for which he and Arthur Harden received the Nobel Prize (Harden 1929 Nobel Lecture). The structure of NAD^+ was finally established in 1936 by Otto Warburg (shown in Figure 1.1).

NAD^+ is formed by two nucleotide units joined by their phosphate groups with one nucleotide attached to an adenosine ring and the other nucleotide attached to a nicotinamide (shown in Figure 1.1).

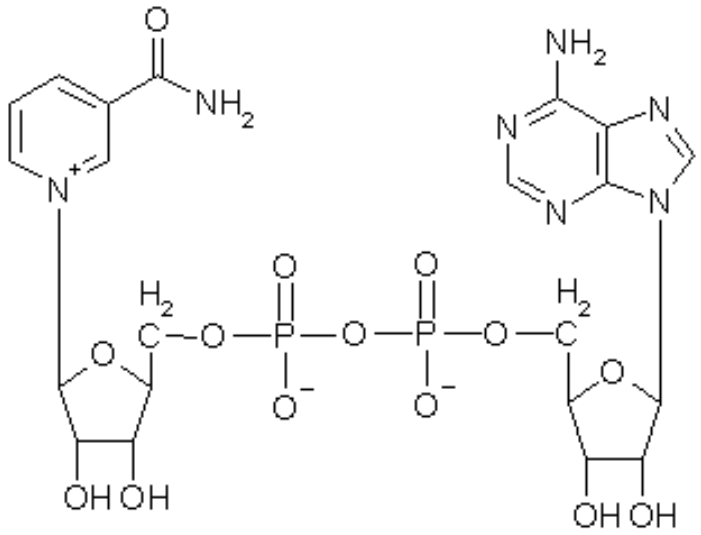

Figure 1.1 Structure of NAD^+. The structure of NAD^+ has two nucleotide units joined by their phosphate groups. An adenosine group is attached to one nucleotide and a nicotinamide is attached to the other nucleotide.

1.1.2 NAD as a cofactor.

NAD^+ was recognised during the last century as the major hydrogen ion carrier for its involvement in a multitude of metabolic processes. Its main role is as a cofactor transferring electrons from one reaction to another. For this reason it is present in two forms in cells, the oxidised form NAD^+ (which accepts electrons) and the reduced form NADH shown in Figure 1.2.

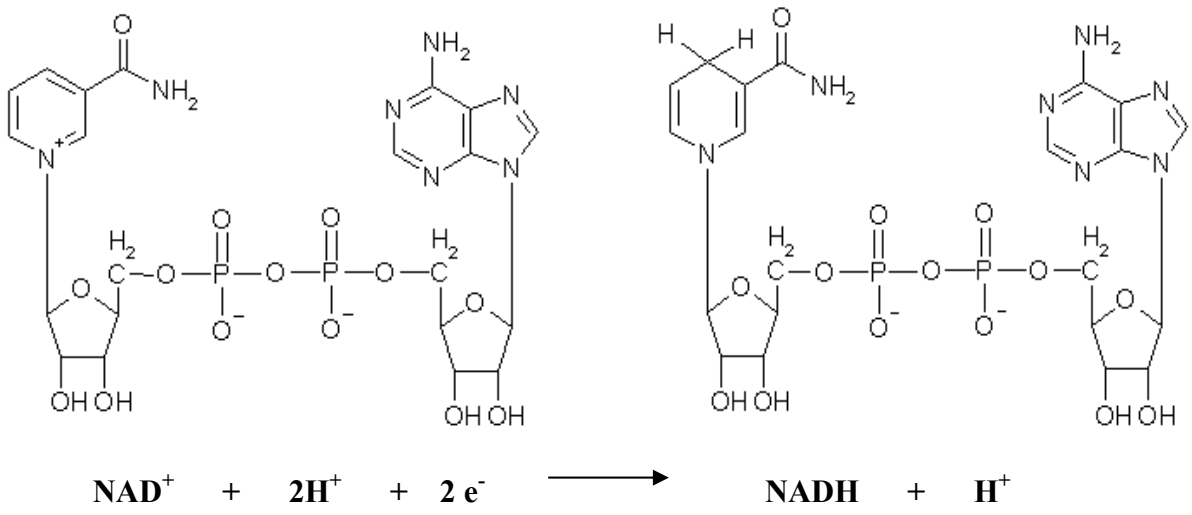

Figure 1.2. Structure and redox reaction of nicotinamide adenine dinucleotide (NAD^+). The conversion to NADH requires two electrons, one that attaches to the positively charged nitrogen in the nicotinamide group. This reaction is reversible and capable of releasing hydrogen ions and replenishing concentrations of NAD^+.

NAD^+ can also be converted by NAD kinase to NADP which is also a powerful reducing agent forming NADPH. Although the chemistry of $NADP^+$ is similar to that of NAD^+ it has different roles being mainly involved in synthesis of lipids and nucleic acids. Of all these redox reactions the addition and removal of hydrogen ions does not alter the nucleotide structure of the molecule therefore not resulting in a net loss of NAD^+ and its derivates.

Concentrations of NAD^+ and its derivatives have been measured in various tissues, cells and organelles. In plants NAD^+ and NADH concentrations in mitochondria are ~2mM,

chloroplasts ~0.4mM and in the cytosol ~0.6mM (see Table 1.1) (Igamberdiev & Gardeström 2003), reviewed in (Noctor, Queval, & Gakiere 2006).

	NAD(H)	NADP(H)
Mitochondria	2mM	0.3mM
Chloroplast	0.4mM	0.4mM
Cytosol	0.6mM	0.3mM

Table 1.1 Concentrations of NAD(H) and NADP(H) in plant cell organelles.

1.1.3 NAD as a substrate.

In addition to NAD^+ acting as a cofactor in redox reactions it can also be consumed as a substrate. There are four different protein modifications involving the degradation of NAD^+ as a substrate, which will be dealt with later in greater detail (illustrated in figure 1.4).

1. Mono ADP ribosylation. ADP ribosylation reactions were first reported in the 1960's following research on the diptheria toxin (Honjo et al. 1968). This activity was later discovered in eukaryotic cells. It involves the cleavage of the nicotinamide unit of one NAD^+ and the transfer of the ADPribose unit onto an acceptor protein, (reviewed in Hassa et al. 2006). Mono ADP ribosylation only involves the attachment of one ADPribose unit on the target protein. Most eukaryotes possess enzymes with poly ADP ribosylation activity but this is performed by different enzymes.
2. Poly ADP ribosylation. This involves the production of large ADP ribose polymers through the addition of many ADP ribose units catalysed by the enzymes poly ADP ribose polymerases (PARPs). First identified in 1963, these poly ADP ribose polymers (PAR) form huge branched structures often comprising of 300-400 units each (Chambon et al. 1963). This will be discussed in detail in section 1.3.

3. Cyclic ADP ribosylation. The importance of intracellular calcium release has long been a subject of research and most is achieved through secondary messengers (reviewed in Berridge (1993)). In 1984 inositol triphosphate (IP3) was discovered as the first of several specific calcium releasing secondary messengers (Burgess et al. 1984). The addition of NAD^+ to sea urchin homogenates generated a release of calcium and required the enzymatic conversion of NAD^+ (Lee & Aarhus 1995). The active molecule in this was later identified as cyclic ADP ribose, now recognised as a powerful calcium mobilisizing agent. The enzyme responsible for producing cyclic ADP ribose is known as ADP ribose cyclase, first (mis-) identified as a NAD^+ glycohydrolase (Kim, Jacobson, & Jacobson 1993). The first ADP ribosyl cyclase was identified in *Aplysia californica* (Hellmich & Strumwasser 1991) and since then calcium signalling mediated by cyclic ADP ribose has been widely documented in a variety of tissues and organisms. Cyclic ADP ribosylation in plants was first shown in beetroot vacuoles with a cyclic ADP ribose IP3 gated calcium release (Allen et al. 1995) and has since been shown to be involved in many pathways, such as an ABA dependent pathway (Wu et al. 2003) resulting in stomatal closure (Leckie et al. 1998). Despite evidence for cyclic ADP ribose activity in plants to date no known homologues of ADP ribosyl cyclases have been identified.
4. Protein deacetylation/NAD^+ dependent protein deacetylation. This is performed by a group of enzymes known as sirtuins, so called due to their similarity to yeast silent information regulator (sir2) genes. They work by removing the acetyl group on lysine residues found on histones and other proteins, a role implicated in chromatin condensation and gene silencing, longevity and DNA repair. This will be discussed in detail in Section 1.2.

A summary of these NAD+ degrading reactions is shown in Figure 1.3. A common feature of all the NAD^+ degrading enzymes is the production of nicotinamide, which acts as an inhibitor on the activity of these enzymes Both the PARPs and sirtuins will each be discussed in greater detail later in this chapter but it is important to view these enzymes within the context of the NAD^+ salvage pathway in order to understand the vital link NAD^+ has between energy metabolism, transcription and signal transduction.

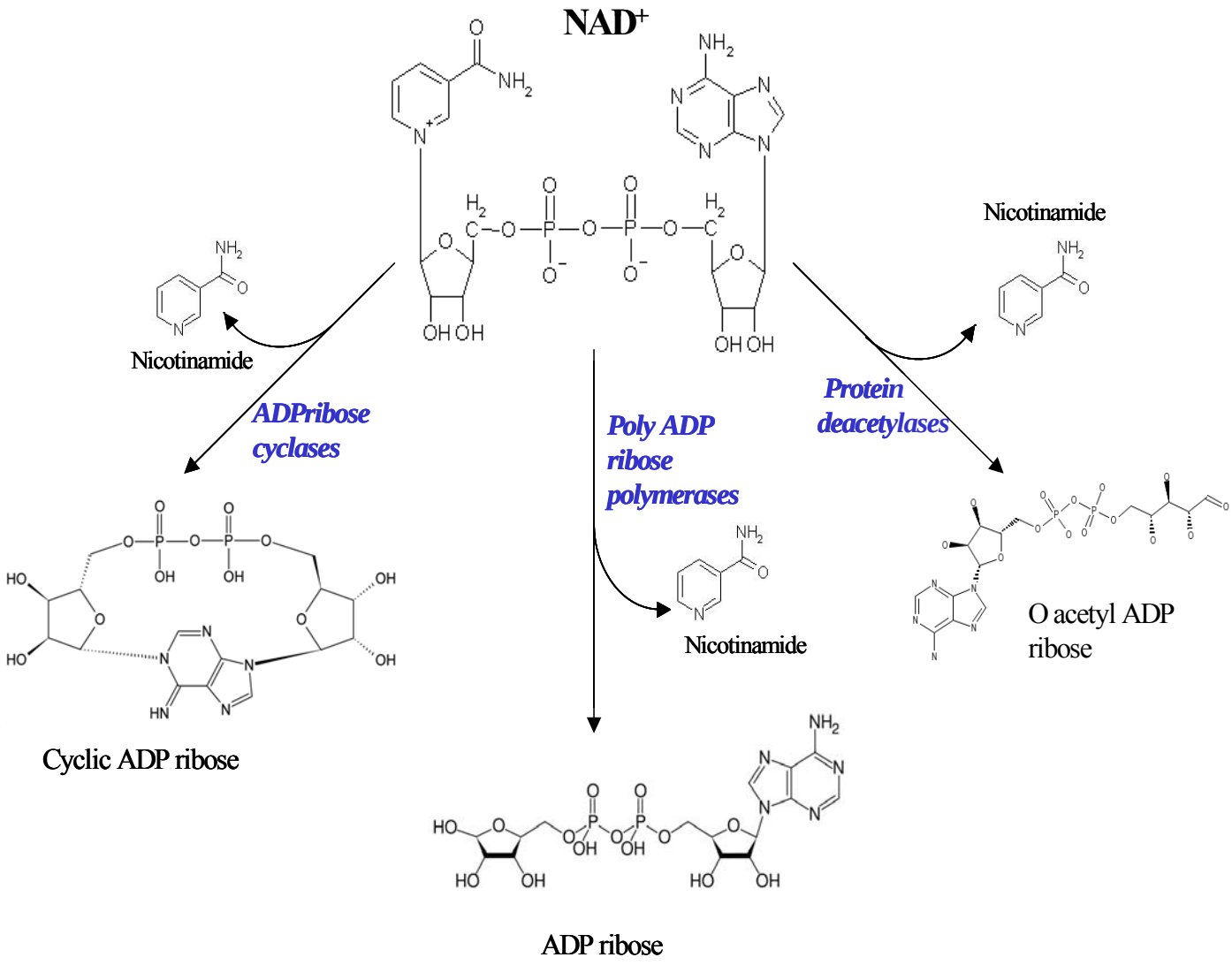

Figure 1.3 Enzymes involved in breakdown of NAD^+. NAD^+ is degraded by three groups of enzymes, ADP ribose polymerases (both mono- and poly-) breakdown NAD^+ and transfer ADPribose to target proteins. ADPribose cyclases break NAD^+ producing cyclic ADP-ribose and ADPribose. Protein deacetylation enzymes break NAD^+ to 0-Acetyl ADP ribose. All NAD^+ degrading enzymes produce nicotinamide.

1.2 Protein deacetylation.

1.2.1 NAD^+ dependent protein deacetylation.

The acetylation state of histones plays an important role in the regulation of gene expression. There are three groups of proteins that deacetylate histone, although this work focuses on the group of histone deacetylases that are NAD^+ dependent. NAD^+ dependent histone deacetylases are a phylogenetically conserved group of proteins found in eukaryotes, prokaryotes and archeal species. NAD^+ dependent histone deacetylases are commonly called sirtuins in the literature and will be referred to as such in this thesis. Sirtuins were first identified as proteins responsible for the silencing of repeated DNA sequences in yeast DNA at telomeres, mating type loci and rDNA. This repression of transcription of mating-type genes maintains the cell-mating type of yeast. Transcriptional gene silencing is achieved through the removal of an acetyl group on histones proteins causing them to form a more compact and closed structure so that the machinery required for transcription cannot reach the DNA (schematic diagram shown in Figure 1.4).

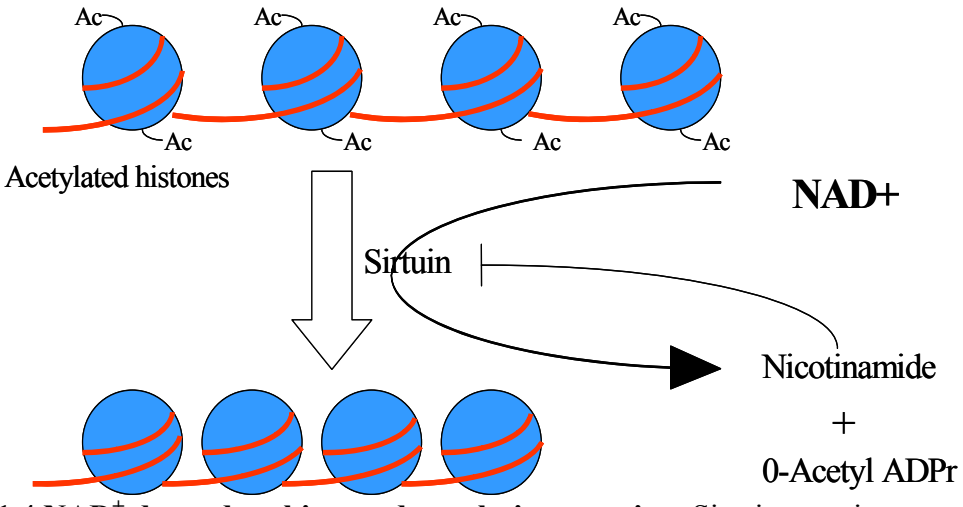

Figure 1.4 NAD^+ dependent histone deactylation reaction. Sirtuin proteins remove the acetyl groups (Ac) on histone lysines allowing the histones to condense into a more tightly grouped structure. The transcription machinery cannot reach the DNA and these genes are silenced. The reaction of the sirtuins requires the one NAD^+ for one lysine deacetylated. The breakdown of NAD^+ produces 0-Acetyl ADPribose and nicotinamide, the latter acting as an inhibitor on the activity of the sirtuins.

Since the first sirtuin gene in yeast was characterised another 4 sirtuin genes in yeast have been identified and 7 sirtuin genes in humans (Frye 1999). So far one of two sirtuins have been identified in every species examined (Brachmann et al. 1995).

Classification of the human sirtuin genes with homology to yeast sir2 by Frye showed two of the human sirtuin proteins did not have histone deacetylase activity but were capable of degrading radiolabelled NAD^+ and transferring a phosphate group onto bovine serum albumin, suggesting that these sirtuins have ADP ribosyl transferase activity (Frye 1999). Since then an increase in research into these interesting proteins has uncovered a wide variety of protein targets and functions, which will be detailed later in this chapter.

1.2.2 Sirtuins and transcription regulation.

Sirtuins were first shown to be histone deacetylases. This results in the histone proteins having a more condensed structure, which prevents the transcription machinery access to DNA. Hence, this results in 'gene silencing' (illustrated in Fig 1.4).

Most of the work on sirtuins transcriptional regulation has been done in mammalian systems and most of these examples are mammalian unless otherwise stated. Sirtuins have been shown to deacetylate other transcription factors, such as PPARγ, PGC-1α and HNF4α which are important for their in role in mobilisation of fat stores and glyconeogenesis. SIRT1 (the first of the 7 mammalian sirtuins identified and named SIRT1-7) has been shown to deacetylate transcription factors involved in cell responses to genotoxic and oxidative stress, such as FoxO, p53, and Ku70 whose activity depends on their acetylation state. Mammalian SIRT1 deacetylation of cell cycle regulator p53 prevents transcriptional induction of powerful apoptosis protein Bax (Vaziri et al. 2001). SIRT1 deacetylation of Ku70 prevents the translocation of Bax protein from the cytoplasm to mitochondria, further reducing the ability to initiate apoptosis (Cohen et al. 2004a). p53 has been shown to have a role as a tumour

suppressor and SIRT1 has been implicated as being a target for cancer therapy because of its control on p53 activity (Heltweg et al. 2006)

SIRT1 has also been shown to deacetylate the transcription factor NF-kappaB, reducing its activity as a signal for neuronal cell death (Chen et al. 2005). SIRT1 activation has been shown to protect against neuronal injury in axons of Wallerian low degeneration mice. This has been reinforced by similar work in *C. elegans* and mice with gene deletions causing Huntington disease (reviewed in Sinclair 2005a).

1.2.3 Sirtuins and DNA repair.

DNA in eukaryotic cells undergoes more than $1x10^5$ DNA lesions per day that require repair, and for this they have 5 main routes of repair mechanisms for maintaining DNA stability and correcting mutations (Barnes & Lindahl 2004). Despite this, DNA mutations increase with age and there is growing evidence supporting the view this increase in DNA lesions is a major cause in the manifestation of aging (Lombard et al. 2005). The yeast Sir2 has been shown to interact with Hdf1, which is essential for double stranded DNA repair and sir2 mutant yeast show an increase in sensitivity to DNA damaging agents (Astrom et al.1999; Tsukamoto et al. 1997).

Work on mutant mice lacking SIRT6 showed early embryonic lethality, a loss of subcutaneous fat, and severe metabolic defects. An increase in DNA breaks was seen as a result of UV-B and ionising radiation. Although the mice showed no abnormalities at birth after 2-3 weeks they failed to thrive and died at 24 days old. The SIRT6 mutant mice also developed severe degenerative defects normally associated with the aging process, such as increase lymphocyte apoptosis and loss of subcutaneous fat (Lombard et al. 2008; Mostoslavsky et al. 2006).

In mammalian cells SIRT1 associates with the RNA binding protein HuR and maintains an elevated level of SIRT1 RNA (Gorospe & de Cabo 2008). SIRT1 has been shown to

deacetylate Nijmegen breakage syndrome (NBS1) protein which is important for recognising damage in DNA and mounting the cellular response to DNA stand breaks (Yuan et al. 2007).

1.2.4 Sirtuins, calorie restriction and longevity.

For many centuries the positive effect of a calorie restricted diet have been long known to cause an increase in lifespan and a decrease in age related diseases such as cardiovascular disorders, cancer and diabetes. It was not until the 1930's that McCay provided the first scientific study showing that rats fed on a measured diet had an increased lifespan compared to freely fed counterparts (McCay et al. 1935). The connection between sirtuins and longevity was first uncovered in budding yeast *Sacchromyces cerevisiae*. Studies in yeast ageing published in 1950's showed that yeast has a finite number of replications producing daughter cells. Therefore the replicative life span in yeast was defined as the number of daughter cells produced before senescence (Mortimer & Johnston 1959). Although yeast replicative lifespan was shown to be increased if grown on glucose restricted media, the first involvement of sirtuins altering lifespan was shown in a yeast mutant screen grown on normal and calorie restricted media. A deletion of the yeast sir2 gene shortened replicative lifespan (Kennedy et al. 1995; Imai et al. 2000) and an overexpression increased replicative lifespan (Kaeberlein et al. 1999). In *Drosophila melanogaster* it was shown that the sirtuin gene was induced by a calorie restricted diet and that sirtuin mutants raised on a calorie restricted diet did not have an increase in lifespan. Furthermore an overexpression of sirtuin gene resulted in an increase in lifespan on normal food but not on a calorie restricted diet (Rogina & Helfand 2004). This was repeated using WT *Drosophila* and the chemical activator resveratrol and showed that lifespan was increased in normal media but not on calorie restriction (Wood et al. 2004a). In *C. elegans* an overexpression of sirtuin gene resulted in an increase in lifespan (Tissenbaum & Guarente 2001).

The health benefits of longevity and its related decrease in age associated illness has been the subject for much research in mice due to their relevance to humans. Mice raised on a calorie reduced diet showed significant decreases in body temperature, heart rate, blood pressure and glucose and insulin levels (Anson et al. 2003).

The Guarente Laboratory was the first to investigate sirtuins in mammals. Overexpression of the mouse Sir2 homolog in fibroblast cells showed that these cells exhibited a reduction in fat production and storage. In addition when these cells were treated with the sirtuin activator resveratrol they exhibited an increase in fat mobilization, although no theory connecting longevity and calorie restriction is postulated in this paper (Picard et al. 2004b).

Research on 12 day old rats grown on a calorie restricted diet showed an increase in levels of Sirt1 in many vital organs. Serum from these rats was added to human embryonic kidney cells and shown to suppress the powerful apoptosis promoter protein Bax. Furthermore a decrease in levels of insulin and insulin-like growth factor receptor (IGF-1) was found in these cells (Cohen et al. 2004b). Work in mammals has shown that SIRT1 (the first of 7 human sirtuin genes) represses the critical transcription factor PPARγ that regulates fat mobilisation from white adipose tissue (Picard et al. 2004a). In hepatocytes sirtuin operates in a complex with transcription factors PGC-1α and HNF4α upregulating gluconeogenic genes and downregulating glycolytic genes (Rodgers et al. 2005). Activation of SIRT1 by resveratrol decreases fat accumulation in white adipose tissue and because of its role in glyconeogenesis could be a target for therapy for type II diabetes (Lagouge et al. 2006; Milne et al. 2007).

A large body of work has since been developed on the role of sirtuins in calorie restriction although a mechanism is still unclear. However, the research does link calorie restriction and energy metabolism and the activity of sirtuins, to processes long believed to be involved in controlling longevity. A review of the different theories linking calorie restriction and sirtuins are found in Sinclair 2005b and Guarente 2005) and summarised in Figure 1.5.

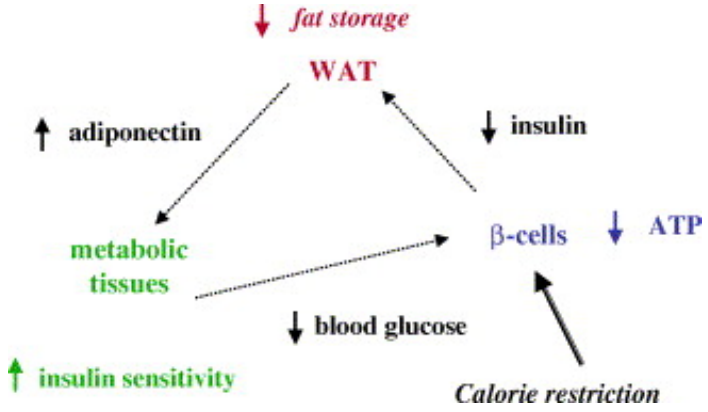

Figure 1.5 Proposed mechanism of calorie restriction in mammals. Under conditions of calorie restriction less insulin is secreted from pancreatic β-cells resulting in mobilization of fat from white adipose tissue. The resulting increase in glucose in metabolic tissues causes an increase in sensitivity to insulin and a reduction in blood glucose. (Taken from Guarente 2005).

1.2.5 Activities of Human sirtuin genes.

Because of the central role of NAD^+ on energy metabolism there has been recent evidence pointing to sirtuins being involved in other stress responses. Seven sirtuin genes have been identified in humans which catalyse 2 different reactions; protein deacetylation (SIRT1, 2, 3, 5 and 7) and protein ADP ribosylation (SIRT4 and 6) (Haigis & Guarente 2006). Because of the requirement for NAD^+ in both reactions, sirtuins provide a vital link connecting energy availability within the cell and metabolic and environmental stress responses. The sirtuin most extensively studied is human SIRT1, the homolog of yeast sir2, although the volume of work on the other human sirtuin genes is becoming increasingly available. The main roles of human sirtuin proteins are summarised in Table 1.2.

Table 1.2 Summary of activities of seven human sirtuin genes.

Mammalian sirtuin	Activities involved	References
SIRT1	1. Prevention of apoptosis via transcription factors FOXO, p53, ku70. 2. Glyconeogenesis, insulin secretion and mobilisation of fat storage via PPARγ. 3. Prevention of neurodegradation by deactylation and prevention of neuron cell death signal Nkappaβ. 4. Deacetylation of Nijmegen breakage syndrome (NBS1) protein implicated in cellular responses to DNA damage	(Vaziri et al. 2001; Cohen et al. 2004a; Picard et al. 2004b; Chen et al. 2005; Yuan et al. 2007; Gorospe & de Cabo 2008)
SIRT2	Deacetylation of tubulin in myelin sheath known to be down regulated in malignant brain tumours.	(Li et al. 2007; Hiratsuka et al. 2003)
SIRT3	Expression shown to be increased in brown adipose tissue of mice exposed to the cold and also activates transcription factor PGC-1α	(Shi et al. 2005).
SIRT4	SIRT4 ADP ribosylation of glutamate dehydrogenase, insulin degrading enzyme and ATP carrier protein in pancreatic β cells negatively regulates insulin secretion.	(Haigis et al. 2006; Ahuja et al. 2007)
SIRT5	Chronic alcohol consumption downregulates SIRT5 and its interaction with PGC-1α in rat liver cells resulting in mitochondrial dysfunction.	(Lieber et al. 2008)
SIRT6	Mice lacking SIRT6 suffer an increase in DNA damage resulting in early embryonic lethality, loss of subcutaneous fat and severe metabolic defects Many of the defects seen are indicative of the effects of aging	(Mostoslavsky et al. 2006; Lombard et al. 2008)
SIRT7	Nuclear protein deacetylating histones and RNA polymerase I. Mice lacking SIRT7 suffer decrease in response to DNA damaging agents and 20% increase in apoptosis	(Ford et al. 2006; Vakhrusheva et al. 2008)

1.2.6 Characteristics and structure of sirtuin genes

Crystals of human sir2 protein (SIRT1) were shown in 2001 to have a 307 amino acid conserved catalytic core (Finnin, Donigian, & Pavletich 2001).

Two main features are shared amongst the sirtuin family of proteins and characterise their structure, a large domain containing a Rossman fold and a smaller zinc binding domain. Between the two domains an interface or groove is formed (illustrated in Fig 1.6).

The sequence of the larger domain is found in many diverse NAD^+ binding proteins and includes some of the typical sequences such as the Gly-X-Gly important for the NAD^+ phosphate binding, a small pocket and charged residues for ribose binding. This large domain is formed of 6 β strands, which form a parallel β sheet and 6 α helixes that fit tightly onto the β sheet. The smaller zinc binding domain consisting of 3 small antiparellel β sheets, an α helix and a zinc atom tetrahedrically bound by four cysteine residues.

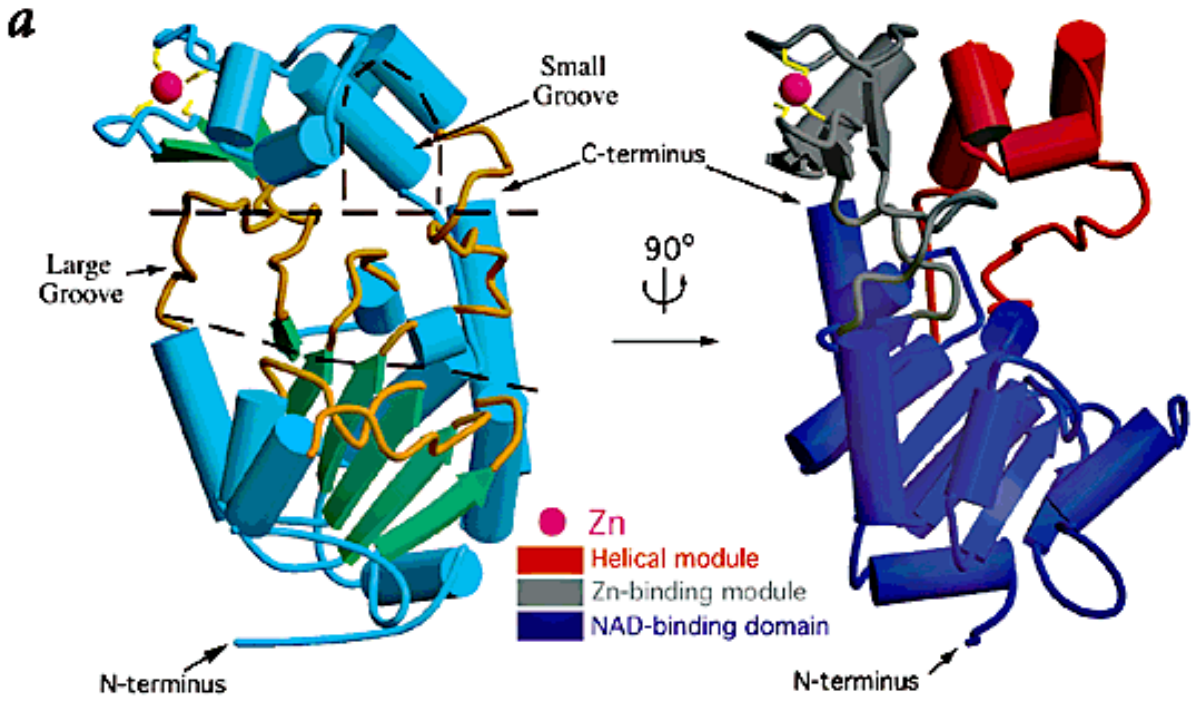

Fig 1.6 The structure of Sir2. Sirtuin consisting of two domains connected by several conserved loops and viewed from two positions rotated by 90º. The large groove in Sirt2 is coloured yellow in the left structure. The NAD^+ binding domain consists of a Rossmann fold (right, seen in blue) and a smaller domain made up of two modules; one in grey binding a zinc atom (magenta) and the other containing a hydrophobic pocket (red). Taken from (Finnin, Donigian, & Pavletich 2001).

1.2.7 Activators and inhibitors of sirtuins.

Activity of sirtuins produces sirtuin inhibitor nicotinamide (Bitterman et al. 2002) and 0-acetyl APD ribose (Tanner et al. 2000). The production of nicotinamide acts as a non-competitive inhibitor on the forward deacetylation reaction (Bitterman et al. 2002) and that its absence increases sirtuin activity.

In yeast it was shown that increasing the activity of the nicotinamidases (enzymes responsible for the removal of nicotinamide) induced longevity without altering the level of NAD^+ in cells (Anderson et al. 2003). At first the mechanism of this inhibition was thought to be due to nicotinamide binding to the NAD^+ binding site of sirtuins (Anderson et al. 2002) although this has since been disproved. The mechanism of this inhibition arises from nicotinamide ability to condense with the sirtuin forming a sirtuin: ADPribose: acetyl-lysine intermediate (Jackson et al. 2003). During the lifetime of this intermediate nicotinamide occupation of the catalytic binding site can result in the reformation of NAD, thus reversing the reaction (Avalos et al. 2005).

A powerful activator of sirtuins is resveratrol (3,5,4'-trihydroxystilbene), a phytoalexin produced by plants in response to pathogen attack. Application of resveratrol has been shown to extend lifespan in yeast (Howitz et al. 2003), *C. elegans*, *D. melanogaster* (Wood et al. 2004b) and fish (Valenzano et al. 2006). In middle aged obese mice on a high fat diet the addition of resveratrol dramatically increased lifespan and survival whilst also decreasing age related effects such as an increased sensitivity to insulin (Baur et al. 2006). In non-obese mice the addition of resveratrol to middle aged mice showed the same reduction in age related metabolic defects but no increase in lifespan (Pearson et al. 2008). However in a conflicting report using 3 different yeast strains resveratrol had no effect on telemetric silencing, ribosomal DNA integrity, or lifespan (Kaeberlein et al. 2005). The molecular basis for this activation revealed that sirtuin activation by resveratrol was only observed using an artificial

fluorescent acetyl- peptide as substrate. Resveratrol dependent activation was shown to be dependent on the presence of a covalently attached fluorophore from the artificial substrate. No resveratrol activation was observed when the same peptide, lacking the fluorophore was used. This has also been shown for mammalian sirtuin genes in vitro (Borra, Smith, & Denu 2005). Therefore the activation of mammalian sirtuins by resveratrol must be carefully interpreted (reviewed in Denu 2005).

1.2.8 Sirtuin genes in *A. thaliana*

There has been one published report on one of the two sirtuin genes in rice, characterising the gene as encoding a nuclear protein and expressed highly in dividing cells (Huang et al. 2007). Rice lines with knocked down sirtuin expression resulted in an increase in hydrogen peroxide, DNA fragmentation, and cell death. Overexpression of the sirtuin gene resulted in plants that were more tolerant of oxidative stress. Microarray analysis on the sirtuin RNAi line revealed a down regulation of genes involved in the hypersensitive response and programmed cell death. There are two sirtuin genes in *A. thaliana* first identified through sequence homology in 2000 (Frye 2000a). However, despite the recent flurry of research into sirtuin genes in many other organisms there has been no further work published on sirtuins in *A. thaliana*.

1.3 Poly ADP ribosylation.

ADP ribosylation is characterised by the transfer of ADP ribose units from the catalysis of NAD^+ onto acceptor proteins, the stages of which are shown in Figure 1.7. The enzymes responsible for this reaction are classed into two families; the mono ADP ribosylating enzymes which transfer one ADP ribose unit and the poly ADP ribose polymerases (PARPs) which transfer many ADP ribose units forming a large ADP ribose polymer onto acceptor proteins. Removal of these ADP ribose units is catalysed by poly ADP ribose glycohydrolases (PARG) enzymes, which are the primary enzymes responsible for the breakdown of poly ADP ribose (PAR) polymers in vivo (Alvarez-Gonzalez 1988).

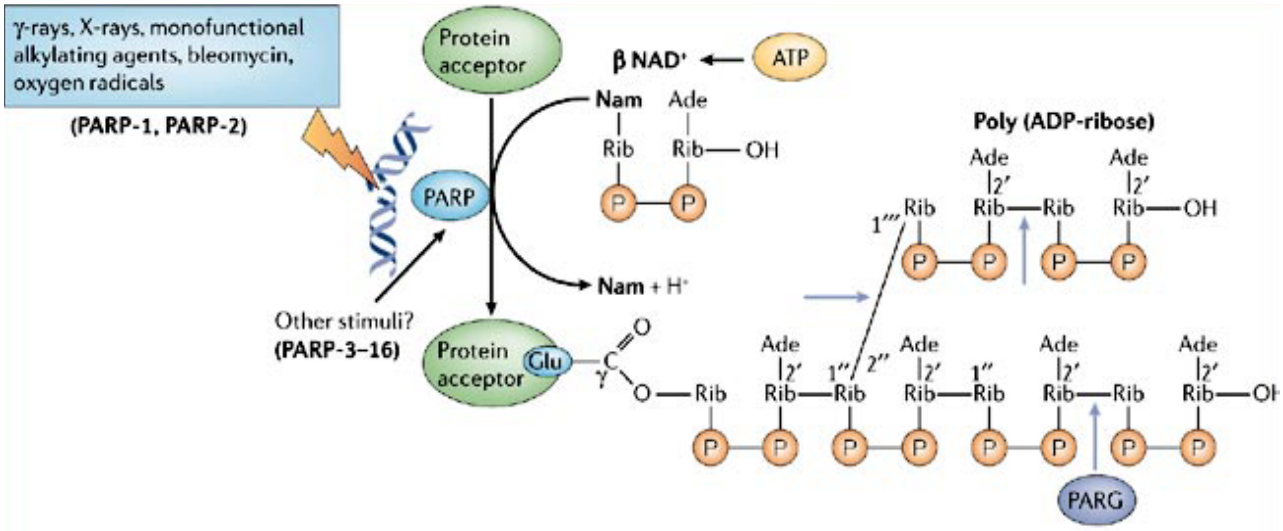

Figure 1.7 ADP ribosylation reaction by poly ADP ribose polymerases (PARP) enzymes. In response to DNA damage, PARP enzymes attach to DNA and hydrolyse NAD^+ releasing a hydrogen ion, nicotinamide and an ADP ribose unit that is transferred to an acceptor protein. Protein elongation and branching of the polymer occurs with the addition of successive ADP ribose units attached by glycosidic bonds. Poly ADP ribose glycohydrolase (PARG) cleaves glycosidic bonds between ADP ribose units. Figure taken from (Schreiber et al. 2006).

The poly ADP ribosylation reaction was first identified in 1963 by P. Mandel et al when NAD^+ was incorporated into nuclear hen liver extracts. The determination of the catalytic domain structure of chicken (Ruf et al. 1996) and mouse PARP1 (Oliver et al. 2004) protein

showed homology with the ADP ribosylating toxin from *C. diphtheriae*. Since then the PARP signature sequence in the catalytic domain has been used to search the non-redundant protein databases (BLAST) for other PARP proteins. PARP enzymes have been found in humans (Amé et al. 2004) as well as characterised in *Drosophila* (Uchida et al. 1993), mice (de Murcia et al. 1997), *C. elegans* (Gagnon et al. 2002) and *A. thaliana* (Lepiniec et al. 1995). The identification of such a large family of PARP in many organisms illustrates the potential importance of ADP ribosylation in maintaining cellular functions.

PARP enzymes are an ancient family of proteins, being found in eukaryotes and prokaryotes such as eubacteria and archeal species (Faraone-Mennella et al. 1998). Surprisingly there are no PARP genes found in yeast (Hassa et al. 2006).

1.3.1 Formation of ADP ribose polymer.

Poly ADP ribose (PAR) is a linear or branched polymer of repeating ADP ribose units linked by glycosidic ribose-ribose bonds (Juarez-Salinas et al. 1982). The synthesis of PAR requires NAD^+ as a substrate and the activity of PARP enzymes is dependent on the cellular concentration of NAD^+ (Kim et al. 2005). All PARP enzymes also possess automodification activity, most likely by covalent auto-ADP ribosylation. In fact PARP 1 was shown to be the main acceptor of poly ADP ribose in vivo (Ogata et al. 1981).

There are four stages in the formation of poly ADP ribose,

1. Initiation. Auto mono ADP ribosylation of glutamate residues in the automodification domain.
2. Elongation. The first covalently attached mono ADP ribose unit acts as a starting point for the addition of further ADP ribose units through glycosidic ribose-ribose bonds.

3. Branching of polymer. This normally occurs after 20 ADP ribose units. It is because of extensive branching that the polymer can become so large, often incorporating 400 ADP ribose moieties.
4. Release of branched poly ADP ribose polymer. Primarily achieved through the activity of poly ADP ribose glycohydrolase (PARG) enzymes.

The structure of PAR has been shown by many groups, estimated to reach up to 400 units. Branching of the polymer is irregular and occurs on average every 20-50 linear ADP ribose units (Hayashi et al. 1983). Electron microscopy of ADP-ribose polymer is shown in Figure 1.8.

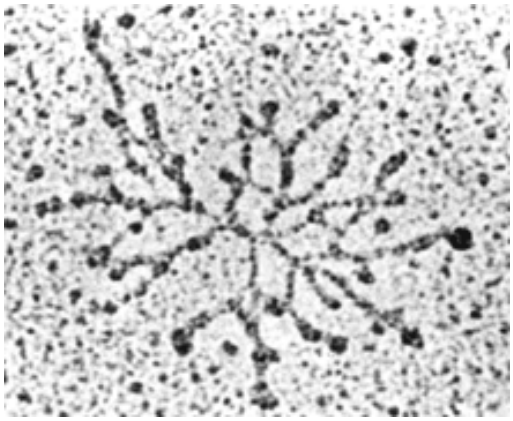

Figure 1.8 Structure of ADP ribose polymer. Visualisation by electron microscopy of ADP ribose polymer purified from calf thymus cells. The polymer is approximately 100nm in diameter. Figure taken from (De Murcia et al. 1983).

Poly ADP ribose is a highly negatively charged polymer and the addition of this to an acceptor protein significantly alters the physiological and biochemical characteristics of the modified protein. This negative charge has been suggested to prevent interactions with other proteins or anionic molecules such as DNA.

1.3.2 Poly ADP ribose acceptor proteins.

At present more than 150 mammalian nuclear protein have been suggested to be modified by the addition of PAR (reviewed in Hassa et al 2006). Most of the proteins associated with PAR are nuclear DNA-binding proteins including PARP itself, histones, topoisomerases, and transcription factors. The modes of action on these are as follows;

PARP enzymes – Poly ADP ribosylation of PARP itself is the most characterised interaction. Automodification of PARP removes its affinity for both NAD and DNA thus decreasing its enzymatic activity. It has been suggested that PARP1 is the most significant acceptor of PAR in intact cells (Ogata et al 1981). There are 15 glutamic acid residues in the automodification domain of PARP enzymes essential for the ADP ribose polymer attachment (Kawaichi et al. 1981).

Histones – the attachment of PAR on to histone tails affects chromatin structure through displacement of histones from DNA (Althaus 1992). Described in section 1.3.3.1.

Transcription factors – the association of large ADP ribose polymers onto transcription factor proteins decreases their DNA binding affinity. For example this has been shown for p53 (Malanga et al. 1998), Ying Yang1 (Oei et al. 1997) and TATA box binding proteins (Oei et al. 1998).

Analyses of the DNA damage repair proteins that act as ADP ribosylation acceptors show that although there is no single invariant amino acid sequence there is a consensus pattern of residues with conserved properties. A typical PAR-binding motif contains two regions, the first is a cluster of positive amino acids, the second is a pattern of hydrophobic amino acids interspersed with basic residues (Pleschke et al. 2000).

1.3.3 Biological functions of PARP activity.

1.3.3.1 PARP role in DNA damage and genomic stability.

The first biological role linked with PARP activity was its involvement in repairing DNA breaks and maintaining genomic integrity in presence of DNA damaging agents (D'Amours et al. 1999). PARP1 is very effective in detecting DNA breaks through its two zinc finger motifs. Although PARP involvement in DNA repair has been shown in many published reports in a variety of organisms the mechanism for how this repair is completed is still unknown.

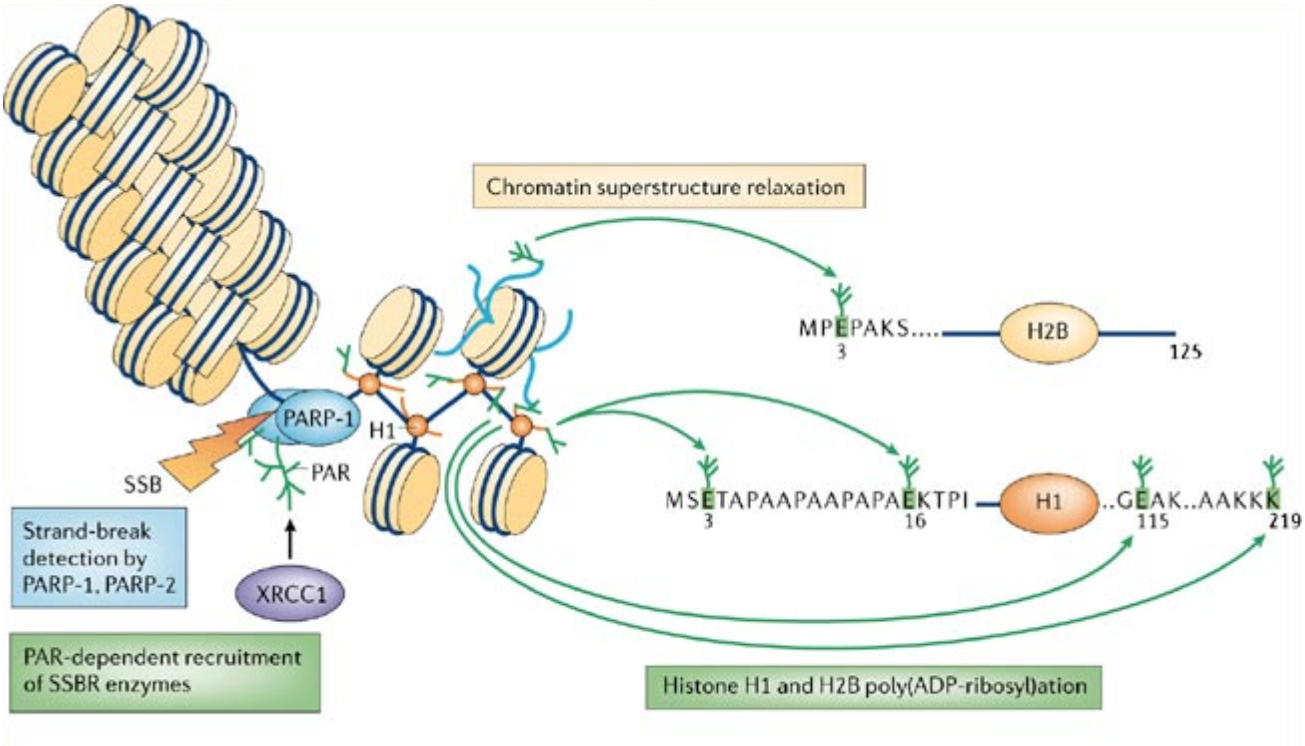

Figure 1.9 PARP1 activity in the repair of DNA breaks and chromatin relaxation. On the detection of DNA strand breaks by PARP1, poly ADP ribose is synthesised on histone proteins at site of the DNA damage. This then acts to recruit DNA repair proteins and to relax the chromatin structure. Figure taken from (Schreiber, Dantzer, Ame, & de Murcia 2006).

PARPS have been implicated in DNA repair and a wide range of other responses including ADP ribosylation of transcription factors and chromatin modifications. Mutational studies in different organisms have helped elucidate PARP mechanisms of DNA damage and given rise

to different hypotheses. Two different laboratories developed mice lacking PARP1 which died after exposure to gamma irradiation and DNA damaging agents methyl nitro urea, MNNG and MMS (Wang et al. 1997; de Murcia et al. 1997; Masutani et al. 2000). Another phenotype observed in these knockout mice was an increase in genomic instability, normally measured as the spontaneous frequency of sister chromatid exchanges, chromatid formation and micronuclei formation. Both of these laboratories reported a decrease in genomic stability after exposure to DNA damaging agents.

Data published on the two PARP genes found in *C. elegans* showed a sharp increase in PAR and a decrease in cellular NAD on the application of high ionising radiation. Furthermore when this was repeated with PARP inhibitors the nematode showed a significant decrease in survival (Dequen et al. 2005).

On detection of DNA strand breaks PARP and binds to damaged DNA (Mathias Ziegler 2001; D'Amours et al. 1999). The mechanisms by which this instigates DNA damage response are unknown although a flurry of research into PARP has produced several hypotheses.

There are three hypotheses for the action of PARP in response to DNA damage.

1. **Activity of poly ADP ribosylation on chromatin structure.** Histones, the major component of chromatin have been shown to be targets of PARP activity in vitro (Poirier et al. 1982a) leading to chromatin decondensation and destabilized nucleosomes (Huletsky et al. 1989). The addition of ADP ribose polymer onto histones, and/or the binding of auto ribosylated PARP at the site of DNA damage leads to a looser chromatin structure (D'Amours et al. 1999). Negatively charged ADP ribose polymers either attached to PARP enzymes or free polymers, acts as an attractive target for histones released from destabilized nucleosomes (Mathis & Althaus 1987;Realini & Althaus 1992). The binding of ADP ribose polymers to

histones could further expose damaged DNA, increasing the access for DNA repair proteins.

2. **PARP and formation of ADP-ribose polymer recruits DNA repair proteins.** A second hypothesis suggests that the poly ADP ribosylation of PARP at the site of DNA damage recruits DNA repair proteins. PARP has been shown to lead to the recruitment of DNA repair proteins, such as Base Excision Repair protein XRCC1 (Masson et al. 1998), and DNA dependent protein kinase (DNA-PK) (Ruscetti et al. 1998).
3. **ADP-ribose polymer acts as a signal for DNA damage.** ADP ribose polymer itself has been shown to act as a signal of the occurrence and severity of DNA damage. A recent study using a PARP1 dependent decrease in cellular NAD^+ uncoupled from the production of PAR, and an in vitro delivery of PAR into cells resulted in cell death after the addition of PAR (Andrabi et al. 2006). The cell death was strongly dependent on the size and dose of ADP ribose polymer (reviewed in Heeres & Hergenrother 2007).

1.3.3.2 Poly ADP ribosylation and the response to stress.

As well as mediating DNA repair PARPs have been implicated in many cellular stress responses. In *A. thaliana* alone, two characterised PARPs have been implicated in responses to Abscisic acid, oxidative stress, DNA damage, salt, and high light (de Block et al. 2005; Vanderauwera et al. 2007). PARPs have been implicated in so many responses in many organisms that they are too numerous to list here. Instead the focus will be on the hypotheses for PARP activity in stress signalling responses.

1. **Role of poly ADP ribosylation in coordinating chromatin structure and transcription**. Poly ADP ribosylation of histones results in decondensed chromatin

with a much looser structure (D'Amours et al. 1999; Poirier et al. 1982a). In the same way that chromatin decondensation can lead to increased access to DNA for DNA repair proteins, access to transcription could be increased. Recent papers on *Drosophila* PARG mutant flies have elucidated a further effect on transcription. In *Drosophila* with reduced PARP activity it has been shown to prevent the accumulation of ADP ribose polymers, chromatin condensation and transcription of highly inducible stress related genes (Tulin & Spradling 2003; Kim et al. 2004).

2. **PARP alteration of Transcription Factor activity.** As well as an alteration of chromatin structure PARPs are also suggest to act as a more classical transcription regulator by altering the function of transcription factors. PARPs activity on transcription factors has been shown by three mechanisms.
    a) **Poly ADP ribosylation of transcription factors**. Studies have shown that the attachment of large ADP ribose polymers to transcription factors affects their DNA binding activities and in turn modifies transcription. Such DNA binding transcription factors include p53, NF-kappaB, B-MYB, and HTLV Tax1. (Anderson et al. 2000; Kameoka et al. 2000; Smith & Grosovsky 1999). However, the action of PARPs on transcription factors is a complex one as some transcription factors can be enhanced by poly ADP ribosylation and others inhibited.
    b) **PARP can bind to promoter DNA.** The finding that PARP1 may bind directly to promotor DNA by recognising DNA sequences or structures have widened understanding of PARPs effect on transcription. PARP binding to DNA promoter sequences can either promote or prevent transcription factor activity. For example PARP has been shown to bind to the promoter of insulin regulator gene Reg

resulting in a reduction of transcription. (Akiyama et al. 2001; Ha, Hester, & Snyder 2002).

c) **Transcription factors can bind directly to the PARP automodification domain.** The transcription factor YY1 binds to the BRCT motif in the automodification domain of PARP1 (Oei et al. 1997) stimulating PARP enzymic activity (Griesenbeck et al. 1999). Transcription factors Oct-1 and B-MYB have also been shown to interact with the automodification domain of mammalian PARP1 (Cervellera & Sala 2000; Nie et al. 1998)

3. PAR polymer formation can function as a cell death signal. This can be further split into two hypothesis

a) In 1985 a mechanism was proposed linking cell death to the overactivation of PARP in response to DNA damage. This hypothesis centred on PARP induced NAD^+ depletion resulting in the utilisation of ATP to form more NAD^+ (Berger 1985). Synthesis of 1 NAD^+ requires 3 ATP (via the NAD^+ salvage pathway) or 5 molecules of ATP (via de novo pathway). In this way cellular NAD^+ and ATP are depleted resulting in cell death (Ha & Snyder 1999). The addition of PARP genes into yeast cells (which otherwise lack both PARP and PARG) resulted in the death of the cells unless a gene encoding PARG was also introduced (Collinge & Althaus 1994; Kaiser et al. 1992). The overactivation of PARP1 in mammalian cells is seen with conditions such as ischaemia (Moroni 2008), inflammation and neuronal diseases such as Alzheimers (Love et al. 1999), and results in a rapid reduction in cellular NAD^+ concentration. Research is in progress on decreasing PARP activity as a possible therapeutic target in the alleviation of these diseases (Virag & Szabo 2002).

b) In 2002 new data published showed an interaction between PARP1 and Apoptosis Inducing Factor (AIF) in PARP knockout mice (Yu et al. 2002). AIF was first identified in 1999 as a mitochondrial flavoprotein found to induce the initial stages of apoptosis through

transportation to the nucleus and chromatin condensation and DNA fragmentation (Susin et al. 1999b). In PARP knockout mice AIF failed to be released from the mitochondria and subsequently conferred cytoprotection against DNA damaging agents. Dawson et al. (2006) reported AIF as a mediator in the cell death response to free PAR delivery. Although no mechanism for this was proposed isolated mitochondria treated with PARP containing nuclear supernatants resulted in a release of AIF. This release of AIF was not reduced with the application of proteases suggesting the stimuli for AIF release is not a protein. However, activated PARP1 from HeLa cells was added to isolated brain mitochondria to examine the release of AIF and it was showed that PAR itself did not induce a release of AIF (Yu et al. 2006). This suggests the possibility of a carrier protein although the mechanism is still far from clear.

1.3.4 NAD metabolism and the control of PARP enzymes.

In cells not exposed to DNA damage the level of ADP ribose polymer is very low. However in response to genotoxic stress the levels of poly ADP ribose can be increase 10-500 fold. The concentration of NAD^+ in unstressed cells is approximately 200-500μM with a half-life of 1-2 hours. In conditions of sustained PARP activity the concentration of NAD^+ can decrease to 10-20% of unstimulated cells. Although the concentration of NAD^+ in cells has a direct control on the activity of PARP enzymes as the levels of NAD^+ are depleted ATP is recruited to form more NAD^+. This depletion leads to a reduction in cellular metabolism and cell death before PARP activity is reduced. The degradation of ADP ribose polymers exhibits a biphasic decay, 85% of ADP ribose polymer synthesised on DNA damage is degraded within 40sec, whilst the remaining fraction is degraded with a half life of 6 minutes. This suggests that on exposure to DNA damage degradation of ADP ribose polymer begins. In contrast constitutive

cellular poly ADP ribose has a half-life of 7 hours (Wielckens et al. 1982). Enzymes responsible for degradation of ADP ribose polymers are the poly ADP ribose glycohydrolases (PARG).

1.3.5 Structure of PARP enzymes

All PARP enzymes display a characteristic 3 domain structure comprising of a DNA – binding domain (DBD), an automodification domain, and a catalytic domain (illustrated in Figure 1.10).

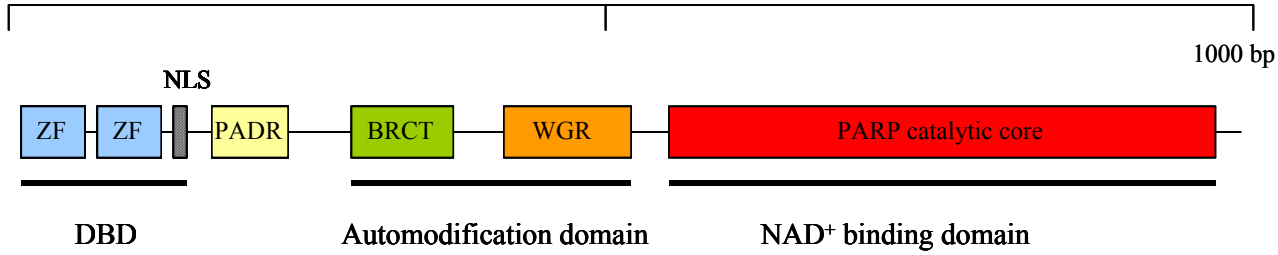

Figure 1.10 Structure of human PARP1. PARP1 from *Homo sapiens* shows three domains. The DNA binding domain (DBD) comprises of two zinc fingers and a nuclear localisation signal, the automodification domain consists of BRCT (Breast cancer 1 protein C-terminus) and a WGR rich region and a PARP catalytic domain.

These domains can be further split into modules. The DNA binding domain binds to single or double strand DNA through two zinc finger motifs. The zinc finger motifs are thought to recognize altered structures in DNA rather than particular sequences and are therefore act as a DNA damage sensor {Menissier-de Murcia et al. 1989).

The automodification domain contains the BRCT region (Breast cancer 1 protein C-terminus) and the WGR domain (characterised by the conserved central motif of tryptophan – glycine – argenine residues).

The largest region of the PARP genes is the PARP minimal catalytic domain a 40kDa region involved in initiation, elongation and branching of ADP ribose polymers. All these domains will be described in more detail in Chapter 4.3.1.

1.3.6 PARP enzymes in plants

Two PARP genes have been identified in *A. thaliana* (Lepiniec et al. 1995). Transient overexpression of *A. thaliana* PARP1 cDNA showed a decrease in DNA breaks and cell death with exposure to mild oxidative stress. Under severe oxidative stress there was an increase in cell death and DNA strand breaks. Similarly in cells with PARP1 antisense expression the opposite effect was seen, an increase in DNA strand breaks with high doses of hydrogen peroxide (Amor et al. 1998). A screen for genes in *A. thaliana* involved in ionising radiation damage showed that both PARP genes were activated (Doucet et al. 2001). Transgenic plants with reduced PARP 1 activity were submitted to drought and high light stress and the transgenic lines were able to maintain energy homeostasis under these stress conditions (de Block et al. 2005). A recent publication using microarray on transgenic plants with reduced PARP activity showed downregulation of wide range genes involved in of stress resistance (Vanderauwera et al. 2007). The hypothesis suggested for this is the overactivation of the PARP genes has a detrimental effect by reducing cellular NAD^+ levels to the extent of inducing cell death and because PARP genes have such an essential role in maintaining levels of NAD^+ it was suggested that the PARP genes may have a role in multiple stress responses. Similar conclusions were drawn when overexpression of PARPs in plants led to an increase in cell death (de Block et al. 2005).

1.4 Poly ADP ribose glycohydrolase (PARG)

PARG was first identified as the enzyme responsible for producing free ADP ribose from polymers of ADP ribose in mammalian cells and possesses endoglycosidic and exoglucosidic activity (Miwa & Sugimura 1971). Although only one PARG gene is present in humans it encodes at least five isoforms (illustrated in Figure 1.11), with each isoform showing different cellular localisations; in the nucleus (hPARG KDa 111), cytoplasmic and nucleus (hPARG KDa 60), mitochondrial (hPARG KDa 55) and two cytoplasmic isoforms (hPARG KDa 102 and 99) (Meyer-Ficca et al. 2004; Meyer et al. 2007).

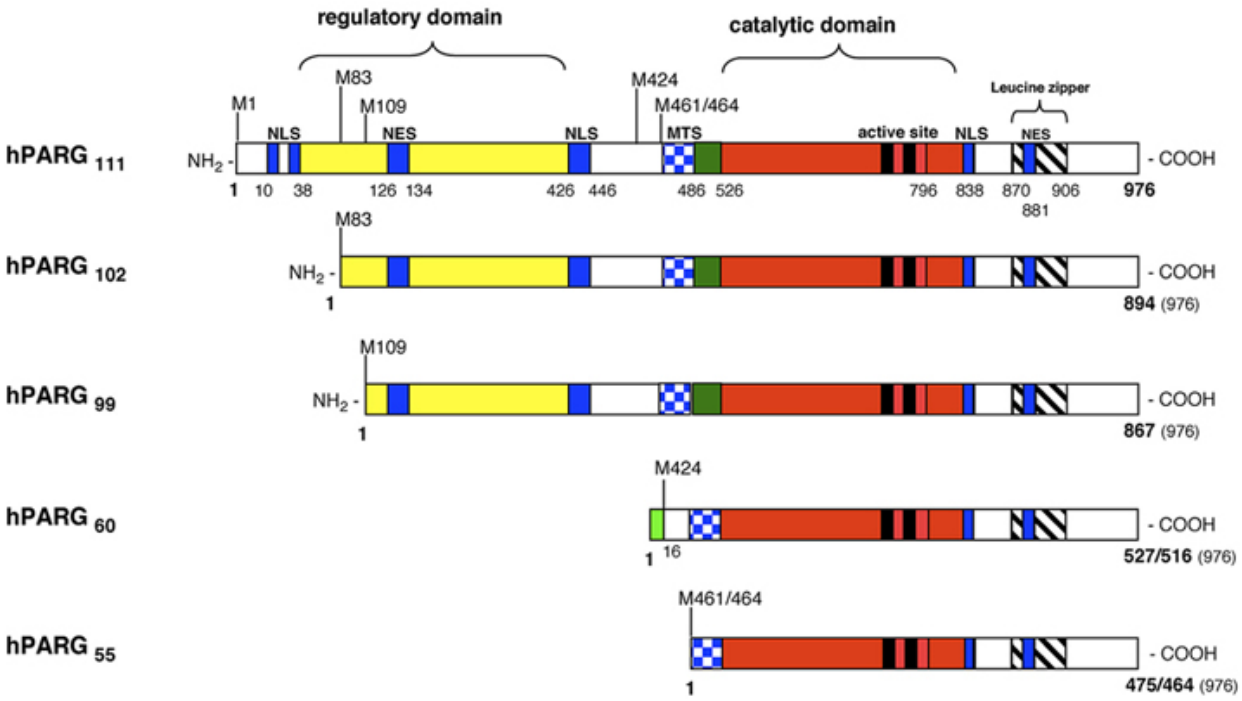

Figure 1.11 Domain architecture of five human PARG isoforms. NLS: nuclear localisation signal and NES: Nuclear export signal found in isoforms PARG KDa 111, 102 and 99. MTS: mitochondrial targeting sequence. PARG 60 contains different N-terminal protein sequences not found in other isoforms. The active site includes conserved residues E728, E738, E756, E757 and T995. (Figure taken from Hassa et al. 2008)

PARG genes have been identified and characterised in other organisms including all mammalian genomes sequenced to date, *D. melanogaster*, *C. elegans* (St Laurent et al. 2007)

and *A. thaliana*. It is interesting that for all these organisms only one PARG gene has been identified but that it possibly encodes multiple isoforms (Lin et al. 1997b). The only exception to this so far are seen in *C. elegans* and *A. thaliana* which both contain two PARG genes (Gagnon et al. 2002; Winstall et al. 1999).

1.4.1 Activity of PARG protein.

The time between identification of the gene encoding PARG and purification of the protein was 25 years and this is attributed to its very low tissue concentration and its instability in later stages of purification. In cells not exposed to DNA damage the concentration of ADP ribose polymers is very low, however it is always 1-2 fold greater than the K_m of PARG. This would suggest that the concentration of poly ADP ribose is sufficient to maintain constant PARG activity even in untreated cells (Alvarez-Gonzalez, Althaus 1989). On increased exposure to DNA damage the concentration of poly ADP-ribose increases proportionally with the number of DNA strand breaks. As mentioned earlier the half-life of ADP ribose polymer synthesised as a result of DNA damage has a very short half life (less than one minute) compared to constitutive ADP ribose polymer (7 hours). PARG also shows preference over catabolism of poly ADP ribose, degrading smaller unbranched polymers more slowly (Hatakeyama et al. 1986). This shows that control over the degradation of polymers is tightly controlled with short polymers degraded more slowly. This would prevent the accumulation of highly modified proteins with large chains of poly ADP ribose attached.

1.4.2 Biological functions of PARG.

PARG enzymes have been much less studied than PARPs, with most of the research into PARP proteins focusing on their control of poly ADP ribosylation. In the past few years work on the activity of PARG itself has appeared and its role is becoming better understood.

The main role for PARG is to control the activity of PARP enzymes. This was shown clearly in yeast *S. cerevisiae* cells, which normally lack both PARP and PARG genes. When human PARP1 gene was introduced to yeast ADP ribosylation activity was seen but the cells did not survive unless human PARG gene was also added (Collinge & Althaus 1994; Kaiser et al. 1992).

The role of PARG enzymes within multicellular organisms has become clearer with the production of mutants lacking PARGs. *Drosophila* mutants lacking the catalytic domain of the PARG gene all died at the larval stage indicating that PARG is essential for the maturation into adult fruit flies (Hanai et al. 2004). Thirty percent of these mutant *Drosophila* did survive until the adult stage if they were grown at a higher than normal temperature of 29°C; however, they displayed progressive neurodegeneration, a shorter lifespan, and the presence of ADP ribose polymer in the central nervous tissue. This suggests an important role for PARGs in regulating the activity of PARP in neuronal tissue. Already research is underway investigating the role of PARG genes in neurological diseases such as Alzheimer and Parkinsons (Kauppinen 2007).

Human embryonic stem cell lines lacking PARG genes resulted in an increase in the sensitivity to DNA damaging agents followed by early apoptosis (Masutani et al 2003). This suggests that PARG is involved in the recovery from DNA damaging agents through efficient poly ADP ribose turnover.

1.4.3 PARG genes in *A. thaliana*.

A. thaliana contains two PARG genes identified through a screen for plants with alterations in circadian rhythm. A single point mutation within one of the two *A. thaliana* PARG genes resulted in an alteration of the timing of transition from vegetative to growth to flowering (Panda, Poirier, & Kay 2002). There is no mechanism to link circadian rhythm to PARG activity. A second PARG gene was identified because it shows large sequence homology to the first PARG gene.

1.5 The NAD salvage and de novo pathways

The common feature between sirtuins, PARPs and ADP ribose cyclases is their utilisation of NAD^+ as a substrate. This removes NAD^+ from the cells and prevents the use of NAD^+ as a cofactor in many metabolic processes. The degradation of NAD^+ produces nicotinamide. The genes of the NAD salvage pathway encode enzymes that convert nicotinamide back in to NAD^+. Sirtuins and PARPs both compete for the substrate NAD^+, which in turn impacts on substrate availability, nicotinamide feed back inhibition of their activity, and the activity of other metabolic processes.

1.5.1 NAD^+ synthesis via the de novo synthesis pathway.

The pathway for the synthesis of NAD^+ can be split into two sections, the de novo and salvage pathway (illustrated in figure 1.12). NAD^+ originates from tryptophan (in animals) (Tanaka & Knox 1959) and L-asparatate in bacteria and plants (Flachmann et al. 1988; Katoh et al. 2006). Through a series of 7 steps it is converted to quinolinic acid from where it is converted to nicotinic acid mononucleotide (NaMN) by the transfer of a phosphoribose group. From here the de novo and salvage pathways converge and NaMN is converted to NAD^+ via

nicotinic acid adenine dinucleotide (NaAD) involving enzymes nicotinic acid mononucleotide adenylyltransferase (NaMNAT) and NAD^+ synthase.

1.5.2 The NAD salvage pathway.

The degradation of NAD^+ as a substrate yields nicotinamide, which is recycled through 4 steps into NAD^+. This pathway from nicotinamide to NAD^+ is known as the NAD salvage pathway and illustrated in Figure 1.12.

The NAD^+ salvage pathway shows variations across different organisms. In plants, labelling studies have shown that the degradation of NAD^+ yields nicotinamide which acts as the substrate for the reforming of NAD^+ (Ashihara et al. 2005). This pathway has also been shown to be the same for bacteria (Berríos-Rivera et al. 2002) and yeast (Sandmeier et al. 2002).

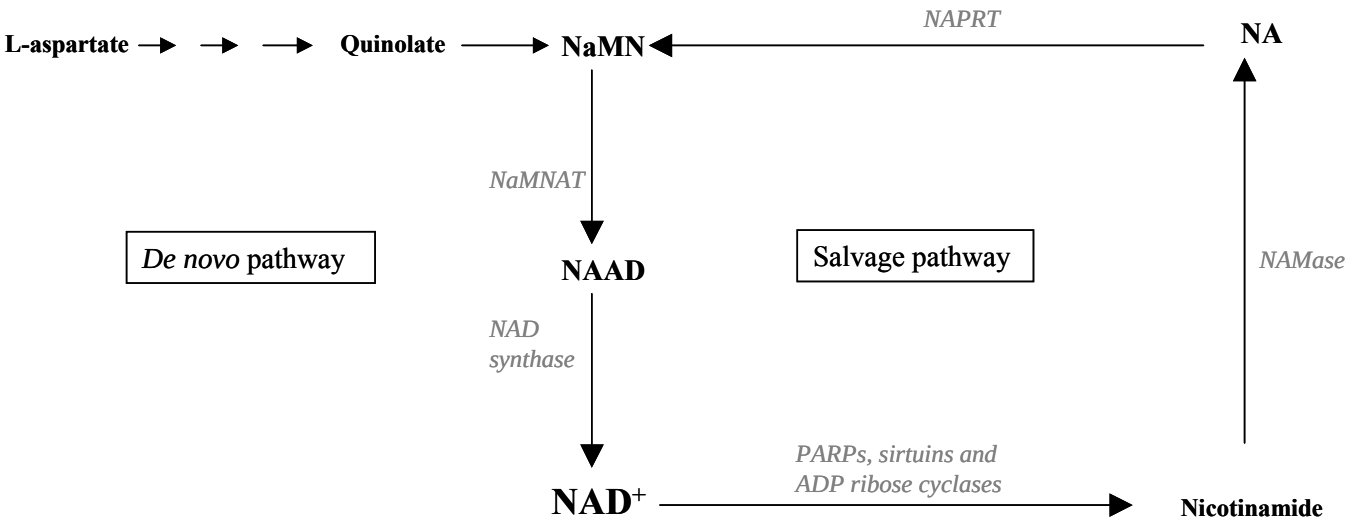

Figure 1.12. NAD^+ de novo synthesis and salvage pathways in plants and bacteria. The de novo pathway involves 7 enzyme steps to convert aspartate via quinolate to nicotinic acid mononucleotide (NaMN). Enzyme names shown in italics, the three enzymes involved in breakdown of NAD^+, sirtuins, ADP ribose cyclases and PARPs (poly ADP ribose polymerases). The enzymes required for the recycling of NAD^+ breakdown products into NAD^+ via the salvage pathway are nicotinamidases (NAMases), nicotinic acid phosphoribose transferases (NAPRT), nicotinic acid mononucleotide transferase (NaMNAT) and NAD synthase.

Nicotinamide is produced from the breakdown of NAD^+ and is converted to nicotinic acid by nicotinamidase enzymes (NAMase; illustrated in Fig 1.12). Nicotinic acid is converted by nicotinic acid phosphoribosyltransferase (NAPRT) to nicotinic acid mononucleotide (NaMN). Here the de novo synthesis and salvage pathways converge. The enzyme NaMNAT performs the conversion of NaMN to NAAD. In the final step NAAD is converted to NAD^+ by an NAD synthase thereby replenishing cellular NAD^+ concentrations. (Pathway reviewed in Hunt, Lerner, & Ziegler 2004).

The NAD salvage pathway in mammals is different as there is no evidence for nicotinamidase enzymes illustrated in Fig 1.13.

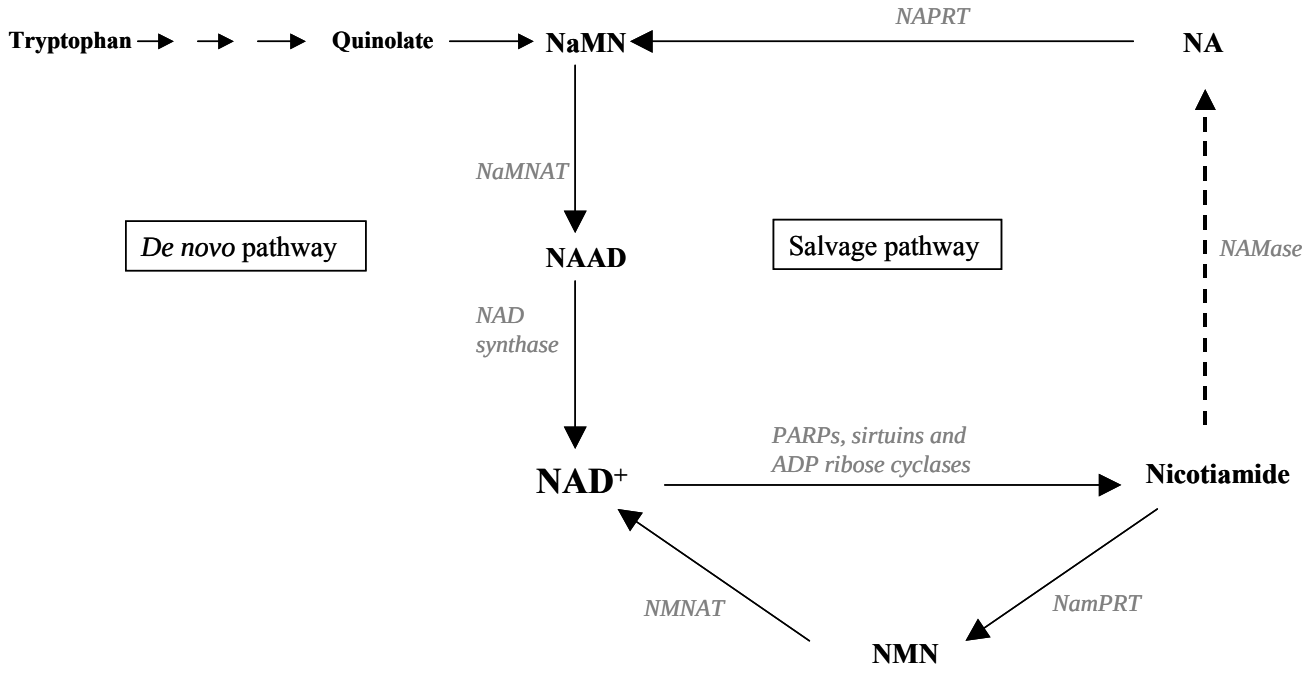

Figure 1.13 Mammalian NAD de novo synthesis and salvage pathways. NAD^+ is degraded into nicotinamide. There is no evidence in mammals for nicotinamidase (NAMase) activity indicated by a dashed line. Nicotinamide is converted to NAD^+ via nicotinamide mononucleotide (NMN) by nicotinamide phosphoribosyltransferase (NamPRT) and Nicotinamide mononucleotide adenylyltransferase (NMNAT). Mammals also have nicotinic acid phosphoribosyltransferase (NAPRT), Nicotinic acid mononucleotide adenylyltransferase (NaMNAT) and NAD synthase enzymes.

In mammals NAD^+ is broken down to produce nicotinamide, which is converted to nicotinamide mononucleotide (NMN) by nicotinamide phosphoribosyltransferases (NamPRT also known as visfatin) and then to NAD^+ by nicotinamide mononucleotide adenyltransferases (NMNAT).

There is no evidence for nicotinamidase enzymes in mammals although other genes of the NAD salvage pathway are present including nicotinic acid phosphoribosyltransferases (NAPRT) that would link nicotinic acid to the NAD salvage pathway. Also present are the enzymes that convert nicotinic acid mononucleotide (NaMN) to nicotinic acid adenyl dinucleotide (NaAD) and NAD^+ by the enzymes nicotinic acid mononucleotide adenylyltransferases (NaMNAT) and NAD synthases (Schweiger et al. 2001b; reviewed in Khan et al. 2007).

1.5.3 Genes of the NAD salvage pathway

1.5.3 Nicotinamidase

Nicotinamidase enzymes catalyse the reaction of nicotinamide (also known as niacin and vitamin B3) to nicotinic acid and ammonia, an activity was first identified in Bakers yeast in 1967 (Bernheim 1967). Nicotinamide acts as an inhibitor on the sirtuin activity (the mechanism of this inhibition was detailed earlier in section 1.2.7).

Because of the inhibitory effects of nicotinamide on sirtuins, nicotinamidases have been implicated in enhancing the protein deacetylase activity in organisms including yeast (Anderson et al. 2002), worms (van der Horst et al. 2007) and *Drosophila melanogaster* (Balan et al. 2008). There is no evidence for nicotinamidase genes in mammals.

In plants the addition of nicotinamide has been reported to lower hydrogen peroxide induced cell death (Amor et al. 1998), and reduce ABA-induced stomotal closure (Leckie et al. 1998).

There have been four *A. thaliana* nicotinamidase genes reported (Hunt et al 2007; Wang et al 2007).

1.5.4 Nicotinic acid phosphoribosyltransferases (NAPRT)

Little is known about the NAPRT enzymes in plants and bacteria. In mammals they do not function in the NAD salvage pathway as nicotinamide is converted directly to NMN (nicotinamide mononucleotide) by NamPRT (nicotinamide phosphoribosyltransferase; see Figure 1.4). NAPRT enzymes are still present in mammals and so there is still a direct link between activity of NAPRT enzymes and cellular NAD^+ concentrations. In mammalian cells expressing NAPRT the addition of nicotinic acid (but not nicotinamide) increased NAD^+ levels and decreased hydrogen peroxide induced cell death (Hara et al. 2007). However, mammals lack the nicotinamidase genes that would link the activity of NAPRT to the NAD salvage pathway.

It was shown in *E. coli* that overexpression of the NAPRT gene resulted in an increase in NAD^+ concentration (Berríos-Rivera et al. 2002). However in yeast it has been shown that an overexpression of the NAPRT gene did not result in an increase in NAD but did cause an increase in lifespan (Anderson et al. 2002)

1.5.5 Nicotinic acid mononucleotide adenylyltransferase (NaMNAT)

NaMNAT enzymes catalyse the conversion of nicotinic acid mononucleotide (NaMN) to nicotinic acid adenine dinucleotide (NAAD) by transferring the adenyl moiety from ATP onto NaMN producing NAAD and pyrophosphate. NaMNAT enzymes display a unique dual specificity for both nicotinic acid mononucleotide (NaMN) and nicotinamide mononucleotide (NMN) and therefore functions in both the NAD salvage and *de novo* pathways (Zhou et al. 2002). The difference in labelling of this enzyme (either NaMNAT or NMNAT) refers to the

substrate the enzyme is acting on. The work presented in this thesis focuses on the NAD salvage pathway and therefore this enzyme will be referred to as NaMNAT.

NaMNAT enzymes have been reported in bacteria (Mehl et al. 2000), yeast (Emanuelli et al. 2003), *D. melanogaster* (Zhai et al. 2008), and humans (Schweiger et al. 2001a). In mammals three NaMNAT enzymes have been characterised and all have the ability to use NMN and NaMN. By contrast *A. thaliana* has only one gene coding for a NaMNAT.

NaMNAT enzymes have been implicated in tumour suppression (Zhou et al. 2002) and also protection against neurodegeneration (Jia et al. 2007).

The only published data on NaMNAT in *A. thaliana* used heterozygous mutant NaMNAT lines. This decrease in NMNAT activity caused depletion in NAD^+ in pollen, which did not affect pollen tube germination but inhibited pollen tube growth. This resulted in the formation of shorter siliques (Hashida et al 2007).

1.6 Aims

The aims of this project were to investigate the role of putative NAD metabolising enzymes in plant responses to stress using *A. thaliana* as the model organism.

For the sirtuins, PARPs, PARGs and NAD salvage pathway gene transcript profiling was used to identify the possible stress responses involving the NAD salvage pathway. Null and transgenic lines were generated to further investigate their role in plant stress responses. Expression and purification of putative NAD salvage proteins in *E. coli* were used to confirm activity.

Chapter 2: Materials and Methods

2.1 Materials

2.1.1 *Arabidopsis thaliana* T-DNA insertion Lines

The *Arabidopsis* T-DNA insertion lines were generated by SALK and were purchased from the Nottingham Arabidopsis Stock Centre (http://nasc.nott.ac.uk/). Those from GABI-Kat were purchased from Max Planck Institute of Plant Breeding Research (Cologne, Germany). All T-DNA insertions were in a Columbia background.

Gene name and number	Insertion line	Company developed
At5g55760	SALK 001493	SALK
At5g09230	GK 349 B06	GabiKat
AtPARP3	SALK 108092	SALK
AtPARP1	GK 380 E06	GabiKat
AtPARP2	GK 420 G03	GabiKat
AtPARG1	SALK 116088 SALK 012110	SALK SALK
AtPARG2	GK 072 B04	GabiKat
NAMase1	GK 121F06	GabiKat

Table 2.1. T-DNA insertion lines for NAD salvage genes.

2.1.2 Chemicals

Unless stated otherwise, all chemicals were purchased from Sigma-Aldrich Chemical Co. Ltd., Dorset, UK or Fisher Scientific (UK) Ltd., Loughborough UK

Restriction enzymes were purchased from Roche (UK) Ltd., Southampton UK

Radioisotopes were from Amersham Biosciences, Bucks UK

Primers for PCR were purchased from MWG Biotech AG, Ebersberg Germany. The primers were supplied desalted and were resuspended to the appropriate concentration in sterile water before use.

Antibiotics were supplied by Sigma-Aldrich Chemical Co. Ltd., Dorset UK All antibiotics used were dissolved in appropriate solvent and filter sterilised.

2.2 Methods

2.2.1 Surface Sterilisation of Seeds

One Covclor 1000 chlorine tablet (Coventry chemicals Ltd UN 2465) was dissolved in 35ml dH_2O with 10µl Triton X-100. 5ml of this was added to 45ml ethanol, mixed gently by inversion and left at room temperature for 5 min. White precipitate was removed by centrifugation at 2000rpm for 5 min (Sorvall Legend RT). Under sterile conditions, seeds to be sterilised were transferred to an eppendorf tube and soaked in 70% ethanol for 2 min. The ethanol was removed and the seeds were soaked in 1ml bleach for 8 min, mixing occasionally by gentle inversion. The bleach was removed; the seeds washed twice in 70% ethanol then left to air dry. Once all traces of ethanol were removed the seeds were then washed 5 times in sterile dH_2O. Seeds were then put onto media plates and left for two days in the dark cold room for two days to stratify. ½ MS growth media for *A. thaliana* seeds contained 2.2g of Murishige and Skoog salts, 0.5g MES and 5g of sucrose in 1litre of dH20. 8% agar was added to the media for plates.

2.2.2 Stress conditions for *A. thaliana Col0* RT-PCR

Reverse transcription PCR (based on a method described by (Fontaine et al 2002) was used to investigate transcript levels of genes in the NAD salvage pathway under a variety of stresses.

Seeds were surface sterilised and then 20 seeds were added to 24 well plates with each well containing 1ml of ½ MS media before stratification in the dark and cold for 2 days. The plates were uncovered and placed in 24 hour light on a shaker set at 40rpm for 7 days when another 1ml of MS media was added. The seedlings were grown for another 4 days for 12 days total. In the sterile hood all media was removed from the plates and a fresh 1 ml MS media added to ensure the same quantity. The plates were returned to the growth room for another 2 hours after which time the control samples were taken and the stress chemicals added (see table 2.2). Seedlings were removed from the wells and gently dried on tissue paper before freezing at –80C at time points 0, 2, 4, 8, 24 and 48 hours.

Stress chemical	Final concentration	Stock dissolved in
Mannitol	2.5 M	½ MS Media
NaCl	200 mM	Water
Hydrogen peroxide	3 mM	Water
Abscisic Acid	50 μM	1% Methanol
Jasmonic Acid	50 μM	Ethanol
LPS	1 μg/ml	
NAA	5 μM	1M NaOH
ACC	200 μM	Water
Salicylic Acid	10 μM	Water
STA	100μg/ml	Water
OKA	1 μM	Water
Brassinosteriod	2.5 μM	Water
Gibberellic Acid	10 μM	Water
MMS	1.2mM	Water
Bleomycin	0.5μg/ml	Water
UV-B	Plates grown in 3μE	
Cold treatment	Plates placed at 4C	
Wounding	Seedling crushed twice with forceps	

Table 2.2. Concentrations for stress conditions for *A. thaliana* seedlings

2.2.3 Genotoxic stress conditions for T-DNA insertion plants

Seeds were surface sterilised and scattered onto ½ MS agar plates (see 2.2.1) before stratifying for 2 days. These were then germinated for 7 days in 24 hour light to ensure that

only germinated seedling of the same size were used. 2ml of ½ MS media and genotoxic chemical was added to each well of a 12 well plate. 10 seedlings were then transferred from the agar plates to each well and the seedling were then grown for another 1-2 weeks. When a phenotype was visible, the seedlings were removed from each well into pre-weighed eppendorfs and incubated overnight in a 90°C oven to remove all water from the seedlings. These were then weighed again for dry weight measurements.

2.2.4 Isolation of Total RNA

Total RNA isolation was preformed using TRI reagent (Sigma-Aldrich Chemical Co. Ltd., Dorset, UK). Approximately 100mg fresh weight plant material was ground to a fine powder in liquid nitrogen using a pestle and mortar. The powder was transferred to a sterile eppendorf tube and 1ml TRI reagent added. The mixture was vortexed briefly and incubated on ice for 5 min. 0.1ml bromochloropropane was added, the sample vigorously shaken for 15 seconds before another incubation for 10 min. The mixture was centrifuged (Eppendorf 5417R) at 12 000 x g for 15 min at 4^{o}C. The colourless upper phase containing the RNA was transferred to a fresh tube, 0.5ml of isopropanol added and the mixed gently. The sample was allowed to stand on ice for 5 min. The solution was then centrifuged at 10 000 g for 10 min at 4^{o}C and the supernatant discarded. The pellet was washed once with ice cold 75% ethanol. After all traces of ethanol had been removed the pellet was resuspended in 50µl DEPC treated water. Contaminating DNA was removed from all RNA preparations using Ambion's DNA-*free* Kit (Ambion (Europe) Ltd, Cambridgeshire UK) following the manufacturer's instructions.

2.2.5 Quantification of DNA and RNA

The quantity and purity of RNA and DNA were determined spectrophotometrically by measuring absorbance at 260 nm and 280 nm. An A_{260} nm of 1 is equivalent to a RNA concentration of 40µg/ml and a DNA concentration of 50µg/ml. The purity of RNA and DNA

is determined by the ratio of absorbance at 260 nm to absorbance at 280 nm. An $A_{260/280}$ ratio of between 1.8 and 2.0 indicates that the nucleic acid is free from protein contamination. The quality of RNA and DNA was determined by agarose gel electrophoresis and the bands checked for signs of degradation (Section 2.2.10).

2.2.6 RT-PCR

The RNA sample (2.5µg) were mixed with 0.25µM oligo dT for 10 min at 70°C and cooled at 4°C. Reverse transcription was carried out in a reaction mixture (25µL) containing AMV reverse transcriptase buffer (Promega UK Ltd, Southampton, UK), 1mM dNTPs (Promega UK Ltd, Southampton, UK), 1 U μL^{-1} RNase inhibitor (Promega UK Ltd, Southampton, UK) and 0·4 UμL^{-1} AMV reverse transcriptase (Promega UK Ltd, Southampton, UK). The reaction was performed at 48°C for 45 min. The enzyme was then heat-inactivated at 95°C for 5 min and the samples diluted 20X to be used for PCR. PCR reactions were performed using 2µL of each 20x diluted cDNA sample in a reaction mixture (25µl) containing 1 x ReddyMix (Abgene, Epsom, UK, contains 1.25 units Thermoprime Plus DNA polymerase, 75mM Tris-HCl (pH8.8), 20mM $(NH_4)_2SO_4$, 1.5mM $MgCl_2$, 0.01% (v/v) Tween 20) 0.2mM each of dATP, dCTP, dGTP and dTTP plus a precipitant and red dye for electrophoresis) and 0.4 µM of each primer.

Gene name and number	Primer name	Sequence
Sirtuin At5g09230	For	TGGTGATATCGAGATTGACG
	Rev	AAGGATGAACCCAACACGAG
Sirtuin At5g55760	For	ACGCAGTTCTCGATAAGCAG
	Rev	AGGTCTCCATTAGCAAGCAG
Nicotinamidase At5g23220	For	ATTCTTTACGCGTCACAACC
	Rev	GCGAGATTCATTAGCGTAGC
Nicotinamidase NAMase1	For	TTCTCGTCATCGATATGCAG
	Rev	TCCTTCACTCCGATCTTGTC
Nicotinamidase At3g16190	For	TCGAGAACATGATCGTCAAG
	Rev	TCACATTGGGATAATCCAGC
PARP AtPARP3	For	CGAGGAGACACACTCGATGAT
	Rev	AACCAACCGTCCACAAGGAACTTT
PARP AtPARP1	For	ACCTCCAGAAGCTCCTGCTAC
	Rev	GTTTTCCACAGGGAACAGTCA
PARP AtPARP2	For	ATTGTGGTTTGACGCCAGTAG
	Rev	GAGGAGCTATTCGCAGACCTT
PARG AtPARG1	For	TTGATTGGAGCTCTTCTTGCATGC
	Rev	AAACGAAGATGCATACCCTGTGTA
PARG At2g31875	For	CGTTTCCGTATATGCGTCACT
	Rev	CATCCATACGAGGCAAAAAGA
NaMNAT	For	CAATCCTCCTACTTTCATGC
	Rev	TGACTTTGAGAGATTCCTCG
NAPRT At4g36940	For	ATC AAT TTC GTT CGT GAT TCG TTA
	Rev	TGC TAG AGC AAC AGC ACA GAA
NAPRT At2g23420	For	AAG TAC TTC GTA GTG CTG ATG G
	Rev	TAA AGC GTC AAT CGT CTC TTC ATT
Actin2 At3g18780	Act2s	GTTGGGATGAACCAGAAGGA
	Act2a	CTTACAATTTCCCGCTCTGC

Table 2.3. RT-PCR primer sequences for genes within NAD salvage pathway.

All PCR products were cloned and sequenced to confirm authenticity (Section 2.2.12). The number of cycles optimised for each primer set is indicated in table 2.4.

Gene	Number of cycles
Sirtuin 09230	29
Sirtuin 55760	31
Nicotinamidase 23220	37
Nicotinamidase 23230	35
Nicotinamidase 16190	29
NAMNAT	32
NAPRT	32
PARP 22470	38
PARP 31320	32
PARP 02390	25
PARG 31870	31
PARG 31865	32
Actin	25

Table 2.4. Optimised number of cycles used to amplify each gene for RT-PCR.

PCR reactions were conducted in a programmable thermocycler (PTC-200 MJ Research): 94°C for 10 minutes, 55°C/1 min, 72°C/2 min, 94/45secs, 55/1 min, 72/1 min (cycle to 94/45 sec) and a 5 min final extension step at 72°C. *ACT2* primers were used as a constitutive control. After amplification, the reaction was resolved by electrophoresis on a 1% agarose gel and stained with ethidium bromide.

2.2.7 Electrophoresis of DNA in Non-Denaturing Conditions

Samples of purified DNA were checked for integrity and molecular weight distribution using agarose gel electrophoresis. 1% (w/v) agarose gels were prepared and run in 1 x TAE (40mM Tris acetate and 1mM EDTA, pH 8.5) containing 0.25µg/ml ethidium bromide. Samples of DNA loaded alongside 1Kb DNA ladder (Promega UK Ltd, Southampton, UK) and the gel was electrophoresed at 5V/cm for 30mins depending on the dimensions of the gel. The PCR products were then quantified by scanning densitometry using Scion Image Beta release 4 (Scion Corporation).

2.2.8 Quantitative PCR

For some of the stress conditions Q-PCR was performed to obtain more accurate results for the changes in transcript level. Quantitative PCR utilises a dye that fluoresces when bound to double strand DNA. Therefore the fluorescence response can be measured in a linear fashion as the concentration of DNA increases over consecutive PCR cycles. Separate primers were designed for Q-PCR to amplify a 300bp fragment over an intron for each of the genes of interest and shown in table 2.5.

Gene name and number	Q-PCR primer sequence
Sirtuin At5g09230	AGAAGCCGCACTCTAAGCAC AGTTACGCTGGATGGAGGAG
Sirtuin At5g55760	TGGGAGGCTAAGTTGAGTGG GCGTGTTGCGAGTGTTCAT
PARP AtPARP3	TGAGCCATGGGAACGTGAGAAGAA AAGCAATGCCAAGCTGCCTTAGAC
PARP AtPARP1	TCCGGAGAAAGAAAGATGCCCAGA GCTGAGTTGCGGGAAATGCTTGAA
PARP AtPARP2	GGACTTGGGATGTGGGATAA GGGGAAGAGTTGGTGTGAAA
PARG AtPARG1	TTCTGGTTCTTCGCCTTTTG CTCGGATGGATGACAATGAA
PARG At2g31875	CTCTTGTTTTTCGCCTCCTG TCTTTTTGCCTCGTATGGATG
UBQ At4g02890	GAGTTCTGCCATCCTCCAAC AACCCTAACGGGAAAGACGA
Actin2 At3g18780	TGAGGTTTCCATCTCCTGCT TGCCAATCTACGAGGGTTTC

Table 2.5. Sequences of Q-PCR primers.

A PCR reaction was set up to amplify the product produced before the band was cloned into TOPO (see section 2.2.10) before being verified by MWG sequence. The concentration of this plasmid DNA was determined spectrophotometrically and dilutions made at 10, 1, 0.1, 0.01, 0.001 and 0 pg/µl. These dilutions were used as standards in order to quantify the

concentration of the cDNA within the stressed samples. 2µl of each of the dilutions was added to 1x Brilliant SYBR green Q-PCR Mastermix (Stratagene) and 500nM of each forward and reverse primer. The reactions were centrifuged briefly to ensure all bubbles were removed. Q-PCR reactions were conducted in a Mx4000 Multiplex Quantitative PCR instrument (Stratagene) and Mx4000 instrument amplification software. The program involved 40 cycles comprising of an initial denaturing step at 95°C for 10min, then cycling between 95C/ 30secs, annealing at 55°C for 1 min and extension at 72°C for 30sec. Each standard curve was created plotting cycle threshold (the cycle number at which fluorescence is above background) against known concentration of dilution. A dissociation plot was analysed for ensure that fluorescence was not due to any spurious dsDNA. When measuring the concentration of gene transcript present in unknown samples the same reaction volumes were used and dilutions for standards were always run at the same time for greater accuracy.

2.2.9 Amplification of genes for cloning

Genes of interest were cloned using the proofreading DNA polymerase KOD HotStart from Novagen (Merck Biosciences Darmstadt, Germany). 200 nM of each forward and reverse primer was added to the following (50 µl total) according to manufacturers instructions.

PCR reactions were conducted in a programmable thermocycler (PTC-200 MJ Research): 94°C for 2 min, 58°C/30sec, 72°C/1 min, 95/30sec, 55/30 min, 72/1 min (cycle to 94/45 sec for 25 cycles) and a 5 min final extension step at 72°C. After amplification, the reaction was resolved by electrophoresis on a 1% agarose gel and stained with ethidium bromide.

2.2.10 Isolation of DNA Fragments from Agarose Gel

The DNA fragment of interest was separated from residual DNA fragments by agarose gel electrophoresis (Section 2.2.10.2). The fragment was excised using a clean, sharp razor blade

and transferred to an eppendorf tube. The DNA fragment was purified using a QIAquick Gel Extraction Kit (Qiagen, West Sussex, UK) following the manufacturer's instructions.

2.2.11 TOPO and pENTR/D Cloning and Sequencing of PCR Products

Successful PCR products to be sequenced were cloned into the pENTR/D vector (Invitrogen) and then transformed into One Shot TOP10 Chemically Competent *E. coli* cells following the manufacture's instructions. Successful transformants were confirmed by colony PCR (Section 2.2.13) and plasmid DNA extracted (Section 2.2.14) was sent for sequencing (MWG Biotech AG, Ebersberg Germany).

2.2.12 Colony PCR

A sterile yellow pipette tip was dabbed onto a bacterial colony then soaked in 5µl dH_2O for 5 min. This was then mixed with 1 x ReddyMix and 100pmol of each primer (forward and reverse). The PCR programme had an initial denaturing step at 94^{o}C for 10 min. This was followed by 25 cycles composing of a denaturing step at 94^{o}C for 30 sec, an annealing step (temp according to primer Tm) for 30 sec and an extension step at 72^{o}C (time according to fragment length). This was followed by a final extension step at 72^{o}C for 5 min. PCR products were analysed by agarose gel electrophoresis (Section 2.2.10.2).

2.2.13 Plasmid DNA Isolation

A single colony was used to inoculate 5ml of LB broth supplemented with the appropriate antibiotic. The culture was grown overnight at 37°C with constant shaking at 200 rpm. The plasmid DNA was isolated from the overnight culture using the QIAprep Spin Miniprep Kit (Qiagen, West Sussex, UK) according to the manufacturer's instructions.

2.2.14 Transformation of Agrobacterium with plasmid DNA

5 µl of plasmid DNA extracted by QIAprep Spin Miniprep Kit was added to 50 µl of Agrobacterium GV3101 cells that had been slowly thawed on ice. These were then quickly frozen in liquid nitrogen and then thawed by incubating at 37°C for 3-5 min. 1 ml of LB broth was added to the cells and incubated at 28°C for 2-4 hours with gentle shaking. Cells were then centrifuged at 3000rpm for 2 min, the supernatant was removed and cells resuspended in 100 µl of LB media. This was then spread onto LB agar plates containing antibiotic for the plasmid and 25 µg/ml for the GV3101 and incubated at 28C for 2 days.

2.2.15 Plant growth conditions.

Enless otherwise stated *A. thaliana* seeds were spread onto moist compost (Levingtons F2; Fisons, Ipswitch UK) and placed in darkness at 4 °C for 2 days. Pots were then transferred to long day growth conditions (16 hour photoperiod, light intensity 200µmol m^{-2} s^{-1}, 22 °C/18 °C day/night temperature and 60% / 70% day/night relative humidity). Seedlings were transferred to individual pots after 7-10 days and watered every 2-3 days.

2.2.16 Transformation of *A. thaliana* with Agrobacterium using floral dip method

Pots of containing 6-8 evenly spaced *A. thaliana* Col0 seeds were grown for about three weeks. When the flower shoots appeared they were removed to encourage more lateral flower stems. The plants were ready to transform when roughly 20% of the flowers had opened.

A single colony of Agrobacterium containing plasmid was used to inoculate 10ml of LB media with antibiotics and grown shaking 28°C for 8 hours before being transferred to 500ml of LB to grow overnight. When the optimum density of cells was reached 0.8-1 the cells were centrifuged at 4500rpm for 10 min. The cell pellet was resuspended in 5% sucrose solution with 0.03% silvet L-77 and the volume adjusted to 500mls. The *A. thaliana* plants were upturned in this solution for 1 min before being covered to increase humidity for 24 hours

room temperature. The plants were then returned to growth room and seeds collected as normal.

2.2.17 Identification of *A. thaliana* transformants.

The vectors used contained a resistant gene for the herbicide Basta (glufosinate ammonium) and resistance to this was used as the selective marker. Seeds collected from floral dip were spread onto soil (about 10 seeds per cm2) and stratified before germinated in growth room. After 4 days growing the seeds were sprayed with 120µg/L Basta in water on alternate days for 8 days. The seedlings without the resistant plasmid bleached and did not survive. Those that survived were transferred to separate pots, grown further and seeds collected. The seeds from these resistant plants were then surface sterilised and spread onto ½ MS agar plates containing 15 µg/ml Basta. Plates were then stratified for 2 days before going into growth room for 12 days. Total seeds and those that had germinated were counted to verify segregation.

2.2.18 Isolation of Plant Genomic DNA

Approximately 200mg fresh weight plant material was ground to a fine powder in liquid nitrogen using a pestle and mortar. The powder was transferred to a sterile Eppendorf tube and 600µl of extraction buffer (1.1% CTAB, 110mM Tris-HCl pH 8.0, 55mM EDTA pH 8.0, 1.54M NaCl pre-warmed to 65°C) was added immediately followed by 1.56µl 20mg/ml proteinase K/ 50mM Tris-HCl pH8.0, 1.5mM calcium acetate. 2% SDS was added and the solution mixed by inversion. The tubes were incubated at 65°C for 1 hour, mixed occasionally by inversion. The tubes were allowed to cool to room temperature and an equal volume of PCI (phenol: chloroform: isoamylalcohol 25:24:1) added. After mixing the tubes were centrifuged at 13 000 rpm (Eppendorf 5415 D) for 2 min, room temperature. The top phase transferred to a fresh eppendorf tube and an equal volume of chloroform:IAA (24:1) added.

After centrifugation (as described previously) the upper phase was transferred to a fresh tube and the DNA extracted again with an equal volume of chloroform:IAA (24:1). The upper phase was transferred to a fresh Eppendorf and 0.6 volume isopropanol added. The tubes were gently rocked for 1-2 min and then incubated at room temperature for 10 min. To pellet the DNA the mixture was centrifuged for 10 min at 13 000 rpm. The supernantant was discarded and the pellet washed twice with ice-cold 70% ethanol. The tube was centrifuged briefly to consolidate the pellet and all traces of ethanol removed. The pellet was re-dissolved in 500µl 0.1 x TE and allowed to re-hydrate on ice for 1-2 hours. Contaminating RNA was removed from DNA preparations by addition of 5µl of RNase stock solution (10mg/ml) followed by incubation at 37°C for 1 hour. An equal volume of PCI (phenol: chloroform: isoamylalcohol 25:24:1) was added and after mixing by inversion the tubes were centrifuged at 13 000 rpm (Eppendorf 5415 D) for 2 min, room temperature. The top phase transferred to a fresh tube and an equal volume of chloroform:IAA (24:1) added. After centrifugation the upper phase was transferred to a fresh tube and 0.35 volume isopropanol and 50µl 3M sodium acetate added. The mixtures were incubated overnight at $^{-}$20°C. To pellet the DNA the mixture was centrifuged for 10 min at 13 000 rpm. The supernatant was discarded and the pellet washed twice with ice-cold 70% ethanol. The tube was centrifuged again to consolidate the pellet and all traces of ethanol removed. The pellet was re-dissolved in 50µl 0.1 x TE and allowed to re-hydrate on ice for 1-2 hour.

Alternatively, genomic DNA was isolated using the Qiagen DNAeasy Plant Kit (Qiagen, West Sussex, UK) following the manufacturer's instructions.

2.2.19 Identification of T-DNA insertion plants

The seeds were bought in at a T2 generation with a known T-DNA insertion within the gene of interest. The large 12 kb T-DNA inserted into the gene effectively inactivates the gene.

Plants were grown for about 2 weeks and genomic DNA extracted from 2-3 leaves. Because the T-DNA insertion is of a known sequence then it is possible to PCR fragments between primers designed to the left and right borders of T-DNA into the gene of interest to identify seedlings with a T-DNA insert. By amplifying the DNA between where the insert should be it is possible to identify if the seedling contains one copy of the wild type gene thus heterozygous. As all the T-DNA insertion line used had a Columbia background, *Arabidopsis thaliana* Columbia (Col0) were always grown and used for PCR as a control.

2.2.20 Phenotypic differences between A. thaliana Col0 and T-DNA insertion plants.

Seeds with a homozygous T-DNA insertion were always grown alongside Col0 to compare for any obvious phenotype. The parameters for this were number of leaves, any lesions on leaves, date of inflorescence, height of inflorescence and day starting and finishing flowering, and time for siliques to dry. This was always carried out in long and short day growing conditions.

2.2.21. Growth conditions for *A. thaliana* seedlings in DNA damaging chemicals.

Seeds were surface sterilised (2.2.1) and spread on MS agar plates in sterile conditions. After 2 days stratification in cold and dark plates were placed in 24 hour light for 7 days. Plants were grown in Costar 24 well microplates (Corning BV Life sciences, the Netherlands). 1ml MS media plus DNA damaging compound was added to each well. Using flamed forceps 3 seedlings from agar places were transferred to each well. Plates were sealed and transferred to 24 hour growth room on shaker and grown with gentle agitation.

Protein expression in *E. coli* BL21 cells

2.3.1 Growth and induction of *E. coli* BL21 cells.

Genes cloned into a vector with a 6x His tag on the C-terminal can be used to purify protein from total extracted protein. The gene of interest was cloned into pEarley 201 obtained from ABRC and transformed into *E. coli* BL21 pLysS cells (Invitrogen) using heat shock method the same as transforming Top10 (section 2.2.10). Single colonies were grown from plates in 5 ml of LB media with antibiotics for 8hours at 37C. This starter culture was then poured into 50ml LB grown until density measured at wavelength 600nm was at 0.6. 1 ml of uninduced sample was taken and centrifuged 12,000 x g for 1ml and the pellet was resuspended in 40 µl of 2x sample buffer (125mM Tris-HCl pH 6.8, 4% SDS, 20% glycerol, 10% merceptanethanol, 2mg bromophenol blue) and boiled for 5 mins. The remaining cells are induced into expressing cloned DNA by adding ITPG (final concentration 0.1mM). The cells are then left for 16 hours shaking at 100 rpm at 20C.

2.3.2 Protein purification from total protein extract from *E. coli* BL21 cells.

Purification of protein under native conditions was always tried first, however if insufficient protein was in the soluble fraction then all the protein was denatured before being bound to the nickel resin. The protein was then refolded on the resin and eluted.

2.3.3 Preparation of nickel resin.

Nickel resin was resususpended by shaking and tapping bottle and 1.5ml added to 15ml falcon tube. The resin was pelleted by low speed centrifugation at 800x g for 1 min and the supernatant gently removed (all centrifugation was performed at 800x g for 1 min unless

stated). 8ml of sterile distilled water was added to the resin and the tube inverted to resuspend the resin. The resin was pelleted by low speed centrifugation and the supernatant removed. For the purification under native conditions 6ml of 1x native binding buffer (50mM NaH_2PO_4 pH 8.0, 0.5M NaCl with 10 mM imidazole from stock containing 3M imidazole, 500 mM NaCl, 20mM sodium phosphate buffer, pH 6) was added and resin resuspended before centrifugation to remove the supernatant. This last step was repeated once more to prepare the nickel resin.

For purification under denaturing conditions 6ml of denaturing binding buffer (8M urea, 20mM sodium phosphate pH 8.0, 500mM NaCl) was added the tube inverted a few times to resuspend the resin. The resin was pelleted by low speed centrifugation and the supernatant removed. This last step was repeated to prepare the resin for denatured cell lysates.

2.3.4 Purification of protein under native conditions.

Cells were pelleted in sorval centrifuge at 3000x g for 10 mins and then resuspended in 8ml 1x lysis buffer (50mM NaH_2PO_4 pH 8.0, 0.5M NaCl) with 8mg of lysozyme before being incubated on ice for 1 hour. Cells were then sonicated on ice with 6 x 10 sec bursts at high intensity with 5 sec cooling time between. To separate the insoluble fraction samples were centrifuged at 3000x g for 15 mins at 4°C and the supernatant transferred to a fresh tube. At each step 20µl of supernatant was added to 2x sample buffer (section 2.3.7) for SDS-PAGE analysis. The 8ml of lysate is added to the prepared resin and kept on ice with gentle agitation for 1 hour for the His tagged protein to bind to the nickel. The resin was settled by low speed centrifugation (800x g 1 min) and the supernatant removed. The resin was resuspended in 8ml of 1x native wash buffer (50mM NaH_2PO_4 pH 8.0, 500mM NaCl and 20mM imidazole) and then pelleted by low speed centrifuge before removing supernatant. This wash was repeated three more times. The resin was resuspended in 8ml of 1x Elution buffer (50mM NaH_2PO_4 pH 8.0, 0.5M NaCl with 250mM imidazole from stock). The plunger from a 10ml syringe

was removed and a small ball of glass wool pushed into the end. A piece of thin tube was attached to the end with a clamp (closed at this stage) and the syringe was held in a vertical position. The resin in elution buffer was transferred to the syringe and the protein eluted in 1ml fractions.

2.3.5 Purification of protein under denaturing conditions.

Cells were pelleted in sorval centrifuge at 3000x g for 10 mins and then resuspended in 8ml of guanidinium lysis buffer (pH 7.8). The resin was gently agitated for 10mins at room temperature to ensure lysis of all cells. The cells were sonicated on ice for three 5 second bursts at high intensity and centrifuged for 15 mins at 3000x g. 20µl of each sample at each stage was retained for SDS-PAGE analysis. The supernatant was transferred to a fresh tube and added to the nickel resin prepared for denaturing conditions. The protein was bound to the nickel using gentle agitation for 30 mins before allowing the resin to settle by low speed centrifugation (800x g 1 min) and supernatant removed. The resin was resuspended in 4ml of denaturing binding buffer then pelleted with a low speed centrifugation and supernatant removed. This step was repeated one more time. To wash the resin was resuspended in 4ml of denaturing wash buffer then pelleted with a low speed centrifugation and supernatant removed. This step was repeated one more time. The resin was washed in 8ml of 1x native wash buffer (50mM NaH_2PO_4 pH 8.0, 500mM NaCl with 10mM imidazole from stock containing 3M imidazole, 500 mM NaCl, 20mM sodium phosphate buffer, pH 6). The resin was pelleted by low speed centrifuge and the supernatant removed. This step was repeated three more time. The resin was resuspended in 1x Elution buffer (50mM NaH_2PO_4 pH 8.0, 0.5M NaCl with 250mM imidazole from stock). Protein was eluted in a 10ml syringe with tubing and a clamp attached to end described in section 2.3.4.

2.3.6 Quantification of protein by Bradford assay

A standard curve was set up using BSA concentrations of 0, 0.25, 0.5, 1 and 1.4 mg/ml. 33 µl of this was added to 1 ml of Bradford reagent (BioRad, Hertfordshire UK) in a 1ml cuvette and mixed by pipetting. The mixture was incubated at room temperature for 5 mins before measuring the absorbance at 595nm. The same volumes were used for the samples with unknown protein concentration and the absorption of each was calculated from the standard curve. 20 µg of protein was run in each lane of SDS-PAGE gel.

2.3.7 SDS-PAGE under denaturing conditions.

The protein gel kit used was the protean mini from BioRad and the manufacturers instruction was used to assemble the protein kit. To obtain optimum protein separation the resolving gel was made up to 10% acrylamide (30:2) with 0.375M Tris HCl pH8.8, 0.1% SDS, 0.1% Ammonium persulphate and 0.1% TEMED. Once the resolving gel had set a stacking gel of 5% acrylamide was poured on top containing 0.125M Tris HCl pH 6.8, 0.1% 0.1% SDS, 0.1% Ammonium persulphate and 0.1% TEMED and a comb for wells added. After the stacking gel had set the comb was removed and the wells washed with water before the gels were assemble in the protein tank and 1x running buffer (0.02M Tris Base, 0.192M glycine, 0.1% SDS, pH 8.3) was poured into the tank to cover both electrodes. 20µg of protein was pipetted into each well and a prestained broad protein marker (NEB Hertfordshire UK) run alongside. The acrylamide gel was electrophoresed at 150V until the dye contained in the samples was at the end of the gel. The glass plates were disassembled and the gels stained in Coomassie blue stain (45% methanol, 10% acetic acid, 0.5g coomassie blue) for 30 mins before destaining (10% methanol, 5% acetic acid).

2.3.8 Electrophoretic transfer of proteins to PVDF membrane

When transferring proteins from acrylamide gel to PVDF membrane then the gels were run as described in section 2.3.7 and disassembled but not stained. PDVF membrane was cut to the same size as the gel and soaked first in methanol for 5 mins and then transfer buffer (28.8g glycine, 6.04g Tris base, 200ml methanol, dH_20 to 2L). After electrophoresis the gel and filter paper were soaked in transfer buffer before being assembled in transfer cassette in order according to manufacturers instructions. The transfer cassette and cooling block were placed in the tank and transfer buffer filled to the top of the tank. The tank was then run at 30V overnight.

2.3.9 Western Blot

After electrophoretic transfer the cassette was disassembled and membranes blocked in TBS Tween (100mM Tris HCl, pH 7.5, 150mM NaCl, 0.05% Tween 20) with 5% dried milk for 1 hour with gentle agitation on very low speed shaker. The membranes were then incubated with the primary antibody diluted 1:2000 in 5% dried milk TBS Tween for one hour. The antibody was removed and can be reused up to three times if stored in the –20C. The membranes were washed three times with TBS Tween for 10mins on shaker between each wash. The membrane was reblocked to 10 mins in 10% dried milk TBS Tween before being removed and incubated with secondary antibody (diluted 1:10000 in TBS Tween) for 1hour shaking. The antibody was removed the membrane washed in TBS Tween gently shaking for 10 mins between each wash. The membranes were placed protein side up on acetate and the chemiluminscent substrate (Pierce 32106) prepared just before use. The chemiluminscent was added to the membranes for 1 min before the excess was removed and a second acetate placed over the membranes. In the dark the membranes were placed within a film cassette and film placed over the top. Exposure times varied with membranes and film was developed.

Chapter 3: Identification and characterisation of two sirtuin genes in *A. thaliana*.

3.1 Introduction.

The silent information regulator (sir2) family of genes were first identified in yeast as controlling yeast replicative life span (Kennedy et al 1995) and for their role in regulation of transcriptional and chromosomal stability. (Kim et al. 1999). The first yeast sirtuin showed protein deacetylation activity although later yeast sirtuin proteins showed ADP ribosylation activity. Protein deacetylation involves the degradation of one NAD^+ for every acetyl group removed producing one molecule of 0-Acetyl ADP ribose (0-AADPr) and nicotinamide. ADP ribosylation involves the breakdown of NAD^+ to transfer ADP ribose onto acceptor proteins and yielding nicotinamide. The most studied activity is the deacetylation of acetylated lysine residues on the N-terminal of histone proteins. This deacetylation results in a more compact and closed structure of the DNA leading to gene silencing (Imai et al. 2000) and shown in Figure 3.1.

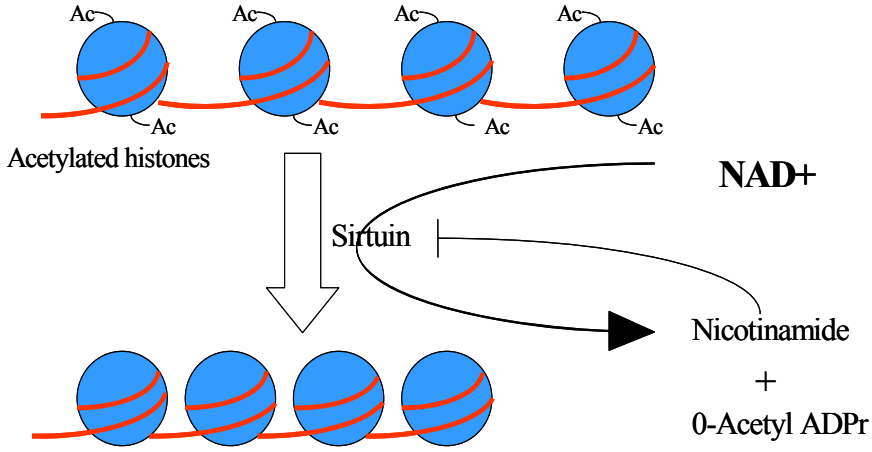

Figure 3.1 NAD^+ dependent histone deactylation reaction. Sirtuin proteins remove the acetyl groups (Ac) on histone lysines allowing the histones to condense into a more tightly grouped structure. The transcription machinery cannot reach the DNA and these genes are silenced.

The sirtuins (so called because of their homology with the yeast silent information regulator genes) are a phylogenetically conserved family of proteins from archean to eubacteria and mammals (Frye 2000a). Although sirtuin genes and their role in many metabolic functions has been characterised in yeast, nematodes and flies, the seven human sirtuins genes (termed SIRT1-7) have been most extensively researched. However, there is a wide difference in functions and localisations of all seven human SIRT genes summarised in Table 3.1.

	Localisation	Role involved
SIRT 1	Nuclear	Aging, insulin secretion, neurodegeneration
SIRT 2	Cytoplasmic	Deacetylates tubulin in myelin sheath
SIRT 3	Mitochondrial	Adaptive thermogenesis
SIRT 4	Mitochondrial	Insulin secretion
SIRT 5	Mitochondrial	Unknown
SIRT 6	Nuclear	DNA and genomic integrity
SIRT 7	Nuclear	DNA damage and genomic stability

Table 3.1 Summary of function and localisation of seven human sirtuin genes.

Sirtuin genes have been identified and characterised in other organisms including *C. elegans* and *D. melanogaster* and purified recombinant protein from both these organisms has been shown to have deacetylase activity. Both *C. elegans* and *D. melanogaster* showed an increase in longevity in the presence of specific sirtuin activators when grown on normal and calorie controlled diets (Wood et al. 2004a). Sirtuin RNAi lines in *D. melanogaster* resulted in early lethality offspring (Kusama et al. 2008).

Although sirtuins were first identified as NAD^+ dependent histone deacetylases some sirtuin proteins did not show this activity. It was Frye who reported that one of the human sirtuin genes did not show histone deacetylation but was capable of transferring a radiolabelled ADP ribose moiety from NAD^+ to bovine serum albumin (Frye 1999).

Sirtuin genes have also been shown to deacetylate a number of other proteins such as p53, and the transcription factors Fox0, Ku70, NF-Kappa β and PGC-1α.

Although there are many different proteins known to be deacetylated by sirtuins the processes affected are metabolic responses to stress (Haigis & Guarente 2006), apoptosis (Sinclair 2005a) cell cycle regulation (Cohen et al. 2004a), and DNA damage (Gorospe & de Cabo 2008).

Because of the range of interesting processes these proteins have been shown to be involved in there has been a flurry of research into sirtuins in many organisms from bacteria to mammals. Sirtuins also represent a vital link between transcription and cellular metabolism through their requirement for NAD^+.

Sirtuins are well characterised in other organisms but so far there has been no published data on the two sirtuin genes in *A. thaliana*.

3.2 Methods and Materials.

3.2.1 *A. thaliana* T-DNA insertion lines.

The Arabidopsis T-DNA insertion lines were generated by SALK and were purchased from the Nottingham Arabidopsis Stock Centre (http://nasc.nott.ac.uk/). Those from GABI-Kat were purchased from Max Planck Institute of Plant Breeding Research (Cologne, Germany) (http://www.gabi-kat.de/). All T-DNA insertions were into a Columbia background.

Gene name and number	Insertion line	Stock Centre
At5g55760	SALK 001493	SALK
At5g09230	GK 349 B06	GabiKat

Table 3.2.T-DNA insertion lines for sirtuin genes in *A. thaliana*. Both lines were generated in *A. thaliana* Col0.

Plants containing the T-DNA insert were identified using protocol described in Methods and Materials (Chapter 2.2.19)

3.2.2 Studies on Transcript levels using Semi-quantitative Reverse Transcriptase PCR (SQRT-PCR)

Transcript levels for sirtuin genes exposed to a variety of different biotic, genotoxic and abiotic stresses were investigated in order to identify the role of sirtuins in stress responses (a full list of stresses tested are listed in Methods and Materials Chapter 2 table 2). cDNA made from extracted RNA was used as template in PCR reactions with primers for sirtuin genes. An actin gene was also amplified as an internal control to compare amounts of cDNA in each reaction (see Methods and Material Chapter 2.2.6). A list of primers sequences is found in Table 3.3.

Gene name and number	Primer name	Sequence	Number of cycles
Actin2 At3g18780	Act2s Act2a	GTTGGGATGAACCAGAAGGA CTTACAATTTCCCGCTCTGC	25
Sirtuin At5g09230	For Rev	TGGTGATATCGAGATTGACG AAGGATGAACCCAACACGAG	29
Sirtuin At5g55760	For Rev	ACGCAGTTCTCGATAAGCAG AGGTCTCCATTAGCAAGCAG	31

Table 3.3. SQRT-PCR primer sequences for *A. thaliana* sirtuin genes and Actin2 gene. Gene products were sequenced by MWG for verification.

PCR products were run on a 1% agarose gel and band intensities analysed by Scion Image. All band intensities were normalised to the actin band before fold differences were compared.

3.2.3 Quantitative PCR (Q-PCR).

The full method described in Methods and Material Chapter 2.2.7. The stresses shown by RT-PCR to have significant differences in response to gene transcript levels were then analysed by quantitative PCR in order to obtain more quantitative results. Q-PCR utilises a fluorescent dye that binds to double stranded DNA with the fluorescence being proportional to the transcript level. Fluorescence levels were analysed using Stratagene Mx4000 instrument and amplification software. PCR products from primers were cloned and sequenced by MWG to verify amplification of the correct sequence. The levels of transcript between samples were compared by amplifying levels of constitutively expressed gene Actin.

Gene name and number	Q-PCR primer sequence
Sirtuin At5g09230	AGAAGCCGCACTCTAAGCAC AGTTACGCTGGATGGAGGAG
Sirtuin At5g55760	TGGGAGGCTAAGTTGAGTGG GCGTGTTGCGAGTGTTCAT
Actin2 At3g18780	TGAGGTTTCCATCTCCTGCT TGCCAATCTACGAGGGTTTC

Table 3.4. Quantitative PCR primer sequences for *A. thaliana* sirtuin and Actin2 genes. Gene products were sequenced by MWG for verification.

3.2.4 Cloning of *A. thaliana* sirtuin genes.

Sequences for both of the *A. thaliana* sirtuin genes were obtained from the Arabidopsis information resource website (www.arabidopsis.org) and primers for cloning into pENTR/D vector (Invitrogen) were designed for this sequence. *A. thaliana* Col0 cDNA was used as template for the PCR reaction (see Methods and Material 2.2.9). After ligation and transfer into *E. coli* Top10 cells (see Chapter 2.2.11) successful transformants were selected by colony PCR (Methods and Material Chapter 2.2.12) and restriction digests of the plasmid insert undertaken before being sent for sequencing at MWG (www.mwg-biotech.com). The advantage of the Invitrogen Gateway cloning system is that is allows transfer of the cloned gene into a variety of different destination vectors without the need for complicated manipulations for plasmid shuffling. All constructs were verified by sequencing by MWG.

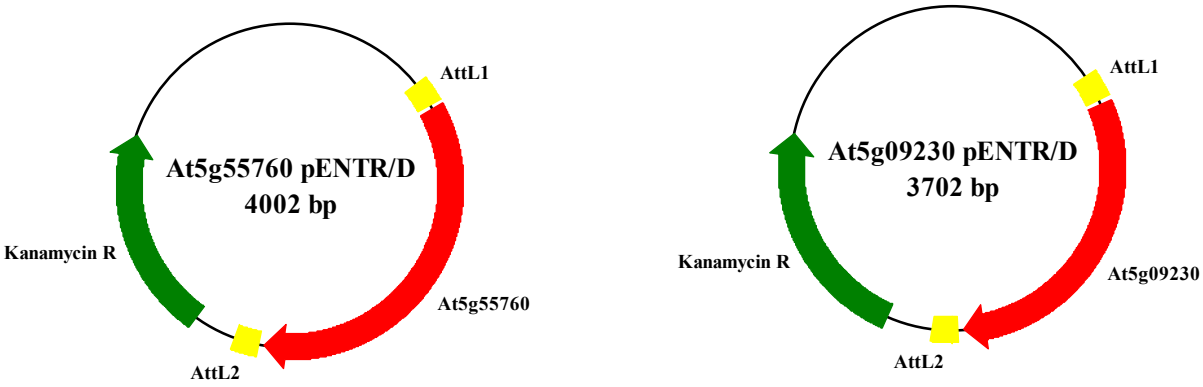

Figure 3.2. Plasmid maps of both putative *A. thaliana* sirtuin genes in Invitrogen entry vector pENTR/D

The *A. thaliana* genes were then transferred to a different destination vectors listed in the table below.

Vector name and manufacturer.	Characteristics	Reference
pDEST17	N-terminal 6xHIS tag	Invitrogen
pDEST 15	N-terminal GST tag	Invitrogen
pGWB6	N-terminal GFP	(Nakagawa et al. 2007)
pGWB5	C-terminal GFP	(Nakagawa et al. 2007)
pEARLEY 501	N-terminal HA tag	Earley KW et al. 2006
pEARLEY 503	N-terminal Myc tag	Earley KW et al. 2006

Table 3.5. Vectors used for expression of sirtuin genes. The table includes vector names, source, and reference for each vector

3.3 Results

3.3.1 Identification and cloning of two sirtuin genes in *A. thaliana*

The catalytic core of sirtuins was identified (Sherman et al. 1999) and confirmed by transferring the human SIRT1 catalytic core to mutant yeast strains to return the silencing phenotype (Brachmann et al. 1995).

The structure of archaean Sir2 homolog was the first sirtuin to be determined (Min et al. 2001) followed by the human SIRT1 sequence (Finnin et al. 2001) and yeast sirtuin (Avalos et al. 2002). All structures revealed two main regions: a large NAD^+ binding domain with a Rossman fold, and a smaller region binding a zinc ion. The larger domain consists of a Rossman fold structure of parallel β sheets similar to domains seen in NAD^+ utilizing enzymes such as dehydrogenases. Mutational studies suggest this domain contains the NAD^+ binding site. The smaller region consists of an antiparallel β- sheet, 2 α helices and a flexible loop. The smaller domain also contains a tetrad of cyseine residues essential for binding of a zinc ion.

Most sirtuins have either N- or C-terminal extensions outwith the catalytic core but the function of this is unknown although it has been suggested to have an autoregulatory role (Zhao et al. 2003).

The protein sequence of the catalytic core of sirtuins was used to interrogate the complete *A. thaliana* expressed sequence tag database using the BLAST algorithm. Two putative sirtuin genes in *A. thaliana* were identified (Hunt et al. 2004).

3.3.1.1 Identification of sirtuin At5g55760 from sequence homology.

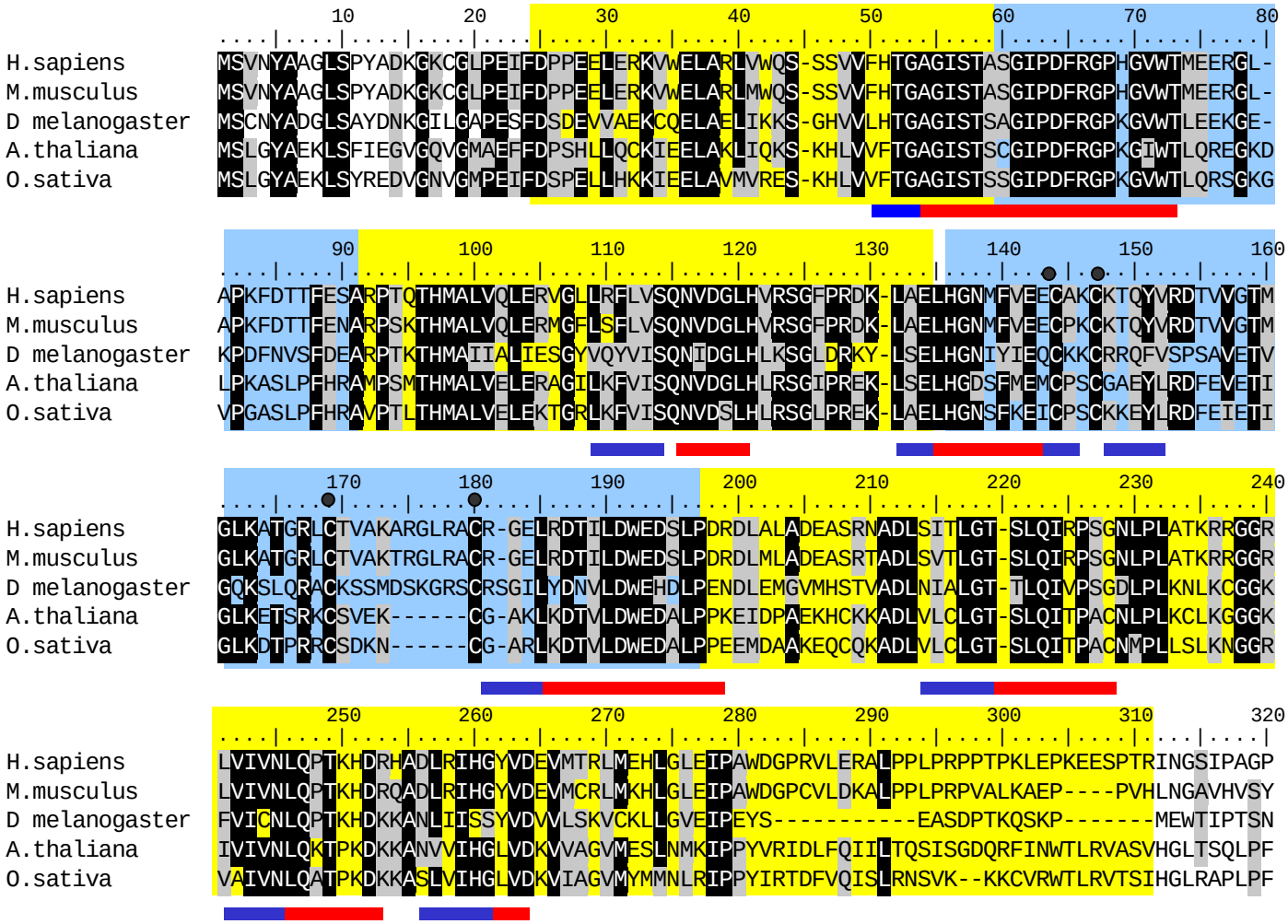

Figure 3.3 Alignment of known sirtuin proteins with putative *A. thaliana* sirtuin protein At5g55760. Sirtuin proteins from *H. sapiens* SIRT6 (NM_016539), *M. musculus* (NM181586), *D melanogaster* NM141733, *O. sativa* Os04g0271000. Sequence homology values for At5g55760 to *H. sapiens* SIRT6 shows 50% identity with 69% similarity, to *M. musculus* show 51% identity with 69% similarity, to *D. melanogaster* show 47% identity with 47% similarity and to *O. sativa* shows 75% identity with 59% similarity. Alignments performed in BioEdit with ClustalW. The sirtuin large domain is shaded in yellow, the small domain in light blue. B strands indicated by blue lines below sequence. Active sites indicated by red bands below sequence. Black dots above sequence indicate the tetrad of cysteine residues required for binding a zinc ion.

Figure 3.3 shows the putative *A. thaliana* gene At5g55760 has most homology to human SIRT6 gene with homology at 50% and similarity of 69% at the amino acid level. Identification of the two sirtuin domains is from comparisons with the crystal structures from

yeast, archean species and human sirtuin SIRT1. The regions of highest sequence homology correlate to the active sites of the protein as shown by the red band underneath the sequence. The 9 areas correlating to the β strands of the Rossman folds also show high similarity between the species.

The At5g55760 protein also contains the tetrad of conserved cysteine residues responsible for binding a zinc ion at residues 144, 147, 169 and 180. Also present is the sequence GAG (residues 53-55) important for the NAD^+ binding.

Human SIRT6 is localised to the nucleus and is involved in DNA stability and age related diseases (Mostoslavsky et al. 2006; Lombard et al. 2008).

3.3.1.2 Sequence homology and identification of At5g09230 in *A. thaliana*

A second putative *A. thaliana* sirtuin gene was identified by BLAST searches of the databases using the catalytic core sequences of sirtuin proteins identified from other organisms (see Figure 3.3). This second putative sirtuin gene shows most homology to human SIRT 4 gene with 42% identity and 62% similarity.

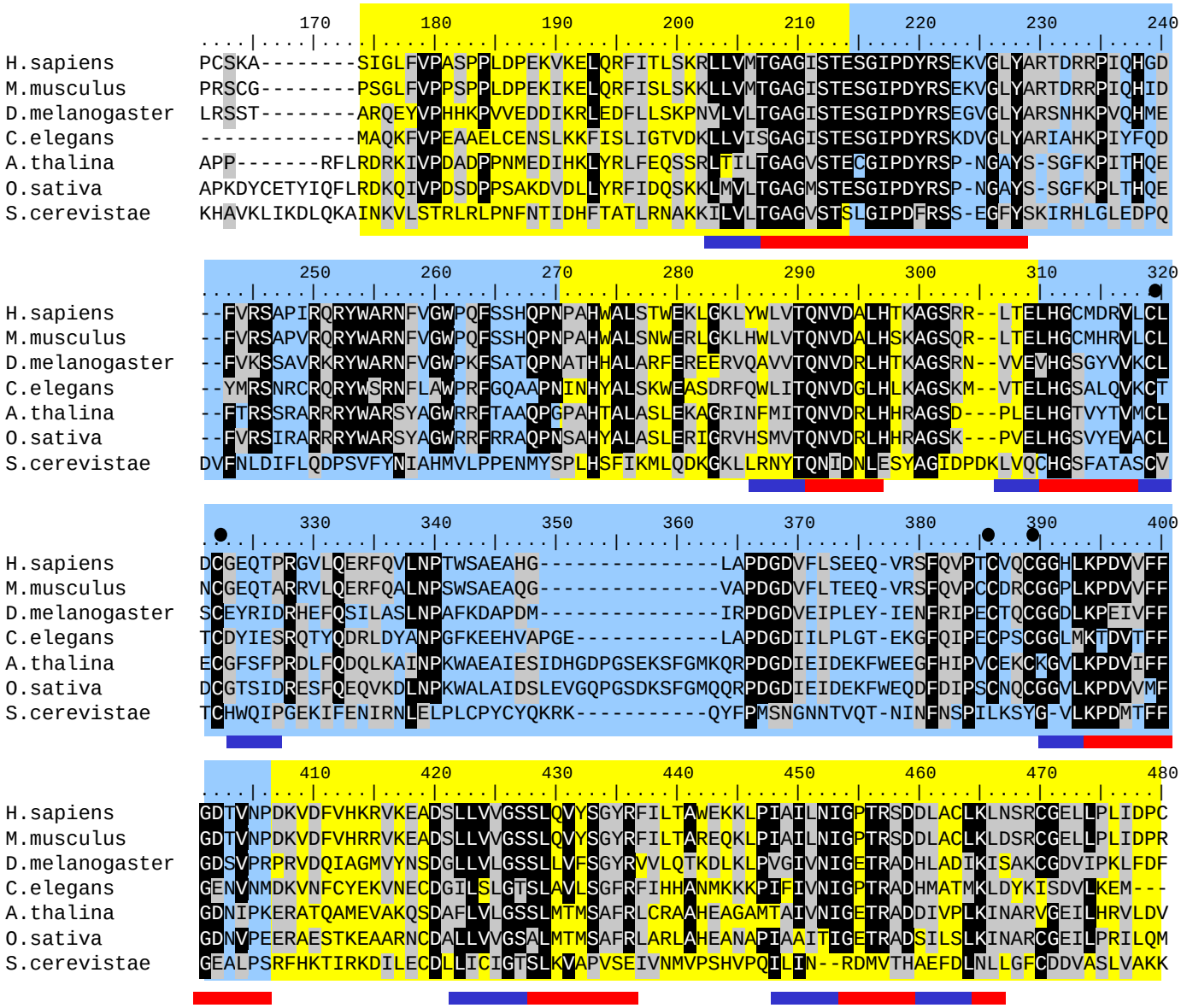

Figure 3.4 Alignment of known sirtuin proteins with putative *A. thaliana* sirtuin protein At5g09230. Sirtuin proteins from *H. sapiens* (NM012240) shows 42% identity and 62% similarity, *M. musculus* (XM 485674), *D. melanogaster* (NM132013), *C. elegans* (NM132013), *O. sativa* (NM001072842) and *S. cerevisiae* (YOL068C). Alignment was performed with ClustalW. The large domain is shaded in yellow, the small domain in light blue. B strands indicated by blue lines below sequence. Active sites indicated by red bands below sequence. Black dots above sequence indicate a tetrad of cysteine residues required for binding a zinc ion.

Figure 3.4 shows the protein for At5g09230 has similar domains to other sirtuin proteins. For example the same 9 β-sheet strands and the four cysteine residues capable of binding the zinc

ion (residues 319, 322, 386, 388). The areas for At5g09230 with the highest similarity between species correlate to the active sites of the protein. Also present is the GAG motif (residues 208-210) thought to bind the NAD^+.

Both putative *A. thaliana* sirtuin sequences show very similar small and large domain structure and zinc binding tetrad of cysteine residues.

In *A. thaliana* there is evidence from Expressed Sequence Tag (EST) data that this sirtuin has 7 different splice variants possibly indicating different localisations (listed in Table 3.6).

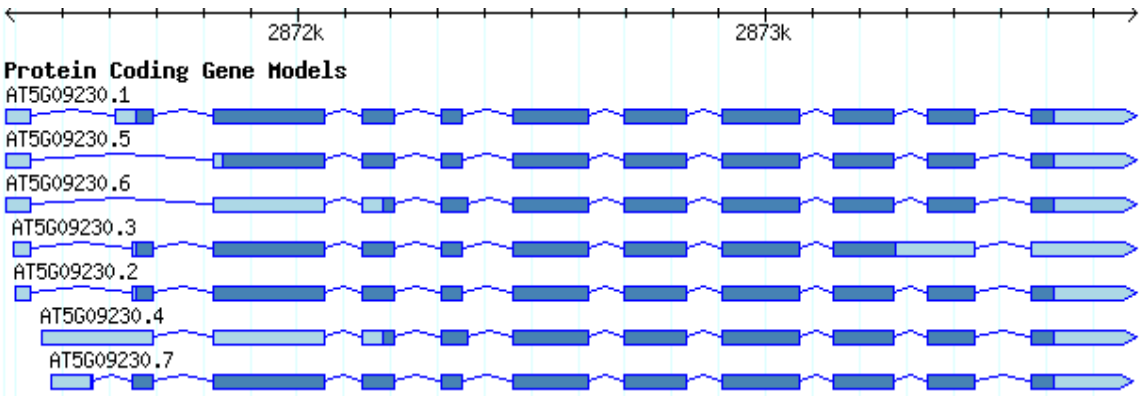

Fig 3.5 Splice variants of At5g09230. This figure was taken from the EST data on the Arabidopsis information resource website (www.tair.org).

The At5g09230 splice variants have been analysed for differences in nuclear localization signals, RNA/DNA binding motifs, vacuolar targeting motifs and perozisomal targeting signals (http://www.psort.org/; http://cello.life.nctu.edu.tw/; http://wolfpsort.org; http://www.psort.org; http://www.cbs.dtu.dk/services/TargetP; http://cello.life.nctu.edu.tw). The consensus amongst these was that different splice variants correlated to different subcellular localizations listed in Table 3.6.

Splice variant	Subcellular localisation
At5g09230.1	Mitochondrial
At5g09230.2	Mitochondrial
At5g09230.3	Chloroplastic
At5g09230.4	Perioxisomal
At5g09230.5	Chloroplastic
At5g09230.6	Perioxisomal
At5g09230.7	Chloroplastic

Table 3.6 Predicted localisations for 7 splice variants for At5g09230. Based on predictions of protein subcellular localisation by sequence analysis (http://wolfpsort.org).
However, it should be noted that these are only predictions based on protein sequence.

3.3.2 Sirtuin gene expression levels in *A. thaliana* Col0 exposed to a variety of different stresses.

One of the first experiments for characterising the two putative *A. thaliana* sirtuin genes was to confirm and investigate gene expression.

Published data from other organisms shows sirtuin gene involvement in a wide variety of metabolic, biotic, and chemical stress responses. Sirtuins have been linked to apoptosis, DNA repair and adaptations to stress conditions. In order to determine if these and other stress conditions induced a change in sirtuin gene expression, *A. thaliana* Col0 seeds were grown in a wide variety of 30 different conditions including abiotic, biotic and DNA damaging agents (see Methods and Materials 2.2.2). Samples were taken over a time course at 0, 2, 4, 8, 24 and 48 hours. RNA was then extracted and cDNA made to examine the change in transcript level

of sirtuin genes. Transcript level were analysed by measuring band intensity after gel electrophoresis. An average and standard error was measured from three biological replicates.

Stress	**At5g55760**					
Time point in hours	**0**	**2**	**4**	**8**	**24**	**48**
Salt	1.00	1.12	1.15	0.91	0.55	0.81
Mannitol	1.00	1.42	1.29	1.05	1.15	0.68
Hydrogen peroxide	1.00	0.98	0.71	0.90	0.50	0.80
Abscisic acid	1.00	0.96	0.81	0.68	0.71	0.70
Ethylene (ACC)	1.00	1.69	1.93	1.68	1.33	1.07
Auxin (NAA)	1.00	1.13	1.21	1.07	1.03	NA
Lipopolysaccharide	1.00	2.18	2.17	1.56	0.79	0.75
Jasmonic acid	1.00	0.67	0.64	0.52	0.44	0.39
Salicylic acid	1.00	1.11	1.00	1.35	0.88	0.61
Wounding	1.00	0.76	0.94	0.91	0.71	NA
Phosphatase inhibitor (OKA)	1.00	1.30	1.00	2.06	1.52	1.66
Kinase inhibitor (STA)	1.00	1.12	0.83	1.05	1.00	0.54
Cold treatment	1.00	1.11	1.39	1.12	1.43	1.11
Phosphate starvation	1.00	2.55	1.66	1.60	1.49	0.82
2,4 DNT (8hours)	1.00	0.85	0.34	0.63	NA	NA
MMS	1.00	1.54	8.79	6.15	4.42	6.16
Bleomycin	1.00	1.89	2.84	1.76	3.47	4.42
UV-B	1.00	1.83	1.27	0.77	1.07	0.54

Table 3.7 Fold differences in transcript levels of *A. thaliana* putative sirtuin At5g55760 using SQRT-PCR under a variety of treatments. Transcript levels were taken at time points 0, 2, 4, 8, 24 and 48 hours. cDNA taken and transcript levels analysed from three separate biological replicates. NA denotes value not available.

From Table 3.7 most of the stress conditions did not show any significant differences, staying around only 1 fold difference between stressed and unstressed. The most significant difference in sirtuin gene expression was with the DNA damaging agents. With MMS (methyl methane sulphonate) there is an increase in At5g55760 transcript levels from 1 to 8.8 within 4 hours, which remains high even at 48 hours at 6 times greater than before the addition of MMS. There is also an increase in gene expression with the addition of Bleomycin, increasing the levels of gene transcript by 3 fold within 4 hours. With 2 hours of resupply of phosphate following 24 hour starvation there was a 2.55 fold increase in At5g55760 gene expression, which later dropped to 1.66 by 4 hours and by 48 hours was 0.82.

Stress	At5g09230					
Time point in hours	**0**	**2**	**4**	**8**	**24**	**48**
Salt	1.00	1.00	0.97	1.02	1.35	1.19
Mannitol	1.00	1.82	1.48	1.67	1.90	1.10
Hydrogen peroxide	1.00	0.83	0.97	1.18	0.67	1.06
Abscisic acid	1.00	1.10	1.06	0.96	0.97	1.28
Ethylene (ACC)	1.00	1.23	1.31	1.24	1.09	1.14
Auxin (NAA)	1.00	1.22	0.97	1.12	1.24	NA
Lipopolysaccharide	1.00	3.61	3.00	2.85	2.15	1.64
Jasmonic acid	1.00	0.59	0.75	0.76	0.56	0.44
Salicylic acid	1.00	0.79	0.88	1.12	0.88	0.75
Wounding	1.00	0.90	0.95	0.15	0.88	0.88
Phosphatase inhibitor (OKA)	1.00	1.30	1.06	1.40	1.50	1.37
Kinase inhibitor (STA)	1.00	1.15	0.99	0.96	1.47	1.09
Cold treatment	1.00	0.90	0.98	0.88	1.08	0.87
Phosphate starvation	1.00	2.17	1.50	1.07	1.09	0.75
2,4 DNT (8hours)	1.00	1.09	0.89	1.12	NA	NA
MMS	1.00	1.68	11.11	6.46	4.50	6.58
Bleomycin	1.00	2.14	3.14	1.84	4.00	4.57
UV-B	1.00	2.71	3.54	1.60	3.53	1.04

Table 3.8 Fold differences in transcript levels of *A. thaliana* putative sirtuin At5g09230 using SQRT-PCR under a variety of treatments. Transcript levels were taken at time points 0, 2, 4, 8, 24 and 48 hours. cDNA taken and transcript levels analysed from three separate biological replicates. NA denotes value not available.

Most of the stress conditions tested did not produce any significant difference in transcript levels of At5g09230 gene, as seen in Table 3.8. The most significant of differences was seen

with MMS, which increases by 11 fold within 4 hours after the addition of the stress. This increase in transcript level was still apparent 48 hours later, remaining at 6.5 fold higher than at 0 hours. Bleomycin and UV-B also showed an increase of 3 fold after 4 hours and this increases by 24 hours to 4 and 3.5 respectively. Lipopolysaccharide also produced an increase of 3.61 fold in only 2 hours although this increase in gene expression decreases by 48 hours.

Both sirtuin genes At5g55760 and At5g09230 show increases in the same stress conditions, namely in response to the DNA damaging agents MMS and Bleomycin, which is similar to published data on the human and mouse sirtuin genes (Lombard et al. 2008).

In order to gain quantitative data for the differences in gene expression quantitative PCR (qPCR) was performed on the same cDNA samples.

3.3.3 Expression studies using quantitative PCR.

3.3.3.1 Expression of sirtuin genes with DNA damaging agent MMS.

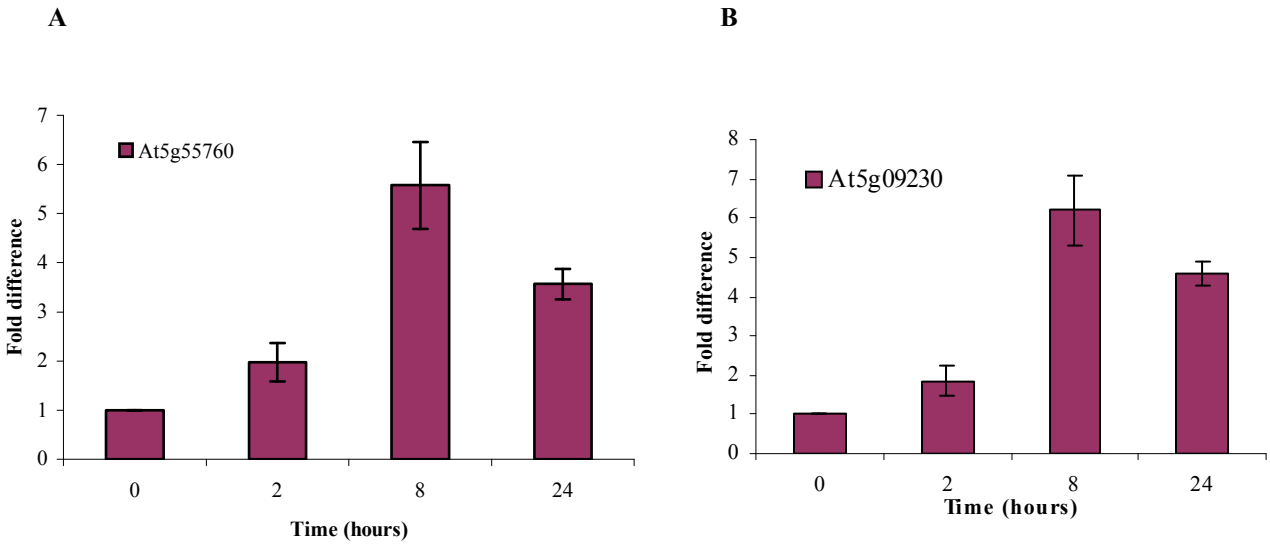

Figure 3.6 Quantitative PCR of transcript levels of putative sirtuin genes in *A. thaliana* Col0 plants exposed to DNA damaging chemical MMS. A. qPCR of At5g55760 gene expression with MMS. B - qPCR of At5g09230 gene expression with MMS. cDNA taken and transcript levels analysed from three separate biological replicates. Transcript level determined by normalization to Actin 2 transcript levels.

The RT-PCR results are consistant with the qPCR data seen in Figure 3.6, which shows an increase in gene expression for both sirtuin genes with the application of MMS. The increase in gene expression for both genes follows a very similar pattern, increasing by 2 fold within 2 hours. The largest increase is seen at 8 hours, about 6 fold for both sequences. Both sequences show a continued increase in transcript levels at 24 hours with At5g55760 at 3.5 and At5g09230 at 4.5 fold.

3.3.3.2 Expression of sirtuin genes with DNA damaging agent Bleomycin.

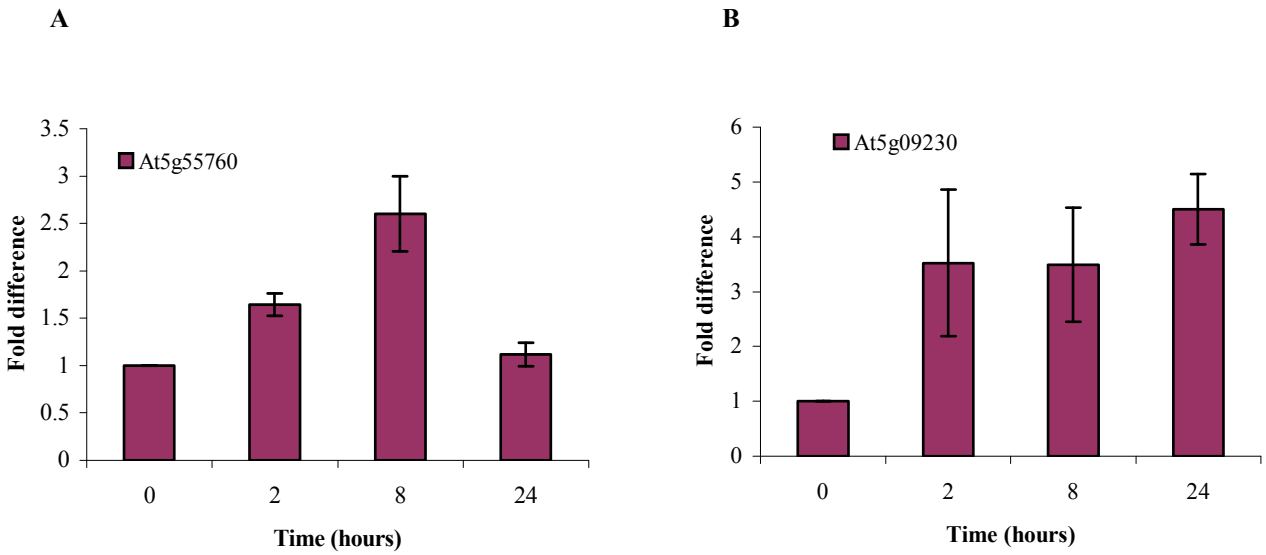

Figure 3.7 Quantitative PCR of putative sirtuin transcript abundance in *A. thaliana* Col0 plants exposed to DNA damaging chemical Bleomycin. A. qPCR of At5g55760 gene expression with Bleomycin. B. qPCR of At5g09230 gene expression with Bleomycin. cDNA taken and transcript levels analysed from three separate biological replicates. Transcript level determined by normalization to Actin 2 transcript levels.

The RT-PCR data show an increase in transcript levels for both genes with the application of Bleomycin, which is reinforced by the qPCR data seen in the figure above. The gene expression patterns for both sirtuin genes are different. At5g55760 shows an increase within 2 hours to 1.5 fold and to 2.5 fold by 8 hours. The level of transcript abundance by 24 hours is returned to the same level as before application of Bleomycin. The gene expression for

At5g09230 shows the largest increase within 2 hours to 3.5 fold, and transcript levels remain high even at 24 hours when levels showed a 4.5 fold increase.

3.3.3.3 Expression of sirtuin genes with UV-B.

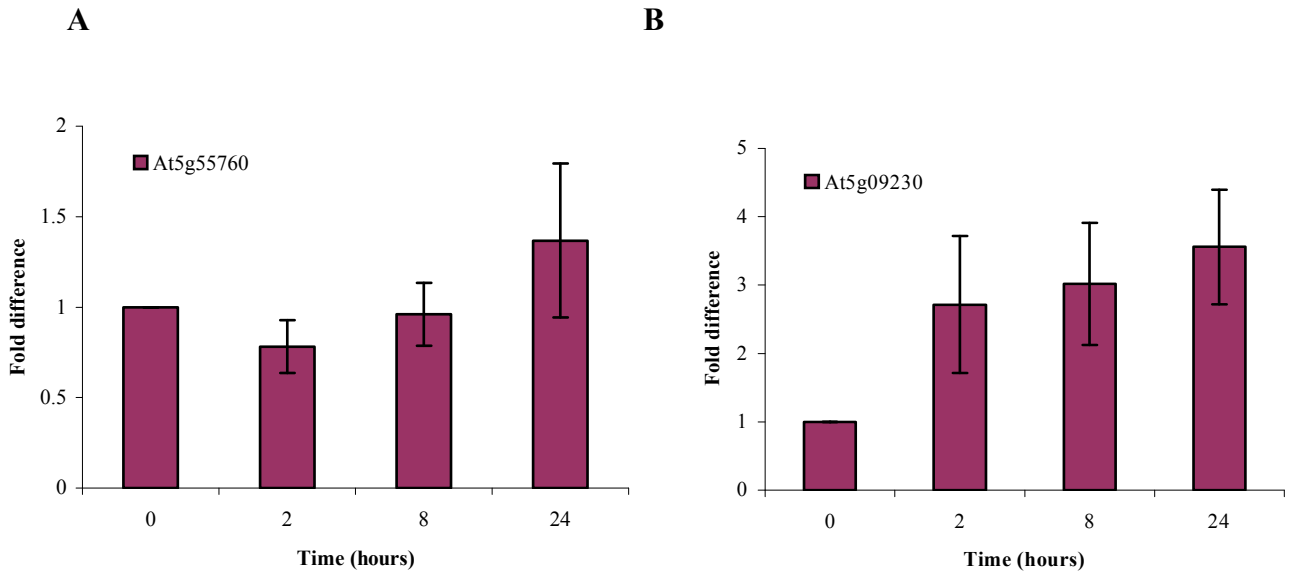

Figure 3.8 Quantitative PCR of transcript abundance of putative sirtuin genes in *A. thaliana* Col0 plants exposed to UV-B. A - qPCR of At5g55760 gene expression with UV-B B - qPCR of At5g09230 gene expression with UV-B exposure. cDNA taken and transcript levels analyzed from three separate biological replicates. Transcript level determined by normalization to Actin 2 transcript levels.

The RT-PCR results show no difference for the abundance of transcript for putative sirtuin gene At5g55760 with UV-B and this is further reinforced by the qPCR results above. The RT-PCR results for At5g09230 show an increase in At5g09230 to 3.5 fold at 4 hours. This data is further reinforced by the qPCR results for At5g09230, which show a 2.5 fold difference in transcript level within 2 hours. This increase in gene expression increases further to 3.5 fold at 24 hours.

3.3.4 Localisation of sirtuin genes in onion epidermal cells.

Sirtuin proteins show differences in subcellular localisation. Of the seven human sirtuins three are targeted to the nucleus (SIRT1, 6 and 7), three sirtuins are localised to the mitochondria (SIRT3, 4 and 5; Michishita et al. 2005) and SIRT2 is cytoplasmic (North et al. 2003). SIRT 6 (the sirtuin with highest homology to At5g55760) has been shown to be targeted to the nucleus in mice (Liszt et al. 2005). Human SIRT4 (most similar to At5g09230) has been shown to be a matrix protein which becomes cleaved at amino acid 28 following transportation into the mitochondria (Ahuja et al. 2007).

In order to identify the cellular localisation of the expressed sirtuin protein, constructs were made with both At5g55760 and At5g09230 cDNA fused to a N-terminal green fluorescent protein (GFP). These constructs were then transiently expressed in onion epidermal cells. The positive control used was the empty vector without a sirtuin gene cloned into it, and the GFP product therefore, should be expressed throughout the onion cell.

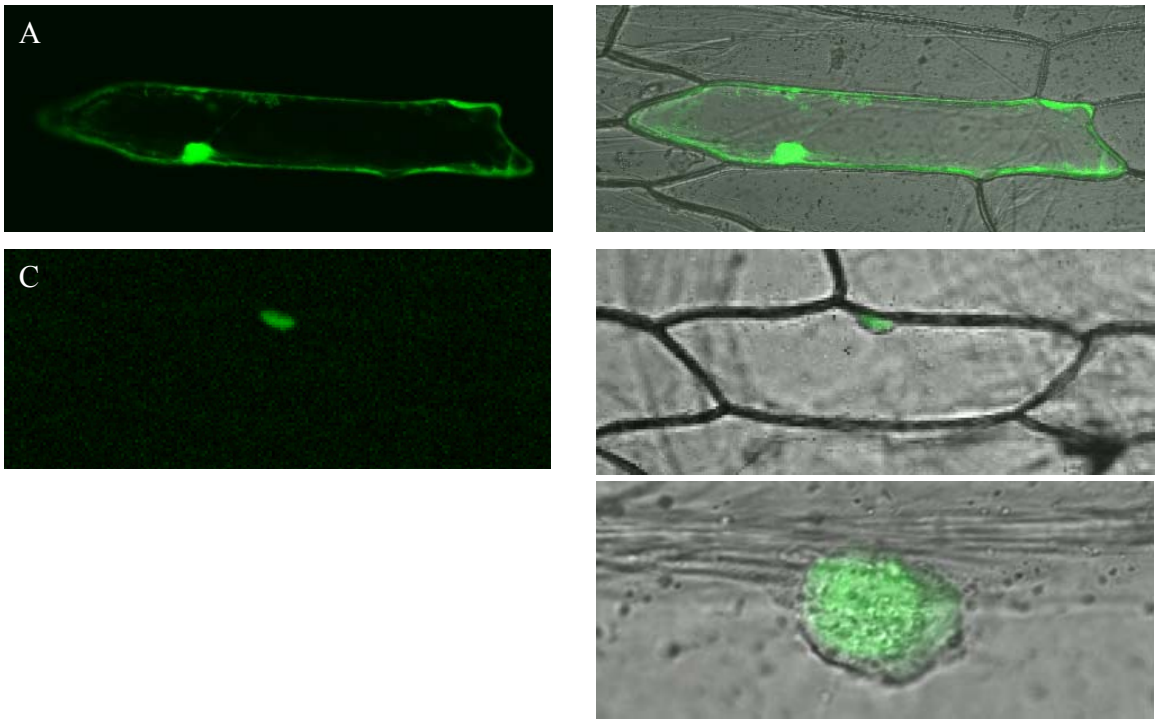

Figure 3.9. Transient expression of the GFP:At5g55760 fusion protein in onion epidermal cells. A and B show the empty vector pGWB6 without At5g55760 expressed throughout the cell. C and D show the sirtuin gene At5g55760 with a N-terminal GFP construct expressed in the nucleus of the cell. E, the nucleus of the cell at increased magnification. This experiment was performed in collaboration with Dr Manuel Paneque.

Figure 3.9 shows cells transfected with a GFP:At5g55760-expressing plasmid exhibited only nuclear fluorescence.

Transient expression of At5g09230 fused to N-terminal GFP tag in onion epidermal cells showed no expression. Further constructs with the At5g09230 fused to N and C-terminal GFP tags were made and transient expression was repeated in both tobacco leaves and onion epidermal cells. However, no expression of the gene was seen.

3.3.5 Protein expression of sirtuin genes in *E. coli*

In order to examine these two putative *A. thaliana* sirtuin genes it was necessary to investigate the protein activity and determine either NAD^+ dependent deacetylation or ADP ribosylation activity. For this the protein from both genes would have to be purified and the activity confirmed. For full details of these methods see Methods and Materials chapter 2.3.1-2.3.6.

The pDEST 17 vector contains a T7 promoter and a T7 RNA polymerase gene, which is fused to the 5' end of the inserted gene. The plasmid also contains a lac repressor gene and a lacZ gene, which controls the expression of the T7 promoter. Under normal conditions the product of the lac repressor gene binds to the lacZ gene preventing transcription of the T7 promotor and the T7 RNA polymerase gene. Protein induction is achieved by IPTG which binds to and inactivates the lac repressor protein. This causes the cell to make T7 RNA polymerase and causes the protein encoded in the plasmid to be expressed. A histidine tag was also fused immediately to the 5' end and in frame with the inserted gene. Protein induction and expression was performed in *E. coli* BL21 cells (Methods and Material 2.3.1). Total protein was extracted from lysed *E. coli* cells and bound to nickel resin. The Histidine tag binds to nickel ions bound to the resin and therefore it is possible to extract the plant sirtuin protein. Extracts were then run on SDS-PAGE and bands analysed after staining.

3.3.5.1 Purification of putative sirtuin At5g55760 protein

When expressing recombinant protein in *E. coli* the resultant protein can be formed either as soluble or insoluble protein. Expression of prokaryotic proteins in eukaryotic cells, high concentration of protein expression and recombinant protein toxicity within the cytoplasm can result in the formation of insoluble inclusion bodies, which are difficult to purify. Therefore optimisation of *E. coli* growing conditions is important to establish a balance between soluble protein and enough protein to purify. Optimisation of protein expression was performed at different temperatures and concentrations of IPTG (seen in Figure 3.10). At5g55760 protein size was predicted to be 55kDa indicated by position of arrow.

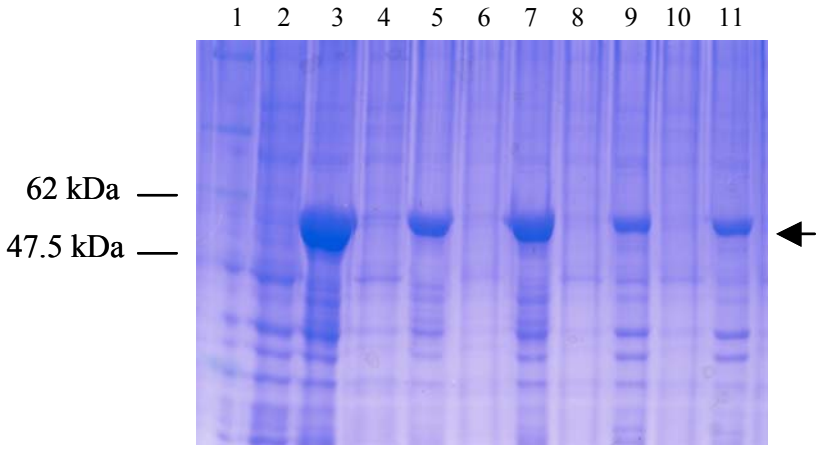

Fig 3.10 Optimisation of At5g55760 protein expression in *E. coli*. Lanes 1- marker. Lane 2 - uninduced total protein and lane 3- total protein induced with 5mM IPTG and grown for 4 hours at 37°C. Lanes 4- uninduced total protein and lane 5- total protein induced with 1mM IPTG and grown for 4 hours at 37°C. Lanes 6- uninduced total protein and lane 7- total protein induced with 0.1mM IPTG and grown for 4 hours at 37°C. Lanes 8- uninduced total protein and lane 9- total protein induced with 5mM IPTG and grown for 4 hours at 20°C. Lanes 10- uninduced total protein and lane 11- induced protein with 1mM IPTG and grown for 4 hours at 20°C. Arrow indicates predicted correct size of expressed protein At5g55760.

For At5g55760 the conditions resulting in the highest yield of protein are seen with 5mM IPTG and grown at 37°C. It was under these conditions that *E. coli* expressing At5g55760 were grown for protein purification with nickel resin (shown in Figure 3.11).

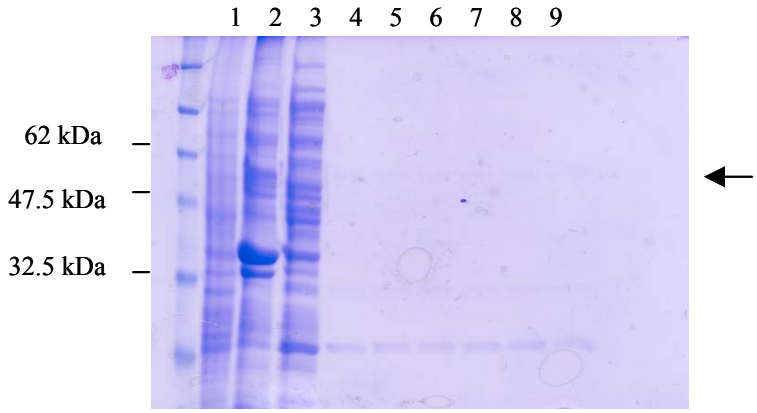

Figure 3.11. SDS-PAGE of purification of sirtuin At5g55760 native protein from *E. coli*. Lane 1- total induced insoluble protein, 2- total induced soluble protein, 3- protein removed after binding with nickel resin, lanes 4-10, eluted protein from nickel column, from 1ml sequential fractions. Arrow indicates predicted size of expressed protein At5g55760.

Despite earlier protein optimisation very little protein was recovered at the correct size of 55kDa. However, the larger band seen in the induced soluble fraction at a smaller size could correspond to degradation product of the induced protein.

To increase the amounts of protein available for purification and to decrease degradation of protein the insoluble protein fraction was denatured with urea and then bound to the nickel resin. This resin was washed and the protein refolded whilst still bound to nickel resin.

Unfortunately very little protein was purified from denatured insoluble protein and contained many more contaminants. This work is being continued to try and optimise the protein purification for enzyme assays to confirm the function of these genes.

3.3.5.2 Purification of sirtuin gene At5g09230.

Protein expression of At5g09230 was also carried out using a plasmid with an N-terminal histidine tag in *E. coli*. Optimisation was first performed in the same way as for At5g55760 by altering the temperature and the concentration of IPTG and shown in Figure 3.12. At5g09230 protein size was predicted to be 42kDa indicated by position of arrow.

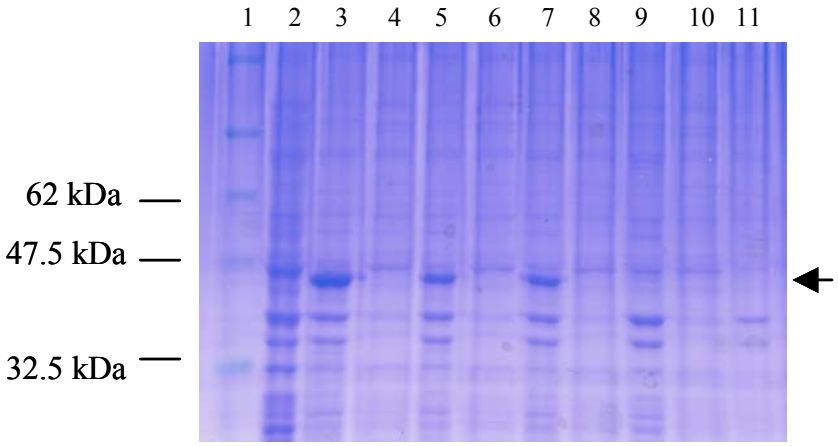

Figure 3.12. Optimisation of At5g09230 protein production in *E. coli*. Lane 1-Marker. Lane 2- uninduced total protein and lane 3- induced protein induced with 5mM IPTG and grown for 4 hours at 37°C. Lane 4- uninduced total protein and lane 5- induced protein induced with 1mM IPTG and grown for 4 hours at 37°C. Lane 6- uninduced total protein and lane 7- induced protein induced with 0.1mM IPTG and grown for 4 hours at 37°C. Lanes 8- uninduced total protein and lane 9- induced protein induced with 5mM IPTG and grown for 4 hours at 20°C. Lanes 10- uninduced total protein and lane 11- induced protein induced with 1mM IPTG and grown for 4 hours at 20°C. Arrow indicates predicted correct size of expressed protein At5g09230.

Expression of At5g09230 in *E. coli* showed the largest induction with 5mM IPTG and grown at 37°C and these conditions were used for purification of protein with nickel resin (shown in Figure 3.13)

.

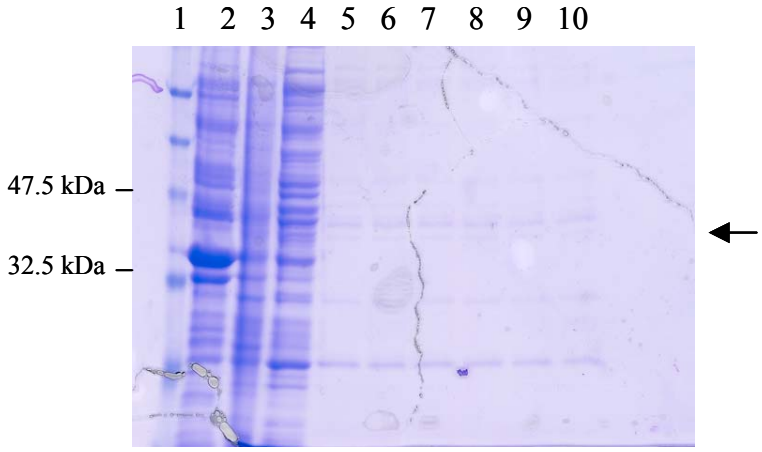

Figure 3.13 SDS-PAGE of native purification of sirtuin At5g09230 native protein expressed in E. *coli*. Lane 1– Marker Lane 2- uniduced total protein, 3– induced insoluble protein, 4- total induced soluble protein, lanes 5-10 protein eluted from nickel resin in 1ml fractions. Arrow indicates predicted correct size of expressed protein At5g09230.

Previous optimisation of At5g09230 (Fig 3.12) did not produce very large amounts of protein and this was also seen for the native protein purification (Figure 3.13). The small amount of protein induced was seen in the insoluble fraction of the total protein. In order to purify insoluble protein the total protein was denatured with urea before being bound to the nickel resin. The bound protein was then refolded on the nickel resin before elution.

Unfortunately despite altering the time, temperature and the concentration of including IPTG, there was only very slight induction of protein. Even after purification there was no protein in the eluted fractions of the correct size. This gene was also expressed in a different strain of *E. coli Rosetta gami*, which were less likely to produce inclusion bodies however protein expression was too low to purify.

Different constructs were made without the Histidine tag, which may have been having an adverse effect on protein expression in *E. coli.* Constructs were made with At5g09230 fused to both C and N-terminal glutathione S-transferase tag, which has been shown to increase

stability of soluble proteins. Despite this, the protein has never been expressed at acceptable levels in *E. coli.*

3.3.6 Generation of transgenic plant lines expressing putative sirtuin genes.

Both putative *A. thaliana* sirtuin genes were cloned into the Invitrogen entry vector as part of the Gateway system (see 3.2.4). From the entry vector both genes were then transferred to destination vectors containing 5' in frame Myc or HA tags under the control of a CaMV 35S promotor, shown in Figure 3.14.

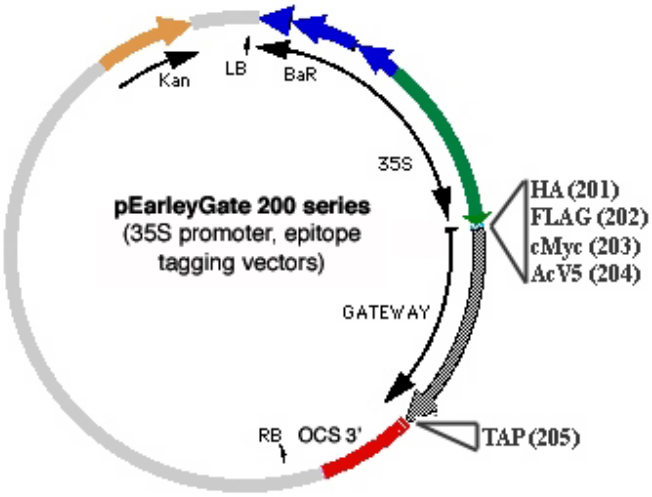

Figure 3.14 Vector map for vector used for transformation into *A. thaliana.* Putative sirtuin gene At5g55760 was fused to 5' HA tag (pEarleyGate vector 201), At5g09230 fused to 5' Myc tag (pEarleyGate vector 203). Vectors developed and obtained from Pikaard Laboratory (Earley KW et al. 2006).

3.3.6.1 Segregation analysis of transgenic lines.

These constructs containing the tagged sirtuin genes were introduced to *A. thaliana* Col0 by *Agrobacterium tumefaciens* infection and the floral dip method (Methods and Material 2.2.14). The vectors used contain the dominant resistance gene for Basta, which is used for selection of successful transformants. It is possible to genotype the T2 generation seeds collected from Basta resistant plants by segregation analysis on media containing Basta. The steps for transformation and segregation of transformants is summarised in Figure 3.15.

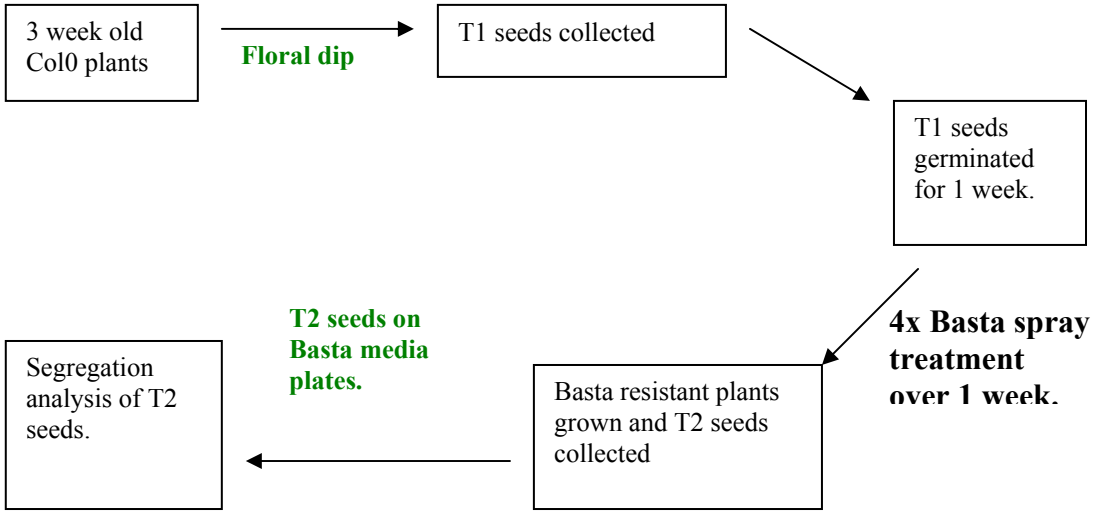

Figure 3.15 Flow diagram showing steps for floral dip of *A. thaliana* Col0 with *Agrobacteria tumerfaciens*.

According to Mendelian genetics the offspring of heterozygous parents will show 1:2:1 segregation as shown in Table 3.9.

	B	**b**
B	BB	Bb
b	Bb	bb

Table 3.9. Mendelian segregation in offspring from heterozygous parent lines. Shows parent genes in bold at the top and the left and the four combinations in the offspring as BB, Bb and bb at a ratio of 1:2:1. The Basta resistance gene is dominant (B) and survival of seedlings on Basta media will be seen in BB and Bb offspring at approximately 75% survival.

Seeds from a heterozygous parent should show segregation of a 1:2:1 ratio according to Mendelian principles, however as heterozygous and homozygous will both survive on Basta

the percentage of surviving seeds will be approximately 75%. Seeds from homozygous parents should be approximately 100%.

T2 seeds were collected from plants which survived the initial Basta screen and were placed on Basta media plates and germination of seeds counted (photograph of plates shown in Figure 3.16). Percentage germination of T2 seeds listed in Table 3.10.

Plant line of parent	**+ / – Basta**	**Percentage of T2 offspring seedlings survived**	**Genotype of T1 parent**
Col0	+ Basta	1.2%	
Col0	- Basta	92%	
55760 H	+ Basta	94%	Homozygous
55760 C	+ Basta	79%	Heterozygous
09230 B	+ Basta	94%	Homozygous?
09230 C	+ Basta	100%	Homozygous

Table 3.10 Segregation analysis of Col0 T2 generation after floral dip transformation with 35S:sirtuin gene. Surviving seedlings counted and recorded as a percentage of total seedlings on the plate. Results shown for Col0 grown on media with and without Basta. Seeds from two lines surviving initial Basta screen for each construct, 35S:Myc:At5g55760 and 35S:HA:At5g09230 shown. Total seeds on each plate between 80-100.

Col0 seeds grown on media without Basta show germination of 92% and with Basta show germination rate of only 1.2%. This confirms that Basta selection was effective.

In Table 3.10 germination of offspring seeds from T1 35S:Myc:At5g55760 H parent line was 94% on Basta media suggesting that line was homozygous for Basta resistance gene. This was also seen for 35S:HA:At5g09230 C line.

T2 offspring from 35S:Myc:At5g55760C showed seedling survival rate at 79% on Basta media suggesting that the T1 parent line was heterozygous.

There was a query over the genotype of 35S:HA:At5g09230 B because the total number of seeds on the plate was only 31 compared to 80-100 for the other lines.

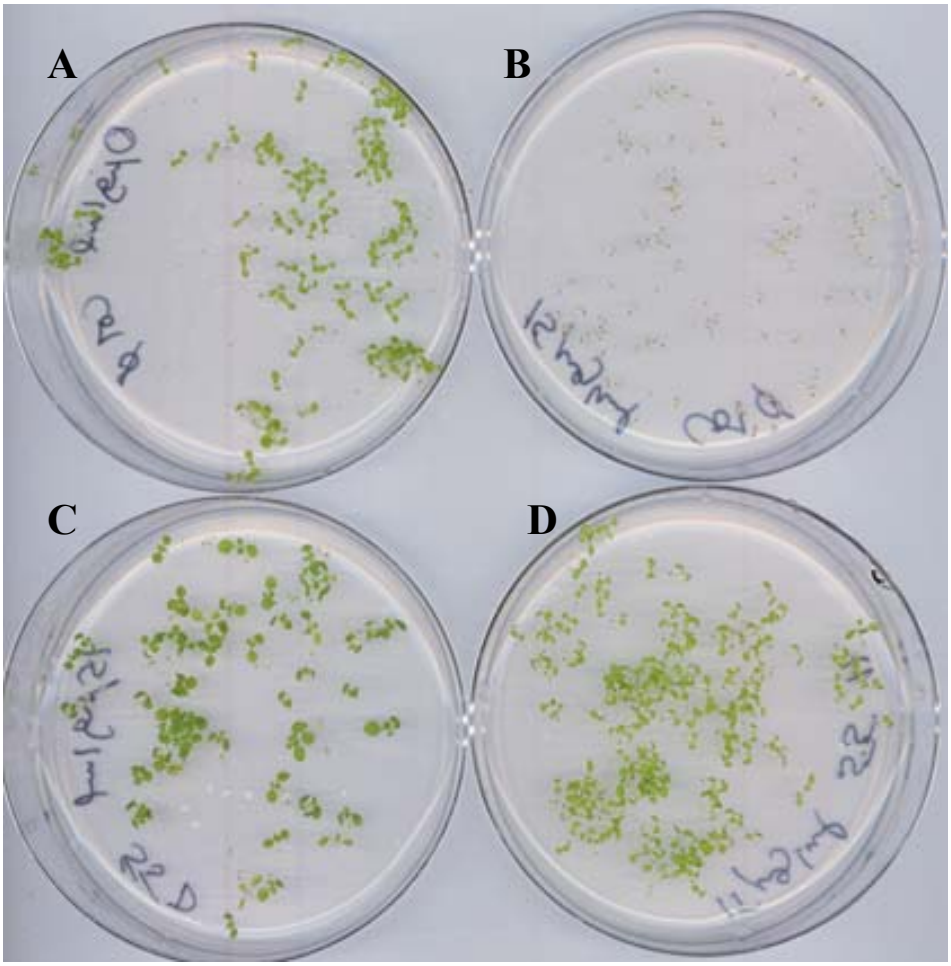

Figure 3.16 Segregation analysis of *A. thaliana* transformants after floral dip with 35S:Myc:At5g55760 construct on Basta media. Plate A- Col0 growing on normal media. Plate B- Col0 seeds growing on plates containing 15µg/ml Basta. Plate C- T2 seeds showing homozygous segregation on 15µg/ml Basta. Plate D- T2 seeds collected after floral dip with plasmid 35S:Myc:At5g55760 and showing heterozygous segregation on 15µg/ml Basta.

3.3.6.2 Identification of 35S:Myc:At5g55760 lines

Primers were designed to putative sirtuin genes over exons that differentiate between cDNA and genomic DNA by band size. Genomic DNA was extracted from T1 plants with Basta resistance and used as template for PCR amplification.

A

B

	PCR band size
cDNA	**352 bp**
gDNA	**497 bp**

C

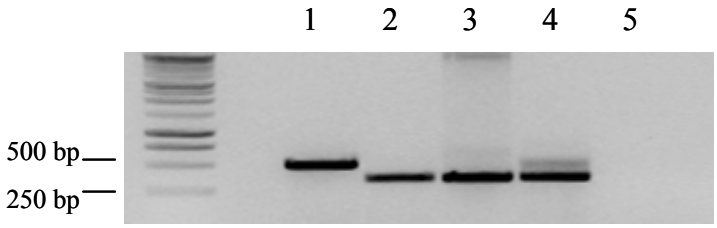

Figure 3.17 Gel electrophoresis of PCR products from genomic DNA template extracted from Basta resistant plants after floral dip with 35S:HA:At5g55760 construct. A - arrows show position of primers on At5g55760 genomic DNA within coding regions. **B** shows band sizes expected with cDNA and genomic DNA. **C** shows gel electrophoresis on genomic DNA extracted from Basta resistant plant for 35S:HA:At5g55760 with homozygous segregation. Lane 1- Col0 gDNA. Lane 2- Col0 cDNA. Lane3- original plasmid used in Agrobacterium for floral dip. Lane 4- gDNA extracted from Basta resistant plant H. Lane 5- no DNA control

Although the difference in band size for gDNA and cDNA controls for At5g55760 gene was not large, it was enough to detect cDNA from genomic DNA template extracted from T1 plant 35S:Myc:At5g55760 H. Presence of a gene product the same size as cDNA for 35S:Myc:At5g55760H suggests successful transformation with the 35S:Myc:At5g55760 construct.

For 35S:Myc:At5g55760C no gene product consistent with cDNA size was detected suggesting that for this line transformation was not successful.

3.3.6.3 Identification of 35S:HA:At5g09230 lines

Genomic DNA was also extracted and PCR repeated for T2 plant lines with 35S:Myc:09230 B and C, which showed homozygous segregation on Basta media plates.

A

B

	PCR band size
cDNA	**185 bp**
gDNA	**250 bp**

C

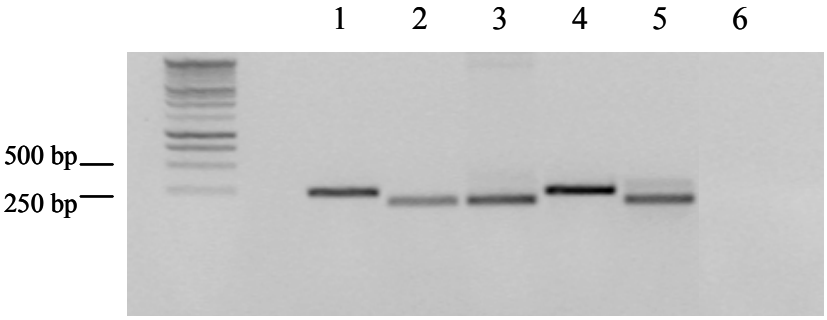

Figure 3.18 Gel electrophoresis of PCR products from genomic DNA template extracted from Basta resistant plants after floral dip with 35S:HA:At5g09230 construct. A- arrows show position of primers on At5g09230 genomic DNA within coding regions. B shows band sizes expected with cDNA and genomic DNA. C shows gel electrophoresis on genomic DNA extracted from Basta resistant plant for 35S:Myc 09230 with homozygous segregation. Lane 1- Col0 gDNA with 09230 primers, lane 2- Col0 cDNA with 09230 primers. Lane3- original plasmid used in *Agrobacterium* for floral dip. Lane 4- gDNA extracted from Basta resistant plant B. Lane 5- gDNA extracted from Basta resistant plant C. Lane 6- No DNA

In Figure 3.18 the genomic DNA extracted from plant line 35S:HA:At5g09230 B showed a band corresponding to gDNA, suggesting it was heterozygous. This backed up segregation analysis because although it showed 92% seedling survival the total number of seeds was very low. However, the gDNA extracted from 35S:HA:At5g09230 C showed a band size corresponding to that of cDNA suggesting that the parent was a successful transformant.

RNA was extracted from the lines 35S:Myc:55760H and 35S:HA:At5g09230 C and cDNA was made. Transcript levels for both sirtuins was compared to constitutively expressed Actin to see if sirtuin expression was higher in the transgenic lines.

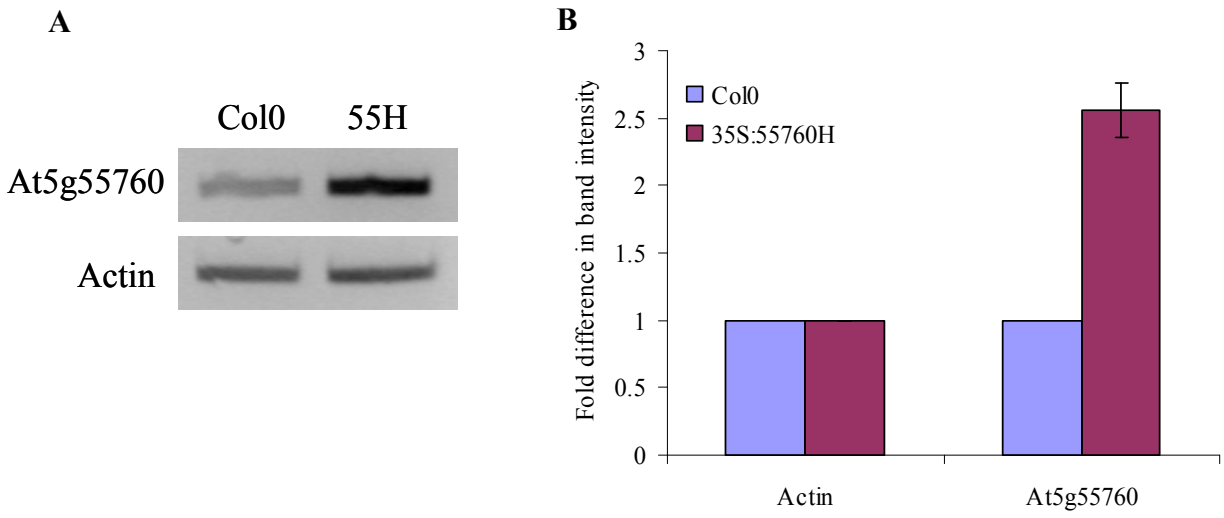

Figure 3.19 RT-PCR for 35S:Myc:At5g55760 H with primers for At5g55760 and actin gene. Comparative PCR between levels of transcript in 35S:Myc:At5g55760 line H and wild type. Actin was used as a control for template DNA. A - shows gel electrophoresis of transcript amplified from 35S:Myc:At5g55760 H (55H) and Col0 with both Actin primers and primers for At5g55760. B shows a graph of the relative band intensities of the gel electrophoresis for gene expression of Actin and At5g55760 in Col0 and 35S:Myc:At5g55760 H.

Gel electrophoresis in Figure 3.19 shows a darker band for At5g55760 transcript for 35S:Myc:At5g55760 H compared to Col0, indicating higher gene expression. An internal control of constitutively expressed Actin shows the same band intensity for both *A. thaliana* and 35S:Myc:At5g55760 H. A comparison of gel electrophoresis band intensity in Scion Image showed amplification of transcript for At5g55760 was 2.8 fold higher in 35S:Myc:At5g55760 H plants.

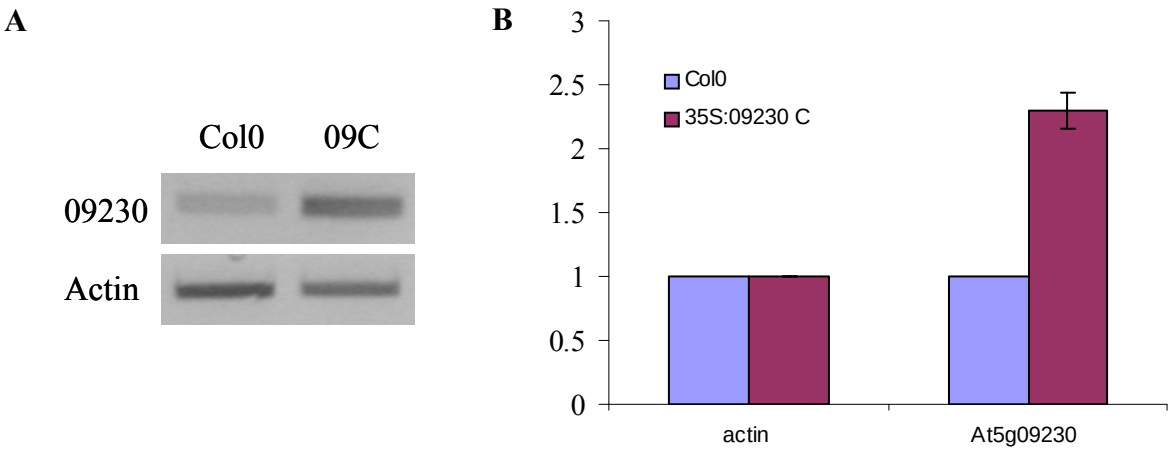

Figure 3.20 RT-PCR for 35S:HA:At5g09230 C line with primers for At5g09230 and actin gene. Comparative PCR between At5g09230 transcript levels in 35S:HA:At5g09230 C and wild type. Actin was used as a control for template DNA. A shows gel electrophoresis of transcript amplified from 35S:HA:At5g09230C (09C) and Col0 with both Actin primers and primers for At5g09230. B shows a graph of the relative band intensities from gel electrophoresis for gene expression of Actin and At5g09230 in Col0 and 35S:HA:At5g09230 C. Quantification was performed using Scion Image.

Gel electrophoresis of At5g09230 transcript amplified from Col0 and 35S:HA:At5g09230 C plants showed higher abundance for 35S:HA:At5g09230 C plants compared with wild type. Internal control of constitutively expressed actin bands showed very similar levels of expression. Measurement of DNA band intensities showed that the At5g09230 transcript was 2.3 fold higher in 35S:HA:At5g09230C plants compared with *A. thaliana* Col0.

3.3.7 Identification of *A. thaliana* plants with T-DNA insertion within sirtuin genes.

Stock centres contain many lines of *A. thaliana* seeds containing transfer DNA (T-DNA) within individual genes. The introduction of a 12 kb region of T-DNA into the coding region of a gene inactivates that gene as transcription is prevented. *A. thaliana* seeds with a 12kb T-

DNA insertion within each sirtuin gene were obtained from the following sources listed in Table 3.11.

Gene name and number	Insertion line	Stock centre
At5g55760	SALK 001493	SALK
At5g09230	GK 349 B06	GabiKat

Table 3.11 *A. thaliana* T-DNA insertion seeds for sirtuin genes and company developed.

The seeds obtained were a mixed population of T2 generation and were confirmed by PCR to have the correct gene knocked out. The method for genotyping the presence of a T-DNA insertion within the correct gene relied on the T-DNA insertion being of known sequence. Primers were designed to amplify outwards from this T-DNA section (see fig 3.21 for a schematic diagram). Amplification of the DNA between the T-DNA insertion into the sirtuin gene was then sequenced by MWG to confirm the exact position of the insertion within the gene. In order to determine if the plant was heterozygous, primers were designed to the sirtuin gene over the point of insertion to confirm the presence of a wild type sirtuin gene.

A. thaliana seeds were grown on soil and homozygous lines were identified by PCR amplification using genomic DNA as template and gene-specific and vector/gene specific primers. In addition, RNA was extracted from plants and cDNA synthesized, and the absence of a PCR amplification product confirmed no transcript was present (described in Methods and Materials chapter 2.2.19)

3.3.7.1 Identification of T-DNA insertion lines for At5g55760

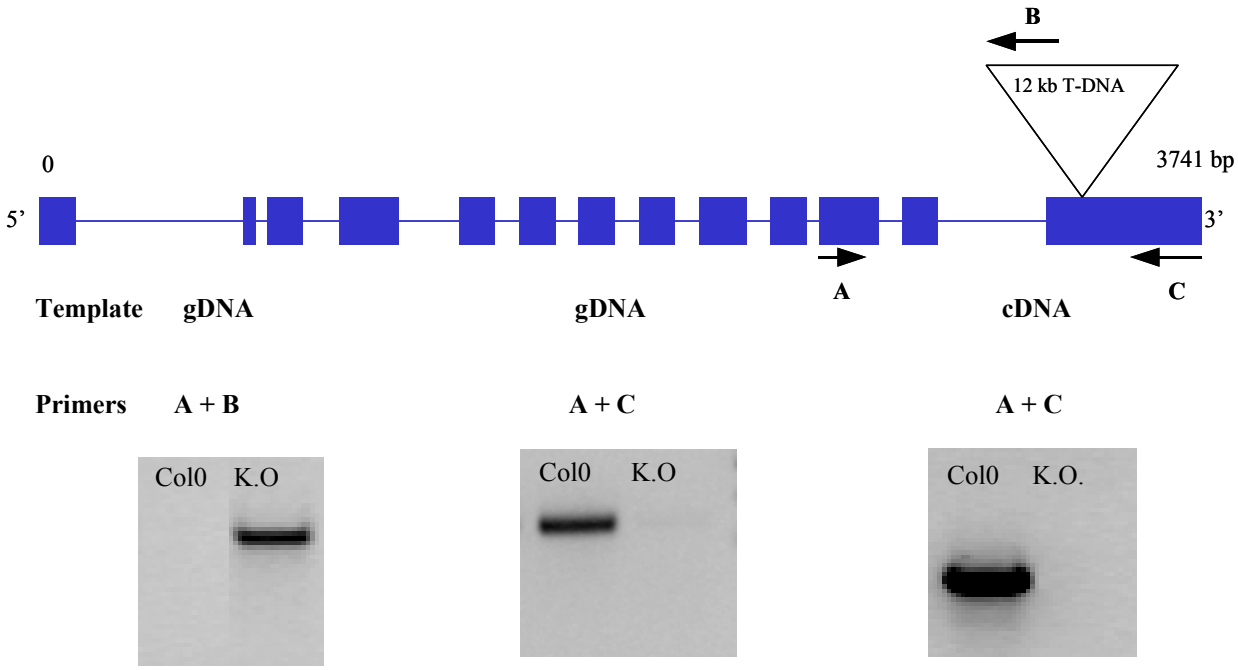

Figure 3.21 Genotyping of A. thaliana At5g55760 null lines. Schematic diagram of 12 kb T-DNA insertion within gene of interest and primer combinations for identifying lines containing insertion. Gel electrophoresis of PCR on genomic DNA and cDNA extracted from *A. thaliana* Col0 and SALK 001493 lines (K.O.) with primers amplifying from T-DNA insertion to At5g55760 gene.

Figure 3.21 shows the position of T-DNA insertion within putative sirtuin gene At5g55760 and the position of primers used for genotyping. Gel electrophoresis showed a band for the presence of T-DNA in the SALK K.O. line, which was absent in Col0. Likewise, primers for wild type gene over the T-DNA insertion point only showed a product for Col0, suggesting that At5g55760 null line was homozygous for the T-DNA insertion.

The absence of sirtuin gene transcript from RNA further confirms that the At5g55760 gene is inactivated.

3.3.7.2 Identification of T-DNA insertion lines for At5g09230

Genotyping of GK 349B06 seeds containing T-DNA insertion within At5g09230 gene was first performed using genomic DNA as template. PCR amplification between the inserted T-DNA and the At5g09230 sequence confirmed the presence of the T-DNA insert. RNA extracted and checked for At5g09230 confirmed the inactivation of the gene by absence of transcript.

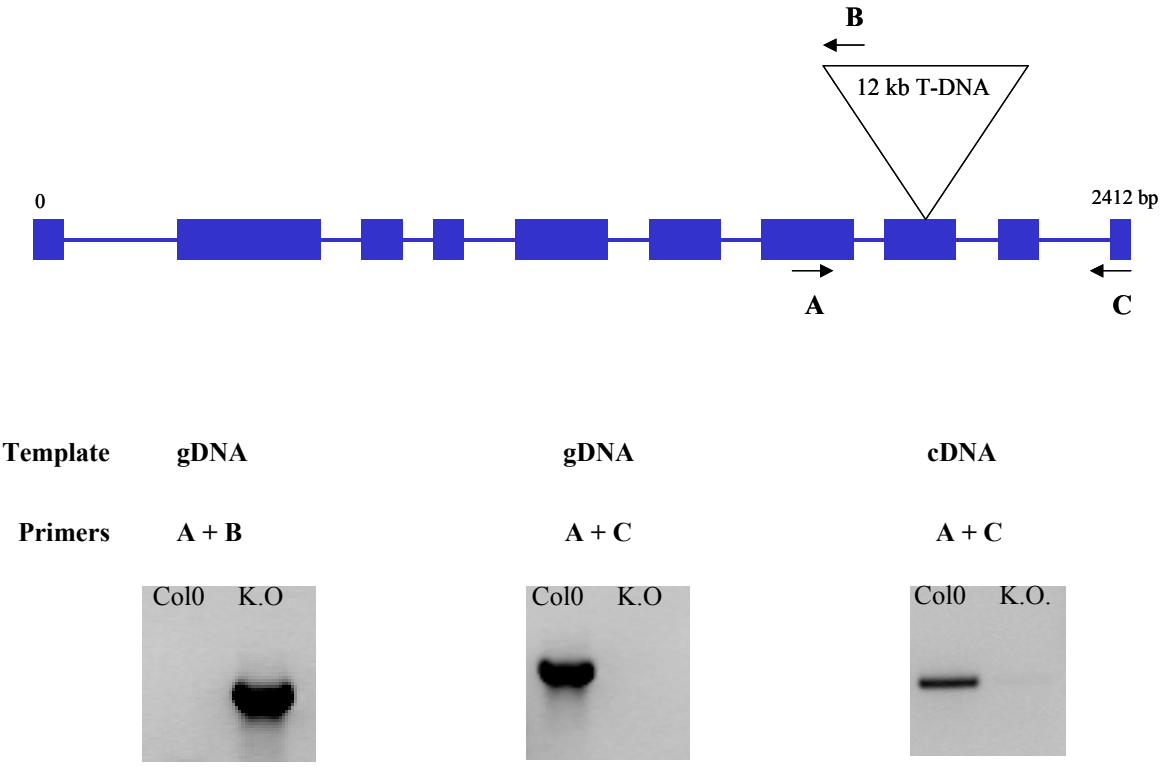

Figure 3.22 Genotyping by PCR of *A. thaliana* At5g09230 null lines. Schematic diagram of position of 12 kb insert into At5g09230 gene and arrows indicated position of primers. Gel electrophoresis of PCR on genomic DNA and cDNA extracted from *A. thaliana* Col0 and GK349B06 lines (KO) with primers amplifying from T-DNA insertion in At5g09230 gene.

In Figure 3.22 the PCR showed the presence of the T-DNA insertion band within the At5g09230 gene in the T-DNA line (KO) and not in *A. thaliana* Col0. Primers amplifying At5g09230 over the point of insertion only amplified in Col0 and not in the T-DNA insertion line suggesting the T-DNA line was homozygous for the T-DNA insertion. The absence of

At5g09230 gene transcript in extracted RNA from the T-DNA insertion line reinforced that At5g09230 was inactivated.

3.3.8 Phenotypes of *A. thaliana* sirtuin null lines under normal growing conditions.

A. thaliana Col0 and plant lines for sirtuin null lines and 35S:sirtuin plants were grown alongside one another in both long and short day conditions. Leaf number and size, date of bolting and flowering were all monitored and no difference was observed.

Figure 3.23 Photographs of sirtuin null lines. WT *A. thaliana* Col0 and null lines for both At5g55760 and At5g09230. Plants were grown in long day conditions and photographed after 3 weeks.

3.3.8.1 Germination of Col0 *A. thaliana* compared with At5g55760 null lines and 35S:Myc:At5g55760 lines.

Genevestigator (https://www.genevestigator.ethz.ch/) compiles microarray information of thousands of microarrays and showed that sirtuin genes had increased expression in germinating seedlings (see Figure 3.24). This was also seen with the Bio-Array Resource for Arabidopsis functional genomics website (http://bbc.botany.utoronto.ca/).

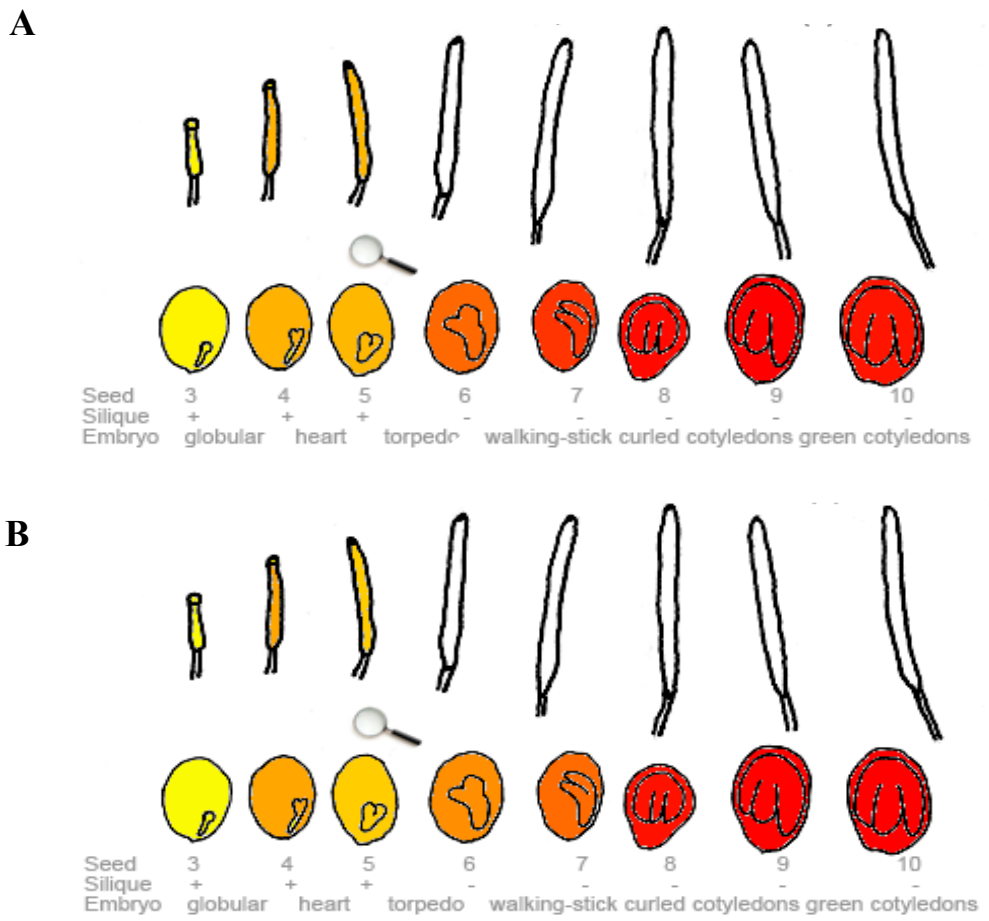

Figure 3.24 Transcript levels of sirtuin genes in germinating seeds of *A. thaliana* Col0 from Bio Array resource for *Arabidopsis* function genomics website. Gene expression levels in seeds for At5g55760 (A) and At5g09230 (B) when compared to Actin2 At3g18780. Yellow colour denotes 1 fold level of gene transcript, orange denotes an increase in gene expression by 1.5 fold and red shows a 16 fold increase in gene expression (Schmid et al. 2005).

In order to investigate any differences in germination between the null and 35S:sirtuin lines, seeds were put on MS media plates and placed in 24 hours light. Germination was then counted every 12 hours for 5 days and percentage germination shown in Figure 3.25.

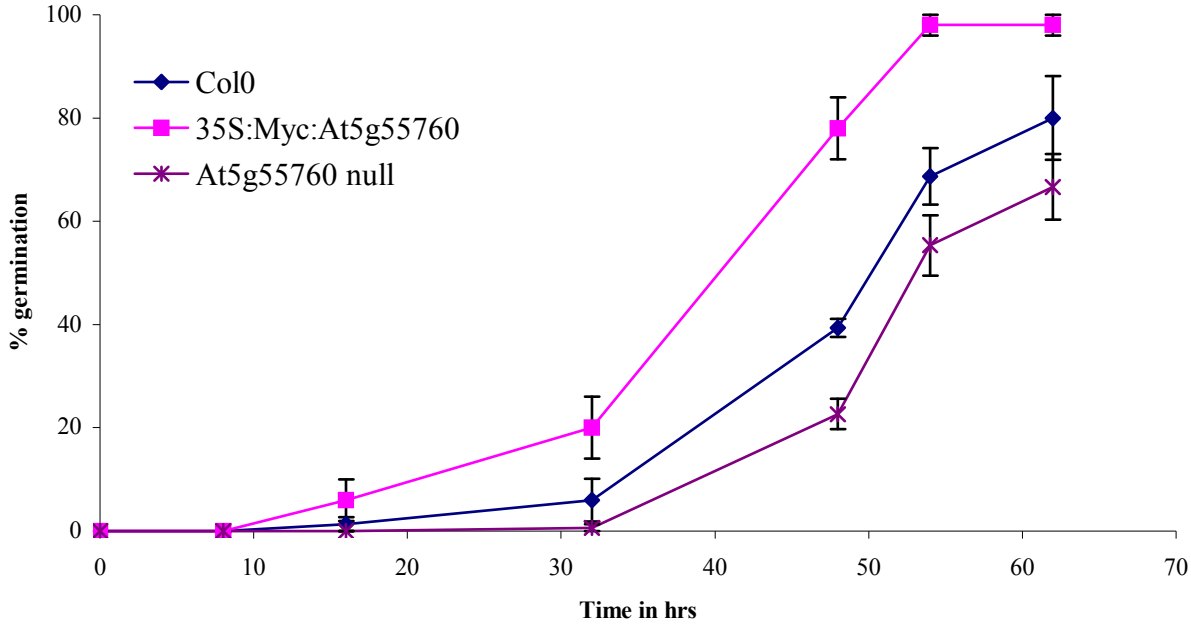

Figure 3.25 Germination of *A. thaliana* Col0, At5g55760 null and 35S:Myc:At5g55760 H seeds on MS media plates. Germination counted twice a day for 3 days. Experiment carried out in triplicate with 50 seeds on each plate and plates were grown in 24 hr light.

Germination of 35S:Myc:At5g55760 seeds was faster than that of Col0. At 32 hours 35S:Myc:At5g55760 seeds had a germination rate of 20% compared with 6% for Col0. This increase in germination rate continued and by 65 hours germination rates of 35S:Myc:At5g55760 were 98% compared with 80% of Col0. It is possible that if this germination study had continued then Col0 would have reached 100% like that of 35S:Myc:At5g55760. Conversely germination of At5g55760 null seeds was lower than that of Col0, with germination not starting until 32 hours, and by 65 hours germination had reached only 67% compared to 80% of Col0. These results suggested that At5g55760 was involved in germination because the At5g55760 null lines showed reduced germination compared with Col0, which was reinforced by the faster germination of 35S:Myc:At5g55760.

In order to ascertain at which stage of germination At5g55760 is involved, this germination experiment was repeated with 2 days of stratification, where the plates are placed in cold and dark conditions for imbibition (shown in Figure 3.26).

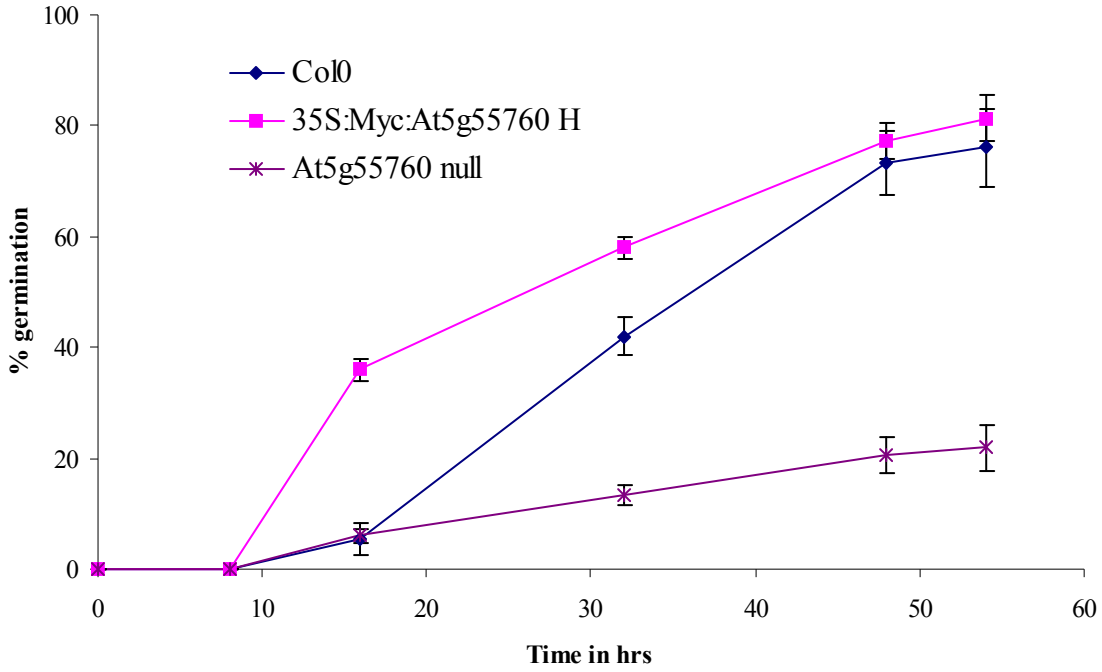

Figure 3.26 Germination of *A. thaliana* Col0, At5g55760 null and 35S:Myc:At5g55760 seeds on MS media plates with two days stratification. Plates were placed in the dark at 4°C condition for 2 days prior to germination in 24 hours light. Experiment carried out three times using 50 seeds on each plate and germination counted twice a day for 3 days.

The differences in germination between the different lines expressing At5g55760 were more pronounced with 2 days stratification. Seeds overexpressing At5g55760 germinated faster than *A. thaliana* Col0 seeds with germination of 35S:Myc:At5g55760 reaching 35% at 15 hours compared with 5% for Col0. However, by 55 hours germination of both lines was 80-85%. This was further reinforced by the very low germination rates for At5g55760 null lines compared with Col0. At 15 hours the difference was small, Col0 and At5g55760 null lines both with 8% germination. However, the difference increased with time, germination of At5g55760 null lines at 55 hours was only 22% compared with 80% for Col0.

Shortly after imbibition, seeds will carry out all the processes required for cell division, including mRNA production, protein synthesis and mobilization of storage reserves. DNA repair occurs as a normal stage of germination shortly after seed imbibition. This pre-

replicative repair stage is important for producing viable embryos. Sirtuins have been shown in many organisms to deacetylate the transcription factor p53 (Vaziri et al. 2001). There is evidence that suggests a p53 dependent DNA repair pathway during seed germination. In seeds with an increase in DNA damage the imbibition period is increased leading to a period of germination arrest whilst the repair mechanisms are carried out (Whittle et al. 2001). From the sirtuin germination data in Figure 3.25 and 3.26 there is a reduction in germination rate in the At5g55760 null lines and this reduction is increased with a period of imbibition. This correlates well with published data where long germination periods and even germination arrest occurs to allow the repair mechanisms to complete their task.

These results suggest that the sirtuin gene At5g55760 is involved in the process of germination possibly at the stage of DNA repair. Similarly when At5g55760 is overexpressed germination rates increase quicker than Col0.

3.3.8.2 Germination of *A. thaliana* Col0 compared with At5g09230 null lines and 35S:HA:At5g09230 lines.

Genevestigator showed that sirtuin gene At5g09230 has increased expression in seeds (Figure 3.24B) and therefore a difference in germination may be seen similar to that seen for plant lines with different expression of At5g55760. *A. thaliana* Col0 seeds were germinated on MS media plates alongside At5g09230 null and 35S:HA:At5g09230 lines.

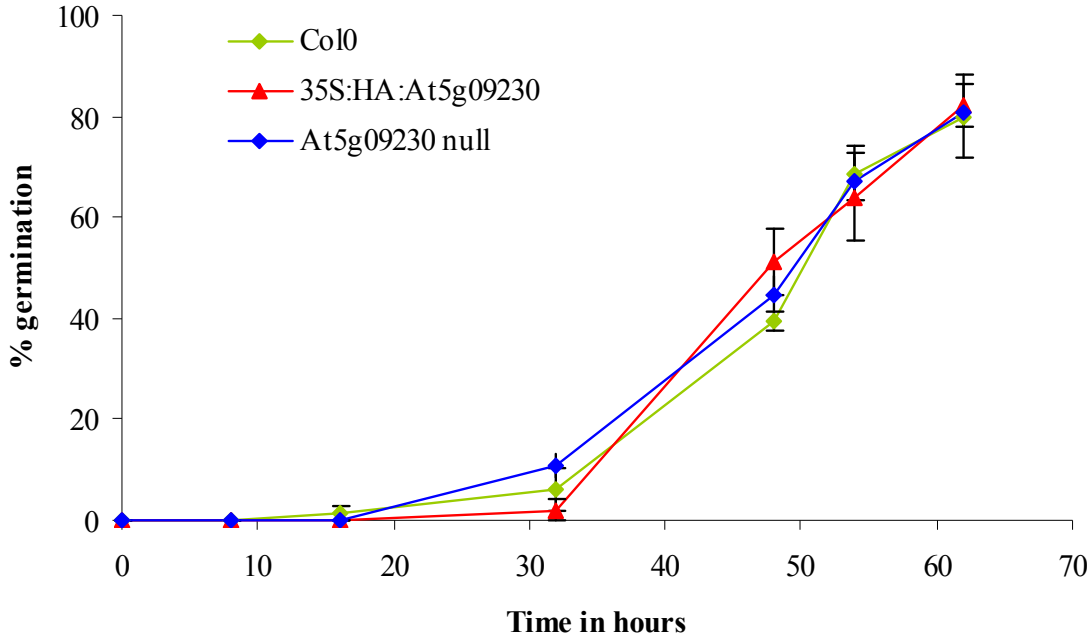

Figure 3.27 Germination of *A. thaliana* Col0 compared with At5g09230 null and 35S:HA:At5g09230 lines on MS media. Germination of seeds was counted twice a day for 3 days and repeated in triplicate with each plate containing 50 seeds.

There was no difference in germination of unstratified *A. thaliana* At5g09230 null lines or 35S:HA:At5g09230 lines when compared with Col0, suggesting that At5g55760 and At5g09230 genes have different roles in germination. However, this germination study was repeated with a 2 day period of stratification to investigate if a difference could be observed.

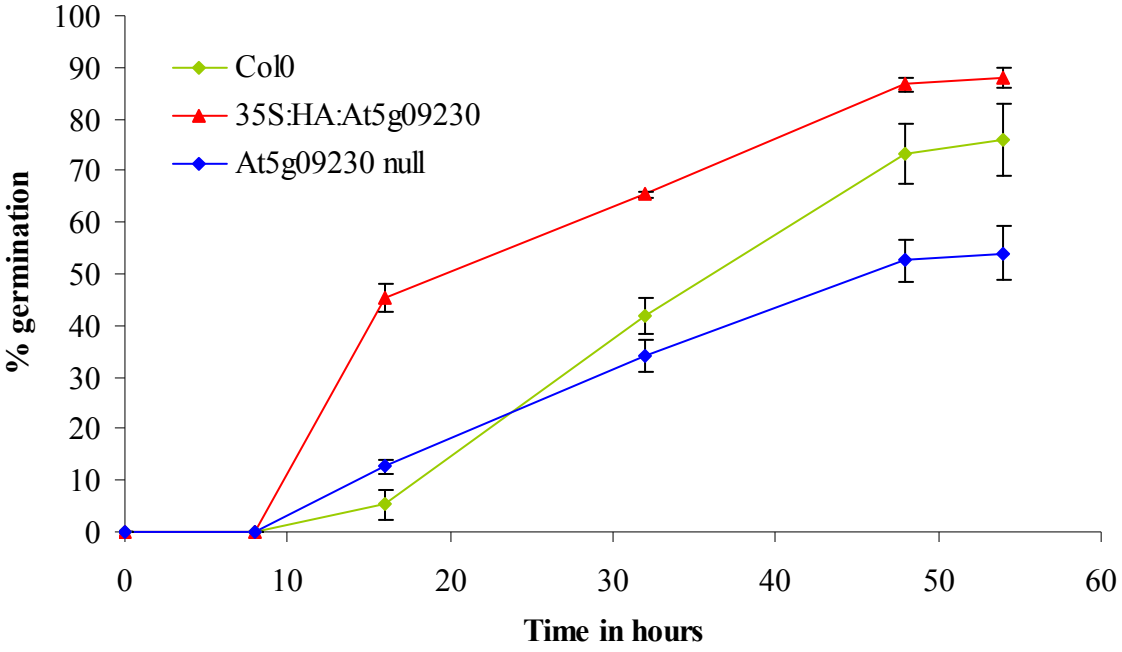

Figure 3.28 Germination of Col0 and At5g09230 null and 35S:HA:At5g09230 lines on MS media plates with two days stratification. Plates were placed in the dark at 4°C for 2 days prior to germination in 24 hours light. . Experiment carried out three times using 50 seeds on each plate and germination counted twice a day for 3 days.

Two days stratification showed a more pronounced difference in germination rates, similar to those for At5g55760. The 35S:HA:At5g09230 seeds showed faster germination, at 16hours 45% germination compared with 7% of Col0. The increased rates remained but by 55 hours was 85% compared with 75% for Col0. Conversely the At5g09230 null lines showed lower rates of germination being 50% at 55 hours compared with 75% for Col0. These results showed that At5g09230 is also involved at the imbibition stage of germination.

3.3.9 Phenotypes of sirtuin null lines and 35S: sirtuin transgenic lines under stress conditions.

Earlier qPCR and RT-PCR results (section 3.3.2 and 3.3.3) showed the largest differences in sirtuin gene transcript levels in genotoxic stress and therefore it would suggest different phenotypes should be seen between lines expressing different levels of sirtuin under stress conditions.

3.3.9.1 Phenotypes of *A. thaliana* Col0 and sirtuin null lines treated with MMS.

Seeds were germinated on MS plates for one week before being transplanted into MS media containing the DNA damaging agent MMS, where they were grown for another two weeks.

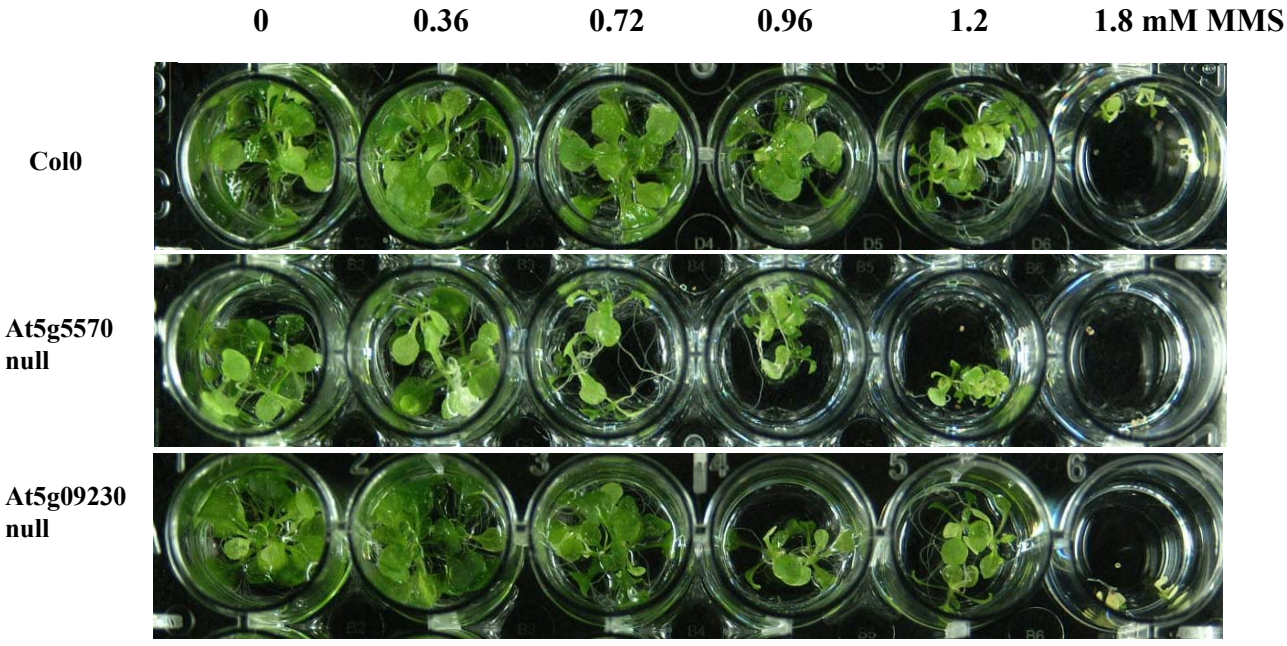

Figure 3.29 *A. thaliana* Col0 and sirtuin null lines exposed to MMS. Top row- Col0, middle row T-DNA At5g55760 plants, bottom row T-DNA At5g09230 in MMS concentrations 0, 0.36, 0.72, 0.96, 1.2, 1.8 mM MMS (left to right). Seedlings were germinated on MS plates for one week before transferring three seedlings to each well with MMS and grown for a further 2 weeks.

Figure 3.29 shows there was no difference in the growth of At5g09230 null plants compared with *A. thaliana* Col0. However, At5g55760 null lines did not grow as well in MMS compared with Col0, they were smaller and displayed chlorosis.

3.3.9.2 Phenotypes of *A. thaliana* Col0 and sirtuin null lines exposed to Bleomycin.

T-DNA insertion plants for both sirtuin genes were also treated with DNA damaging agent Bleomycin.

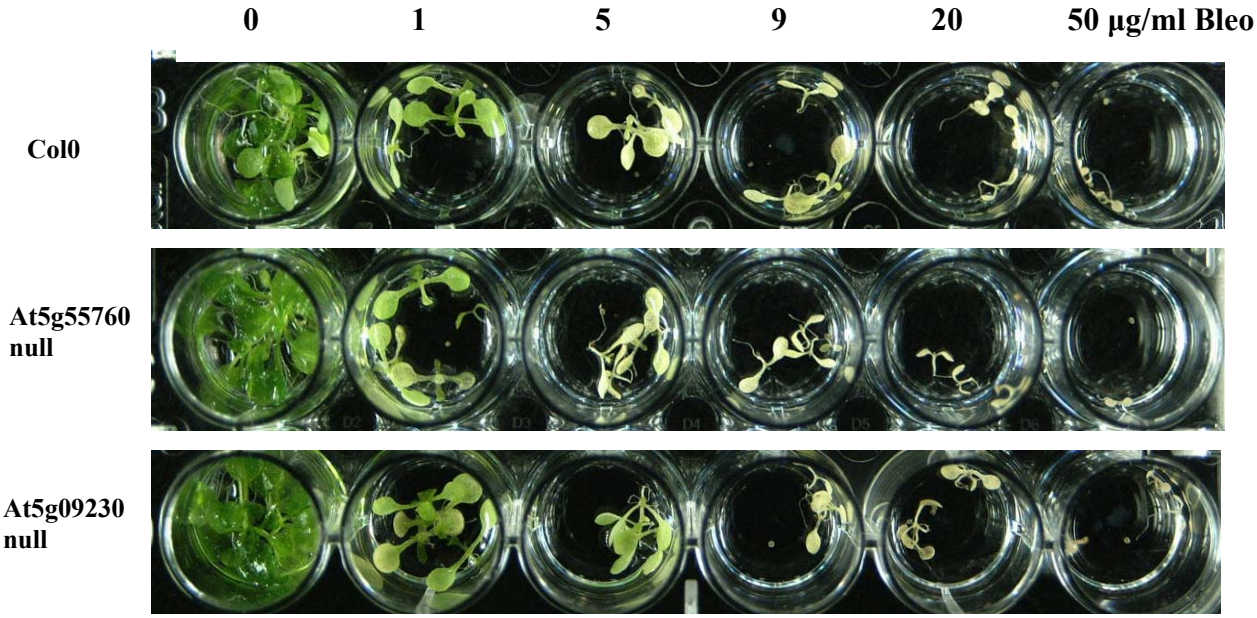

Figure 3.30 *A. thaliana* Col0 and sirtuin null lines grown in media containing Bleomycin. Seeds were germinated on MS plates for one week before transferring three seedlings per well into 1 ml MS media plus Bleomycin at concentrations 0, 1, 5, 9, 20 and 50 µg/ml Bleomycin (left to right).

In Figure 3.30 Col0 and At5g55760 null plants seemed more sensitive of Bleomycin compared with MMS, with both displaying chlorosis at high concentrations of Bleomycin. No obvious difference in phenotype was shown in the null lines treated with bleomycin.

These results suggest a role for At5g55760 in DNA repair in seedlings. This work is ongoing and this experiment has still to be repeated with the 35S:Myc:At5g55760 and 35S:HA:At5g09230 transgenic lines.

3.3.9.3 Comparison of phenotypes of WT and sirtuin null lines exposed to UV-B.

Plants utilise all wavelengths of light, the most important are those within the visible spectrum, which are harvested for photosynthesis. However, wavelengths of light outwith the visible spectrum are important environmental factors for regulating plant growth and development. *A. thaliana* has 3 photoreceptor systems relating to perceiving red/ far red light (controlling leaf expansion, germination and photoperiod), blue/UV-A light (important for hypocotyl elongation) and UV-B light.

UV-B light is damaging to many organisms as it induces the formation of pryrimidine dimers between adjacent pryrimidine bases. UV-B is the most powerful carcinogen in the development of skin cancers in humans (de Gruijl et al. 1999). In plants, exposure to UV-B causes tissue necrosis (Frohnmeyer & Staiger 2003). However, UV-B levels in incident sunlight are very low, although there are fears that depletion in the ozone layer causes an increase in UV-B.

In plants the characteristics of UV-B exposure are desiccation and necrosis, but the UV-B signalling pathway is relatively uncharacterised (Mackerness et al. 2001). A gene identified recently in *A. thaliana* as UV resistance locus 8 (UVR8) as being essential for activating HY5 a transcription factor involved in activating many genes involved in UV-B protection (Brown et al. 2005). It is also interesting that this UVR8 gene has a sequence characteristic of a gene involved in chromatin condensation (Kliebenstein et al. 2002).

The gene expression studies on *A. thaliana* sirtuin genes showed UV-B exposure induced a 3.5 fold increase for At5g09230 (see Table 3.8 and fig 3.8). At5g55760 did not show any upregulation in expression with UV-B.

A. thaliana seeds were grown in short day conditions for 12 days before exposure to 5µE of UV-B light for 24 hours. The plants were then allowed 5 days to recover before phenotypes were observed. Photographs from each stage were taken and shown in Figure 3.31.

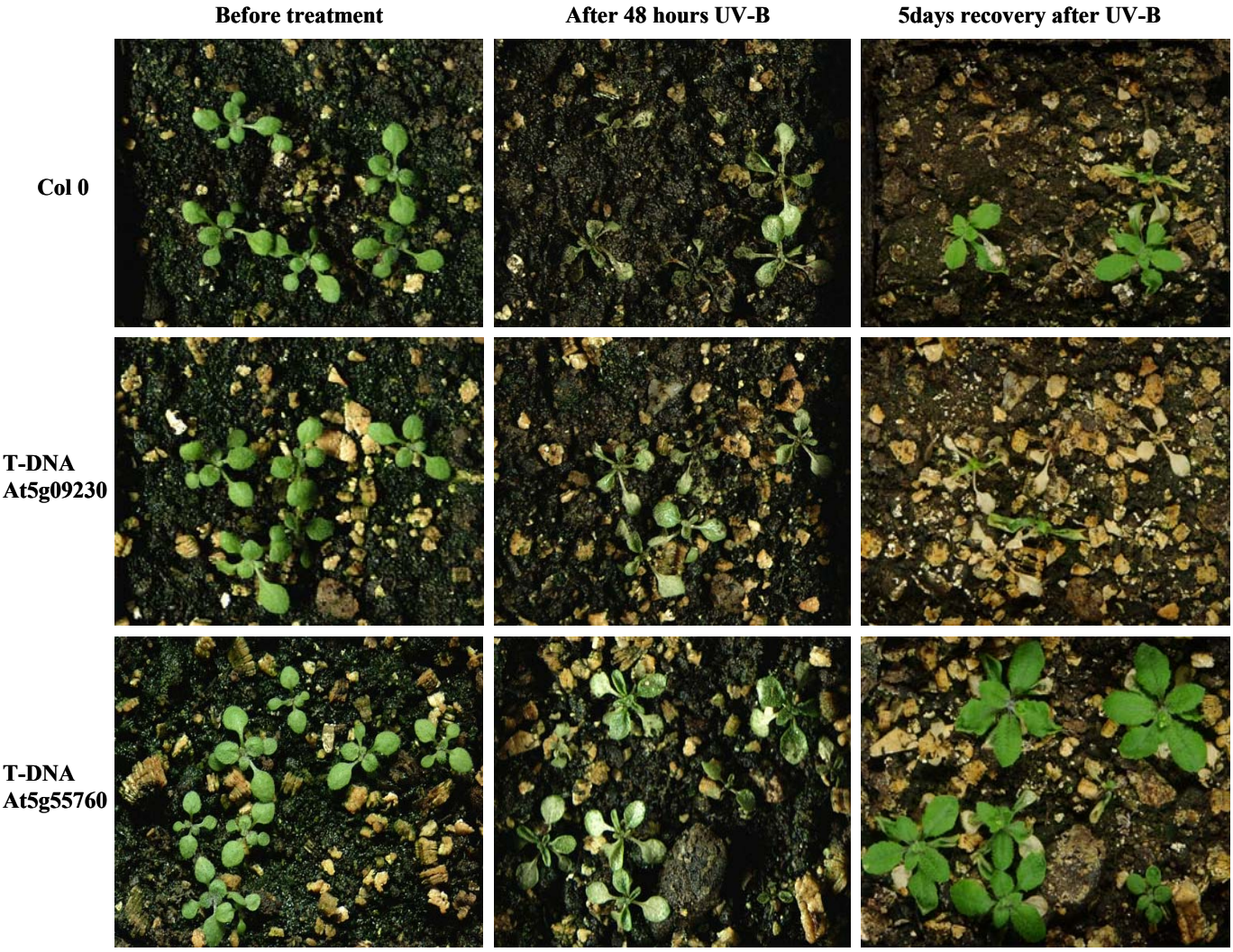

Figure 3.31 *A. thaliana* Col0 and sirtuin null plants exposed to UV-B. Top row – Col0, middle row At5g09230 null, lower row, At5g55760 null plants. Left column shows plants before treatment, middle row is immediately after 48 hours of UV-B stress, and right shows the plants after 5 days recovery.

There was no difference between the Col0 and At5g09230 null lines before treatment or after 48 hours of UV-B treatment. However, after 5 days recovery the Col0 plants had recovered

sufficiently to continue growing and complete their life cycle compared with the At5g09230 null lines, which do not recover and die. Survival rates for these plants were 50% for Col0 compared to 20% for the At5g09230 null lines. Further work to characterise the response of 35S:HA:At5g09230 plants to UV-B is required.

3.3.10 Identification of sirtuins within UV-B signalling pathway.

The UV-B signalling pathway induces a UV-B specific gene UVR8 that activates transcription factor HY5. HY5 then causes the expression of many UV-B protection genes such as Chalcone synthase (CHS).

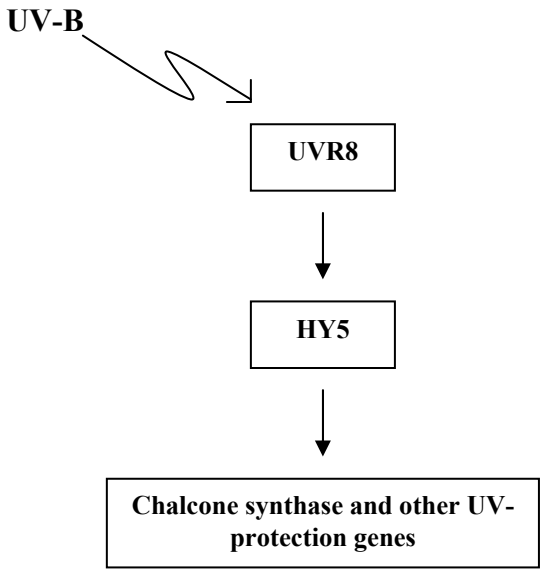

Figure 3.32. Schematic diagram of UV-B signalling pathway. Exposure to UV-B induces a UVR8 specific UV-B signalling gene that activates bZIP transcription factor HY5. HY5 triggers the induction of genes required for plant survival for UV-B exposure.

Null lines carrying T-DNA insertions for both HY5 and UVR8 were obtained from Prof. G. Jenkins, University of Glasgow. Sirtuin gene expression in these mutant lines were analysed to identify where sirtuin genes were in the UV-B signalling pathway. Chalcone synthase (CHS1) transcript was used as a positive control for the level of UV-B exposure.

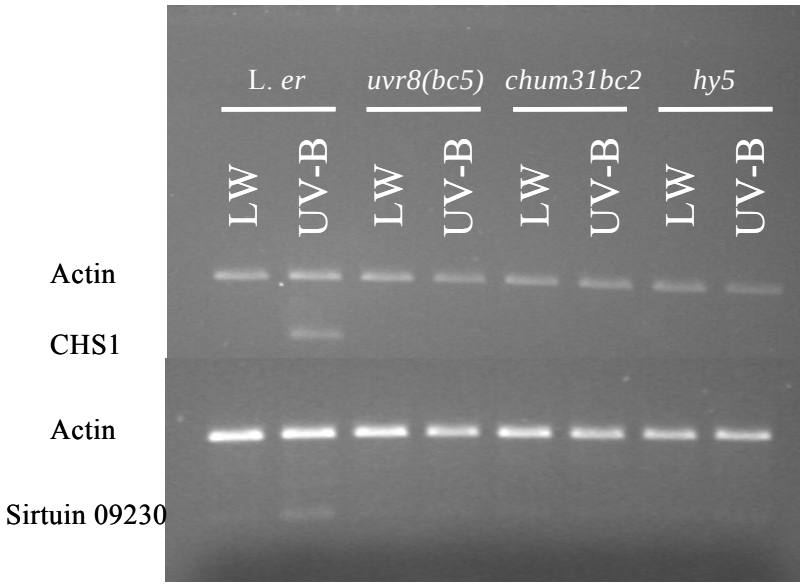

Figure 3.33 Transcript levels for At5g09230 in UVR8 and HY5 null lines. Plants tested included *A. thaliana* L.erecta and T-DNA insertion plants for UVR8 (bc5 and chum31bc2) and HY5. Conditions tested were white light (LW) and UV-B. Transcript levels were analysed for Actin, Chalcone synthase (CHS) and At5g09230. Actin levels were tested for cDNA concentration.

In Figure 3.33 the *A. thaliana* L.er plants CHS and sirtuin gene At5g09230 were both induced by UV-B compared to white light. However, in the uvr8 and hy5 null lines neither CHS nor At5g09230 genes were induced. This suggested that CHS and At5g09230 were downstream of UVR8 and HY5 in the UV-B repair pathway. This was reinforced by the increase in sensitivity to UV-B seen by the T-DNA At5g09230 lines.

3.4 Discussion.

Sirtuins were first identified as NAD dependent protein deacetylases/ ADP ribosyl transferases as playing a critical role in regulating lifespan (Buck, Gallo, & Smith 2004;Frye 2000b). In model organisms they have been implicated in regulating cellular responses to DNA damage (reviewed in Kruszewski & Szumiel 2005 and Gorospe & de Cabo 2008) as well as promoting senescence under conditions of chronic stress through deacetylation of histones and transcription factors (Yang & Sauve 2006; Anastasiou & Krek 2006).

3.4.1 Identification of 2 sirtuin genes in *A. thaliana*

Two sirtuin genes were identified in *A. thaliana* through sequence homology of the catalytic domains identified in other organisms (Haigis et al. 2006). X-ray crystallography of human, yeast and archeal sirtuin proteins identified two main domains (Brachmann et al.1995; Finnin et al. 2001; Sherman et al.1999). The larger domain comprises of a Rossman fold characteristic of an NAD binding domain. The smaller domain contains 4 cysteines, which bind a zinc ion. Both At5g09230 and At5g55760 show high homology to other characterised sirtuins from yeast, humans, Drosophila and mice, with high homology in the regions of β sheet and α helices. The sequence similarity between sirtuins identified in *A. thaliana* and sirtuins characterised in other organisms suggests that the domain architecture is likely to be very similar. Also present are the tetrad of cysteine residues shown in the crystal structure to bind a zinc ion.

Sequence homology of the *A. thaliana* At5g55760 (Figure 3.3) shows most homology to one of the two rice sirtuin genes. A paper published on rice sirtuin genes (OsSRT1 and OsSRT2) showed that RNAi lines for OsSRT1 (homolog of At5g55760) to have an increase in leaf lesions and an increase in DNA strand breaks under normal growing conditions (Huang et al. 2007). Plant leaf lesions are normally associated with a hypersensitive response to pathogen

attack induced by hydrogen peroxide, which is also capable of increasing DNA damage. Consistent with this, RNAi knockdown lines showed an increase in hydrogen peroxide production. Transgenic rice plants overexpressing OsSRT1 had increased resistance to oxidative stress suggesting rice SRT1 has a role in protecting against damage caused by reactive oxygen species.

The closest of the mammalian homologs to At5g55760 is SIRT6, which has been shown to be a nuclear protein with ADP ribosylation activity (Liszt et al. 2005). Mice embryonic fibroblast cells lacking SIRT6 showed slow growth and an increase in sensitivity to ionising radiation but interestingly not to UV-B exposure (Mostoslavsky et al. 2006). Also reported in the same paper were mutant mice lacking the SIRT6 gene, which exhibited a significant increase in chromosomal aberrations including fragmented chromosomes and detached centromeres. At birth the mice did not show any abnormalities but after 3 weeks the mice suffered from several acute degenerative processes and failure to thrive, eventually leading to death before 1 month of age. These included a loss of subcutaneous fat, lymphocyte apoptosis and an increase in DNA damage, all severe metabolic defects normally associated with aging.

The *A. thaliana* gene At5g09230 shows the highest homology to human SIRT4. In mice embryonic fibroblast cells SIRT4 has been characterised as a mitochondrial ADP ribose transferase that ADP ribosylates mitochondrial protein including glutamate dehydrogenase and ATP/ADP carrier proteins (Ahuja et al. 2007; Haigis et al. 2006).

The EST database of *A. thaliana* shows 6 At5g09230 splice variants (Figure 3.5). Differences between the sequences of the splice variants are seen at the ends of the gene and the probable active site of the protein is unchanged. Analyses of these sequences by protein localisation prediction algorithms have suggested that each splice variant could have different localisations (Table 3.6). Northern blot analysis for this gene could identify the functional splice variants although unfortunately the size differences between some of the splice variants

is only ~ 30bp. It is interesting that most other model organisms contain multiple sirtuin genes (humans have 7, yeast 5) *A. thaliana* has only two sirtuin genes, although At5g09230 is suggested to have multiple splice variants. It could be possible that each of the splice variants have different localisation and biological roles, therefore functioning as separate genes products.

3.4.2. Expression of sirtuin genes in *A. thaliana*

Expression of sirtuins in other model organisms are seen in a wide range of responses, to DNA damage (Kruszewski & Szumiel 2005), H_2O_2 (Frescas et al. 2005), apoptosis (reviewed in Buck et al. 2004) and longevity (Lin et al. 2000). Investigations into *A. thaliana* sirtuin gene expression under a variety of stress conditions and treatments might imply a role or function of sirtuins in *A. thaliana*. Compared with other eukaryotes, *A. thaliana* has relatively fewer sirtuin genes suggesting that the plant sirtuins may be involved in more functions than their yeast or animal counterparts.

RT-PCR revealed that At5g55760 was mainly induced by DNA damaging agent MMS. At5g55760 shows highest homology to SIRT6, which has been shown to be significantly induced by DNA damaging agents (Mostoslavsky et al. 2006). Also the rice sirtuin homolog OsSRT1 RNAi knockdown lines have been shown to have more DNA strand breaks compared to wild type plants (Huang et al. 2007).

Although the mechanism of SIRT6 involvement in DNA repair is not known it could be through chromatin modifications at the site of DNA strand breaks or deacetylation / ADP ribosylation of transcription factors or other proteins involved in DNA repair. Interestingly the mice mutants show no difference in sensitivity to UV-B exposure compared to wild type. This is also shown in the RT-PCR and qPCR of sirtuin At5g55760 which shows no change in gene expression to exposure to UV-B.

Gene expression of At5g09230 increased with DNA damaging agents and lipopolysaccharide (LPS). Previous work on mammalian SIRT4 has shown its ADP ribosylation of glutamate dehydrogenase and other proteins known to downregulate insulin secretion (Ahuja et al. 2006). Despite At5g09230 showing highest homology to SIRT4 of the mammalian sirtuins, they may have very different targets and roles within the organism.

At5g09230 also shows an increase in gene expression with lipopolysaccharide (LPS) treatment. LPS is known to cause a large increase in production of nitric oxide in *A. thaliana*. Nitric oxide is a signalling molecule induced by plants in recognition of avirulent pathogen interactions. A rapid burst of Nitric oxide has the ability to induce cell death by the production of reactive oxygen species.

There are different pathways specific to different types of DNA damage. Double strand breaks in DNA (such as induced by ionizing radiation) are repaired by non-homologous end joining (NHEJ) or homologous recombination (HR). Single strand breaks are repaired by Nucleotide excision repair (NER) or Base excision repair (BER) depending on the type of lesion (Hoeijmakers 2001). UV-B causes covalent bonds to form between adjacent cytosine bases causing a bulky dimer in the DNA, normally repaired by NER. More simple single strand breaks can arise spontaneously from endogenous alkylation, oxidation and deamination as well as chemical mutagens such as alkylating agent MMS. These are normally repaired by the BER pathway (Barnes & Lindahl 2004). Interestingly mutants in humans and mice for components in NHEJ, HR and NER cause aging-type phenotypes or no phenotype, whereas mutations in BER are normally lethal (Lombard et al. 2008). The response of At5g55760 to MMS and not UV-B suggests its possible involvements in the BER DNA repair pathway.

3.4.3 Localisation of *A. thaliana* sirtuin protein.

At5g5570 has been shown to be a nuclear protein in onion epidermal cells (Figure 3.9), which is consistent with previous published data on OsSRT1 and SIRT6. The localisation of At5g09230 has still not been established despite being investigated with both N- and C-terminal GFP fusions in onion, tobacco and Arabidopsis. The construct for protein localisation expressed At5g09230 under control of a strong constitutive 35S promoter derived from the cauliflower mosaic virus and it is possible that will such high expression the At5g09230 protein is toxic. Work is currently underway using At5g09230 fused to GFP under control of its own regulatory components.

3.4.4 Protein purification of *A. thaliana* sirtuin genes.

Protein expression of sirtuins was first attempted in *E. coli* because it is quick and inexpensive. Since the end of this project both sirtuins have been expressed in insect cells and soluble protein produced suggesting that a eukaryotic cell is required to produce viable recombinant protein. Difficulties in expressing eukaryotic proteins in prokaryotic systems are well known, as conditions inside a prokaryotic cell (pH, osmolarity) are different from the original source of the gene. The effects of this were problematic, as recombinant protein formed insoluble inclusion bodies, which are aggregates of misfolded protein. Protein from inclusion bodies was difficult to purify as the protein has to be denatured and refolded often resulting in erroneous protein structure.

For this reason optimisation of protein induction was essential to decrease the production of insoluble protein. Optimisation included altering conditions such as temperature, optimum density of *E. coli* cells at the time of induction, duration of protein induction and concentration of IPTG. By altering conditions, smaller quantities of protein were induced often improving correct folding of recombinant protein.

Sirtuin genes were coupled to a Histidine tag which although small could affect the formation of soluble protein. Constructs were also used fusing sirtuin genes to a GST tag often increasing recombinant protein stability and solubility. All of these alterations in growing conditions and constructs were attempted but unfortunately soluble At5g55760 was never obtained and At5g09230 was never induced in *E. coli* BL21 cells. Expression of both sirtuin genes was under the control of T7 promoter and it is possible that at such high expression levels sirtuins could be toxic to *E. coli.* Expression of both sirtuin genes was repeated in another strain of *E. coli*, Rosetta gami, which has one extra rare tRNA designed to enhance disulphide bond formation and more natural protein folding. However, protein recovery was too low to be of value.

3.4.5 *A. thaliana* sirtuin transgenic lines

A. thaliana plants containing T-DNA insertions in each sirtuin gene were identified through PCR of genomic DNA and confirmed by the absence of cDNA sequence. Under normal growth conditions there was no difference in development compared to wild type plants.

Arabidopsis lines with sirtuin genes under control of 35S promoter were generated and identified through segregation analysis using the Bar (Basta) resistance gene. No difference in growth and development of the 35S lines compared to wild type was observed.

The online microarray database Genevestigator identified an increase in sirtuin gene expression in germinating seeds. Investigations into germination of sirtuin null and overexpressing lines showed the knockout lines showed a decrease in germination rate compared to wild type. Similarly, the overexpressing lines had faster germination. The results were similar for both sirtuin genes and more exaggerated with 2 days stratification. Seeds suffer DNA damage as a result of desiccation, which has to be repaired for germination of viable seedlings, during which there is a large surge in transcription. Sirtuin involvement in

DNA repair and regulation of transcription is well documented (reviewed in Anastasiou & Krek 2006) and could possibly explain the reduction in germination seen in T-DNA knockdown lines.

Null lines for At5g55760 show a weak phenotype of smaller plants compared to wild type on the addition of MMS. Null lines for At5g09230 show no phenotype with MMS and a weak phenotype for At5g55760 could result from gene redundancy. In order to safeguard against lethal mutations in one gene, organisms often employ several genes to perform the same function. It is possible that the presence of sirtuin genes is an example of such gene redundancy. In future the generation of plant lines with both sirtuins inactivated may produce a more obvious phenotype with DNA damaging agents.

The sirtuin overexpressing lines were generated late on in this project and responses to DNA damaging agents have not yet been investigated.

3.4.6 Involvement of At5g09230 in UV-B signalling pathway.

RT-PCR and qPCR showed an increase in At5g09230 gene expression with exposure to UV-B. For this reason At5g09230 null lines were tested for their response to UV-B and showed an increase in susceptibility to UV-B damage. Components of the UV-B pathway have been elucidated and a schematic diagram shown in Figure 3.34 (Brown et al. 2005).

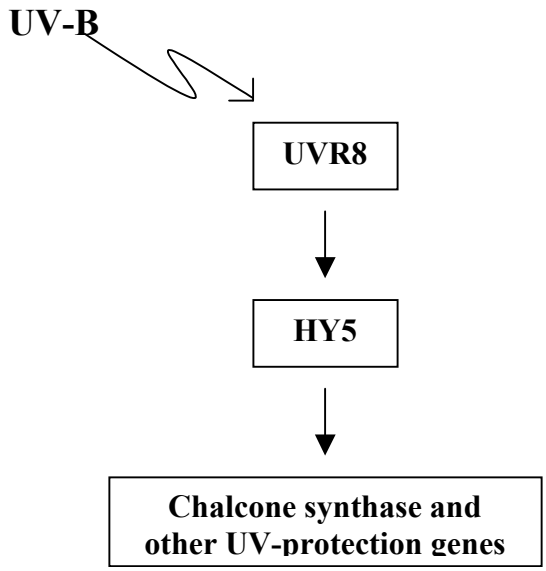

Figure. 3.34 Schematic diagram of components of the UV-B signalling pathway. UV-B exposure induces a specific UV-B signalling gene (UVR8) that activates bZIP transcription factor HY5. HY5 triggers the induction of genes required for plant survival to UV-B exposure.

UV Resistance locus 8 (UVR8) is a UV-B specific gene essential for activating HY5 transcription factor that in turn induces chalcone synthase. Chalcone synthases produces a pigment that shields the plant against the DNA damaging effects of UV-B.

Null lines carrying T-DNA insertions in UVR8 and HY5 genes were grown in white light and UV-B and transcript levels of sirtuin At5g09230 investigated. In this way it was possible to identify that in mutants of UVR8 and Hy5 no transcript for At5g09230 was seen on exposure to UV-B. Presence of transcript for chalcone synthase was used as a positive control for the activation of the UV-B signalling pathway. Therefore sirtuin At5g09230 must be downstream of both of UVR8 and Hy5 in the UV-B signalling pathway.

UVR8 shows sequence and structure homology to a regulator of chromatin condensation (RCC1) protein although chromatin condensation activity has not been shown for UVR8 (Kliebenstein et al. 2002). This is very interesting as it suggests a possible link for At5g09230 involvement in UV-B signal response due to its activity as a chromatin modifier.

Future work using Yeast 2 hybrid assays or sirtuin TAP tag fusions could identify interactors and sirtuin targets that could further define the function of sirtuins.

Chapter 4: Characterisation of PARPs and PARGs in *A. thaliana* and their role in plant stress.

Introduction

Poly ADP ribosylation is characterised by the addition of complex branched poly ADP ribose polymers onto acceptor proteins, catalysed by the poly ADP ribose polymerase (PARP) enzymes. Poly ADP-ribose is a linear or branched polymer of many ADP-ribose units (sometimes up to 400) linked by glycosidic ribose-ribose bonds. The reaction utilises NAD^+ as the substrate and the activity of the PARP enzymes is directly linked to the concentration of NAD^+ in cells (Alvarez-Gonzalez 1988). Once synthesised poly ADP ribose polymers are rapidly degraded by the action of poly ADP-ribose glycohydrolase (PARG), an enzyme that cleaves the glycosidic bonds between the poly ADP-ribose units (Miwa & Sugimura 1971). Therefore the various activities of PARP and PARG enzymes must be tightly regulated in order to respond efficiently to the various stimuli whilst maintaining effective energy homeostasis.

PARP enzymes were first discovered in 1963 by Mandel who showed that hen liver nuclear extracts incorporated NAD^+ into poly ADP ribose. Initially PARP1 was thought to be the only poly ADP ribosylating enzyme in living cells but the generation of PARP1 knockouts in both mice and *Drosophila* that were still capable of producing poly ADP ribose polymers suggested other enzymes were involved. Since then 5 PARP genes with bona fide PARP activity have been discovered in humans (Hassa et al. 2006). In 1971 Miwa identified the first poly ADP ribose glycohydrolase (PARG) enzyme and later also described in detail the branched structure of poly ADP ribose polymer (Miwa & Sugimura 1971).

The activities of PARP genes can be split into 3 groups.

1. Poly ADP ribosylation induced cell death.

This model was first suggested in 1983 by Berger and co-workers after it was found that DNA repair mechanisms were more efficient when PARP1 was inhibited and cells exposed to high DNA damage (Sims et al. 1983). In an attempt to restore NAD^+ levels, NAD^+ is re-synthesised with a consumption of 2-4 molecules of ATP to one NAD^+. This depletion of ATP leads to cellular energy failure and finally necrotic cell death.

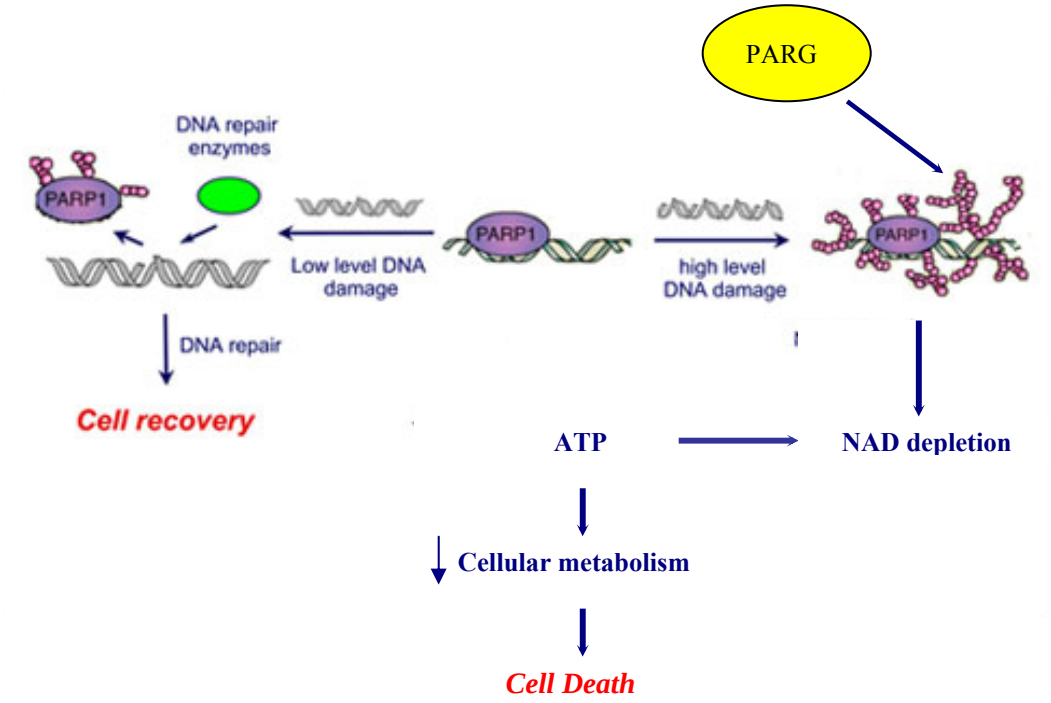

Figure 4.1. Schematic diagram of activity of PARP and PARG proteins. In response to low DNA damage PARP helps recruit DNA repair enzymes to the site of DNA breaks. Overactivation of PARP protein in response to high doses of genotoxicity results in the formation of large branched polymers thereby depleting cellular NAD^+. ATP is utilized to synthesise more NAD^+ (at a rate of 2-4 ATP to 1 NAD^+) resulting in a decrease in cellular metabolism and cell death. PARG proteins remove poly ADP ribose chains, reversing activity of PARP genes by catalyzing the hydrolysis of bonds between the ADP units.

This has been reinforced by the generation of PARP1 knockout mice showing an increase in tolerance to high concentrations of DNA damaging agents (reviewed in Shall & de Murcia 2000). A recent report on *A. thaliana* with negliable PARP activity showed an increased tolerance to a variety of abiotic stresses (Vanderauwera et al. 2007).

A second model has emerged explaining the correlation between PARP activation and cell death using knockout mice showing an NAD^+ reduction may not be totally responsible for

cell death. This model suggests PARP activation and the signal for poly ADP-ribosylation itself induces the translocation of Apoptosis Inducing Factor (AIF) from mitochondria to the nucleus causing DNA fragmentation and apoptosis-like cell death (Yu et al. 2006; Andrabi et al. 2006).

There is a fine balance between the two main activities of PARP, its role in repairing DNA damage, and its role as a cell death signal. Further the activity of PARG and their control over PARP is gathering importance. PARG enzymes are responsible for poly ADPribose degradation by catalysing the removal of poly ADPribose polymer chains from modified proteins. The importance of PARG enzymes on the activity of PARP proteins was demonstrated in yeast, which is normally devoid of PARP enzymes. When yeast was transformed with human PARP genes the cells did not survive unless they were also transformed with PARG genes (Perkins et al. 2001). Mutant *D. melanogaster* lacking PARG genes displayed early embryonic lethality (Hanai et al. 2004) and embryonic stem cells without PARG genes showed increased sensitivity to DNA damaging agents (Masutani et al. 2003).

2. Modulation of chromatin structure.

In 1982 it was shown that poly ADP ribosylated chromatin has a more relaxed structure which was later shown that it was to the extent normally seen in mutated chromatin (Poirier et al. 1982b; Kim et al. 2004). This lead to the 'histone shuttle' hypothesis whereby PARP and PARG activation in response to DNA damage causes the relaxation of DNA allowing DNA repair enzymes access to the site of damage (Althaus 1992).

3. Corepressor/coactivator activity.

PARP1 has been shown to interact with and regulate the function of many transcription factors. Recent research has shown that PARP acts as a repressor or activator of transcription factors, for example NFκB, which has a key role in expression of inflammatory disorders

(Hassa &Hottiger 2002). This coactivator/corepressor function is achieved by phosphorylation of the transcription factor either enhancing or reducing its activity.

PARP activity has been implicated in many biological stress conditions. PARP encoding genes in human cells consists of a large superfamily of 18 members encoding proteins that share a conserved catalytic core. It is hardly surprising that data from mammalian cells show PARP involvement in diverse biological roles such as genomic stability, regulation of telomere maintenance, DNA repair mechanisms, initiation of cell death signalling and apoptosis, and regulation of transcription. Although the role of PARPs enzymes in these biological processes has long been known, the mechanism of the action is still unclear.

Mutant mice lacking the gene encoding PARP1 are healthy and fertile under normal conditions. On exposure to ionising radiation and alkylating agents the mutant mice die rapidly (Wang et al. 1997; de Murcia et al. 1997; Masutani et al. 2000).

Two PARP enzymes have been identified in *A. thaliana* by homology to human PARPs (Lepiniec et al.1995). Experiments using transient overexpression of *A. thaliana* PARP1 cDNA showed a decrease in DNA breaks and cell death with mild oxidative stress. Under severe oxidative stress there was an increase in cell death and DNA strand breaks. Similarly in cells with PARP1 antisense expression the opposite effect was seen, an increase in DNA strand breaks at high doses of hydrogen peroxide (Amor et al. 1998). A screen for genes in *A. thaliana* involved in ionising radiation damage showed that both PARP genes were activated (Doucet et al. 2001). Transgenic plants with reduced PARP activity were submitted to drought and high light stress and the transgenic lines were able to maintain energy homeostasis under these stress conditions (de Block et al. 2005). DNA microarray experiments using transgenic plants with reduced PARP activity showed a wide range of stress resistant phenotypes (Vanderauwera et al. 2007). The explanation for this is that overactivation of PARP activity has a detrimental effect by reducing cellular NAD levels to

the extent of inducing cell death, and because PARPs have such an essential role in maintaining levels of NAD^+, it was suggested that the PARP genes might have a role in multiple stress responses.

Most of the published work on PARGs points to its vital role in maintaining cellular concentrations of NAD^+ by controlling the action of PARPs but more recently work has appeared on the PARGs themselves. PARG proteins have been identified in mammals, insects, nematodes and plants and all share similar features.

A mutation in the *A. thaliana* PARG gene was shown to induce an altered circadian period length affecting the transition from vegetative to flowering growth (Panda et al. 2002). A single point mutation in the within this PARG gene not only revealed a deficiency in PARG activity but also in the automodification of PARP and the transcription levels of circadian rhythm controlled genes.

Mutant *Drosophila melanogaster* without PARG genes exhibit lethality in the larval stage unless grown at 29ºC when it displays progressive neurodegenerative with the accumulation of poly ADP-ribose in the central nervous system (Hanai et al. 2004). Mice lacking two exons in a PARG genes show an increased sensitivity to DNA damaging agents and an increase in inflammation responses (Cortes et al. 2004), whilst mice lacking PARG completely show early embryonic lethality (Koh et al. 2004).

Methods

4.2.1 Semi Quantitative Reverse Transcriptase PCR (SQRT-PCR).

To investigate the effects of stress on PARP and PARG gene expression *A. thaliana* Col0 seedlings were exposed to a variety of different biotic, genotoxic and abiotic stresses (for full list see Chapter 2 Table 2). Sterile seeds were grown in liquid media for two weeks before the treatment was applied and samples were taken at 0, 2, 4, 8, 24 and 48 hours (for full methods see Chapter 2.2.2). Two μg of total extracted RNA was used to make cDNA. A twenty times dilution of this cDNA was used as template for both RT-PCR (Chapter 2.2.6) and quantitative PCR (Chapter 2.2.8). Primers used and numbers of cycles for SQRT-PCR are shown in Table 5.1.

Gene name and number	Primer name	Sequence	Number of cycles
PARP AtPARP3	For Rev	CGAGGAGACACACTCGATGAT AACCAACCGTCCACAAGGAACTTT	38
PARP AtPARP1	For Rev	ACCTCCAGAAGCTCCTGCTAC GTTTTCCACAGGGAACAGTCA	32
PARP AtPARP2	For Rev	ATTGTGGTTTGACGCCAGTAG GAGGAGCTATTCGCAGACCTT	25
PARG AtPARG1	For Rev	TTGATTGGAGCTCTTCTTGCATGC AAACGAAGATGCATACCCTGTGTA	31
PARG At2g31875	For Rev	CGTTTCCGTATATGCGTCACT CATCCATACGAGGCAAAAAGA	32
Actin2 At3g18780	Act2s Act2a	GTTGGGATGAACCAGAAGGA CTTACAATTTCCCGCTCTGC	25

Table 4.1 Primer sequences for *A. thaliana* PARP and PARG genes and the number of cycles used for RT-PCR. All products for RT-PCR were sequenced by MWG for verification.

4.2.2 Quantitative PCR (qPCR).

cDNA synthesized from mRNA extracted from *A. thaliana* Col0 exposed to stress treatments (for full methods see Chapter 2.2.2 and 4.2.1) was also analysed by qPCR in order to obtain more accurate results. qPCR utilises a fluorescent dye that bids to double stranded DNA with the fluorescence being proportional to the cDNA level. The PCR reaction amplifies the cDNA present in template sample, which is measured by the fluorescence. qPCR was performed and fluorescent analysed using Stratagene Mx4000 instrument amplification software. The same template cDNA was used as in the section above. Each of the three replicates was analysed three times. qPCR requires primers designed across an intron for each gene. qPCR primer sequences are listed below in Table 4.2.

Gene name and number	**Q-PCR primer sequence**
PARP AtPARP3	TGAGCCATGGGAACGTGAGAAGAA AAGCAATGCCAAGCTGCCTTAGAC
PARP AtPARP1	TCCGGAGAAAGAAAGATGCCCAGA GCTGAGTTGCGGGAAATGCTTGAA
PARP AtPARP2	GGACTTGGGATGTGGGATAA GGGGAAGAGTTGGTGTGAAA
PARG AtPARG1	TTCTGGTTCTTCGCCTTTTG CTCGGATGGATGACAATGAA
PARG At2g31875	CTCTTGTTTTTCGCCTCCTG TCTTTTTGCCTCGTATGGATG
UBQ At4g02890	GAGTTCTGCCATCCTCCAAC AACCCTAACGGGAAAGACGA
Actin2 At3g18780	TGAGGTTTCCATCTCCTGCT TGCCAATCTACGAGGGTTTC

Table 4.2 Real time primers sequences for *A. thaliana* PARP and PARG genes. All products were sequenced to confirm authenticity.

4.2.3 *A. thaliana* PARP and PARG null lines.

A. thaliana PARP and PARG null lines were generated by SALK and purchased from the Nottingham Arabidopsis Stock Centre (http://nasc.nott.ac.uk/). T-DNA insertion lines generated by GabiKat were purchased from the Max Planck Institute of Plant Breeding Research (Cologne, Germany), (http://www.gabi-kat.de/). All T-DNA insertion lines were generated into an *A. thaliana* Columbia (Col0) background.

Gene name and number	Insertion line	Stock centre
AtPARP3	SALK 108092	SALK
AtPARP1	GK 380 E06	GabiKat
AtPARP2	GK 420 G03	GabiKat
AtPARG1	SALK 116088 SALK 012110	SALK SALK
AtPARG2	GK 072 B04	GabiKat

Table 4.3 Details of *A. thaliana* PARP and PARG null lines.

Seeds obtained were a T2 generation and therefore contained a mixture of homozygous, heterozygous and wild type Col0. Identification of plants with homozygous insert was performed as outlined in Chapter 2.2.19.

4.3.1 Structure of PARP genes

PARP genes contain a common C-terminal catalytic domain containing the 'PARP signature', a highly conserved region of 50 amino acids characterised by a NAD^+ acceptor site and residues essential for initiation, elongation and branching of the ADP ribose polymer (Oliver et al. 2004).

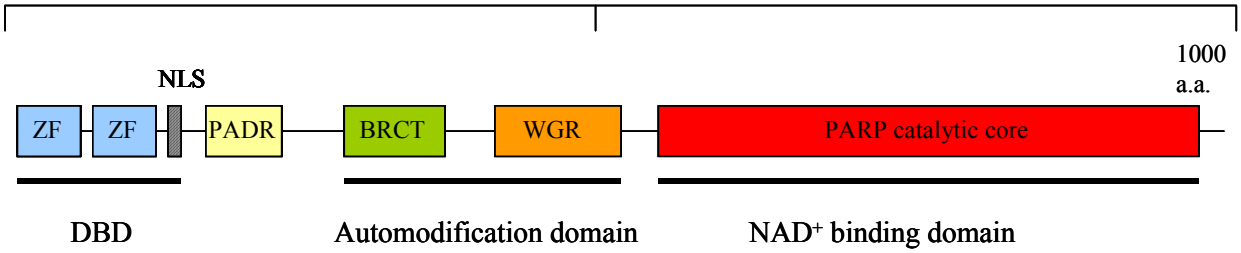

Figure 4.2 Structure of human PARP1. PARP1 from *Homo sapiens* shows three domains. The DNA binding domain (DBD) comprises of two zinc fingers and a nuclear localisation signal, the automodification domain consists of BRCT (Breast cancer 1 protein C-terminus) and a WGR rich region and a PARP catalytic domain. Between the DBD and automodification domain is the PADR domain.

Humans contain 18 different genes encoding PARP proteins illustrating the potential importance of poly ADP ribosylation in regulating cellular functions. The most characterised of the ADP ribosylation enzymes is human PARP-1. It displays a characteristic 3 domain structure including a DNA binding domain at the N-terminus followed by the automodification domain and the PARP catalytic domain at the C-terminus (see Figure 4.2; Kameshita et al. 1984)

These domains can be further split into modules. The DNA binding domain binds to single or double strand DNA through two zinc finger motifs. The zinc finger motifs are thought to recognize altered structures in DNA rather than particular sequences and are therefore act as a DNA damage sensor (Menissier-de Murcia et al. 1989). Research on the presence of two separate zinc finger motifs suggests very different roles with the first zinc finger stimulating

PARP activity to double and single DNA strand breaks and the second zinc finger may act exclusively to single DNA strand breaks (Gradwohl et al. 1990). Following the zinc finger domains is a nuclear localisation signal (KRK 207-211).

The automodification domain contains the BRCT region and the WGR domain. The BRCT domain (Breast cancer 1 protein C-terminus) found at residues 386-414 has not been studied extensively although several studies suggests it contains a weak leucine zipper motif and that its role is essential to auto-modification. The BRCT domain is found in many diverse DNA damage and cell cycle proteins suggesting this domain recognises phosphorylated peptides and mediates protein-protein interactions involved in cell cycle and DNA repair mechanisms. (Williams et al. 2003).

The WGR domain is characterised by the conserved central motif of tryptophan – glycine – argenine residues and is found in a variety of enzymes including polyA polymerases. This region has not been extensively characterised and its function is unknown although it may have DNA binding properties.

The PADR domain is found in poly ADPribose polymerases but the function of this domain is unknown.

The largest region of the PARP genes is the PARP minimal catalytic domain a 40kDa region involved in initiation, elongation and branching of ADP ribose polymers. The molecular mass of HsPARP1 is 55kDa. Although this is the active site of the enzyme the catalytic activity of this domain is not stimulated by DNA strand breaks. Also within this PARP minimal catalytic domain is the 'PARP signature' region of 50 amino acids (starting N907) characterised by a common NAD acceptor site and the residues essential for initiation, branching and elongation of poly ADP ribose polymers (Oliver et al. 2004).

4.3.2 Identification of AtPARP1 from sequence homology and BLAST

The first PARP in *A. thaliana* (PARP 1 AtPARP2) was identified by sequence homology to animal PARP proteins (Lepiniec et al. 1995). Whilst this gene contained the conserved C-terminal PARP catalytic domain it lacked the N-terminal zinc finger domains normally associated as the DNA break sensor. A second *A. thaliana* PARP sequence has been identified (AtPARP2) and transcripts of both PARP genes increased rapidly following ionising radiation (Doucet et al. 2001).

All PARP genes characterised encode a 40kDa catalytic domain shared amongst all PARP enzymes. This core catalytic domain sequence was used to interrogate the *A. thaliana* translated genome sequence using the BLAST algorithm (http://blast.ncbi.nlm.nih.gov/Blast.cgi and http://www.arabidopsis.org/Blast/index.jsp). As well as the 2 previously characterised PARP genes another putative PARP gene in *A. thaliana* was identified.

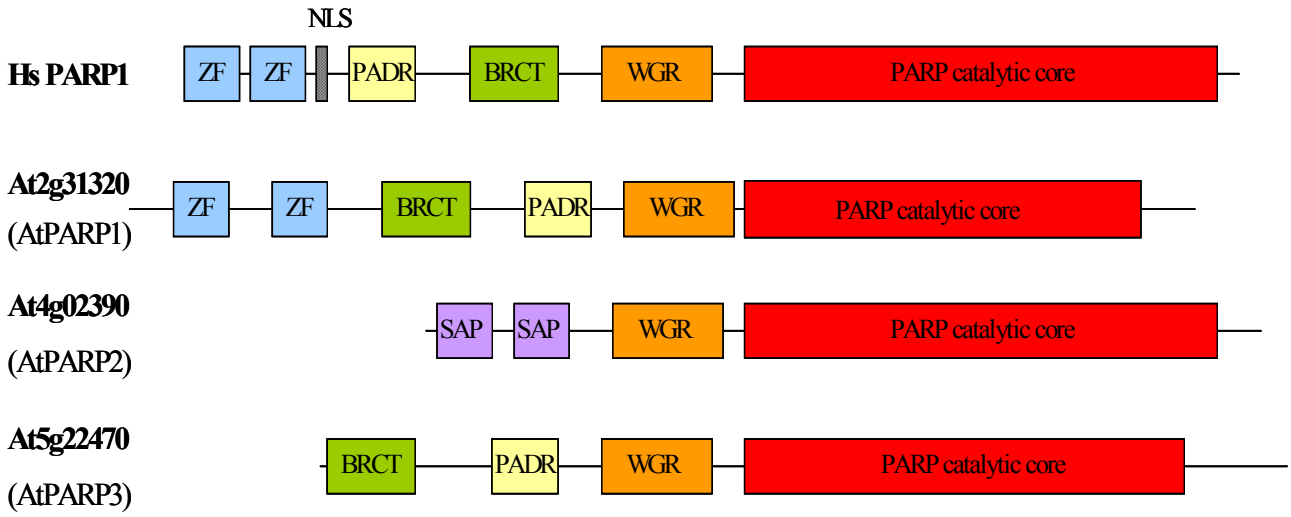

Figure 4.3 Domain architecture of the human PARP1 protein and three putative *A. thaliana* PARP sequences. ZF are two zinc finger domains, PADR is a domain found in ADP ribose synthetases, BRCT is the Breast cancer tumour repressor, WGR is the nucleic acid binding domain and the PARP catalytic domain comprises of the regulatory region of the enzyme. Two SAP domains are found on AtPARP3 at the N-terminal end.

As seen in Figure 4.3 all three *A. thaliana* PARP sequences contain very similar domains, each possess the domains for the automodification module (WGR domains) and the catalytic core. The nuclear localisation signal found in human PARP1 (KRK 207-211) is also found in AtPARP1 (AtPARP1) after the two zinc finger motifs at residues KRK 207-209.

One obvious difference is the presence of the two SAP domains in AtPARP2 (AtPARP2). The SAP domain (after SAF-A/B, Acinus and PIAS) is a putative DNA/RNA binding domain found in many nuclear and cytoplasmic proteins and has been shown to bind to scaffold attachment regions. It was first seen in PIAS sequences (protein inhibitors of activated STAT) which are thought to be transcriptional coregulators (Kotaja et al. 2002). The properties of DNA binding explains the increase in activity of AtPARP2 in response to ionising radiation despite the absence of zinc fingers (Doucet et al. 2001).

Collectively the domains and activities of PARP genes suggest important roles in a variety of nuclear functions.

Further analysis of the PARP active site reveals many similar features between *A. thaliana* PARPs and human PARP1. The active site of this protein contains a β-α-β-α loop motif responsible for NAD^+ binding. This domain spans amino acids 662-1014 and the crystal structure of the core catalytic domain in HsPARP1 shows an evolutionarily conserved glutamate residue (E970 in HsPARP1). Mutational studies of this residue decreased the enzyme activity to that of mono ADP ribosylation suggesting a role for this amino acid in chain elongation. (Ruf et al. 1996; Marsischky et al. 1995).

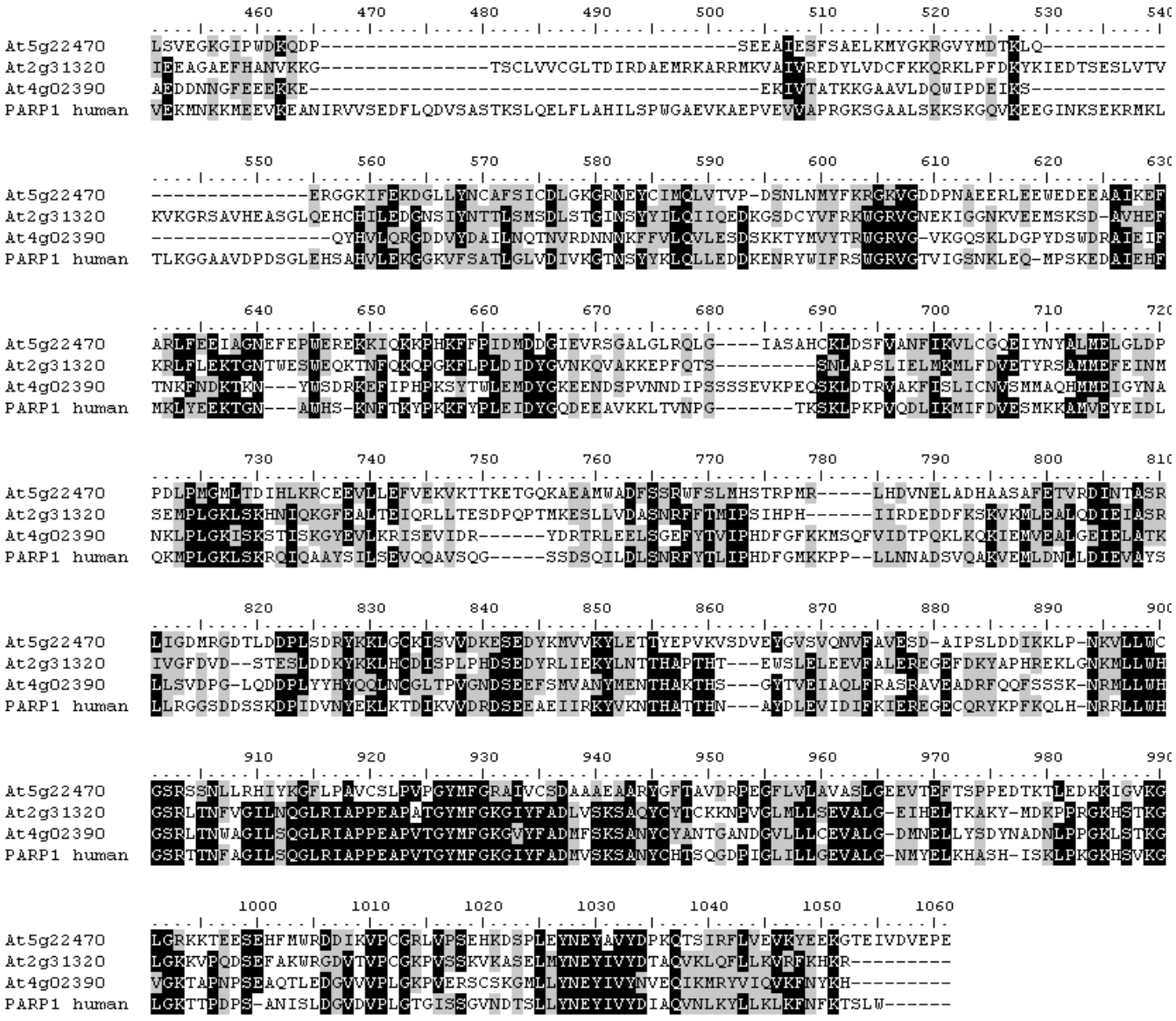

Figure 4.4 Sequence homology of HsPARP1 and three putative PARP proteins from *A. thaliana*. Sequence homology of PARP1 from *Homo sapiens*, two characterised PARPs from *A. thaliana* and one putative PARP sequence (AtPARP3). Sequence similarity of HsPARP1 protein to AtPARP2 showed 42% homology with 61% similarity, to AtPARP1 38% homology with 55% similarity, and to AtPARP3 27% homology with 45% similarity. Sequence alignments were performed in BioEdit with ClustalW.

The sequence alignments in Figure 4.4 show the area of most significant homology is the C-terminal catalytic core.

4.3.3 Analysis of PARP expression under stress conditions using SQRT-PCR and qPCR.

Gene transcript levels for a variety of stress conditions were first analysed using SQRT-PCR, which although only semi-qualitative, is fast and inexpensive. Treatments showing changes in transcript were then repeated using qualitative PCR (full method in Chapter 2.2.6 and list of treatments in Table 2.2).

Stress	**AtPARP3**					
Time point in hours	**0**	**2**	**4**	**8**	**24**	**48**
Salt	1.00	7.62	12.23	8.31	6.06	0.48
Mannitol	1.00	2.91	6.23	5.55	3.51	2.18
Hydrogen peroxide	1.00	NA	NA	NA	NA	NA
Abscisic acid	1.00	11.64	32.44	22.28	13.19	8.43
Ethylene (ACC)	1.00	0.95	2.09	NA	NA	NA
Auxin (NAA)	1.00	11.66	19.22	5.11	6.48	NA
Lipopolysaccharide	1.00	0.94	2.70	1.41	0.21	1.18
Jasmonic acid	1.00	0.80	1.06	1.96	1.28	1.09
Salicylic acid	1.00	0.80	1.84	0.50	1.55	1.04
Wounding	1.00	0.53	2.42	3.14	0.96	0.84
Phosphatase inhibitor	NA	NA	NA	NA	NA	NA
Kinase inhibitor	NA	NA	NA	NA	NA	NA
Cold treatment	NA	NA	NA	NA	NA	NA
Phosphate starvation	NA	NA	NA	NA	NA	NA
MMS	1.00	1.35	2.80	2.27	1.12	1.36
Bleomycin	1.00	3.55	5.66	4.57	2.22	2.37
UV-B	1.00	2.20	2.70	1.57	1.96	0.82

Table 4.4 Fold differences for AtPARP3 expression in response to stress conditions at 0, 2, 4, 6, 24, 48 hours. Transcript levels are expressed compared to actin expression. Samples were prepared in triplicate and results presented as averages. NA indicates where transcript levels were so low it was impossible to take an accurate reading of expression.

Gene expression levels for AtPARP3 in Table 4.4 showed increases with salt, mannitol, Abscisic acid, Auxin, MMS and Bleomycin in different degrees. However, they all showed the same temporal pattern with the largest increase seen between 0 and 2 hours and the highest level of transcript present at 4 hours. After 4 hours there was a decrease in gene expression although it never returned to the level before the addition of the stress condition. For example the result for Abscisic acid treatment showed the largest increase in expression to 11.6 fold between 0 and 2 hours, rising to 32 fold at 4 hours. This then decreased to 22 fold, 13 fold and 8 fold at time points 8, 24 and 48hours, respectively.

Stress	AtPARP1					
Time point in hours	**0**	**2**	**4**	**8**	**24**	**48**
Salt	1.00	1.06	1.16	1.07	1.10	0.62
Mannitol	1.00	0.75	0.82	0.76	1.04	0.81
Hydrogen peroxide	1.00	0.67	0.80	2.65	7.53	7.48
Abscisic acid	1.00	0.95	0.48	1.20	0.82	0.42
Ethylene (ACC)	1.00	1.09	1.18	1.13	1.19	0.50
Auxin (NAA)	1.00	0.95	0.84	0.82	0.76	0.40
Lipopolysaccharide	1.00	0.68	0.61	10.68	1.05	1.34
Jasmonic acid	1.00	0.92	1.22	1.19	1.19	0.60
Salicylic acid	1.00	0.88	0.89	0.98	1.02	0.64
Wounding	1.00	0.49	0.71	1.12	0.82	0.26
Phosphatase inhibitor	1.00	1.66	0.65	0.89	1.02	0.64
Kinase inhibitor (STA)	1.00	4.77	2.67	1.78	2.10	0.67
Cold treatment	1.00	1.26	1.88	1.20	1.16	1.01
Phosphate starvation	1.00	2.13	1.85	1.38	1.22	0.72
MMS	1.00	1.30	5.03	4.37	2.90	3.18
Bleomycin	1.00	2.90	5.47	3.81	3.13	3.95
UV-B	1.00	0.93	1.87	0.67	1.72	0.59

Table 4.5 Fold differences for AtPARP1 expression in response to stress conditions at 0, 2, 4, 6, 24, 48 hours. Transcript levels were expressed compared to actin expression. Three biological triplicates were performed and results presented as averages. NA indicates where expression was too low to be measured accurately.

The most significant increase in gene expression for At2g31329 is seen with MMS and Bleomycin. MMS shows an increase to 5 fold by 4 hours which remains high dropping to 3 fold by 48 hours. Bleomycin increases to nearly 3 fold within 2 hours and to 5.5 fold by 4 hours. This also remains high at 4 fold by 48 hours.

Stress	AtPARP2					
Time point in hours	**0**	**2**	**4**	**8**	**24**	**48**
Salt	1.00	1.95	2.13	1.76	1.75	1.52
Mannitol	1.00	2.09	1.77	1.76	1.65	1.61
Hydrogen peroxide	1.00	2.91	4.35	3.57	3.90	3.20
Abscisic acid	1.00	1.40	0.94	1.00	0.86	2.55
Ethylene (ACC)	1.00	1.11	1.20	1.01	1.22	0.43
Auxin (NAA)	1.00	1.01	1.17	0.88	0.62	0.47
Lipopolysaccharide	1.00	00.93	0.66	0.96	0.70	0.92
Jasmonic acid	1.00	0.60	0.82	0.64	0.57	0.37
Salicylic acid	1.00	0.61	0.95	0.82	0.62	0.51
Wounding	1.00	0.49	0.75	0.85	0.64	0.26
Phosphatase inhibitor	1.00	2.36	0.94	1.09	1.07	0.84
Cold treatment	1.00	1.82	2.09	0.93	1.01	0.84
Phosphate starvation	1.00	1.67	1.56	1.18	1.26	0.65
MMS	1.00	1.74	8.43	8.53	5.65	8.06
Bleomycin	1.00	7.01	15.87	9.53	10.21	12.61
UV-B	1.00	0.86	1.44	1.09	2.40	2.30

Table 4.6 Fold differences for AtPARP2 expression in response to stress conditions at 0, 2, 4, 6, 24, 48 hours. Transcript levels were expressed compared to actin expression. Samples were prepared in triplicate and results presented as averages. NA indicates where transcript levels were so low it was impossible to take an accurate reading of expression.

The most significant results for gene expression of AtPARP2 are also seen with MMS and Bleomycin. MMS increases to 8.4 fold by 4 hours, and although it falls to 5 fold at 24 hours it remains higher than before the addition of MMS. Bleomycin increases by 7 fold within the first 2 hours of treatment and increases to nearly 16 fold by 4 hours. Again, although this falls over the next hours it still remains high at 10 fold by 24 hours.

4.3.3 Quantitative PCR of PARP genes

4.3.3.1 With Abscisic acid

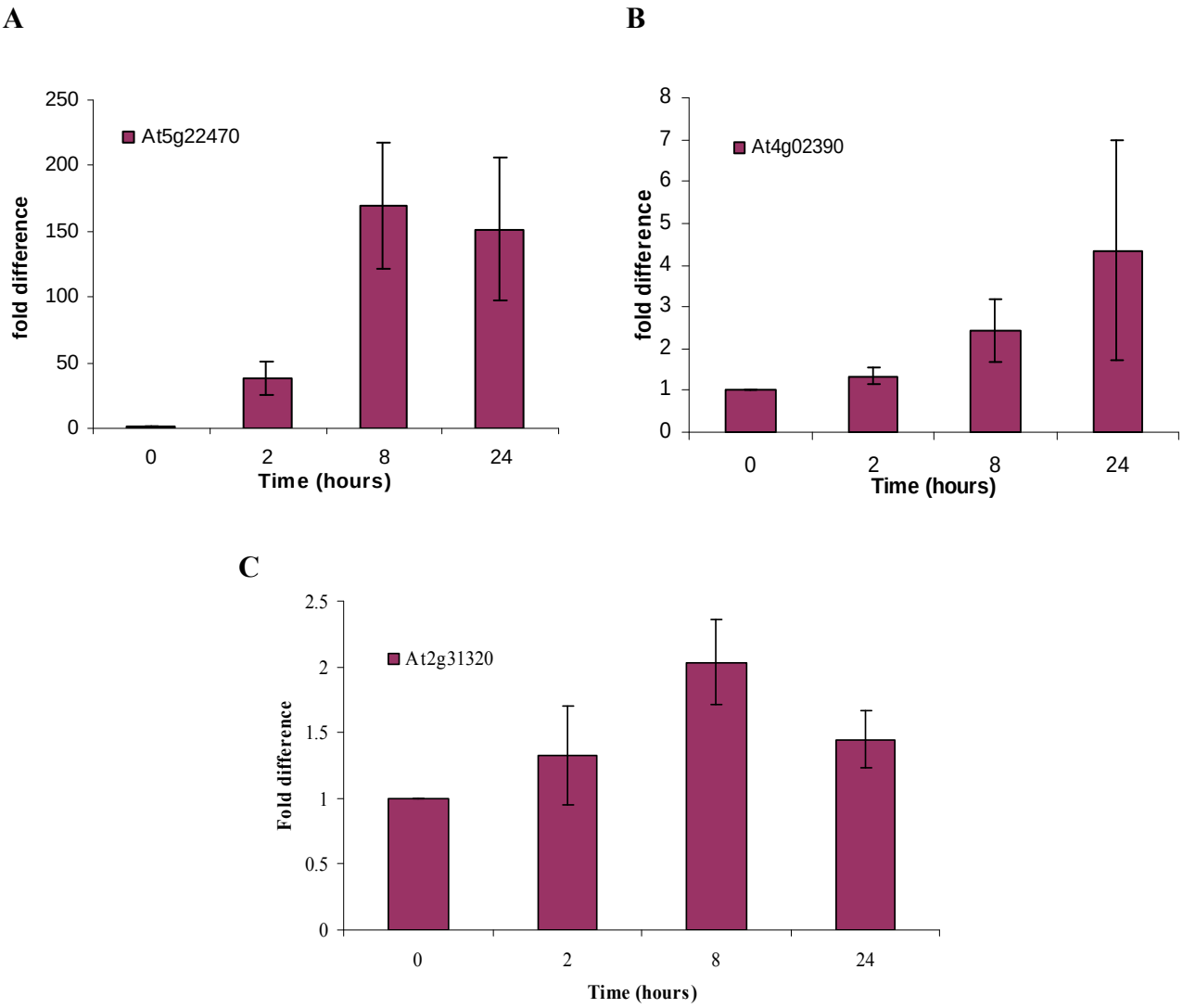

Figure 4.5 qPCR of PARP gene expression with exogenous ABA treatment. Fluorescence levels are expressed relative Actin expression **A**, qPCR of fold difference in transcript expression of AtPARP3. **B**, qPCR of AtPARP2. **C,** qPCR of AtPARP2. cDNA samples from each three biological replicates were analysed in triplicate and results given as averages and error bars indicate standard error.

Figure 4.5 shows the expression of AtPARP3 and AtPARP2 increased with Abscisic acid application but to very different degrees. AtPARP2 increases 5 fold by 24 hours but with a large variation. AtPARP3 expression increased dramatically to nearly 50 fold within the first

two hours and continued to 170 fold by 8 hours. There was a slight decrease by 24 hours to 150 fold.

4.3.3.2 Quantitative PCR of PARP genes with DNA damaging agent MMS.

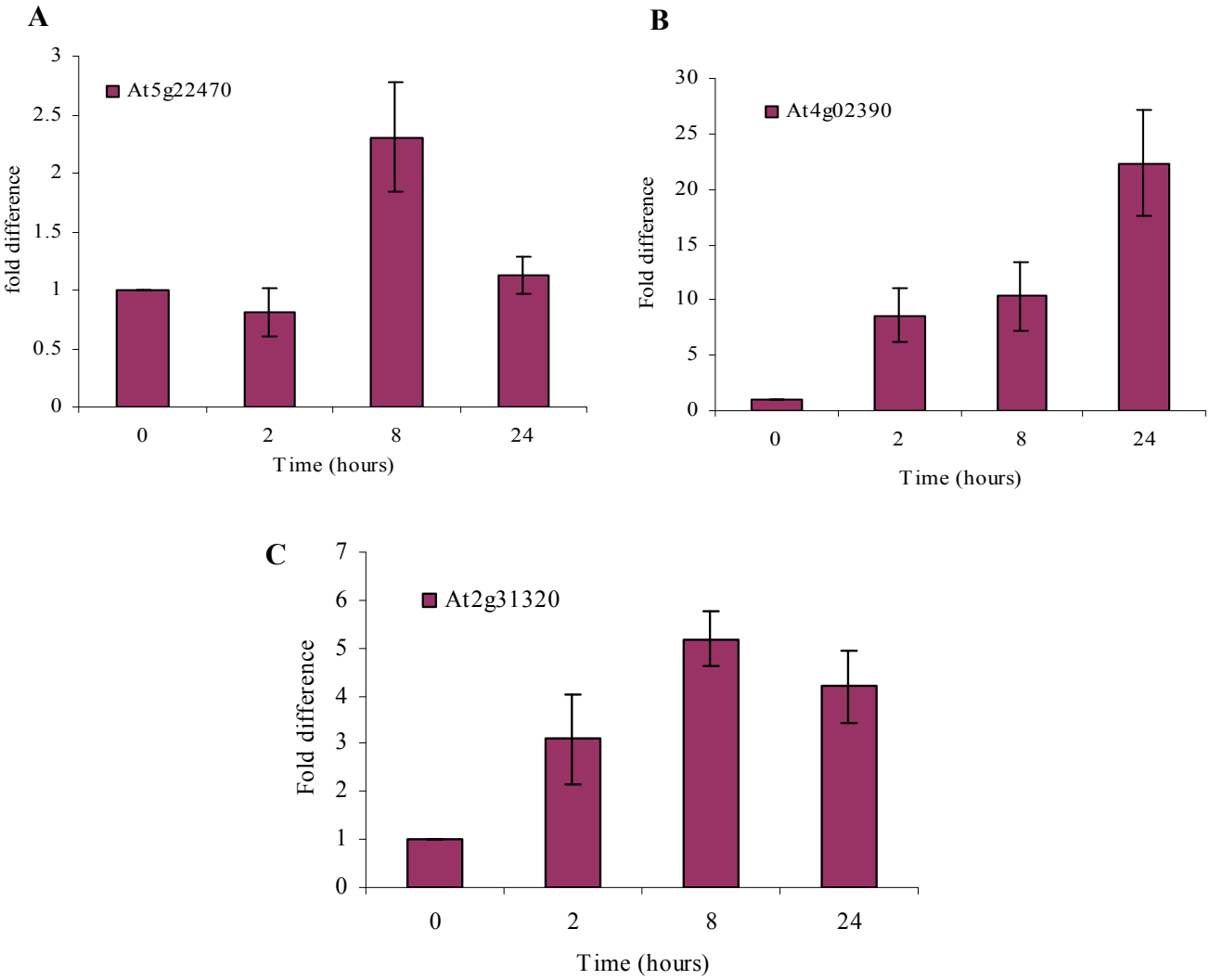

Figure 4.6 qPCR of PARP gene expression with exogenous MMS application.
Fluorescence levels are expressed relative Actin expression **A**, qPCR of fold difference in transcript expression of AtPARP3. **B**, qPCR of AtPARP2. **C**, qPCR of AtPARP2. Each of three biological replicates were analysed in triplicate and results presented as average. Standard error indicated by error bars.

The biggest increase was seen for AtPARP2, which increased by 8 fold within 2 hours and by 23 fold at 24 hours. Interestingly the transcript levels showed two main increases, the first within 2 hours and the second between 8-24 hours. AtPARP1 showed an increase with MMS

to 3 fold by 2 hours, 5 fold by 8 hours and 4 fold by 24 hours. There was no change in transcript level for AtPARP3.

4.3.3.3 Quantitative PCR of PARP genes with DNA damaging agent Bleomycin.

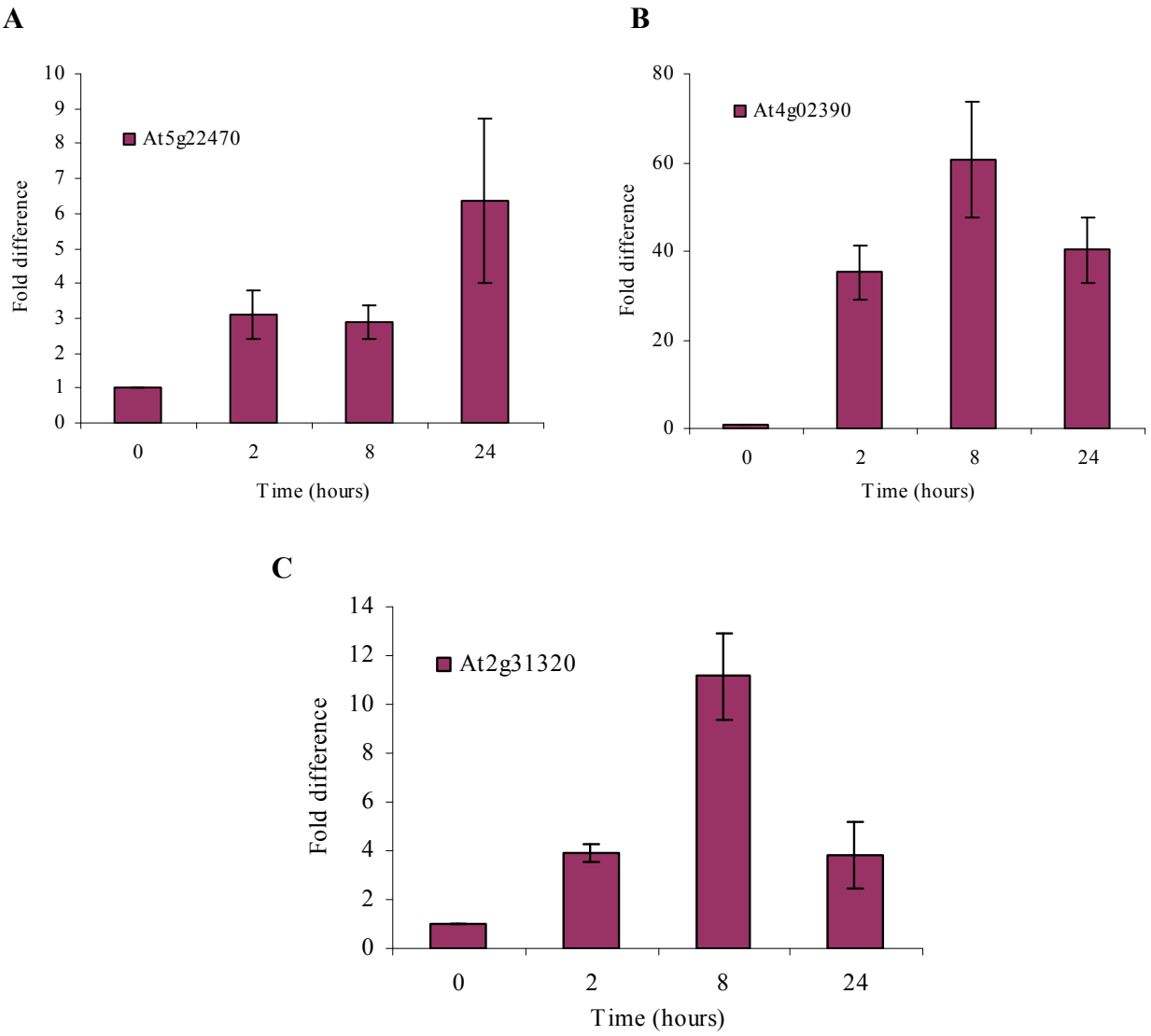

Figure 4.7 qPCR of PARP gene expression with Bleomycin. Fluorescence levels are expressed relative to Actin expression. **A,** qPCR of fold difference in transcript expression of AtPARP3. **B**, qPCR of AtPARP2. **C,** qPCR of AtPARP2. cDNA of each of three biological replicates were analysed in triplicate and averages presented. Error bars indicate standard error.

RT-PCR data showed that all three *A. thaliana* PARP gene expression increases in response to Bleomycin stress with the biggest increase in AtPARP2. The qPCR shown in Figure 4.7 shows the largest of the increases was seen within 2 hours of the addition of Bleomycin, up to

37 fold. Transcript level increased further to 60 fold by 8 hours before decreasing to 40 fold by 24 hours. The expression of AtPARP3 followed a different pattern, increasing to only 3 fold within 2 hours and then the largest increase between 8 and 24 hours to 7 fold. At3g31320 increased by 4 fold within the first 2 hours, 11 fold by 8 hours and then decreases to 4 fold at 24 hours after Bleomycin.

4.3.4 Identification of T-DNA insertion lines for *A. thaliana* plants.

In order to fully characterise the role of these putative PARP genes in *A. thaliana*, plant lines containing a 12kb T-DNA insertion within the respective PARP genes were acquired (Table 4.3 shows plant lines and the stock centre developed). These seeds were the T2 generation and confirmation of a homozygous insertion within the correct gene was performed using PCR. Primers were designed between the left border of the known T-DNA sequence and the gene of interest. Presence of an amplified band indicated an insertion within the gene. To confirm whether the insert was heterozygous or homozygous the gene was amplified over the point of T-DNA insert.

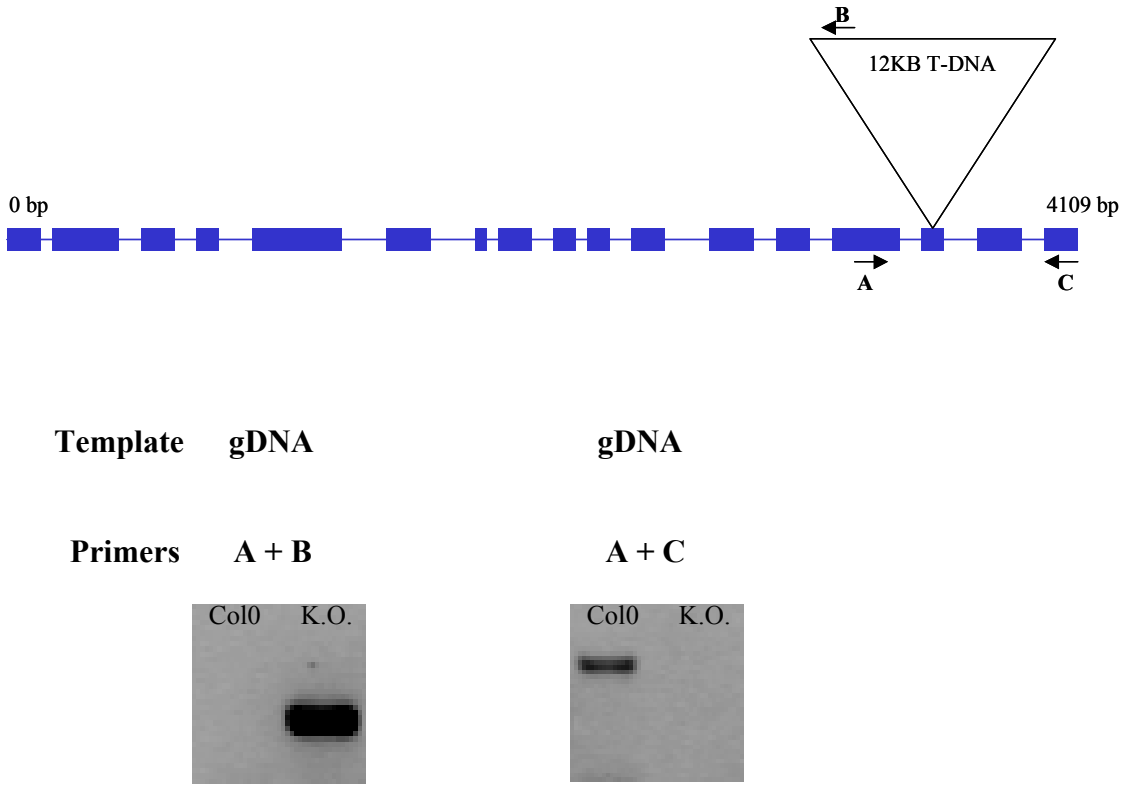

Figure 4.8 Identification of *A. thaliana* homozygous AtPARP2 null line by PCR genotyping. Schematic diagram of 12 kb T-DNA insertion within gene of interest and primer combinations for identifying lines containing insertion. Gel electrophoresis of PCR on genomic DNA extracted from *A. thaliana* Col0 and GK420G03 lines with primers amplifying from T-DNA insertion to AtPARP2 gene.

The presence of an amplified band from the T-DNA fragment into the AtPARP2 gene shows the plant has the T-DNA insertion. The absence of an amplified fragment of the PARP gene over the point of insertion suggests that the plant is homozygous for the T-DNA insertion.

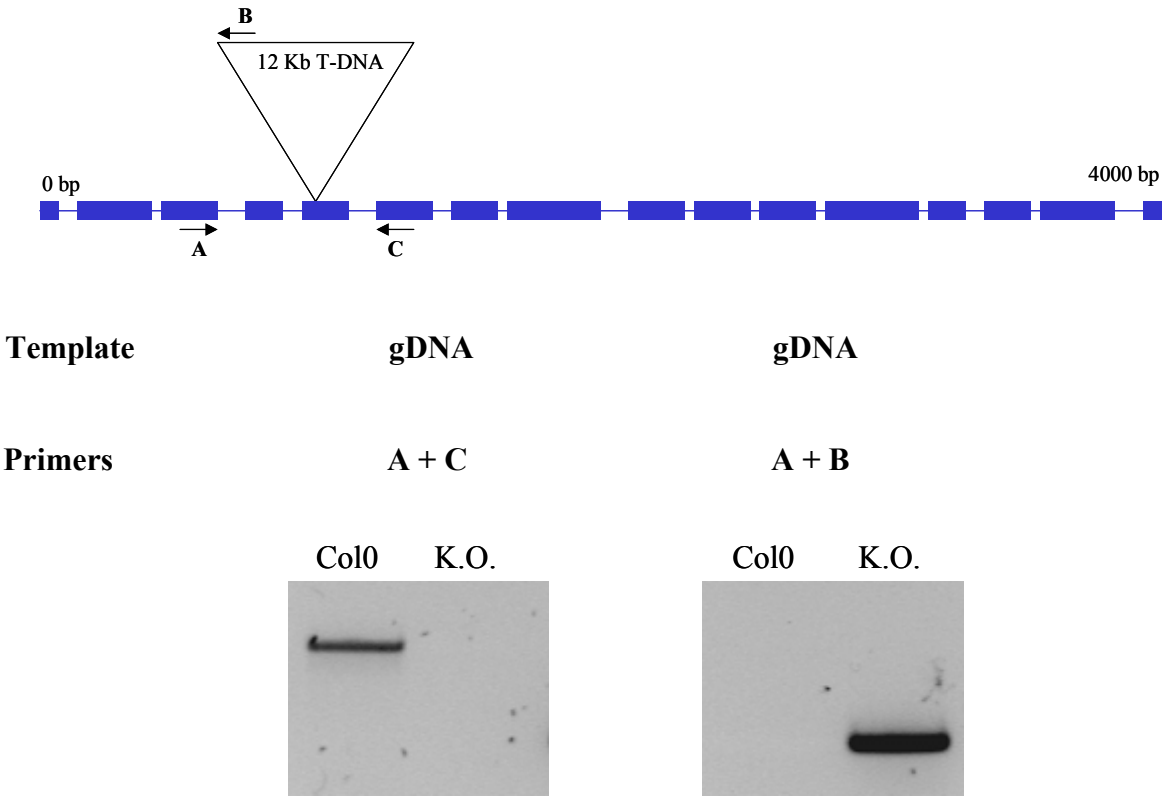

Figure 4.9 Identification of *A. thaliana* homozygous AtPARP1 null line using PCR genotyping. Schematic diagram of 12 kb T-DNA insertion within gene of interest and primer combinations for identifying lines containing insertion. Gel electrophoresis of PCR on genomic DNA extracted from *A. thaliana* Col0 and GK380E06 (KO) lines with primers amplifying from T-DNA insertion to AtPARP1 gene.

The presence of an amplified band from the T-DNA into the AtPARP1 gene showed that the KO plant contained the T-DNA insert. Primers designed over the site of T-DNA insertion showed a band for Col0, which was absent in the KO. This suggested that the KO was homozygous for the T-DNA insert.

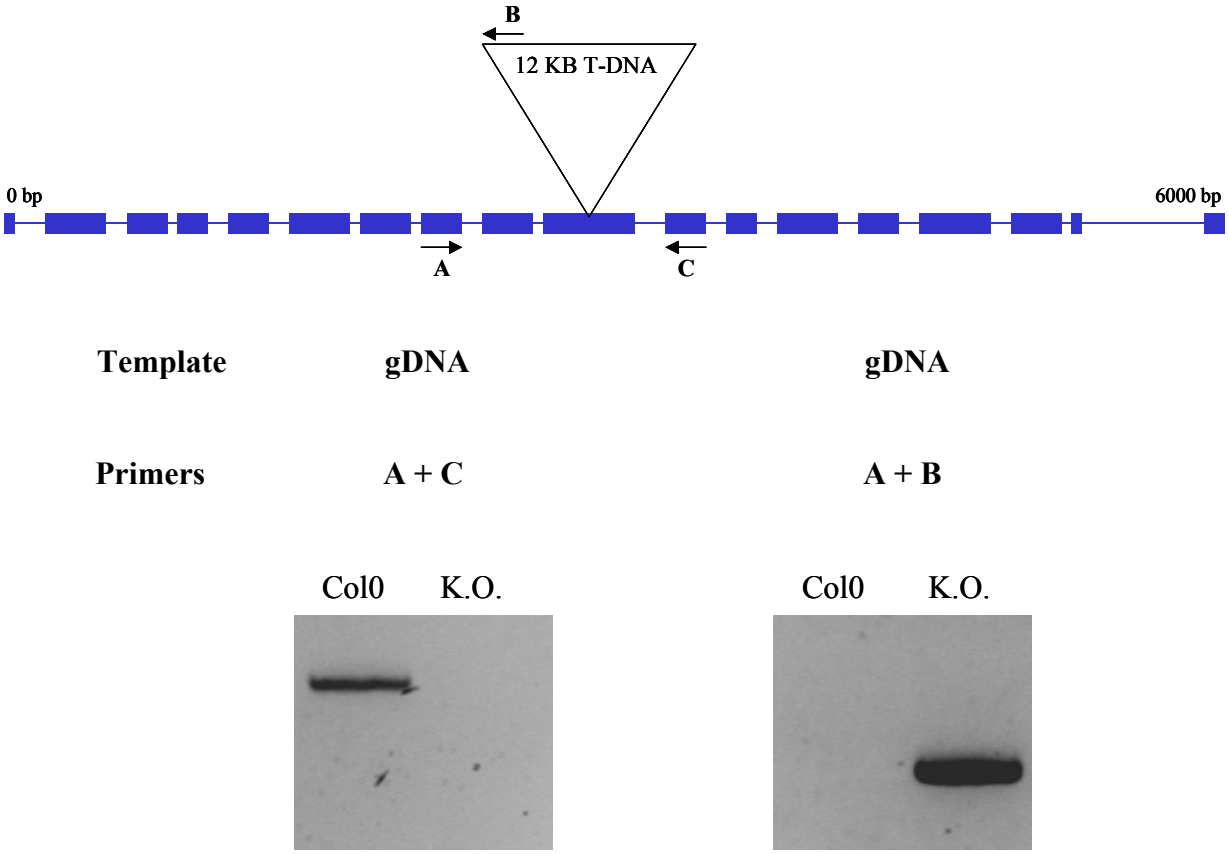

Figure 4.10 Identification of homozygous AtPARP3 null line using PCR genotyping. Schematic diagram of 12 kb T-DNA insertion within gene of interest and primer combinations for identifying lines containing insertion. Gel electrophoresis of PCR on genomic DNA extracted from *A. thaliana* Col0 and N653425 (KO) lines with primers amplifying from T-DNA insertion to AtPARP3 gene.

Gel electrophoresis showed a band for AtPARP3 in *A. thaliana* Col0 but not the T-DNA knockout (KO) line. Primers between the T-DNA insertion and AtPARP3 gene only amplified DNA in the T-DNA line. This suggested that the knockout line was homozygous for the T-DNA insertion in AtPARP3.

4.3.5 Phenotypes of *A. thaliana* PARP null lines.

PARP null lines were grown alongside Col0 in both long and short day conditions and leaf size and number, day of bolt and flowering were observed. There was no difference in the growth of the null lines compared with Col0.

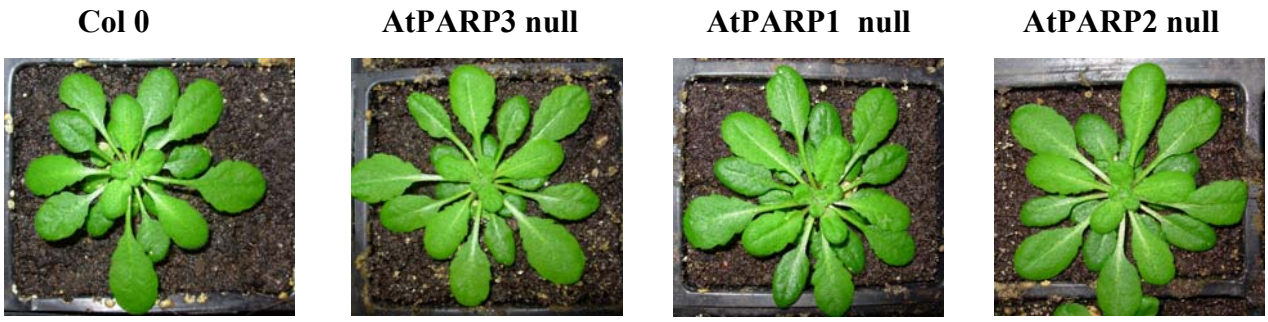

Figure 4.11. Photographs of plants of Col0 and PARP null lines. Plants were grown in long day conditions and photographs taken after 26 days.

4.3.6 Phenotypes of PARP null lines treated with DNA damaging agents.

From the RT-PCR and qPCR results the expression of PARP genes was greatly increased in the presence of DNA damaging chemicals. Therefore PARP T-DNA insertion lines were grown in media containing MMS and Bleomycin to analyse for differences in tolerance of DNA damage.

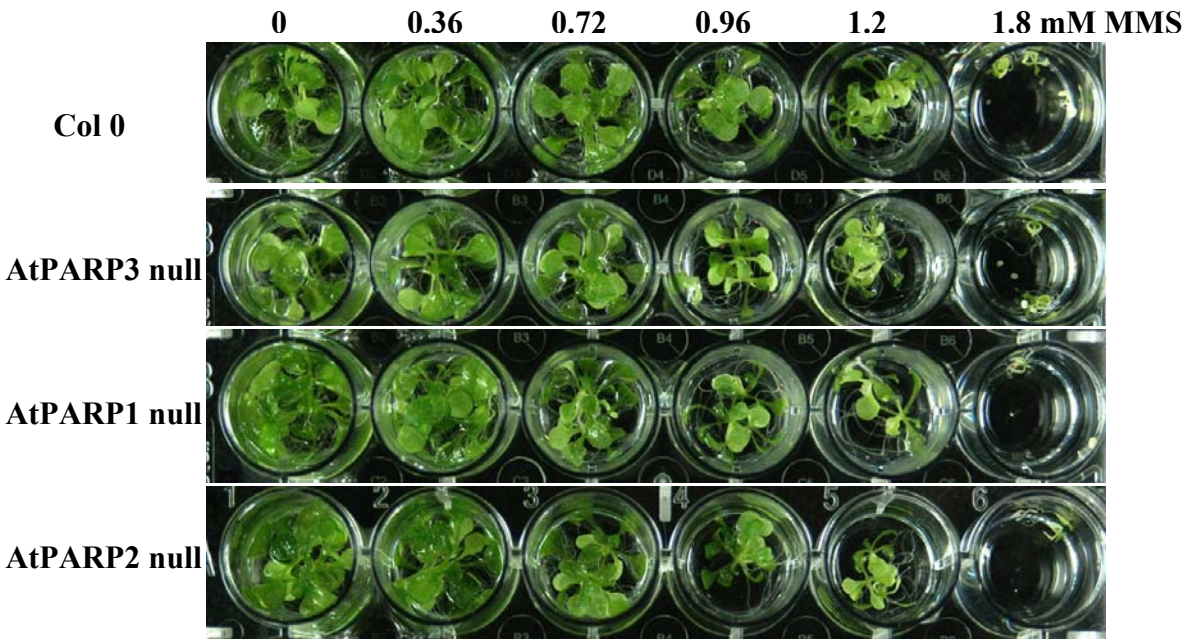

Figure 4.12. Photographs of Col0 and PARP T-DNA insertion plants grown in DNA damaging chemical MMS. Seeds were germinated on MS plates for one week before transferring 3 seedlings into each well with media containing MMS (0, 0.36, 0.72, 0.96, 1.2, 1.8mM MMS left to right) and grown for a further two weeks.

None of the PARP null lines showed any clear difference from Col0 in tolerance or susceptibility in the presence of either MMS (Figure 4.12). Similar results were obtained with Bleomycin and UV-B treatment (data not presented).

PARG genes in *A. thaliana*.

4.3.6 Identification of two PARG genes in *A. thaliana*

PARG enzymes catalyse the removal of poly ADPribose polymers allowing the acceptor protein to return to its unmodified state, and producing free ADP-ribose.

Although the activity was discovered 30 years ago (Miwa & Sugimura 1971)the protein was not purified until 1986 probably due to its high sensitivity to proteases (Hatakeyama et al. 1986). The protein has since been purified from a variety of different organisms and tissues but shows considerable variation in activity, localisation and molecular weight. In 1997 a

gene from humans encoding an enzyme with poly ADPribose glycohydrolase activity was identified and when the protein was expressed in *E. coli* it yielded two active enzymes at both 58kD and 110kD (Lin et al. 1997a; Amé et al. 1999).

To date only one PARG enzyme has been identified in humans, (Meyer et al. 2003; Meyer et al. 2007), bovine (Lin et al. 1997a), mice (Cortes et al. 2004), rat (Shimokawa et al. 1999) and *D. melanogaster* (Uchida et al. 1993) and although different isoforms of the protein are found in each of these organisms. Only *C. elegans* (Gagnon et al. 2002) and *A. thaliana* each contain 2 functional PARG genes (Panda et al 2002).

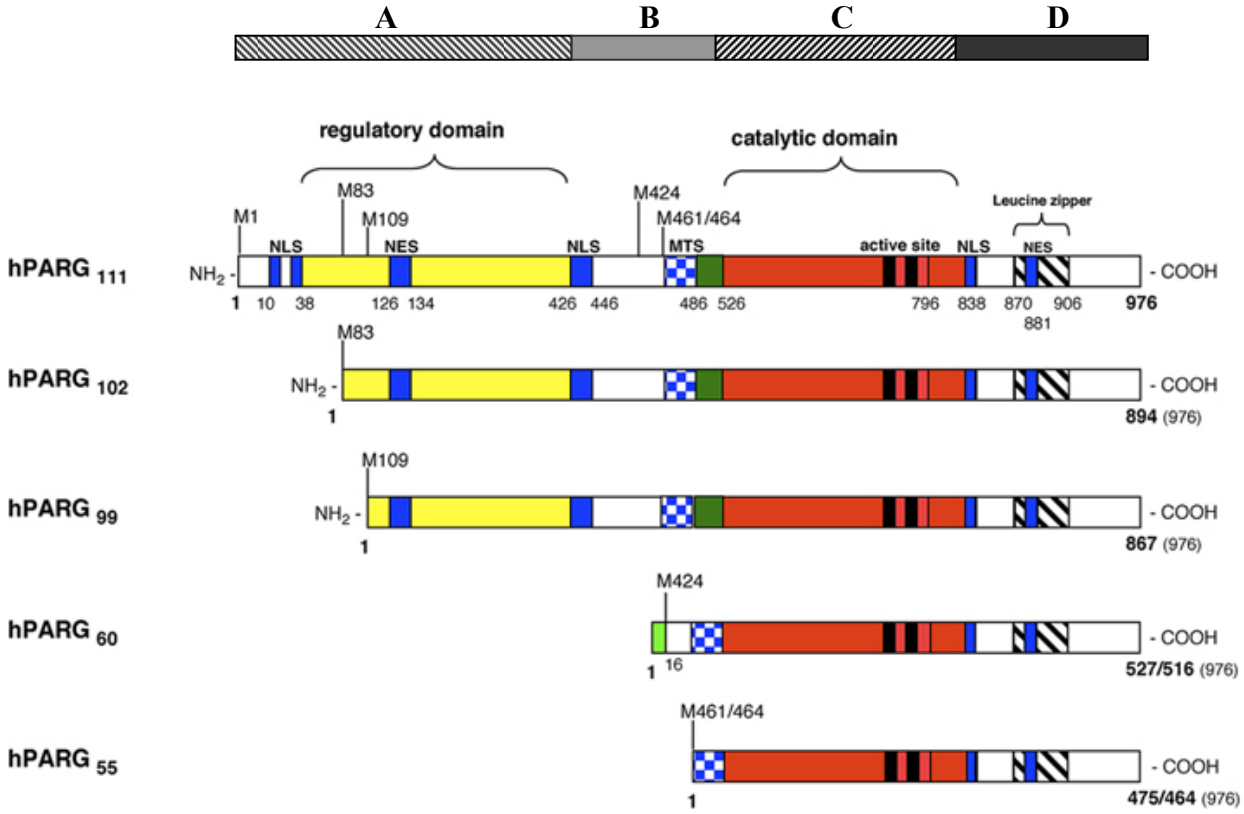

Figure 4.13 Domain architecture of five human PARG isoforms. HsPARG shows two main domains, regulatory domain A and the catalytic domain (made up of domains B, C and D). NLS: nuclear localisation signal and NES: Nuclear export signal found in isoforms PARG kDa 111, 102 and 99. MTS: mitochondrial targeting sequence. PARG 60 contains different N-terminal protein sequences not found in other isoforms. The active site includes conserved residues E728, E738, E756, E757 and T995. (Figure taken from Hassa & Hottiger 2008).

PARG proteins contain 2 main domains (seen in Figure 4.13), a regulatory domain (region A) and a catalytic domain (comprising of motifs B, C and D). This catalytic domain is

characterised by three sections with B and D having an α helical structure and region C predominantly β sheet (Meyer et al. 2003). Throughout all species the region of highest similarity is located at the C-terminus and investigations into the activity of PARG enzymes links this region to the catalytic domain (Amé et al. 1999). The main differences in the five human PARG gene splice variants are seen in the N-terminal regulatory domain. Within this domain a putative nuclear localisation signal (NLS) at amino acid 422-447 (the sequence of which shows sequence similarity to PARP1 NLS) and a nuclear export signal (NES) are observed (Lin et al. 1997b).

In 2002 a screen for genes involved in regulating the circadian clock identified a mutant with a longer period length that affects the transition from the vegetative to flowering development (Panda, Poirier, & Kay 2002). The lesion in this mutant was identified through map based cloning and found to be in AtPARG1 (AtPARG1), a putative PARG gene. The PARG sequence was used to interrogate the *A. thaliana* translated genome sequence using the BLAST algorithm (http://blast.ncbi.nlm.nih.gov/Blast.cgi and http://www.arabidopsis.org/Blast/index.jsp). Another putative PARG gene in *A. thaliana* was identified at At2g31865 (AtPARG2).

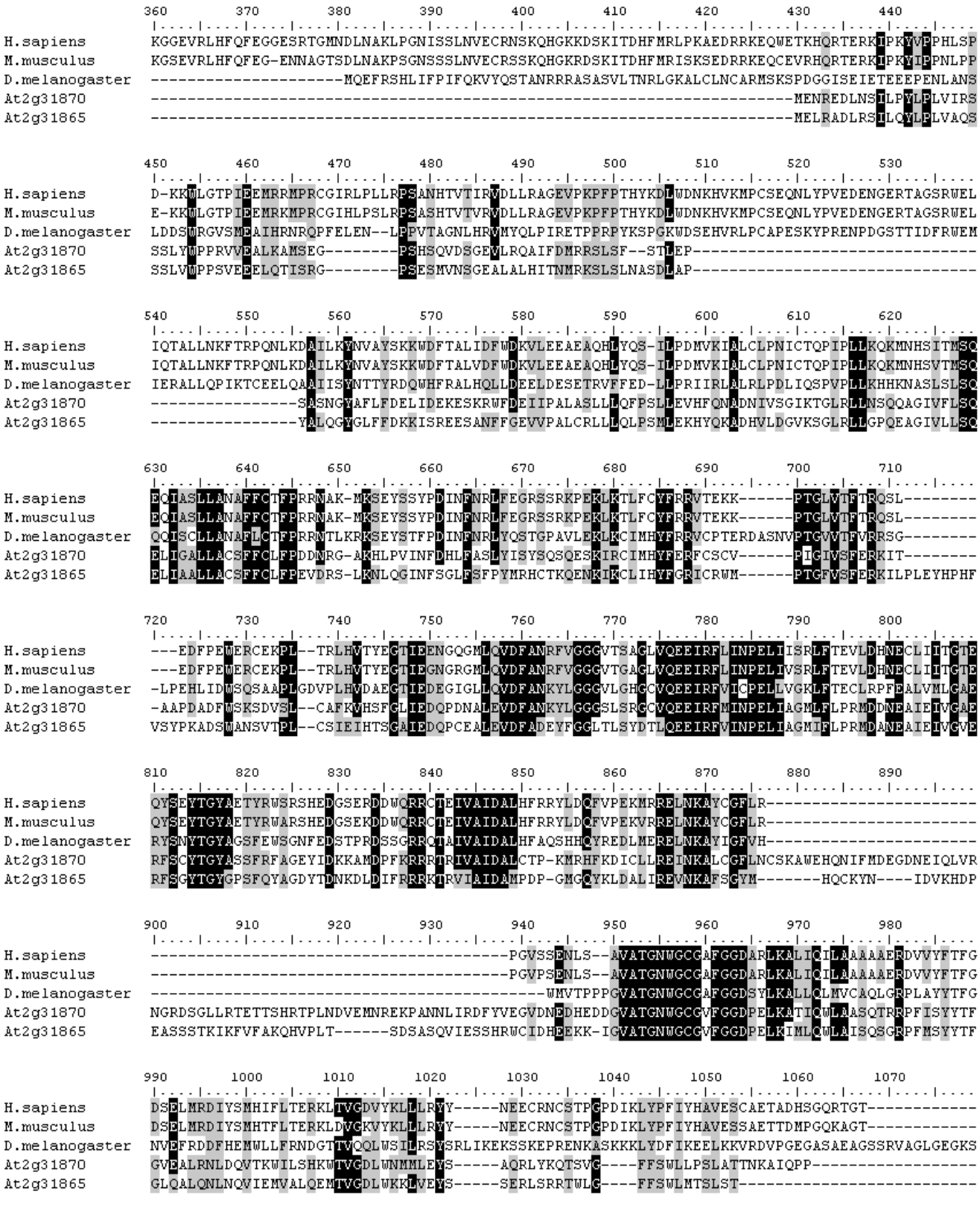

Figure 4.14 Sequence homology of putative *A. thaliana* PARGs. Sequence homology of PARGs from *H. sapiens* (NM003631), *M. musculus* (NM011960) *and D. melanogaster* (NM057973) with AtPARG1 and AtPARG2. Sequence homology of AtPARG2 to *H. sapiens* is 30% with a similarity of 49% at amino acid level, to *D. melanogaster* 32% with 49% similarity, and to *M. musculus* 30% with 49% similarity.

Through mutational analyses three motifs have been identified that are vital for PARG function; these are VDFAN (residues 758-762), a glycine rich sequence of GGG (residues 766-768) and QEE (residues 776-768; Patel et al. 2005). All of these are present in the two *Arabidopsis* PARG proteins (see Figure 4.14), although AtPARG2 contains only two of the three glycine residues (766-767). All of these important sequences are found in region C of the catalytic domain. Also present is the tyrosine residue at 814 which is essential for binding of the potent PARG inhibitor 8-(aminohexyl)amino-ADP-HPD (Koh DW et al. 2003). The five human PARG gene splice variants show differences in the N-terminal regulatory domain containing a NLS and NES. However this N-terminal regulatory region of PARG is completely absent in the putative *A. thaliana* PARG genes.

4.3.6.1 Analysis of AtPARG1 expression under stress conditions using SQRT-PCR

A. thaliana Col0 seedlings were exposed to a variety of stress treatments and transcript levels of PARG genes were measured using RT-PCR (see Chapter 2.2.6 and 4.2.1 and Table 2.2 for full list of treatments).

Stress	**AtPARG1**					
Time point in hours	**0**	**2**	**4**	**8**	**24**	**48**
Salt	1.00	1.02	0.96	0.99	0.92	0.18
Mannitol	1.00	0.85	0.91	1.47	2.19	1.97
Hydrogen peroxide	1.00	0.49	0.53	0.67	0.29	0.52
Abscisic acid	1.00	0.96	0.56	0.42	0.74	0.58
Ethylene (ACC)	1.00	0.66	0.69	0.25	0.23	0.20
Auxin (NAA)	1.00	0.92	1.03	0.23	0.67	NA
Lipopolysaccharide	1.00	1.68	1.16	0.72	0.57	0.61
Jasmonic acid	1.00	0.71	0.68	0.62	0.57	0.44
Salicylic acid	1.00	1.54	1.66	1.43	1.00	0.47
Wounding	1.00	0.72	0.99	0.83	0.85	0.18
Phosphatase inhibitor	1.00	0.86	0.71	0.24	0.32	0.46
Kinase inhibitor (STA)	1.00	3.18	2.16	2.26	1.69	0.99
Cold treatment	1.00	1.00	1.78	0.86	0.98	0.96
Phosphate starvation	1.00	3.59	4.43	2.07	1.14	0.32
MMS	1.00	1.35	2.80	2.27	1.12	1.36
Bleomycin	1.00	3.55	5.66	4.57	2.22	2.37
UV-B	1.00	2.20	2.70	1.57	1.96	0.82

Table 4.7 Fold differences in AtPARG1 expression in response to stress conditions at 0, 2, 4, 6, 24, 48 hours. Transcript levels are expressed compared to actin expression. Samples were taken from three separate biological replicates and results presented as averages. NA indicates expression levels were too low to measure accurately.

The most significant of the results in Table 4.7 for gene expression of AtPARG1 was seen with the application of DNA damaging agents MMS, Bleomycin and UV-B light exposure. With Bleomycin the levels of cDNA increased by 3.5 fold in the first 2 hours and by 5.6 by 4 hours. This decreased but remained high at 4.5 fold by 8 hours before decreasing further to 2.3 at 24 hours. MMS and UV-B exposure showed a similar pattern with the highest levels seen at 4 hours after exposure (2.8 fold for MMS and 2.7 for UV-B) although this level decreased to untreated level by 48 hours. An increase was also seen with phosphate starvation. This experiment was performed over a 24 hour period of phosphate starvation followed by phosphate resupply at which point the timed samples were taken. Within 2 hours of phosphate resupply there was an increase in AtPARG1 transcript level to 3.5, which increased to 4.4 by 4 hours. Transcript level decreased to 2 and 1 at 8 hours and 24 hours respectively. There was a slight decrease in gene expression with hydrogen peroxide, Abscisic acid, ethylene and Jasmonic acid, where the amount of transcript falls to half of the untreated samples within the first 2 hours. This then remained low until 48 hours after treatment.

4.3.6.2 Analysis of AtPARG2 expression under stress conditions using SQRT-PCR

Stress	At2PARG2					
Time point in hours	**0**	**2**	**4**	**8**	**24**	**48**
Salt	1.00	1.77	2.30	2.50	3.46	1.67
Mannitol	1.00	1.05	1.10	1.35	1.27	1.18
Hydrogen peroxide	1.00	1.09	1.02	1.53	0.74	0.52
Abscisic acid	1.00	1.84	0.96	1.23	1.27	1.18
Ethylene (ACC)	1.00	.81	1.21	1.01	0.71	0.61
Auxin (NAA)	1.00	1.03	1.31	1.10	0.66	0.61
Lipopolysaccharide	1.00	0.83	1.03	0.91	0.80	0.87
Jasmonic acid	1.00	1.53	1.93	1.48	1.11	3.16
Salicylic acid	1.00	1.86	2.61	2.96	2.16	2.15
Wounding	1.00	1.67	1.42	1.04	0.80	2.17
Phosphatase inhibitor	1.00	1.68	0.88	0.76	0.87	1.06
Kinase inhibitor (STA)	1.00	5.79	2.79	1.52	3.08	0.84
Cold treatment	1.00	0.80	1.60	1.10	0.94	0.84
Phosphate starvation	1.00	2.42	1.94	0.64	0.57	0.14
MMS	1.00	2.34	3.85	4.26	2.45	2.96
Bleomycin	1.00	2.36	4.00	3.24	2.60	3.04
UV-B	1.00	1.20	2.30	1.39	3.71	3.53

Table 4.8 Fold differences for AtPARG2 in response to stress conditions at 0, 2, 4, 6, 24, 48 hours. Transcript levels were expressed in relation to actin expression. Experiment was repeated from three biological replicates and results presented as averages. NA denotes levels of expression were too low to measure accurately.

Table 4.8 shows the most significant changes in transcript level were seen with the addition of MMS, Bleomycin and UV-B light exposure although the patterns of expression were different. For MMS the levels increased to 2.3 fold by 2 hours, 3.8 by 4 hours to the highest point of expression of 4.2 fold at 8 hours. This then decreased to 2.4 by 24 hours and then

increased slightly to 3 fold at 48 hours. With the application of bleomycin the highest expression of 4 fold was seen at 4 hours and this then decreased to 3.2 by 8 hours and 2.6 by 24 hours, followed by an increase to 3 fold at 48 hours. UV-B light exposure showed a steady increase in gene expression with the highest level of 3.7 at 24 hours, which decreased to 3.5 by 48 hours. There was also a slight increase in gene expression with salt, increasing to a 1.77 fold by 2 hours, 2.3 by 4 hours and 3.46 by 8 hours. This then decreased to 1.67 by 48 hours.

4.3.7 Expression of PARG genes using qPCR.

4.3.7.1 Transcript level of PARG genes with DNA damaging agent MMS.

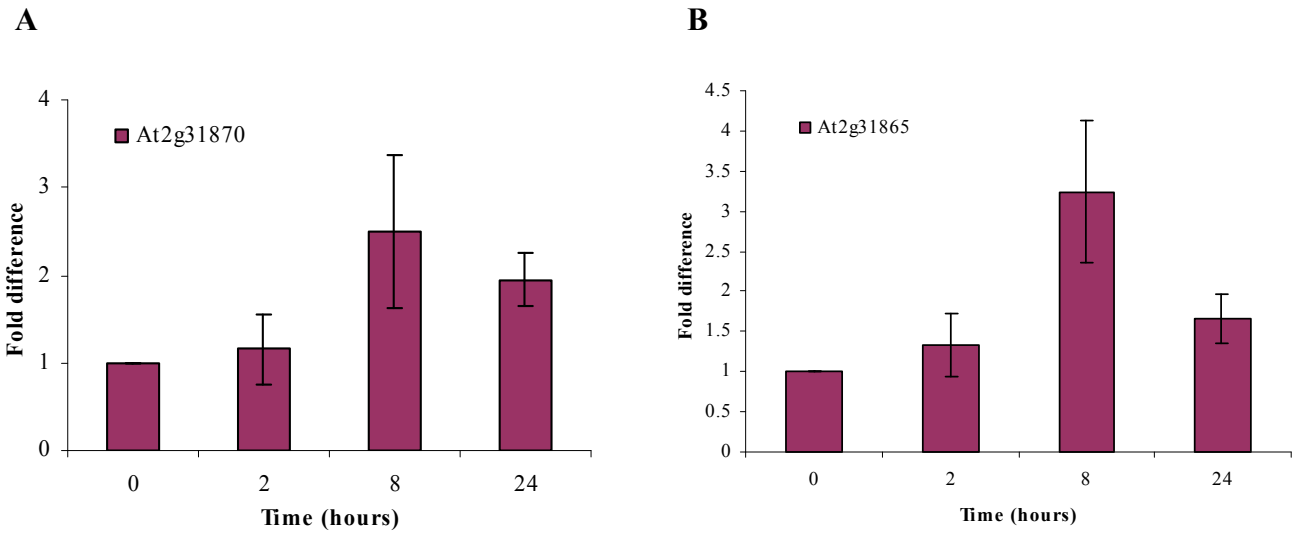

Figure 4.15 Quantitative PCR of PARG gene expression with MMS treatment.
Fluorescence levels were expressed relative to actin **A**, qPCR of fold difference in transcript levels of AtPARG1. B qPCR of AtPARG2. cDNA samples for each of the three biological replicates were repeated in triplicate and presented as averages. Standard error is indicated by error bars.

Expression of both of the *A. thaliana* PARG genes increased in response to MMS by 2.5-3 fold. It is interesting that the main increase in expression is seen between the time points 2 and 8 hours. By 24 hours the expression has decreased to nearly that of before the addition of MMS.

4.3.7.2 Transcript levels of PARG gene expression with Bleomycin treatment.

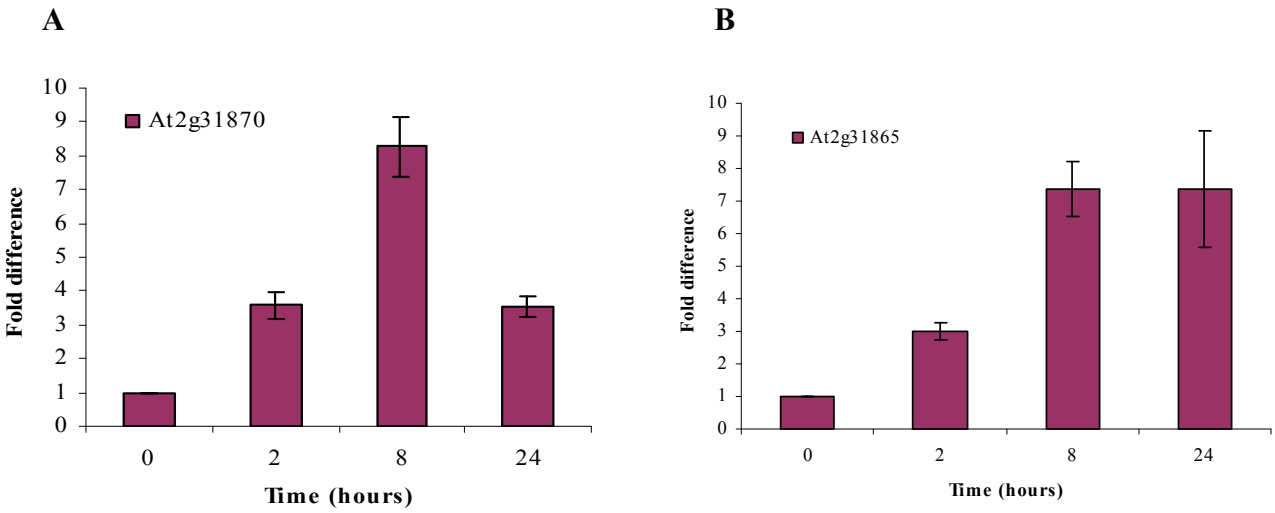

Figure 4.16 Quantitative PCR of PARG gene expression with exogenous ABA treatment. Fluorescence levels are expressed relative Actin expression **A**, qPCR of fold difference in transcript expression of AtPARG1. **B**, qPCR of AtPARG2. cDNA samples from each three biological replicates were analysed in triplicate and results given as averages and error bars indicate standard error.

Expression of both *A. thaliana* PARG genes increased significantly after addition of Bleomycin. Both genes increased by about 3.5 fold within 2 hours and to 8 fold by 8 hours. However at 24 hours AtPARG2 remained high at an 8 fold increase compared to AtPARG1 at 24 hours, which reduced to 3 fold. The largest of the increases in transcript was seen between 2 and 8 hours. This pattern was the same as seen in the previous RT-PCR data (Tables 4.7 and 4.8).

4.3.7.3 Transcript level of PARG genes with UV-B light exposure

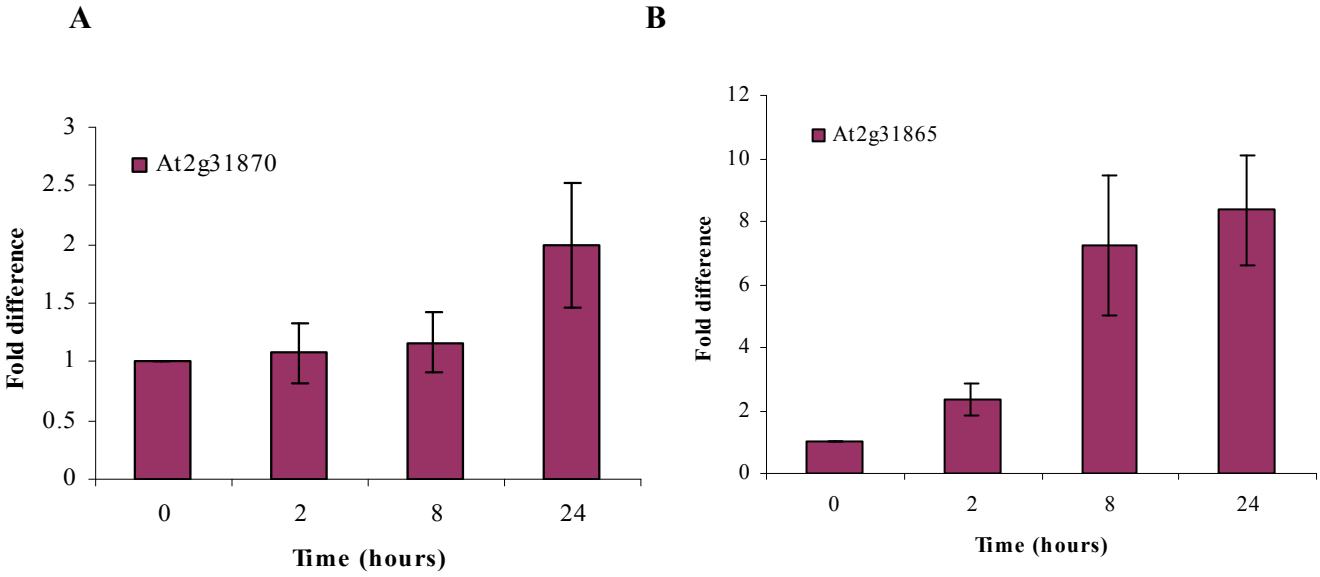

Figure 4.17 Quantitative PCR of PARG gene expression with exposure to UV-B light. Fluorescence levels are expressed relative Actin expression A. qPCR showing fold difference in transcript level of AtPARG1. B. qPCR of AtPARG2. Fluorescent levels were compared to actin. cDNA samples from each three biological replicates were analysed in triplicate and results given as averages and error bars indicate standard error.

Both genes showed very different responses to UV-B stress with AtPARG1 showing no difference in gene expression. However AtPARG2 increased to 2 fold by 2 hours, 7 fold by 8 hours and at 24 hours expression increased by 8 fold. It is interesting that for Bleomycin and MMS both genes showed very similar patterns of expression as well as similar fold differences at the same time points.

4.3.8 Identification of *A. thaliana* PARG null lines.

Three *A. thaliana* plant lines were obtained with 12 kb T-DNA insertions in each PARG gene (shown in Table 4.9). Plants that were homozygous for the T-DNA insertion were identified by PCR using primers designed to the T-DNA sequence and the PARG gene. RNA was extracted from plants and cDNA synthesized, and the absence of a PCR amplification product confirmed no transcript was present (described in Chapter 2.2.19 and 4.5.4)

Gene name and number	Insertion line	Stock centre
AtPARG1	SALK 116088	SALK
AtPARG2	GK 072 B04	GabiKat

Table 4.9 *A. thaliana* T-DNA insertion lines for PARP and PARG genes and the companies where they were generated.

4.3.8.1 Identification of *A. thaliana* AtPARG1 null lines.

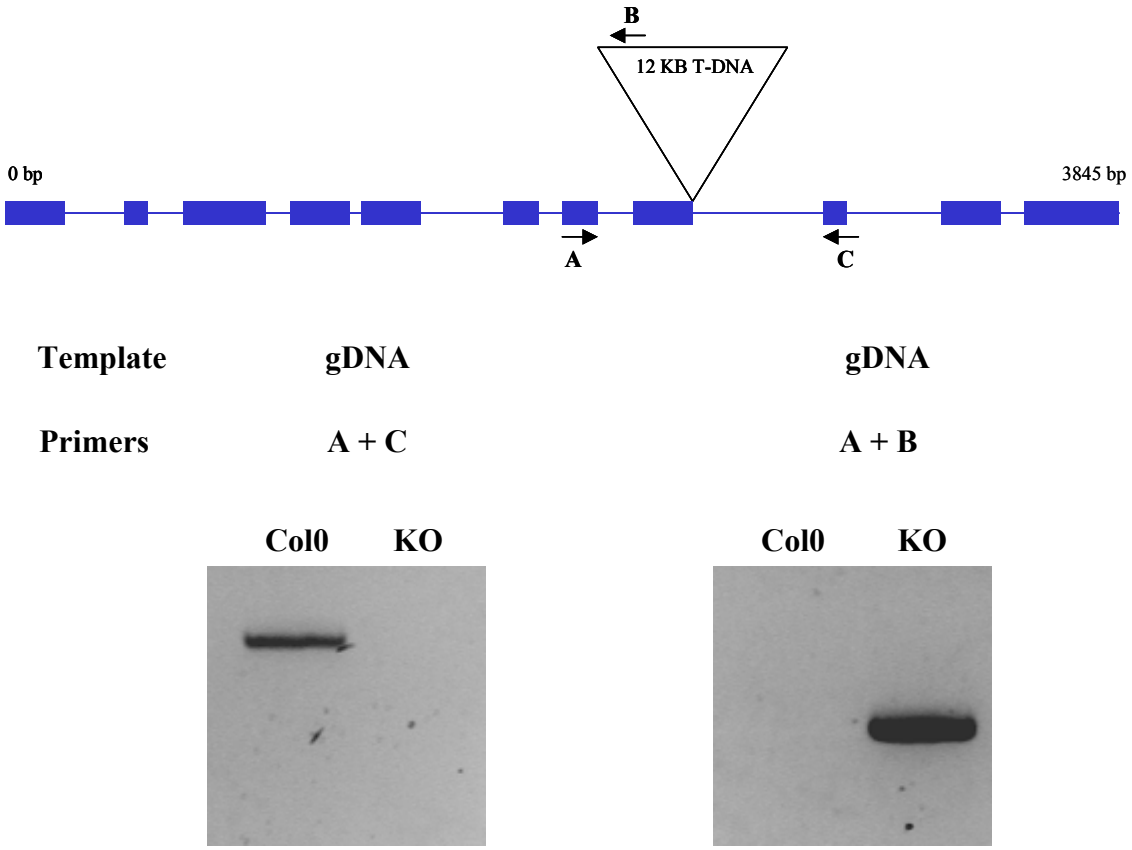

Figure 4.18 Identification of homozygous AtPARG1 null lines by PCR genotyping. Schematic diagram of 12 kb T-DNA insertion within gene of interest and primer combinations for identifying lines containing insertion. Gel electrophoresis of PCR on genomic DNA extracted from *A. thaliana* Col0 and N616088 (KO) lines with primers amplifying from T-DNA insertion to AtPARG1 gene.

Figure 4.18 showed a PCR band amplifying DNA between inserted T-DNA and AtPARG1 gene in the knockout (KO) line indicates the presence of T-DNA insert. Primers designed to the wild type allele over the site of T-DNA insertion only amplify DNA for Col0 suggesting that this knockout line is homozygous for the T-DNA insertion.

4.3.8.2 Identification of AtPARG2 null lines.

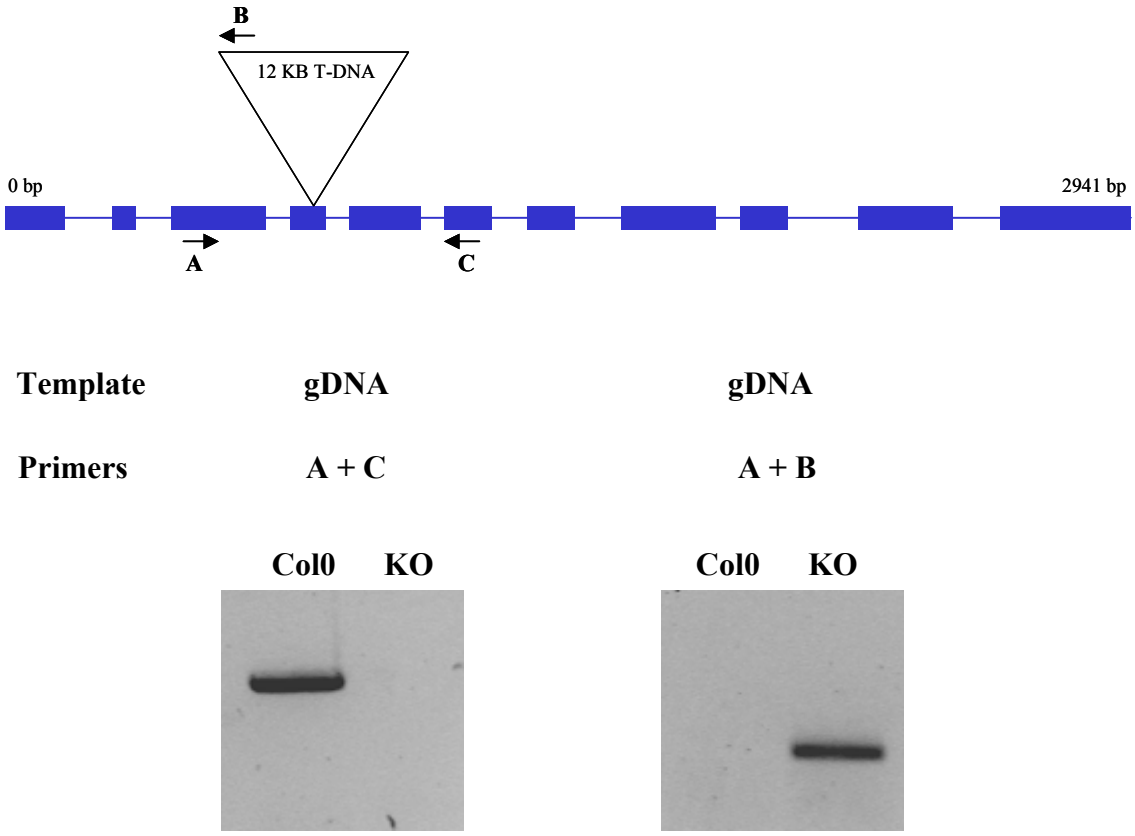

Figure 4.19 Identification of homozygous AtPARG2 null line using PCR genotyping. Schematic diagram of 12 kb T-DNA insertion within gene of interest and primer combinations for identifying lines containing insertion. Gel electrophoresis of PCR on genomic DNA extracted from *A. thaliana* Col0 and GK072B04 (KO) lines with primers amplifying from T-DNA insertion to AtPARG2 gene.

Figure 4.19 showed a PCR product for the T-DNA insertion for the knockout line but not in *A. thaliana* Col0 plant. The absence of a band for the wild type allele for the AtPARG2 null line suggests that it is homozygous for the T-DNA insertion.

4.3.8.3 Phenotypes of PARG null lines.

A. thaliana Col0 plants were grown alongside PARG null lines in both long and short day growth conditions. Plants were observed for differences in development, leaf size, leaf number, day of bolt and date of flowering.

Figure 4.20 Photographs of *A. thaliana* Col. AtPARG1 and AtPARG2 null lines. Plants were grown in long day growth conditions and photographed after 3 weeks.

There was no difference in size of PARG null lines compared with Col0. However, plants null for AtPARG1 showed an early flowering phenotype, 6 days earlier than Col0 (see Figure 4.21). This was observed in both short and long day growing conditions.

Figure 4.21. Photograph of early flowing phenotype of AtPARG1 null lines compared with Col0. T-DNA AtPARG1 are on the left and *A. thaliana* Col0 on the right. Plants were grown in long day growth conditions and photograph taken after 4 weeks.

There was no difference in flowering time between AtPARG2 null lines and Col0.

4.3.8.4 Phenotypes of *A. thaliana* PARG null lines in response to DNA damaging agents.

Seeds were stratified on MS plates for 2 days before germination for 7 days in 24 hour light. Five seedlings were then transferred to individual 1ml well plates containing MS media plus either MMS or Bleomycin. After 14 days growing in 24 hour light seedlings were removed from liquid media, dried overnight and dry weight recorded (see Chapter 2.2.18).

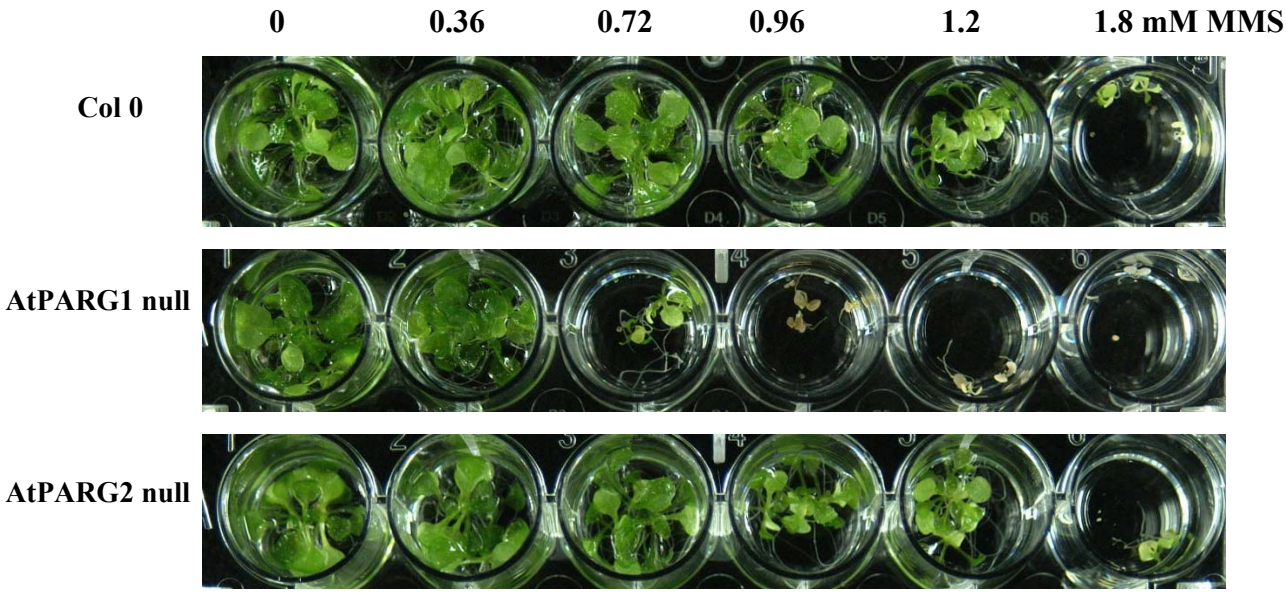

Figure 4.22 Photographs of *A. thaliana* Col0 and PARG null lines grown in MMS. Seeds were germinated on MS agar plates for one week in 24 hour light after 2 days stratification. Three seedlings were then transferred to each 1ml well on 24 well plates containing MS media and concentrations of MMS (from left to right) 0, 0.36, 0.72, 0.96, 1.2 and 1.8 mM MMS. Seedlings were then grown for a further two weeks in 24 hour light before samples were removed for dry weight measurement. Three biological triplicates were performed.

Seedlings grown without MMS showed no difference in size but at 0.72mM MMS most the AtPARG1 null lines are very much smaller. At 0.9, 1.2 and 1.8 mM MMS the AtPARG1 null seedlings are yellow and dead. There was no difference observed between Col0 and AtPARG2 null plants. In order to quantify the differences in plant growth with MMS treatment dry weight measurements were taken for all three biological replicates and presented as average (shown in Figure 4.23)

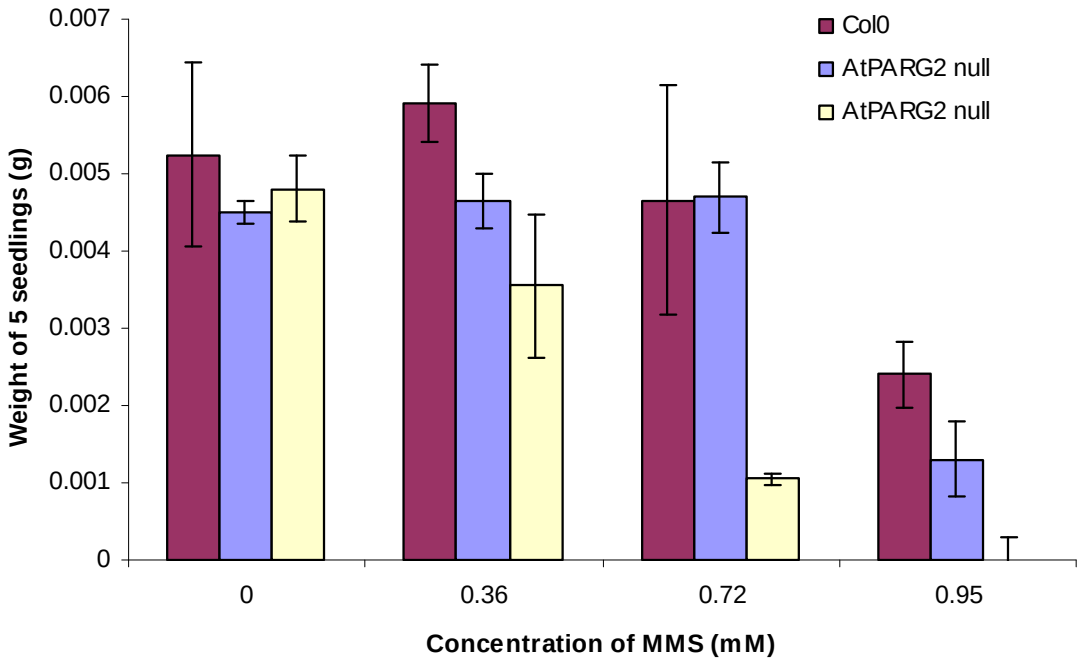

Figure 4.23 Dry weights for Col0 and PARG null lines grown in MMS for 2 weeks. Seedlings were germinated on MS agar and 24 hour light for 1 week before three seedlings transferred into 1ml well containing MS media and MMS for 2 weeks (shown in Figure 4.22). Seedlings were then removed for dry weight measurements. Experiment was repeated in triplicate and averages presented. Error bars indicate standard deviation.

There was no difference in size of *A. thaliana* Col0 and AtPARG1 null lines grown in absence of MMS. However at 0.36 and 0.72 mM MMS Col0 grew better than the AtPARG1 null line. At 0.96 mM MMS all the AtPARG1 null line were dead and there was such little plant material that the weight was negligible. There was no difference in dry weights of the AtPARG2 null line compared with the Col0.

4.3.8.5. Phenotypes of PARG null lines with DNA damaging agent Bleomycin.

Seeds were germinated on MS agar plates in 24 hour light for 1 week before seedlings being transferred into 24 well plates containing 1ml MS media and Bleomycin. These were grown in 24 hours light for 2 weeks (see Chapter 2.2.18 for full details).

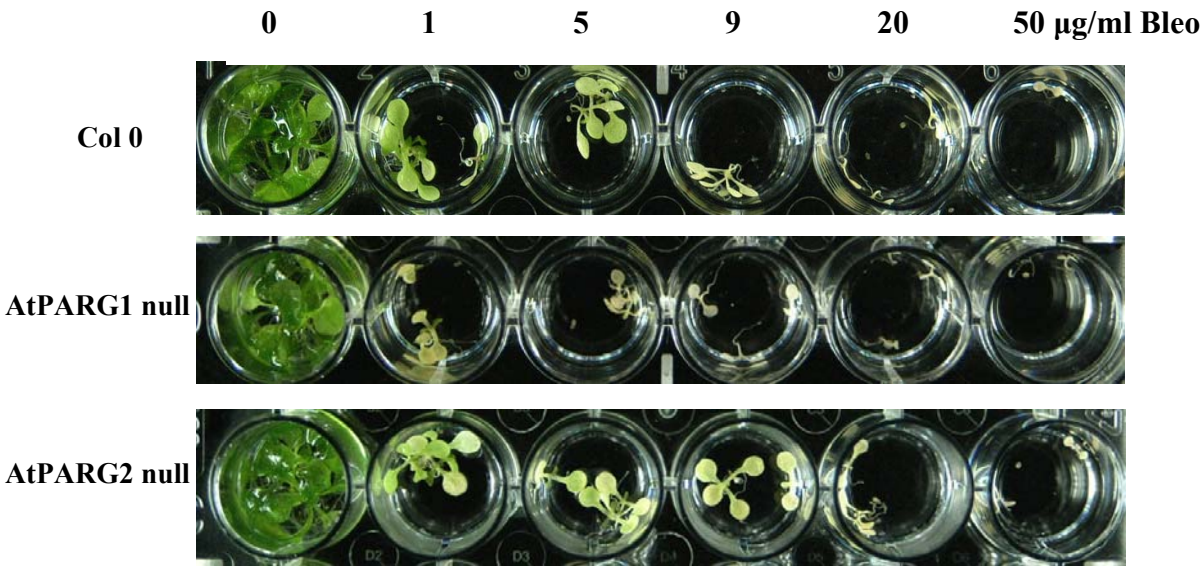

Figure 4.24. Photograph of *A. thaliana* Col and PARG null lines grown in Bleomycin. Seeds were first germinated on MS agar for 1 week in 24 hour light. Three seedlings were transferred to 1ml wells with MS media and Bleomycin at concentrations 0, 1, 5, 9, 20 and 50 µg/ml (left to right). Experiment was repeated in triplicate.

There was no obvious difference between Col0 seedlings and PARG null lines grown without Bleomycin. At 1µg/ml Bleomycin AtPARG1 null lines were smaller and more chlorotic than Col0 and AtPARG2 null plants. At all higher concentrations of bleomycin AtPARG1 null plants were are smaller and more susceptible to Bleomycin than Col0.

4.4 Discussion

4.4.1 Structure of PARP proteins and identification of novel Arabidopsis PARP gene AtPARP3

Two PARP genes (AtPARP1 and AtPARP3) have previously been identified in *A. thaliana* (Babiychuk et al. 2002; Lepiniec et al. 1995). Another previously unreported PARP gene has been identified as AtPARP3, through sequence homology to the PARP1 catalytic site (Hunt et al 2004).

A comparison of the domains found in 3 putative *A. thaliana* PARP and human PARP1 is shown in Fig 4.3. All 4 PARPs contain the catalytic core and the WGR region of the automodification domain. AtPARP1 shows most homology to human PARP1 with characteristic 3 domain structure comprising of a DNA binding domain, automodification domain, and a catalytic core. These 3 domains can be split further, the DNA binding domain consists of two zinc finger motifs, shown to act as DNA damage sensors (Ménissier-de Murcia et al. 1989). The automodification domain is made up of the BRCT (Breast Cancer C-terminal) domain which is present in many proteins involved in cell cycle and DNA damage (Williams et al. 2003) and a WGR domain with a conserved rich sequence of tryptophan – glycine – argentine. The function of both the BRCT and WGR domains is unknown.

AtPARP2 does not contain the BRCT or PADR domain and instead of zinc finger motifs, contains 2 SAP domains in the DNA binding regions. SAP domains are putative DNA binding domains found in many nuclear proteins. They were first identified in transcriptional regulator proteins PIAS (protein inhibitors of activated STAT; Liu et al. 2001).

AtPARP3 contains the BRCT, PADR and WGR domains but no DNA binding domain suggesting it may not act in response to DNA strand breaks. The domain with most homology to PARP1 is in the catalytic core.

The catalytic core of all PARP proteins consists of a 40kDa catalytic site that is responsible for the initiation, elongation and branching of ADP ribose polymers (Ruf et al. 1996; Marsischky. 1995).

4.4.2 PARP Gene expression

Expression of the three putative PARPs in *A. thaliana* show all are induced by DNA damage although AtPARP1 and AtPARP2 much more so than AtPARP3. This correlates well to the absence of a DNA binding domain in the structure of AtPARP3 protein.

This response in PARP gene expression to DNA damaging agents is consistent with previous published data on the two characterised PARP genes in Arabidopsis and PARP genes in other model organisms (Lepiniec et al. 1995; Doucet et al. 2001).

Previous investigations on two *A. thaliana* PARP genes (AtPARP1 and AtPARP2) showed that both genes are upregulated in response to DNA breaks caused by ionizing radiation (Doucet et al 2001). The AtPARP2 gene has also been shown to be induced by other environmental stresses such as drought and some heavy metals (Doucet et al. 2001). Cultured soybean cells expressing antisense PARP2 were shown to inhibit H_2O_2 induced cell death (Amor et al. 1998). *A. thaliana* plants with reduced PARP activity had inhibited cell death rates and plants were more tolerant of a broad range of abiotic stresses including drought, high light, and heat (de Block et al. 2005). One interpretation of these results is that with reduced PARP activity cells are better able to maintain energy homeostasis as there is a decrease in the depletion of NAD^+, which under normal conditions would cause cell death (Vanderauwera et al. 2007). However, in plants there have been no reports of correlation between NAD^+ concentration and PARP activity.

HsPARP1 has been shown to detect DNA breaks through its two zinc fingers and binds to the DNA at the site of damage (Gradwohl et al. 1990; Ikejima et al. 1990; Ménissier-de Murcia et al. 1989). The mechanisms by which PARPs mediate responses to DNA damage are unknown although several hypotheses exist to explain it (see Chapter 1.3.3.1)

The first hypothesis proposes that in response to stress (in this case heat) PARP1 is activated and modifies chromatin proteins leading to decondensation and transcriptional activation. In response to DNA damage PARPs are known to poly ADP ribosylate histones which disrupts chromatin and destabilizes nucleosomes (Huletsky et al. 1989; De Murcia et al. 1986). This leads to a change in the regulation of transcription.

A second hypothesis suggests that the poly ADP ribosylation of PARP at the site of DNA damage recruits DNA repair proteins. PARP has also been shown to lead to the recruitment of DNA repair proteins, such as Base Excision Repair protein XRCC1 (Masson et al. 1998), and DNA dependent protein kinase, DNA-PK (Ruscetti et al. 1998)

4.4.3 Expression of putative AtPARP3 gene.

Gene expression of the previously unreported putative PARP AtPARP3 gene showed an upregulation in response to the plant stress hormone Abscisic acid, salt, mannitol, auxin and DNA damaging agents. These results suggest that AtPARP3 is under a more general hormonal control. The level of transcript for AtPARP3 appears to be tightly controlled, as it is either absent or present in very high levels. This tight control of expression is presumably because hormonal pathways are more part of normal cell function, compared to the response to DNA damage, which arises spontaneously.

Abscisic acid is a hormone involved in the response to drought and water stress as it controls the closing of stomata, reducing transpiration, and preventing further water loss. It is also vital in breaking seed dormancy in the early stages of germination. Plant responses to drought and

salt are closely related and the mechanisms overlap, possibly explaining the upregulation of PARP AtPARP3 to salt and mannitol. Abscisic acid deficient mutants of Arabidopsis are affected in their response to numerous stress conditions such as drought, salt and cold (reviewed in Leung & Giraudat 1998).

Abscisic acid mediates plant signalling responses to salt, drought and cold treatment so it follows that an increase in salt would result in a release of ABA and the induction of AtPARP3. In these experiments expression of AtPARP3 was higher with ABA application than with salt and probably attributable to the concentration of salt and ABA used in this experiment.

ABA also mediates the transition from dormant seed to the early stages of germination. The online microarray database shows that AtPARP3 is expressed mostly in seeds (https://www.genevestigator.ethz.ch/). It could be possible that AtPARP3 is mainly expressed at germination.

The signalling pathways involving Abscisic acid, and salt stress are fairly well characterised with many mutants in the components of the pathways. Future work could investigate AtPARP3 transcript level in these mutant lines to identify the mechanisms controlling AtPARP3 expression. Abscisic acid is a general abiotic stress hormone and could offer exciting and practical applications for engineering plants with altered tolerance to environmental stress.

AtPARP3 expression appears to be upregulated by auxin, a plant hormone principally involved in phototropism and cell elongation. It is also the key hormone initiating cell regeneration in response to wounding (Mishra et al. 2006). However wounding does not induce any increase in AtPARP3 transcript level.

4.4.4 PARP T-DNA lines.

Homozygous *A. thaliana* plant lines with T-DNA insertions in each of the PARP genes were obtained from the Arabidopsis Stock centre in Nottingham (http://www/nasc.nott.ac.uk/). Plants with homozygous T-DNA insertion were identified by PCR of genomic DNA and confirmed by absence of transcripts. Under normal growth conditions in both short and long days no difference in growth or development was observed. Unfortunately these were obtained late on in this project and time only allowed for experiments testing these PARP inactivated lines with DNA damaging agents. There was no difference in susceptibility to DNA damaging agents for the PARP null lines when compared with wild type plants. This could due to gene redundancy. In order to protect against lethal mutations in one gene, higher organisms evolve several genes at different loci to perform the same function. It is possible that the presence of 3 *A. thaliana* PARP genes could be an example of such gene redundancy. De Block and co-workers suggested PARPs induce cell death in plants (De Block et al. 2005); overactivity of PARP enzymes depletes cellular NAD and causes cell death. It was observed that a decrease in PARP activity leads to an increase in tolerance to a broad range of stress conditions by maintaining energy homeostasis. However, the PARP null lines do not show any increase in tolerance to DNA damaging agents which would appear inconsistent to this hypothesis. Further studies into the effect of altered PARP activity on the concentration of NAD would confirm or disprove this theory.

4.4.5 PARG enzymes.

PARG reverse the activity of PARP by breaking the bonds between ADP ribose units. Only one PARG gene has been identified in all model organisms except *C. elegans* (St Laurent et al. 2007) and here in *A. thaliana*, both of which contain two PARG genes. However, the organisms with only one PARG gene produce many isoforms, the human PARG gene for

example gives rise to 5 isoforms all with different localisations (Fig 4.13) Differences between the isoforms occur at the N-terminal end of the protein. The catalytic domain of PARG proteins was used to interrogate the translated *A. thaliana* genome database and two putative PARG genes were identified (Hunt et al 2004).

The structure of PARG genes shows 2 main regions, the N-terminal putative regulatory domain containing a nuclear localisation signal and a C-terminal catalytic domain. Interestingly the N-terminal regulatory domain is entirely absent from both *A. thaliana* PARG genes, making them most similar to human PARP isoform HsPARG55. HsPARG55 lacks the Nuclear localisation signal and the regulatory domain and is targeted only to the mitochondria (Meyer et al. 2007). One Arabidopsis PARG gene had already been identified through its involvement in circadian rhythm (Panda et al. 2002). This report showed that a mutation in the TEJ (AtPARG1) gene resulted in an alteration in photoperiod, causing a change in the transition from vegetative growth the flowering growth. The other PARG sequence identified through BLAST search showed up a previously unreported and novel PARG encoded by the gene AtPARG2.

4.4.6 Gene expression of PARGs

The transcript levels for both *A. thaliana* PARG genes showed to be increases with the addition of DNA damaging agents as well as for kinase inhibitor for AtPARG1 and phosphate starvation for AtPARG2. It is perhaps unsurprising that DNA damaging agents should cause an increase in the expression of PARG genes since they also induced such a high expression in PARP genes. Increased activity of PARP proteins leads to a large accumulation of ADP ribose polymer that can result in a depletion of NAD and cell death. Therefore the activity of PARG proteins has to be tightly controlled in order for PARP to respond to the damage in DNA without causing cell death by causing metabolic failure.

4.4.7 PARG null lines.

Plants that were null for AtPARG1 showed an early flowering phenotype in both long and short day conditions. This interesting observation confirmed the alteration in photoperiod identified by the TEJ mutant (Panda, Poirier, & Kay 2002). One possible connection between circadian rhythm and PARG activity is through cyclic ADP ribose, which is formed by the degradation of NAD^+ by ADPribose cyclases. Circadian oscillations in the concentration of cADP ribose coordinate with circadian oscillations in the concentration of cellular calcium (Dodd et al. 2007; reviewed in Harrisingh & Nitabach 2008). However, although cADP ribosylation activity has been identified in plants, to date no genes encoding ADP ribose cyclases have been isolated. This early flowering phenotype could arise as a possible result of interplay between ADPribose cyclases and PARP/PARG enzymes competing for NAD as a substrate. It could also be possible that PARGs not only use poly ADP ribose as a substrate, but also cyclic ADP ribose, which would partially explain this phenotype. A possible explanation for this phenotype could be that cADP ribose levels are depleted by the reduction in PARG activity resulting in a change in circadian rhythm.

Also, PARGs control on PARPs activity of transcription factors and chromatin modifications (detailed in Chapter 1.3.3.2) could result in an alteration in circadian rhythm although there is no published data to support this.

AtPARG1 null lines show increased susceptibility to DNA damaging agents. It is interesting that the AtPARG1 null lines, but not the PARP null lines that show a difference in tolerance to genotoxicity.

There are two main theories as to how an accumulation of ADP ribose polymer may initiate the cell death response (detailed in Chapter 1.3.3.2)

A decrease in PARG activity would support the hypothesis that overactivation of PARP by a following DNA damage leads to a reduction in cellular NAD^+ that would cause cell death

(Bouchard et al. 2003). This was seen in *A. thaliana* with reduced PARP activity causing an increased tolerance to a wide range of abiotic stresses. The reason suggested was that because PARP proteins are not consuming NAD^+ a more efficient cellular energy homeostasis is maintained (Vanderauwera et al. 2007; De Block et al. 2005).

More recently a second mechanism linking increased PARP activity and cell death has been published. An increase in PARP activity has also been shown to be cause apoptosis by causing the release of the powerful apoptosis inducing factor from the mitochondria (Yu et al. 2006). Once in the nucleus AIF induces chromatin condensation and DNA fragmentation (Susin et al. 1999b). Although the mechanism for this release of AIF by PARP is unknown, PARP1 deficient mice fibroblasts show impaired AIF translocation to the nucleus with the application of DNA damaging agents (Yu et al. 2006). The reduction in PARG activity could cause an increase in ADP ribose polymer leading to this translocation of AIF. However, there is no evidence for the presence of AIF in plants and the finding here could indicate another ADPribose polymer induced cell death pathway that is AIF independent.

Clearly PARGs control of PARP activity in response to DNA damage is tightly controlled in order to repair breaks in DNA whilst still allowing efficient cellular metabolism.

Chapter 5: Identification and characterisation of NAD salvage pathway genes in *A. thaliana.*

5.1 Introduction

Sirtuins, PARPs and ADP ribose cyclases utilize NAD^+ as a consumable substrate releasing nicotinamide and an ADP ribose moiety. NAD^+ is an essential coenzyme required for a multitude of chemical reactions and therefore organisms have to maintain a reservoir of NAD^+ in cells. The NAD salvage pathway comprises of enzymes required to reform NAD^+ after its degradation by sirtuins, PARPs and ADP ribose cyclases. The NAD salvage pathway was first characterised in mammals using ^{14}C- Nicotinic acid (Preiss & Handler 1958).

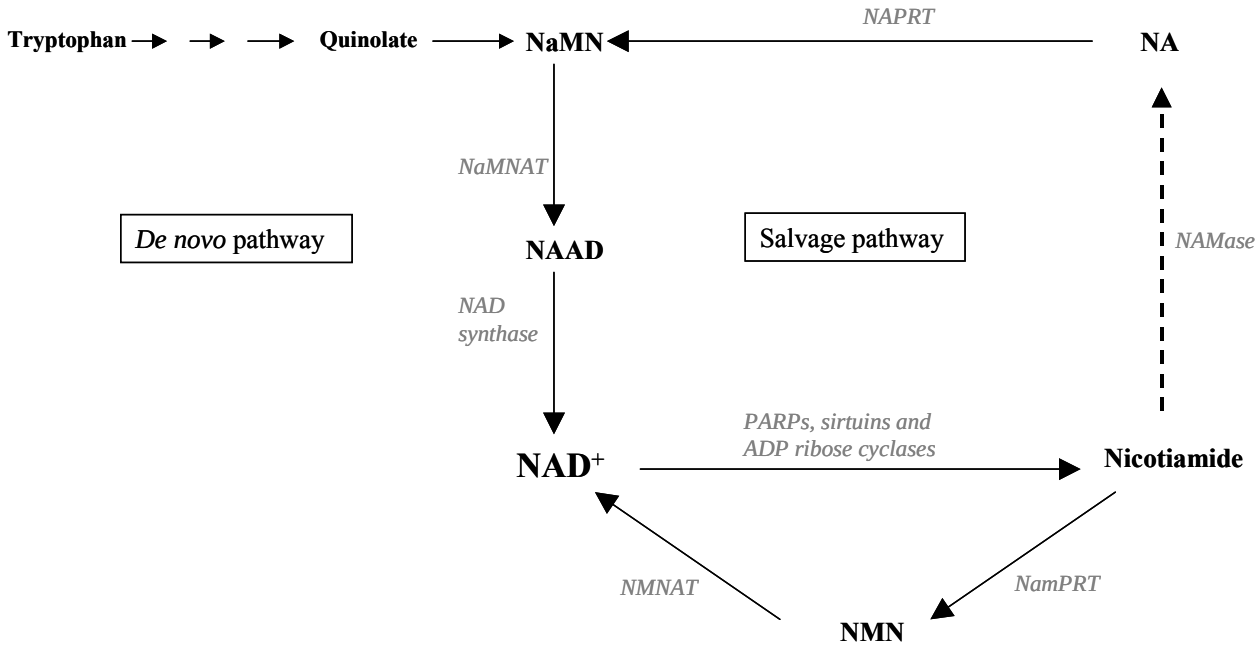

Figure 5.1 Mammalian NAD salvage pathway. NAD^+ is degraded into Nicotinamide. In mammals there is no evidence for nicotinamidase (NAMase) proteins indicated by a dashed line. Nicotinamide is converted to NAD^+ to Nicotinamide mononucleotide (NMN) by nicotinamide phosphoribosyltransferase (NamPRT) and nicotinamide mononucleotide adenylyltransferase (NMNAT) enzymes. The pathway in mammals requires nicotinic acid phosphoribosyltransferases (NAPRT), nicotinic acid mononucleotide adenylyltransferases (NaMNAT) and NAD synthase enzymes.

In mammals NAD^+ is broken down by PARPs, sirtuins and ADP ribose cyclases to produce nicotinamide, which in mammals acts as substrate for the reforming of NAD^+ (see Fig 5.1). Nicotinamide is converted to nicotinamide mononucleotide (NMN) by nicotinamide phosphoribosyltransferases (NamPRT also known as visfatin) and then to NAD^+ by nicotinamide mononucleotide adenyltransferases (NMNAT). There is no evidence for nicotinamidase enzymes in mammals although other genes of the NAD salvage pathway are present including nicotinic acid phosphoribosyltransferases (NAPRT) that would link nicotinic acid to the NAD salvage pathway. Also present are the enzymes that convert Nicotinic acid mononucleotide (NaMN) to Nicotinic acid adenyl dinucleotide (NaAD) and NAD^+ by the enzymes nicotinic acid mononucleotide adenylyltransferases (NaMNAT) and NAD synthases (Schweiger et al. 2001b; reviewed in Khan et al. 2007).

5.1.1 NAD salvage pathway in plants and bacteria.

Labelling studies have identified the steps of the NAD salvage pathway in plants (Ashihara et al. 2005) and the pathway shown in Figure 5.2.

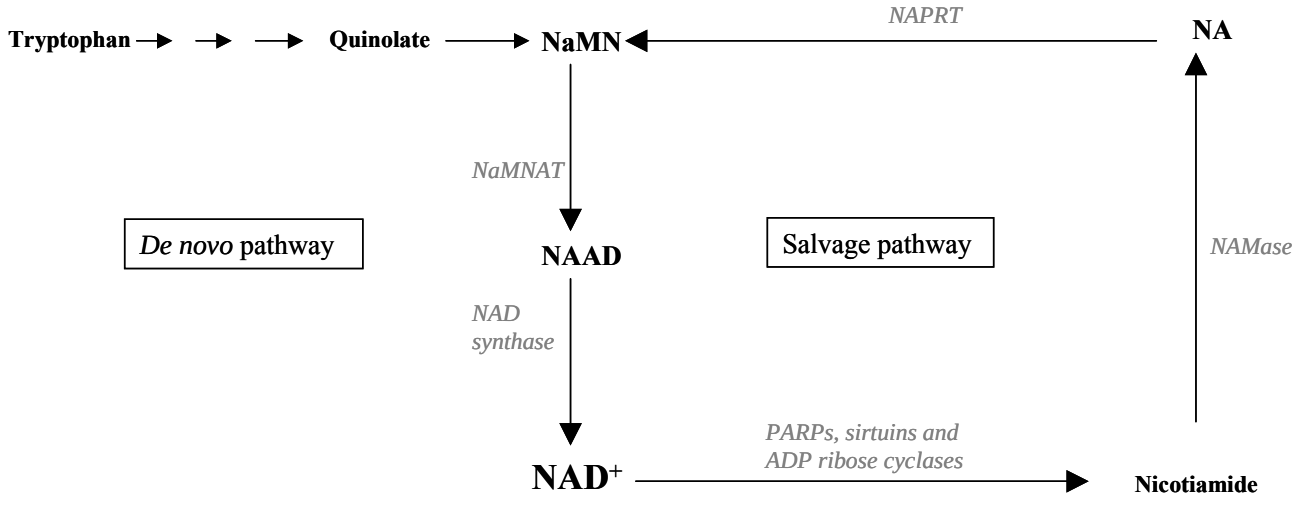

Figure 5.2 NAD salvage pathway in plants. The breakdown of NAD^+ produces nicotinamide, which is converted to nicotinic acid (NA) by nicotinamidases (NAMase). NA is converted to nicotinic acid adenyl dinucleotide (NAAD) via nicotinic acid mononucleotide (NaMN) by nicotinic acid phosphoribosyltransferases (NAPRT) and nicotinic acid mononucleotide adenylyltransferases (NaMNAT). NAD synthases perform the last step converting NAAD to NAD^+.

These studies have shown nicotinamide is converted to nicotinic acid by nicotinamidase enzymes (Ashihara et al. 2005; see Figure 5.2). The addition of a mononucleotide group by nicotinic acid phosphoribosyl transferase (NAPRT) converts nicotinic acid to mononucleotide (NAMN). This is then converted to nicotinic acid adenine dinucleotide (NAAD) by nicotinic acid mononucleotide adenyltransferase (NaMNAT; Hunt et al. 2004). NAD synthetase completes the last step of nicotinic acid adenine dinucleotide to NAD^+. This pathway has also been elucidated in yeast, which also contains nicotinamidase enzymes (Sandmeier et al. 2002) and *E. coli* (Berríos-Rivera et al. 2002).

5.1.2 Nicotinamidases

The activity of the sirtuins, PARPs and ADP ribose cyclases degrade NAD^+ as a substrate producing nicotinamide, the production of which acts as inhibitor to both sirtuins and PARP enzymes. Although at first the mechanism of this inhibition was thought to be due to the nicotinamide binding to the NAD^+ binding site of sirtuins (Anderson et al. 2002) it is now known that nicotinamide acts as a non-competitive inhibitor on the forward sirtuin reaction (Bitterman et al. 2003).

In the last decade there has been more research on the activity of sirtuins. Sirtuins have been shown to confer longevity on a variety of organisms from yeast to mammals (see section 1.2.4.) but they are inhibited by nicotinamide. Lifespan of yeast is dramatically increase with the application of nicotinamide (Anderson et al. 2003). The nicotinamidase gene in yeast (pnc1) was first identified in 2002 and later shown by two groups to govern lifespan removing the nicotinamide that inhibits sirtuin activity (Anderson et al. 2003; Gallo et al. 2004). These studies showed that PNC1 activity causes sufficient depletion in nicotinamide to increase activity of sirtuins and increase longevity of the yeast. In both *C. elegans* and *D. melanogaster* the activity of nicotinamidase has been shown to affect sirtuin activity and longevity. In *C. elegans* a deletion of nicotinamidase gene caused a reduction in longevity

whilst overexpression increased lifespan (van der Horst et al. 2007). This has also been shown in *D. melanogaster* (Balan et al. 2008).

In plants the addition of nicotinamide has been reported to lower hydrogen peroxide induced cell death (Amor et al. 1998), and reduce ABA-induced stomotal closure (Leckie et al. 1998). To date four *A. thaliana* nicotinamidase genes have been reported (Hunt et al. 2007, Wang et al. 2007).

5.1.3 Nicotinic acid phosphoribosyltransferases (NAPRT)

These enzymes catalyse the second step in the NAD salvage pathway converting nicotinic acid to nicotinic acid mononucleotide (NaMN). In yeast the strong link between the activity of sirtuins and regulation of the NAD salvage pathway was further reinforced by work on the NPT gene (yeast NAPRT homolog). Overexpression of the yeast NPT1 gene enhanced sirtuin mediated longevity and gene silencing but did not affect the overall levels of NAD^+ (Anderson et al. 2002). A deletion of the NPT1 gene cancels the increase in lifespan caused by calorie restriction (Sandmeier et al. 2002; Lin et al. 2000).

Despite mammals having a different NAD salvage pathway mammalian cells still contain functional NAPRT genes. The addition of nicotinic acid increased cellular NAD^+ levels and decreased oxidative cell death (Hara et al. 2007). The function of these NAPRT genes in mammals is not well understood.

5.1.4 Nicotinic acid mononucleotide adenylyltransferase (NaMNAT)

NaMNAT enzymes catalyse the conversion of nicotinic acid mononucleotide (NaMN) to nicotinic acid adenine dinucleotide (NaAD). NaMNAT enzymes display a unique dual specificity for both nicotinic acid mononucleotide (NaMN) and nicotinamide mononucleotide (NMN) and therefore functions in both the NAD salvage and *de novo* synthesis pathways

(Zhou et al. 2002). The difference in labelling of this enzyme (either NaMNAT or NMNAT) refers to the substrate the enzyme is acting on. The reactions involved are shown below.

Figure 5.3 Enzymic activities of N(a)MNAT enzymes. Although only one enzyme, N(a)MNAT can convert NMN to NAD and NaMN to NaAD.

The work reported here focuses on the NAD salvage pathway and therefore this enzyme will be referred to as NaMNAT.

NaMNAT enzymes have been identified in bacteria (Mehl et al. 2000), yeast (Emanuelli et al. 2003), *D. melanogaster* (Zhai et al. 2008), and three NaMNAT in humans (Schweiger et al. 2001a). Properties and activities of human NaMNAT reviewed are in (Berger et al. 2005).

Recently there has been more work on NaMNAT enzymes because their activity is very low in tumour cells.

NMNAT also catalyses the rate limiting step for the conversion of anticancer drug tiazofurin to its active form. Resistance to tiazofurin is associated to the low activity of NaMNAT in cancer cells (Zhou et al. 2002; Sorci et al. 2007).

NaMNAT has also been implicated in protection against neurodegeneration, the main cause for diseases such as Parkinson disease and Alzheimers. NMNAT null lines of Wallerian mice (a mutant strain of mice with a slow axon degeneration) have shown that NMNAT is essential for delaying neuronal degeneration (Jia et al. 2007). This response was suggested to be mediated by the activity of sirtuins, which when upregulated also protects against neurodegeneration (Araki et al. 2004).

In this study the aim was to identify nicotinamidases, NAPRT and NaMNAT genes in *A. thaliana* and to further investigate their activity.

5.2 Materials and methods

5.2.1 Reverse transcriptase PCR (RT-PCR).

Transcript levels for NAD salvage genes exposed to a many different biotic, genotoxic and abiotic stresses were examined in order to identify the role of putative NAD salvage pathway sequences in stress responses (a complete list of stress conditions in Materials and Methods Chapter 2 Table 2). Two µg of extracted total RNA was used to make cDNA, which was then used as template in PCR reactions amplifying putative NAD salvage sequences. Actin was used as an internal control to normalize for differences in the concentration of cDNA. All products of the PCR were cloned and sequenced by MWG Biotech.

Gene name and number	Primer name	Sequence	Number of cycles
NAMase (At5g23220)	220 L4 220 R4	ATT CTT TAC GCG TCA CAA CC GCG AGA TTC ATT AGC CTA CG	37
NAMase (NAMase1)	230 for 230 rev	TTCTCGTCATCGATATGCAG TCCTTCACTCCGATCTTGTC	35
NAMase (At3g16190)	161 for 161 rev	TCGAGAACATGATCGTCAAG TCACATTGGGATAATCCAGC	29
NAPRT	420 L2 420 KR	AAG TAC TTC GTA GTG CTG ATG G TAA AGC GTC AAT CGT CTC TTC ATT	32
NaMNAT	NaMNAT L3 NaMNAT R2	CAA TCC TCC TAC TTT CAT GC TGA CTT TGA GAG ATT CCT CG	32

Table 5.1 Primers sequences for amplification of putative *A. thaliana* NAD salvage pathway sequences. Names and numbers of cycles using in RT-PCR also listed.

5.2.2 Cloning of *A. thaliana* NAD salvage genes.

Sequences for the three nicotinamidase genes, one NAPRT and one NaMNAT were obtained from the Arabidopsis information resource website (http://www.arabidopsis.org/) and primers

designed to the sequences for cloning into the pENTR/D vector (Invitrogen) (full methods see Chapter 2.2.9 - 2.2.11). Plasmids containing the correct gene were identified through colony PCR (Chapter 2.2.12) and restriction enzyme digests (Chapter 2.2.13) before verification by DNA sequencing. From the pENTR/D vector, the putative NAD salvage genes were transferred into Gateway destination vectors pDEST17 and pDEST15 (illustrated below Figure 5.4) for protein expression studies.

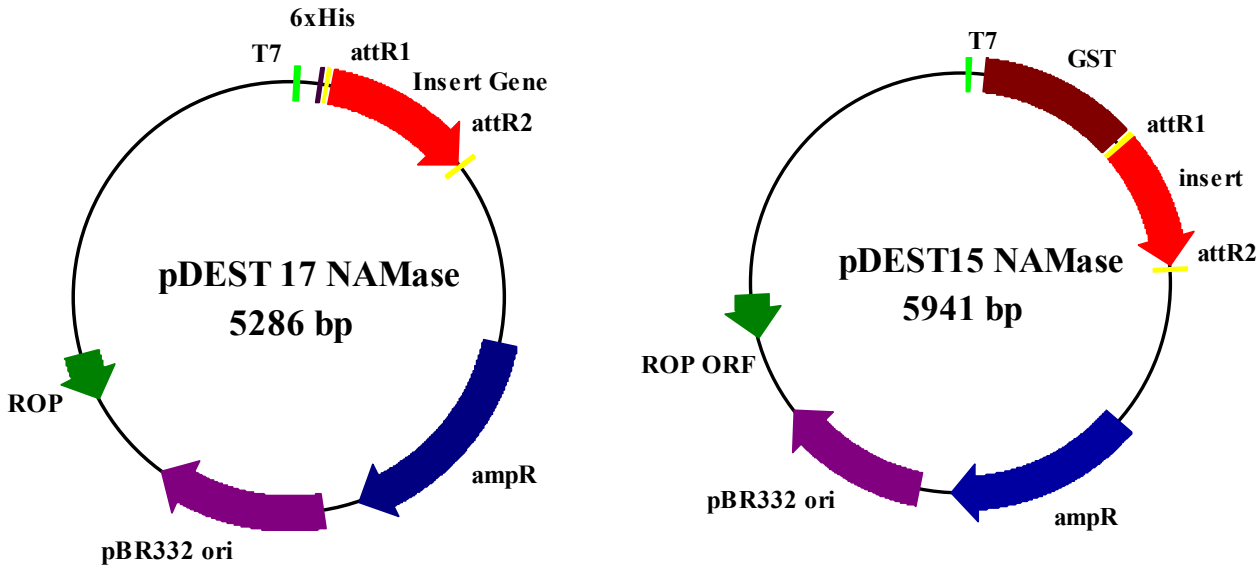

Figure 5.4 Vector maps for pDEST17 and pDEST15. Position of the NAMase gene is shown as insert. The vector includes att sites, promotor and antibiotic resistance genes.

These vectors were then used for protein expression in *E. coli*

5.2.3 Protein expression of NAD salvage genes in *E. coli*

pDEST 17 containing the inserted gene was used to transform *E. coli* BL21 pLysS cells and successful transformants were identified by restriction digests and DNA sequencing. Protein induction was achieved by the addition of IPTG, which binds to and inactivates the lacZ repressor gene. This results in production of T7 RNA polymerase and causes the protein encoded in the plasmid to be expressed. pDEST 17 vector contains an N-terminal 6x Histidine tag fused to the gene insert, which allows the protein to bind to nickel resin.

Conditions for protein expression were optimised to increase the amount of soluble protein produced by altering the concentration of IPTG added, temperature, and period of induction. For the genes of the NAD salvage pathway 0.1mM IPTG was added to *E. coli* cells at optimum density of A_{600} 0.8-1 and grown for 16 hours at 18ºC before cell lysis. The recombinant protein was purified using nickel charged resin (see Methods and Materials 2.3.1 for full description of method).

5.2.4 Nicotinamidase assay.

Nicotinamidases catalyse the reaction

$$\text{Nicotinamide} + H_2O \longrightarrow \text{Nicotinic acid} + \text{Ammonia.}$$

Concentration of protein was measured using BioRad Bradford reagent (see Chapter 2.3.6). Reactions were set up in triplicate in 150µl total volume using 0, 1, 5, 10 and 20µl of purified protein with 10mM phosphate buffer (pH 7.5), 150mM NaCl, 1mM $MgCl_2$, and with 0 or 8mM nicotinamide. Reactions were incubated at 30ºC for 1 ½ hours as described previously (Frothingham et al. 1996). Controls included boiled purified protein. Reactions were placed on ice before being analysed by HPLC for the production of nicotinic acid.

5.2.5 NAPRT assay

Concentration of purified NAPRT protein was quantified using BioRad Bradford reagent (see chapter 2.3.6). Reactions were set up using 0, 1 and 10µl of protein eluted in 100µl total reaction with reaction buffer containing 50mM Tris HCl (pH 7.5), 10mM $MgCl_2$, 0.4mM 5-phosphoribosyl 1-pyrophosphate and 2mM ATP. Substrate nicotinic acid was added at 0 or 5mM. Reactions were set up in triplicate including boiled purified NAPRT protein as controls. Reactions were incubated at 37ºC for 1½ hours before being placed on ice and analysed by HPLC.

5.2.6 NaMNAT assay

Concentration of purified NaMNAT protein was determined using BioRad Bradford reagent (see Chapter 2.3.6). 0, 1, 2, 5, and 10µl of eluted protein was used in triplicate for reactions in 100µl total with 40mM Tris-HCl (pH 7.5), 3.4mM ATP and 18mM MgCl2. Substrate concentrations for NaMN or NMN were added at 0, 1, 2, 3 mM. Controls included boiled eluted NaMNAT protein. Reactions were incubated at 37ºC in a waterbath and placed on ice before analysis by HPLC.

5.2.7 HPLC analysis

HPLC apparatus used was a Thermo scientific SpectraSystem AS3000 (Thermo Fisher Scientific Inc, A gradient of 0.01M potassium phosphate buffer pH5.5 (eluant A) and methanol (eluant B) was set up for times; 0 mins eluant A 100%, eluant B 0%; 15minutes eluant A 88%, eluant B 12%; 17.5 minutes eluant A 55%, eluant B 45%; 20 minutes eluant A 30% eluant B 70%; 25 mins eluant A 30% eluant B 70%; 30 minutes eluant A 100%; 35 minutes eluant A 100% eluant B 0%.

Peak identities were confirmed using standards at 1, 0.1 and 0.01mM in triplicate and analysed by retention time and 280/260 nm absorbance ratios. Concentration/peak area plots were developed for quantification. Standards were checked everyday to ensure reliability of separation and any chromatographic modification of system.

5.3 Results

5.3.1 Identification of Nicotinamidases

The sequence of *S. cerevisiae* PNC1 gene and *E. coli* PncA gene was used to search the translated *A. thaliana* genome database using the BLAST algorithm. Three putative nicotinamidase genes were identified (Hunt et al 2004).

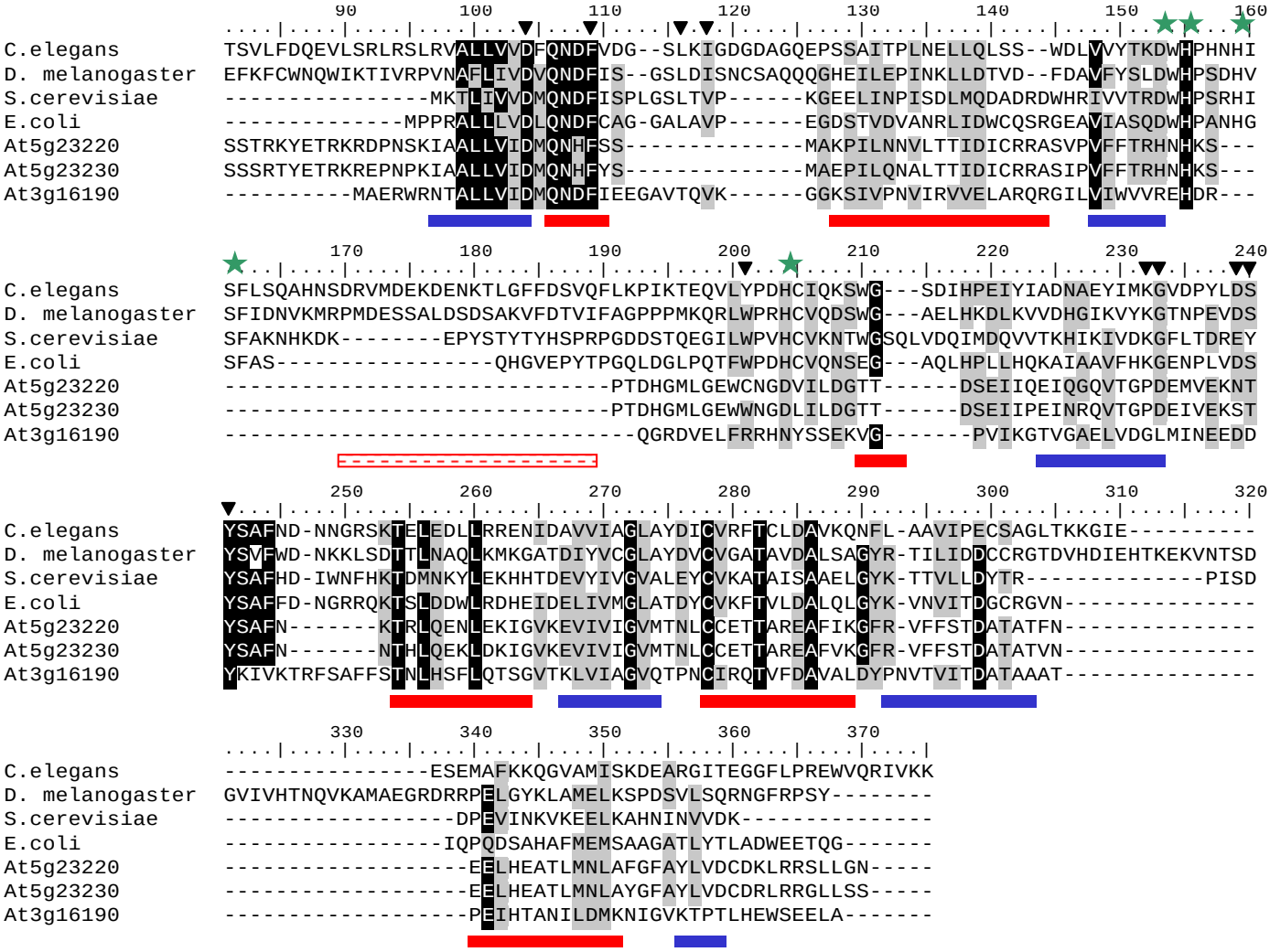

Figure 5.5 Sequence homology for putative *A. thaliana* nicotinamidases. Alignments for three putative Nicotinamidase sequences encoded by genes At3g16190, At5g23220 and At3g16190 to *C. elegans* (Y38C1AA.3), *D. melanogaster* (NP_732446), *S. cerevisiae* PNC1 (NP_011478), *E. coli* (P21369). Sequence alignments performed in BioEdit with ClustalW. β strands indicated by blue line underneath sequence, α helices by red line. Residues described as important for catalytic activity indicated by triangle above sequence.

Figure 5.5 shows three sequences that show homology to other characterised nicotinamidases, At5g23230 (NAMase1), At5g23220 (NAMase2) and At3g16190 (NAMase3). Homology to other characterised nicotinamidase genes is highest in the proposed catalytic regions at residues 98-110 and 240-300. Recently the crystal structure of *E. coli* nicotinamidase PNC1 has been published and it is from here that the annotation of the β sheets and α helices were taken (Hu et al. 2007b). Nicotinamidase enzymes display an unexplained affinity for Nickel resin and indicated on Figure 5.5 are the residues D153 H155 H159 S161 and H204 predicted to give this affinity for nickel resin. *A. thaliana* nicotinamidases appear to lack the α helix positioned between residues 170-190.

5.3.2 Nicotinamidase gene expression levels in *A. thaliana* Col0 exposed to different stress conditions.

Nicotinamidase gene expression was investigated in *A. thaliana* Col0 seeds grown in a variety of 30 different conditions including abiotic and biotic stress and DNA damaging agents (see Methods and Materials 2.2.2). Samples were taken over a time course at 0, 2, 4, 8, 24 and 48 hours. RNA was then extracted and cDNA made to examine the change in transcript level of nicotinamidase genes using SQRT-PCR (Chapter 2.2.6). Expression of gene was measured by analysing band intensity of gel electrophoresis of SQRT-PCR amplification products. Transcript levels were compared to Actin expression and results presented as averages.

5.3.2.1 Gene expression of NAMase2 with different stress treatments.

Stress	NAMase2					
Time point in hours	**0**	**2**	**4**	**8**	**24**	**48**
Salt	1.00	0.95	1.27	0.80	1.02	1.24
Mannitol	1.00	2.38	2.03	1.45	1.15	0.74
Hydrogen peroxide	1.00	0.66	0.67	0.44	0.30	0.31
Abscisic acid	1.00	4.25	7.94	5.25	6.71	17.55
Ethylene (ACC)	1.00	0.76	0.77	0.25	0.38	0.58
Auxin (NAA)	1.00	0.85	0.43	0.27	0.48	NA
Lipopolysaccharide	1.00	2.29	1.17	1.05	0.73	0.45
Jasmonic acid	1.00	1.13	0.45	0.83	0.64	0.67
Salicylic acid	1.00	1.17	2.22	2.60	2.04	1.29
Wounding	1.00	0.82	1.76	1.94	2.56	4.28
Phosphatase inhibitor	1.00	1.42	0.90	1.50	1.09	1.68
Kinase inhibitor	1.00	0.48	0.21	0.29	2.13	4.23
Cold treatment	1.00	1.19	1.11	1.27	1.49	1.12
Phosphate starvation	1.00	3.21	2.35	1.48	1.53	1.46
2,4 DNT (8hours)	1.00	1.29	1.14	1.15	NA	NA
MMS	1.00	0.98	1.54	0.68	0.47	0.69
Bleomycin	1.00	1.08	1.29	0.93	1.01	1.27
UV-B	1.00	0.14	0.15	0.12	0.04	0.08

Table 5.2 Summary of fold differences in the expression of putative AtNAMase2 using RT-PCR under different stress conditions. Transcript levels are expressed compared to actin expression. Samples were prepared in triplicate and results presented as averages. NA indicates where transcript levels were so low it was impossible to take an accurate reading of expression.

The most significant results in Table 5.2 for NAMase2 were seen with Abscisic acid, which increased from 1 to 4.25 within 2 hours. This continued to rise to 7.94 by 4 hours but dropped to 5.25 at 8 hours. The transcript level remained high at 6.71 by 24 hours and at 17.55 by 48 hours. The increase was also seen with phosphate starvation, which caused an increase to 3.25 within 2 hours of phosphate resupply. This then dropped to 2.35 by 4 hours and remained at about 1.5 until 48 hours.

A notable decrease in gene expression was seen to UV-B. Within 2 hours of UV-B exposure the transcript levels of NAMase2 fell from 1 to 0.14 and remained low at approximately 0.1 until 48 hours after exposure to UV-B.

5.3.2.2 Gene expression of NAMase1 with different stress treatments.

Stress	NAMase1					
Time point in hours	**0**	**2**	**4**	**8**	**24**	**48**
Salt	1.00	1.44	1.95	1.20	1.81	1.98
Mannitol	1.00	2.07	1.98	1.97	2.03	1.79
Hydrogen peroxide	1.00	0.99	1.10	1.10	1.07	1.35
Abscisic acid	1.00	1.24	1.82	1.37	2.14	NA
Ethylene (ACC)	1.00	1.09	1.45	1.37	1.47	2.54
Auxin (NAA)	1.00	1.03	1.21	0.77	1.56	NA
Lipopolysaccharide	1.00	1.87	1.75	1.65	1.46	1.26
Jasmonic acid	1.00	0.76	0.88	0.96	0.75	0.88
Salicylic acid	1.00	1.18	1.18	1.43	1.31	1.32
Wounding	1.00	1.15	0.96	1.16	1.17	1.22
Phosphatase inhibitor	1.00	1.44	1.29	1.95	1.59	2.26
Kinase inhibitor (STA)	1.00	0.58	0.39	0.45	NA	NA
Cold treatment	1.00	1.25	1.26	1.15	0.98	0.56
Phosphate starvation	1.00	1.65	1.35	1.19	0.44	0.97
2,4 DNT	1.00	1.20	0.98	2.31	NA	NA
MMS	1.00	1.86	6.06	3.80	1.66	2.26
Bleomycin	1.00	1.56	1.00	2.42	4.08	6.78
UV-B	1.00	0.13	0.10	0.13	0.12	0.20

Table 5.3 Summary of fold differences in the expression of putative AtNAMase1 using RT-PCR under different stress conditions. Transcript levels are expressed relative to actin transcript levels. Samples were prepared from three biological replicates and results presented as averages. NA indicates such low transcript levels that it was impossible to take an accurate reading of expression.

Table 5.3 shows the most significant changes in AtNAMase1 transcript levels were seen with DNA damaging agents. MMS caused an increase in expression from 1 to 6 fold within the first 4 hours but this then dropped to 3.8 at 8 hours and returned to approximately 2 for 24 and 48 hours. Bleomycin caused an increase mainly at 8 hours to 2.42 and continued to increase to 4 by 24 hours and 6.78 at 48 hours. UV-B caused a decrease in NAMase1 similar to NAMase2. After 2 hours of UV-B NAMase1 transcript levels decreased from 1 to 0.13, and to 0.10 by 4 hours. This remained low at 0.13 by 8 hours and 0.12 at 24 hours before a small increase to 0.2 at 48 hours.

5.3.2.3 Gene expression of NAMase3 with different stress treatments.

Stress	NAMase3					
Time point in hours	**0**	**2**	**4**	**8**	**24**	**48**
Salt	1.00	1.24	1.44	1.06	1.36	2.06
Mannitol	1.00	1.86	1.61	1.98	2.11	2.32
Hydrogen peroxide	1.00	1.08	0.94	0.94	0.80	1.12
Abscisic acid	1.00	1.10	1.41	1.54	1.79	3.49
Ethylene (ACC)	1.00	1.07	1.23	1.09	0.99	1.87
Auxin (NAA)	1.00	1.39	1.88	1.30	3.09	NA
Lipopolysaccharide	1.00	2.19	1.72	1.60	1.51	1.19
Jasmonic acid	1.00	0.64	0.68	0.72	0.65	0.67
Salicylic acid	1.00	1.40	1.79	1.81	1.81	1.78
Wounding	1.00	0.82	1.76	1.94	2.56	4.28
Phosphatase inhibitor	1.00	1.03	1.14	1.47	1.39	1.74
Kinase inhibitor (STA)	1.00	0.39	0.34	0.29	NA	NA
Cold treatment	1.00	1.17	1.14	0.97	0.73	0.65
Phosphate starvation	1.00	0.91	0.79	0.73	0.78	0.84
2,4 DNT	1.00	1.45	1.02	2.08	NA	NA
MMS	1.00	0.99	4.10	1.94	1.94	2.59
Bleomycin	1.00	1.45	2.03	2.63	5.87	6.38
UV-B	1.00	0.13	0.15	0.14	0.17	0.23

Table 5.4 Summary of fold differences in the expression of putative AtNAMase3 by RT-PCR under different stress conditions. Transcript levels are presented compared to actin expression. Experiment was repeated in triplicate and results presented as averages. NA indicates where transcript levels were so low it was impossible to take an accurate reading of expression.

The most significant changes in AtNAMase3 gene expression are seen with the DNA damaging agents (Table 5.4). MMS causes a rise in transcript level from 1 to 4 fold by 4 hours, this then drops to 1.94 at 8 and 24 hours and 2.59 at 48 hours. Bleomycin causes an increase to 1.45 within 2 hours and 2.03 at 4 hours. This continues to rise to 2.63 at 8hours, 5.87 at 24 hours and 6.38 at 48 hours. UV-B causes a big drop in gene expression from 1 to 1.13 within 2 hours and this then decreases dramatically to 0.15, 0.14, 0.17 and 0.23 at 4, 8, 24 and 48 hours respectively.

5.3.3 Expression of putative Nicotinamidases in *E. coli* and purification of protein.

In order to fully characterise the nicotinamidase genes in *A. thaliana* it was necessary to test the protein activity. *A. thaliana* nicotinamidase genes were cloned into Invitrogen pDEST 17 vector for the expression of proteins within *E. coli* BL21 pLysS cells. The pDEST 17 vector contains a T7 promotor and a lacZ repressor gene. The vector was transferred into the E. coli BL21 pLysS cells and successful transformants grown up in LB media to an optimum density of A_{600} 0.8-1. The addition of IPTG induces the expression of the inserted nicotinamidase gene fused to an N-terminal Histidine tag. The cells were lysed and total protein released was mixed with Nickel charged resin, which was then washed and the purified protein eluted from the resin.

5.3.3.1 Purification and activity of putative nicotinamidase AtNAMase2 protein.

The *E. coli* BL21 pLysS cells containing pDEST17 vector and NAMase2 were grown in LB and induced with 0.1mM IPTG for 16 hours at 18ºC. After cell lysis the total protein was bound to nickel resin. The resin was washed four times to remove impurities and protein bound to nickel was eluted in fractions. Protein samples were then run on SDS-PAGE and visualised using blue Coomassie stain (full method in chapter 2.3.1 and 5.2.3). The predicted size for NAMase2 was 22kDa.

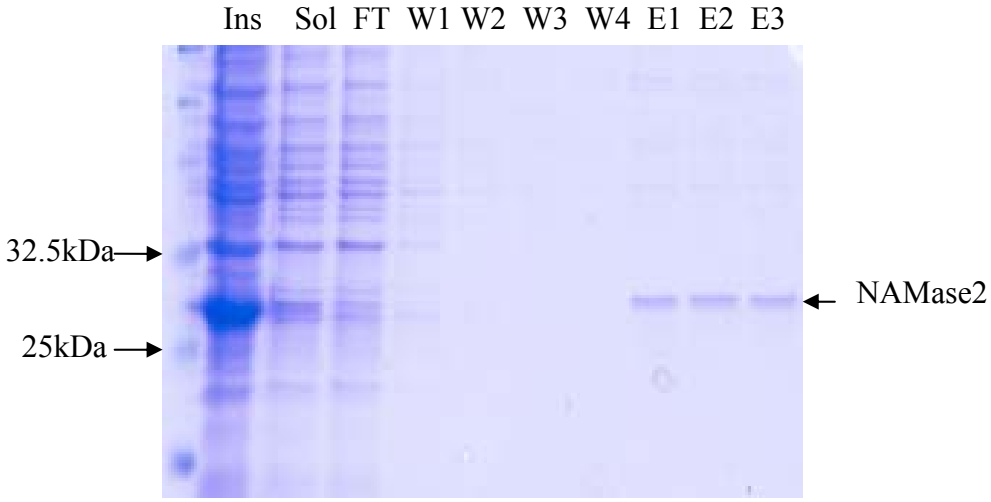

Figure 5.6 SDS-PAGE gel of *A. thaliana* NAMase2 expressed in *E. coli* BL21 cells. Lanes on gel from left to right are Marker, Induced insoluble fraction (Ins), soluble induced fraction (sol), flow through of protein after addition of nickel resin (FT), washes 1-4 (W1-4), protein elutions (E1-3). Arrow indicates purified protein of correlating to predicted size of NAMase2.

Purified protein (and controls of nicotinamide and nicotinic acid) was then set up in triplicate for nicotinamidase assay at 30ºC for 1½ hours before analysis with HPLC for the production of nicotinic acid.

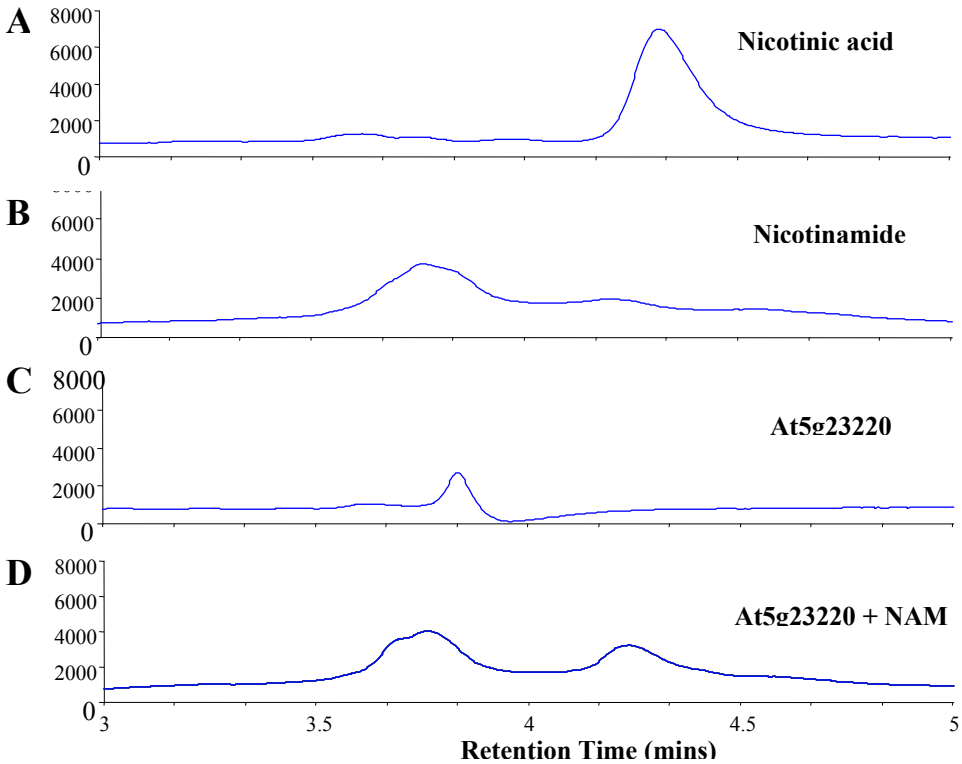

Figure 5.7 HLPC chromatogram of product for NAMase2 nicotinamidase assay. A, and B- shows graphs of control peaks for nicotinic acid (A) and nicotinamide (B). C- shows chromatogram of products of nicotinamidase assay containing NAMase2 purified protein and no substrate. D- shows peaks for products of assay containing NAMase2 protein and 8mM substrate nicotinamide. The assay was repeated in triplicate although only one representative chromatogram is presented.

The HPLC chromatogram showed that control nicotinic acid had a clear peak at retention time 4 mins 20 seconds, and nicotinamide at 3 mins 40 seconds. Only purified NAMase2 protein has a peak at 3 mins and 50 seconds. When purified NAMase2 and nicotinamide substrate were analysed there were three peaks present, one correlating to purified protein NAMase2 and another nicotinamide (seen at 3 mins 40 seconds and 50 seconds) and another clear peak at 4 mins 25 seconds which correlates to the control peak for the production of nicotinic acid. Authentic standards were used to quantify the concentration of nicotinamide produced in the enzyme assay.

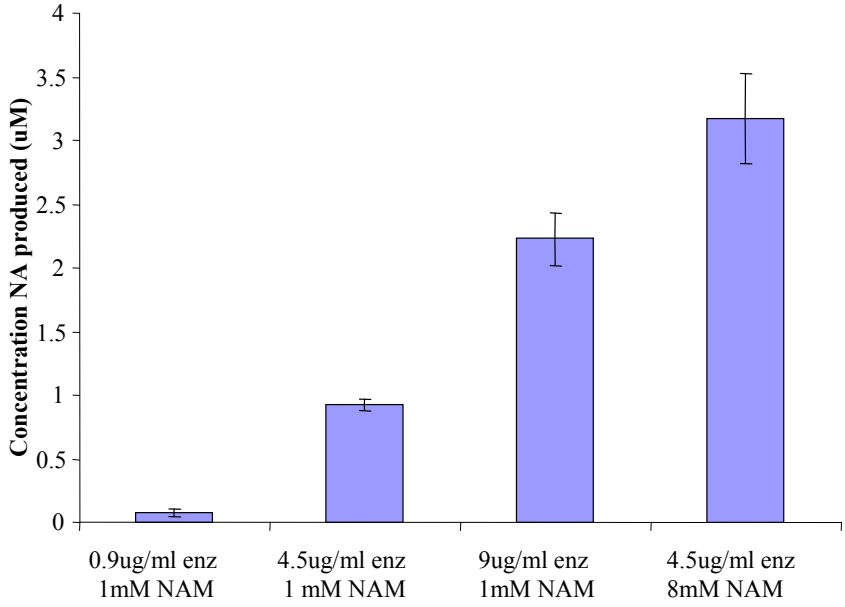

Figure 5.8 Nicotinamidase activity of purified NAMase2 protein. Nicotininamidase assay was performed with increasing amounts of and nicotinamide (NAM) and purified NAMase 2 protein. Nicotinic acid produced was analysed by HPLC. Standards of nicotinic acid were used to equate concentration / chromatogram peak area graphs, which were used to determine concentration of nicotinic acid produced. Assay was performed in triplicate and concentrations of nicotinic acid produced are presented as averages and error bars indicate standard deviation.

These results in Figure 5.8 showed that purified protein from nicotinamidase NAMase2 produced nicotinic acid in the presence of nicotinamide. This production of nicotinic acid increased with increasing amounts of enzyme and substrate. Protein concentration, substrate concentration and the concentration of nicotinic acid produced over time were used to determine the activity of the protein. The specific activity of this protein was calculated at 1.6 +/- 0.15 nmol nicotinic acid produced/ µg purified protein/hour.

5.3.3.2 Purification and activity of putative AtNAMase1 in *E. coli.*

E. coli BL21 pLysS containing pDEST 17 vector with NAMase1 were induced with 0.1mM IPTG for 16 hours at 18ºC and the cells lysed. Total protein was mixed with nickel column and purified protein eluted (full method in Chapter 2.3.1 and 5.2.3). The size of NAMase1 protein was predicted to be 22kDa.

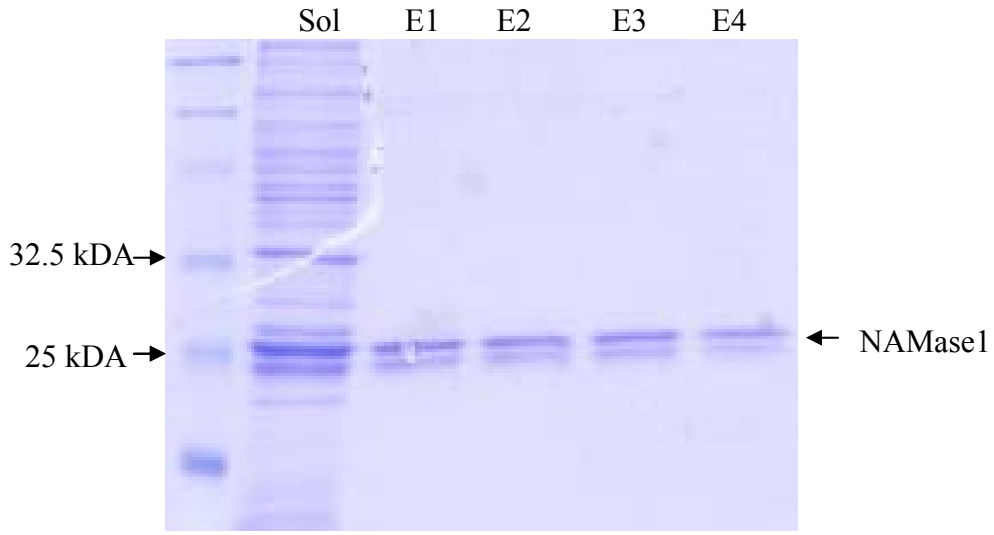

Figure 5.9 SDS PAGE gel of NAMase1 protein expressed in *E. coli* BL21 cells. Gel shows lanes from left to right, protein marker, induced soluble fraction (sol), four purified protein elutions (E1-4).

SDS-PAGE in Figure 5.9 showed the induced protein band in the soluble fraction. The eluted protein only showed two clear bands at about 25kDa, which is 3 kDa larger than predicted. The purified protein and controls was set up for nicotinamidase assay for 1½ hours at 30ºC and products analysed by HPLC.

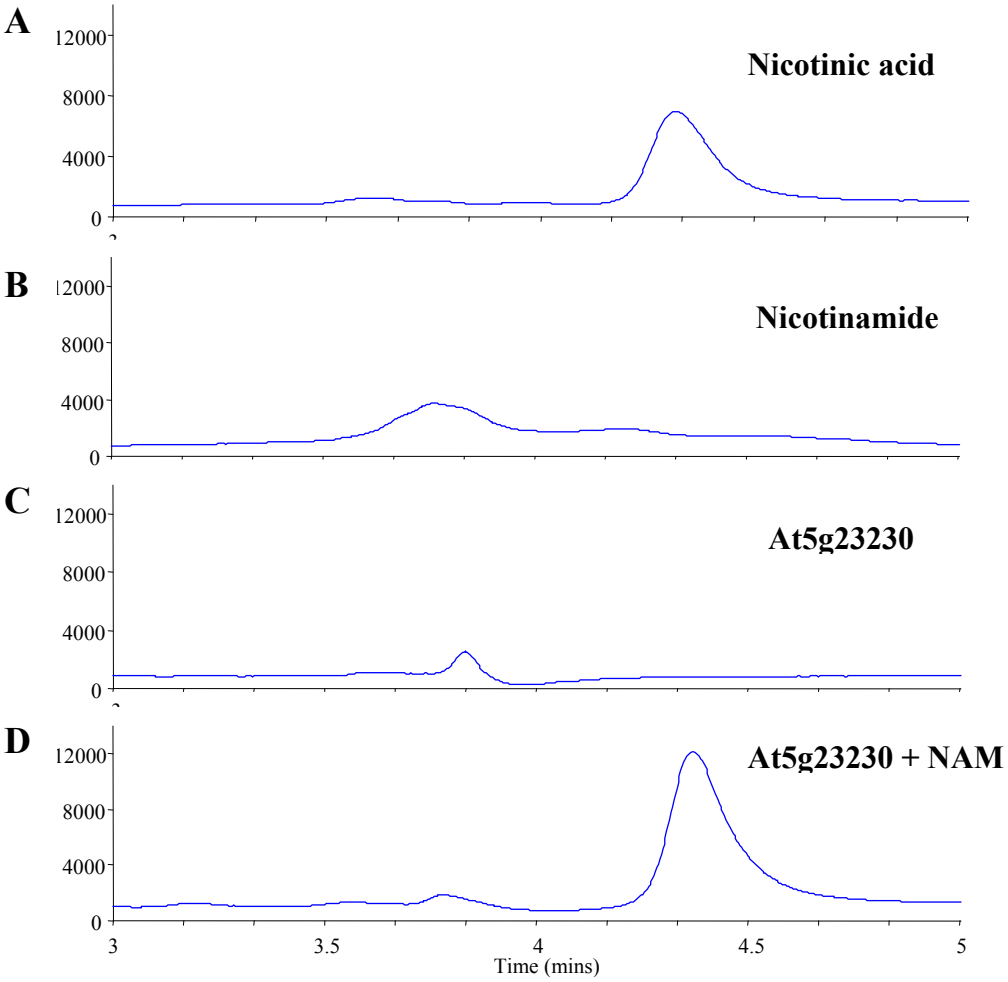

Figure 5.10 HLPC chromatogram of products for NAMase1 nicotinamidase activity. A, and B, shows graphs of control peaks for nicotinic acid (A) and nicotinamide (B) standards. C- shows chromatogram of nicotinamidase assay containing purified NAMase1 protein. D- shows chromatogram for products of assay containing purified NAMase1 protein and 8mM substrate nicotinamide (NAM). The assay was repeated in triplicate although only one representative chromatogram has been presented.

Figure 5.10 shows two clear peaks at 4 mins 20 seconds for nicotinic acid and 3 mins 45 seconds for nicotinamide were observed. Purified protein from NAMase1 without substrate showed a small peak at 3 mins 50 seconds. NAMase1 protein and nicotinamide substrate shows one small peak correlating to protein at 3 mins 50 seconds and one extra large peak at 4 mins 20 seconds, the same retention time as nicotinic acid. The large peak is not present when only NAMase1 protein was analysed.

Standards of nicotinamide were used to quantify the concentration produced in the enzyme assay.

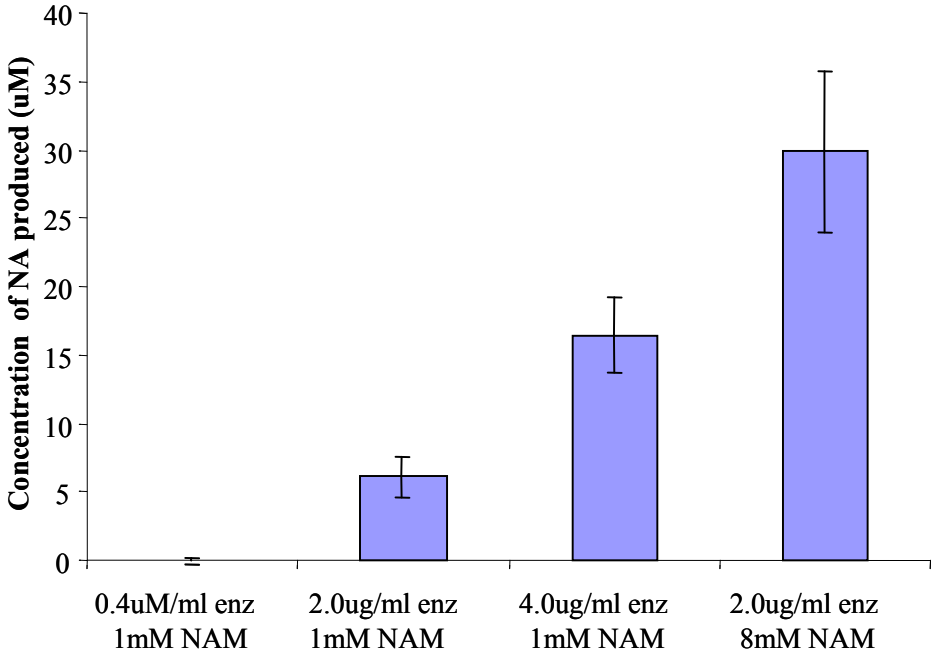

Figure 5.11 Nicotinamide activity of NAMase1 purified protein. Nicotininamidase assay was performed with varying concentrations of and nicotinamide (NAM) and purified NAMase 2 protein. Products of nicotinamidase assay were analysed by HPLC. Peak areas from standards of nicotinic acid were used to determine the concentration of nicotinic acid produced in nicotinamidase assay. Assay was performed in triplicate and concentrations of nicotinic acid produced are presented as averages and error bars indicate standard deviation.

When the peak area was analysed there was an increase in production of nicotinic acid with an increase in NAMase1 protein and also with an increase in nicotinamide substrate. The specific activity of this protein is 2.7 +/- 0.5nmoles nicotinic acid produced /µg nicotinamidase /hr.

5.3.3.3 Purification and activity of putative nicotinamidase NAMase3 protein.

E. Coli BL21 pLysS cells were transformed with construct of vector pDEST17 containing NAMase3 sequence, and were induced with 0.1mM IPTG and grown for 16 hours at 18ºC.

Cells were lysed and total cell protein was mixed with nickel resin. After 4 washes protein bound to nickel resin was eluted from the resin. NAMase3 was predicted to be 21 kDa. (full method in Chapter 2.3.1 and 5.2.3). Protein samples from stages of protein purification were run on SDS-PAGE gel

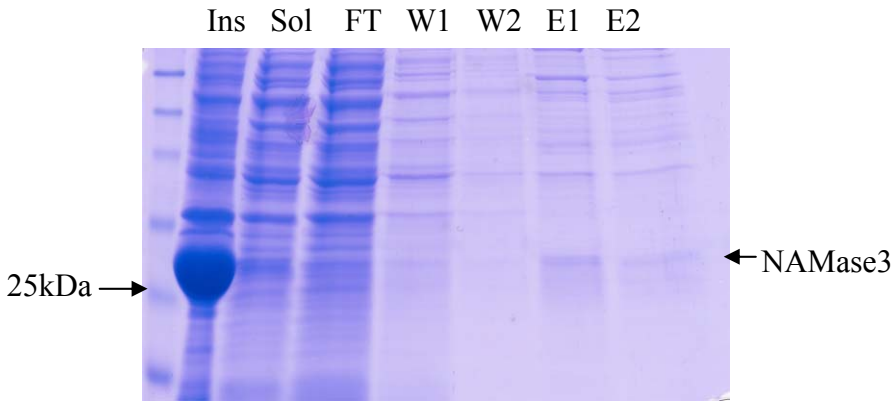

Figure 5.12 SDS PAGE of NAMase3 protein expression in *E. coli*. Lanes on gel from left to right are Marker, Induced insoluble fraction (Ins), soluble induced fraction (sol), flow through of protein after addition of nickel resin (FT), washes 1 and 2 (W1 and W2) and two protein elutions (E1 and E2).

Protein size was predicted to be 21 kDa although the large band induced is a little larger at above 25 kDa. The wash fractions contained many protein bands and the protein eluted showed more contamination than for the other nicotinamidase proteins. However, eluted protein was used for nicotinamidase assay and products analysed by HPLC.

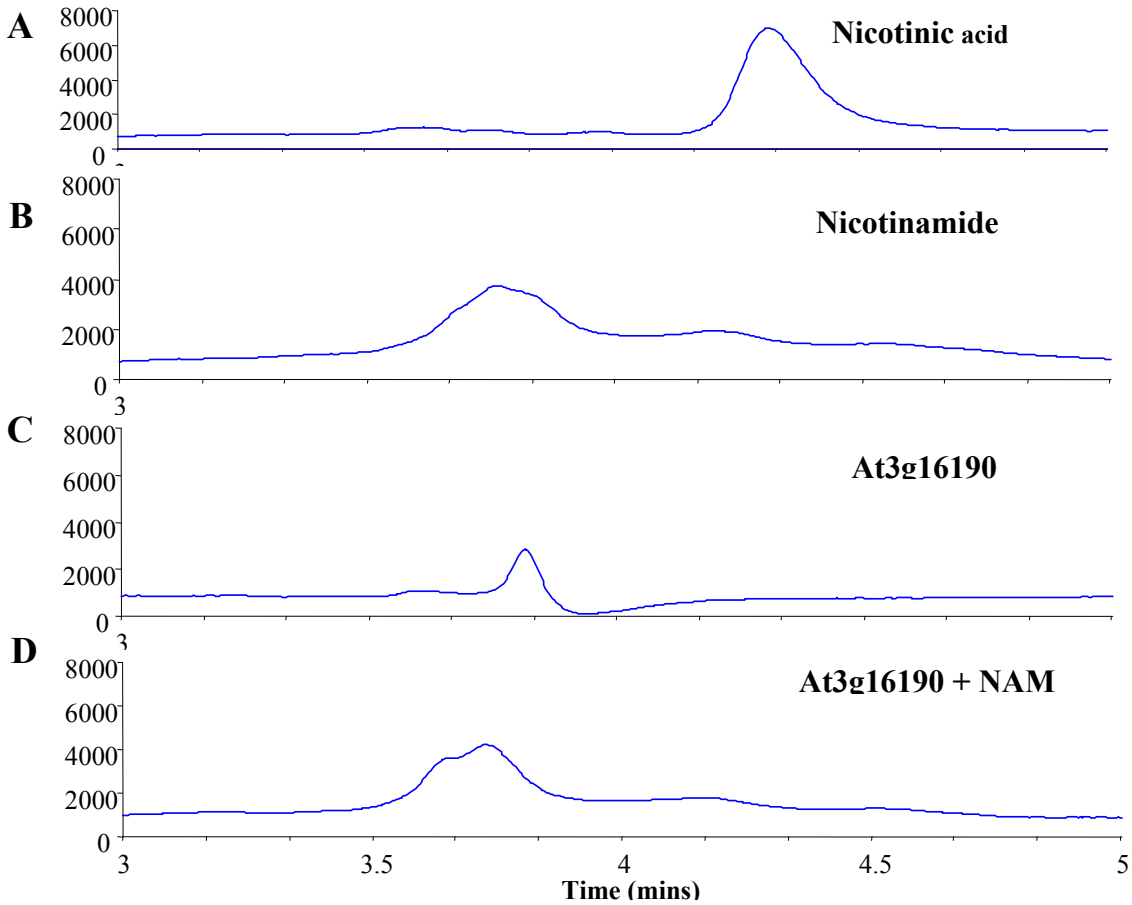

Figure 5.13 HLPC chromatogram of products of nicotinamidase activity of NAMase3 protein. A, and B, show chromatograms of standards for nicotinic acid (A) and nicotinamide (NAM; B). C- peaks of nicotinamidase assay containing purified NAMase3 protein. D- shows chromatogram for products of assay containing purified NAMase3 protein and 8mM substrate nicotinamide (NAM). Although only one representative chromatogram has been presented the assay was repeated in triplicate.

Controls reactions for nicotinic acid and nicotinamide show peaks at 4 mins 20 seconds and 3 mins 45 seconds respectively. The graph for NAMase3 protein shows only one peak at 3 mins 50 seconds. For NAMase3 and nicotinamide substrate only shows two peaks, one at 3 mins 40 seconds correlating to nicotinamide and one at 3 mins 50 for the NAMase3. However, there is no peak at 4 mins 20 seconds for the production of nicotinic acid.

Standards of nicotinamide were used to quantify the concentration of the nicotinamide produced in the enzyme assay. A graph of nicotinamidase activity is shown in in Figure 5.14.

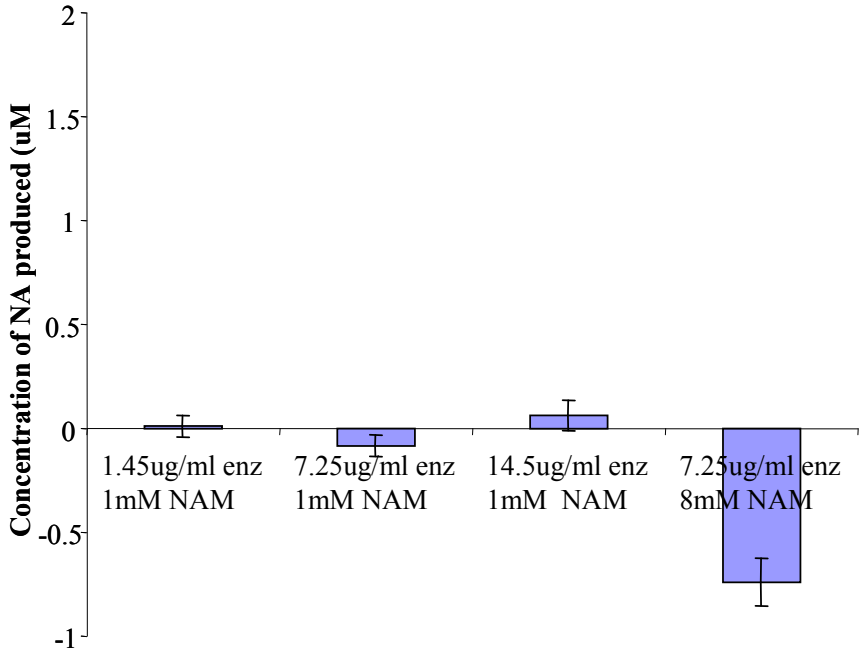

Figure 5.14 Nicotinamide activity of NAMase3 purified protein. Nicotininamidase assay was performed with increasing amounts of and nicotinamide (NAM) and purified NAMase 3 protein. Products of nicotinamidase assay were analysed by HPLC. Peak areas from standards of nicotinic acid were used to determine the concentration of nicotinic acid produced in nicotinamidase assay. Assay was performed in triplicate and concentrations of nicotinic acid produced are presented as averages and error bars indicate standard deviation.

The reaction of purified NAMase3 with nicotinamide substrate did not produce any nicotinic acid (Figure 5.14). The HPLC did not show any peak correlating to nicotinic acid production. When the area of these peaks was analysed there was actually a decrease in the area where a peak for nicotinic acid should be.

5.3.2 Nicotinic acid phosphoribosyltransferase (NAPRT) enzymes.

Nicotinic acid phosphoribosyltransferase is a member of the phosphoribosyltransferase superfamily. It utilizes 5-phosphoribosy 1-pyropyruvate (PRPP) as a substrate in the reaction

Nicotinic acid + PRPP ⟶ Nicotinic acid mononucleotide + PPi

5.3.2.1 Identification of NAPRT gene in *A. thaliana*.

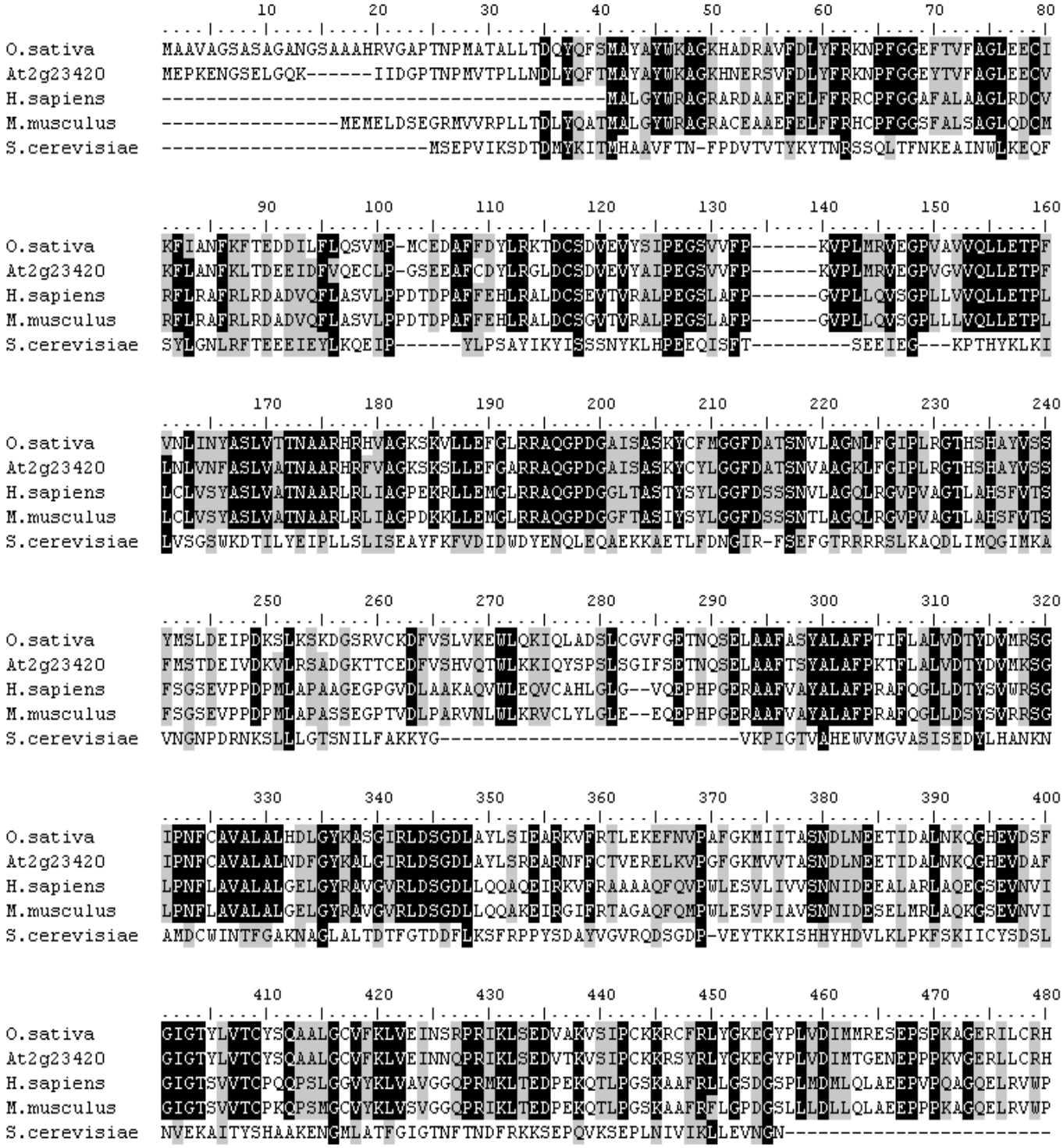

Figure 5.15 Sequence homology for putative *A. thaliana* NAPRT sequence At2g23420. Shows sequence homology with NAPRT from *O. sativa* Os04g0429800 (NP_001052813) is 74% with 88% similarity, with *Homo sapiens* (NP_660202) shows 45% homology and 64% similarity, to *M. musculus* (NP_766195) 44% homology and 64% similarity and with *S. cerevisiae* (NP_014852) 22% homology and 38% similarity at an amino acid level. Alignments were performed in BioEdit with ClustalW.

The structure of two NAPRT enzymes have recently been resolved by crystallography from yeast and *Thermoplasma acidophilum* (Chappie et al. 2005; Shin et al. 2005). However, as these proteins show only about 20% homology to NAPRT from *A. thaliana* it is questionable how relevant any structural correlations would be (Figure 5.15). However, the consensus between NAPRT enzymes (and their related QRPT enzymes) is that they contain an N-terminal domain, a central active domain and a more variable C-terminal domain. The active site forms a pocket lined with basic and aromatic residues, with the pyrophosphate located at the entrance interacting strongly with residues RLDSGDL positioned at residues 337 (Shin et al. 2005).

5.3.2.2 Purification and activity of putative *A. thaliana* NAPRT At4g23420 protein.

The *A. thaliana* gene At4g23420 was cloned into the pDEST17 vector and expressed in *E. coli* BL21 pLysS cells. Recombinant protein was induced with 0.1mM IPTG for 16 hours at 18ºC. After cell lysis total protein was mixed with nickel charged resin to purify protein (full method in Chapter 2.3.1 and 5.2.3). NAPRT At2g23420 was predicted to be 64kDa in size. (This work was performed in collaboration with Dr. Emma Travis).

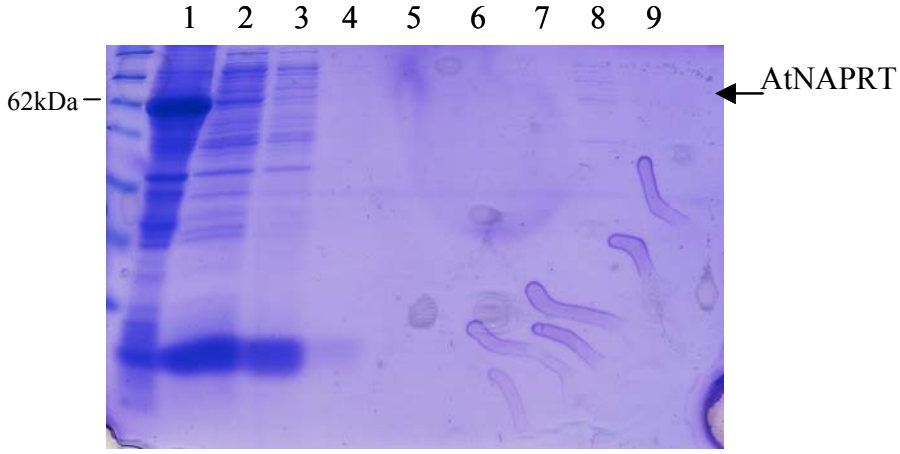

Figure 5.16 SDS-PAGE of purification of putative NAPRT protein At2g23420 expressed in *E. coli*. Lane 1- total induced insoluble protein, 2- total induced soluble protein, 3- flow through protein after binding with nickel resin, 4-7 four consecutive washes of nickel resin, 8 and 9 eluted purified NAPRT protein. (This work was performed in collaboration with Dr. Emma Travis).

The purified NAPRT protein was used to set up NAPRT assays in triplicate (see Chapter 5.1.3). Concentrations of protein and substrate were varied and the reaction products analysed by HPLC.

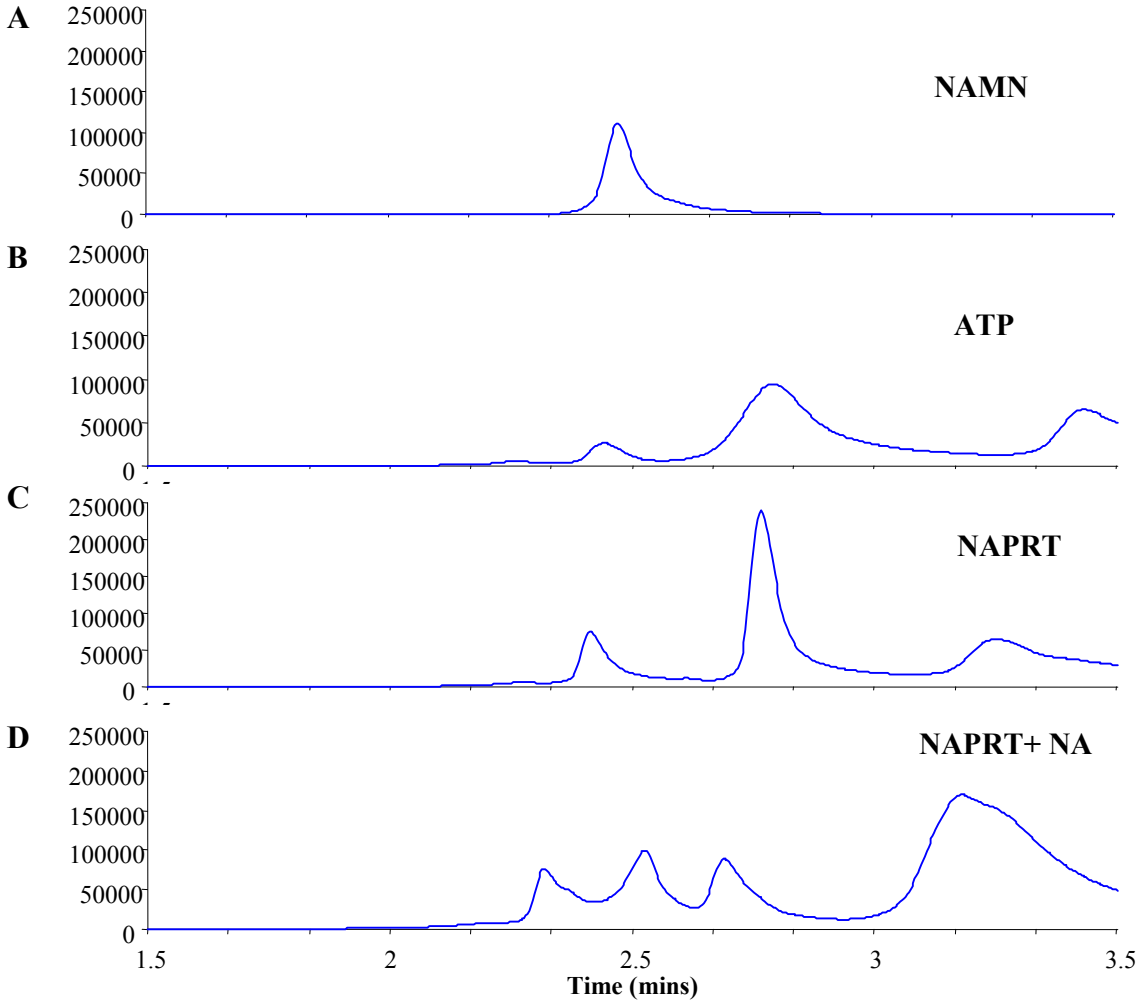

Figure 5.17 HPLC Chromatogram of products of NAPRTase activity of purified NAPRT At2g23420 protein. A and B shows control chromatogram of NAMN (A) and ATP (B) standards. C shows chromatogram of nicotinamidase assay containing purified NAPRT enzyme alone, D shows chromatogram for products of assay containing purified NAPRT enzyme plus nicotinic acid (NA) substrate and ATP required for reaction. The assay was repeated in triplicate although only one representative chromatogram has been presented.

The peak for product NAMN shows a clear peak at 2.5 mins retention time. The control for ATP (required for the NAPRT reaction) shows 3 peaks at 2.5, 2.8 and 3.5minutes. The NAPRT enzyme alone shows three peaks at very similar retention times as ATP at 2.5, 2.8

and 3.2 mins. The reaction containing both purified NAPRT enzyme and substrate 4 peaks are seen; three of these correspond to peaks for enzyme and ATP at 2.4, 2.7 and 3.2 mins. An extra peak is seen at 2.5 mins, which corresponds to the production of NAMN.

5.3.3 Nicotinic acid mononucleotide adenylyltransferase (NaMNAT) enzymes.

NaMNAT enzymes catalyse the conversion of nicotinic acid mononucleotide (NaMN) to nicotinic acid adenine dinucleotide (NaAD). NaMNAT enzymes display a unique dual specificity for both nicotinic acid mononucleotide (NaMN) and nicotinamide mononucleotide (NMN) and therefore functions in both the NAD salvage and *de novo* pathways. They work by transferring an adenyl from ATP onto NaMN resulting in the formation of NaAD and pyrophosphate.

NaMNAT enzymes have been identified in bacteria (Mehl et al. 2000), yeast (Emanuelli et al. 2003), *D. melanogaster* (Zhai et al. 2008), and humans (Schweiger et al. 2001a). Three NaMNAT enzymes have been identified in human the properties and activities of which are reviewed in Berger et al. 2005.

A putative NaMNAT enzyme in *A. thaliana* was identified by comparing translated sequences from characterised NaMNAT is other organisms to the translated *A. thaliana* genome database using the BLAST algorithm (Hunt et al. 2004).

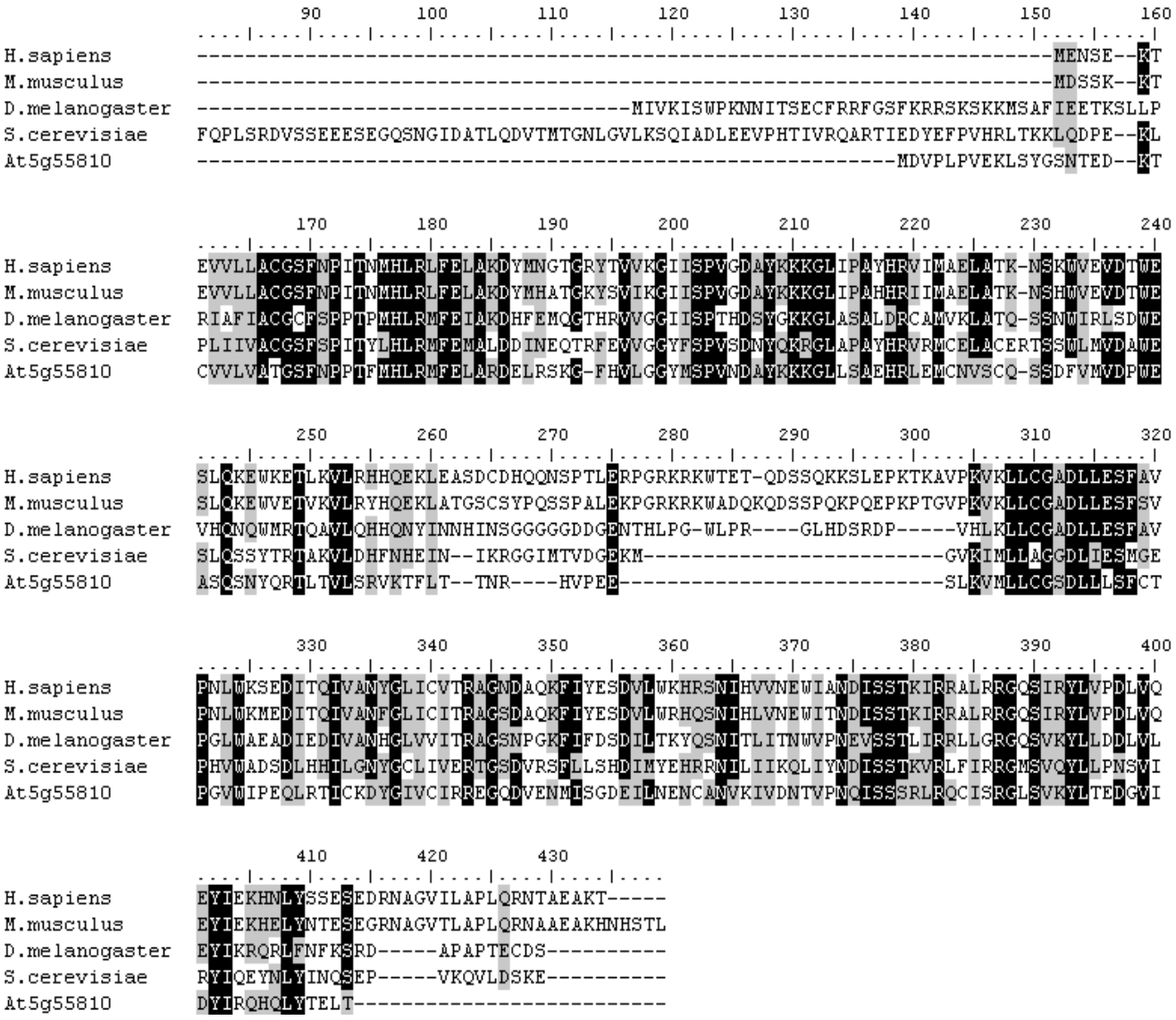

Figure 5.18 Sequence homology for putative *A. thaliana* NaMNAT At5g55810 sequence. At5g55810 alignment with *H. sapiens* NMNAT1 (NP_073624) shows 38% homology and 57% similarity, to *M. musculus* (NP_597679) 37% homology with 56% similarity, to *D. melanogaster* (NP_733064) 36% homology and 57% similarity and to *S. cerevisiae* (NP_011524) 39% homology and 60% similarity at an amino acid level.

The structure of human NaMNAT has been shown by x-ray crystallography to consists of a 6 stranded β-sheet covered by α-helices (Werner et al. 2002). Two conserved motifs necessary for N(a)MN are found in all NaMNAT enzymes consisting of an N-terminal sequence GXFXPX(T/H)XXH and a C-terminal sequence SXTXXR. Both these motifs are found in the *A. thaliana* gene At5g55810 at residues 168-177 and 378-382 (Figure 5.18).

5.3.3.1 Purification and activity of putative NaMNAT At5g55810 protein.

At5g55810 was cloned into the pDEST 17 vector (see Chapter 5.2.2) and induced for 16 hours at 18ºC with 0.1mM IPTG. Total protein was mixed with nickel charged resin to purify the NaMNAT protein (full protein purification method in Chapter 2.3.1 and 5.2.3) Samples were run on SDS-PAGE gel (Figure 5.19). The size of At5g55810 was predicted to be 30kDa. (This work was performed in collaboration with Dr. Emma Travis).

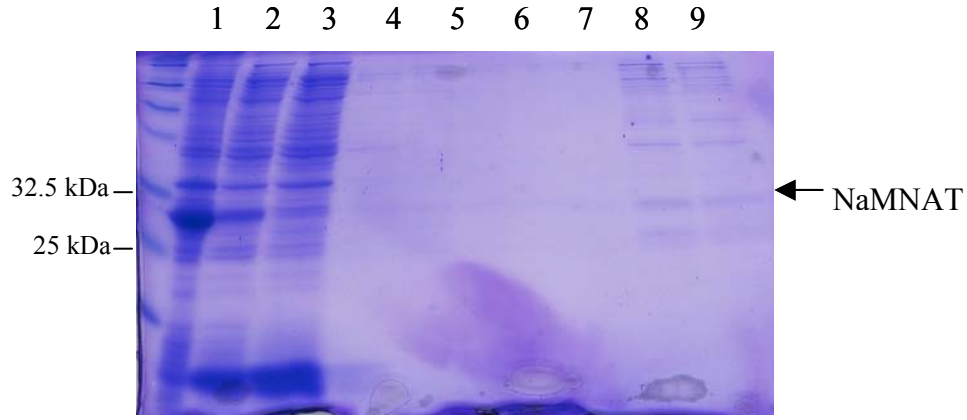

Figure 5.19 SDS-PAGE of purification of NaMNAT At5g55810. Lane 1- total induced insoluble protein, 2- total induced soluble protein, 3- flow through protein after binding with nickel resin, 4-7 four consecutive washes of nickel resin, 8 and 9 eluted purified NAPRT protein.

Purified protein was used to set up for NaMNAT assay in triplicate (Chapter 5.1.4) Concentrations of NMN substrate and enzyme were varied and the products of the NaMNAT assay were analysed by HPLC.

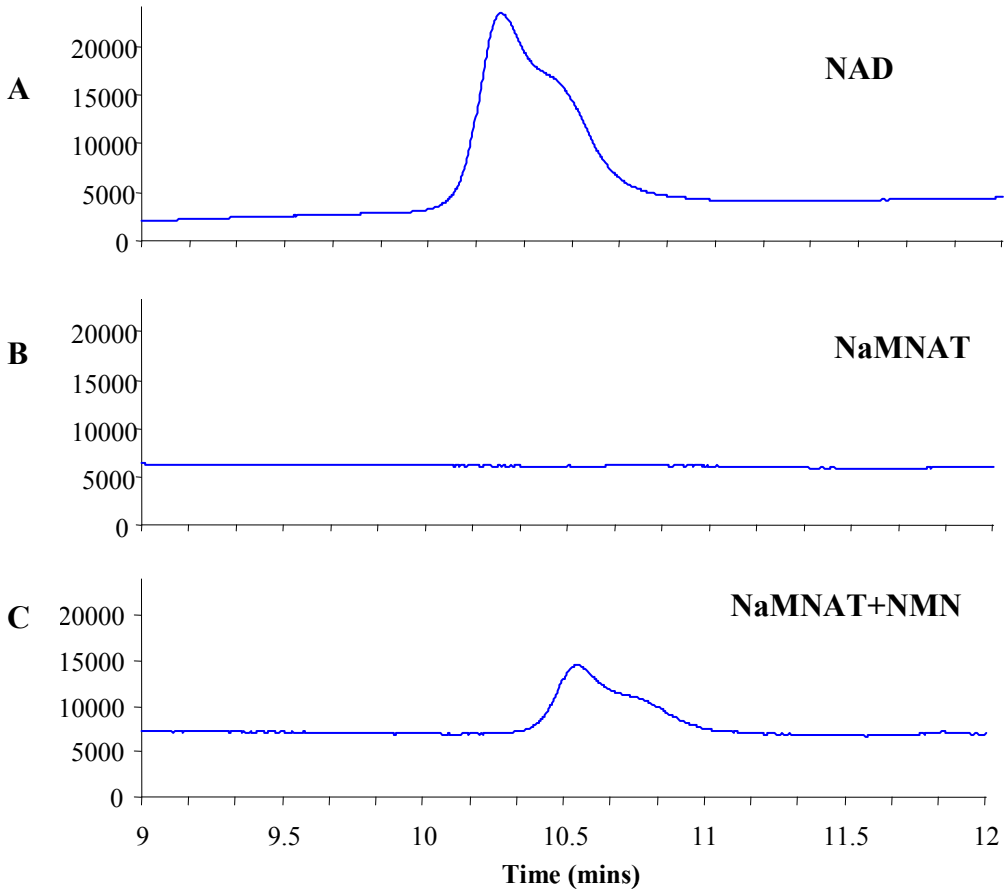

Figure 5.20 HLPC chromatogram of products of NaMNATase assay using purified At5g55810 protein. A, shows chromatogram of control peaks NAD standard. B- shows chromatogram of NaMNATase assay containing purified NaMNAT protein. C- shows chromatogram for products of NaMNATase assay containing purified NaMNAT protein and 8mM substrate nicotinamide mononucleotide (NMN). The assay was repeated in triplicate although only one representative chromatogram has been presented

The control for NAD^+ product shows characteristic two peaks at 10.5 minutes retention time. The HPLC for only purified At5g55810 protein only does not show any peaks at the time corresponding to any formation of NAD^+ product. The graph for purified NaMNAT protein plus substrate NMN shows the formation of the NAD^+ two peaks at 10.5 minutes suggesting that At5g55810 functions as a NaMNAT enzyme. The chromatogram for substrate NMN showed a peak at approximately 4 mins and is therefore not represented.

The purified NaMNAT enzyme was also able to convert NaMN to NaAD, and displays dual substrate specificity identified in all other NaMNAT enzymes.

Standards of known NAD^+ concentrations were used to plot and a calibration curve of concentration /peak areas. The area of NAD^+ peak formed during the HPLC of the NaMNAT assay was used to determine the concentration of NAD^+ produced by the NaMNAT protein. From this activity and kinetics were calculated.

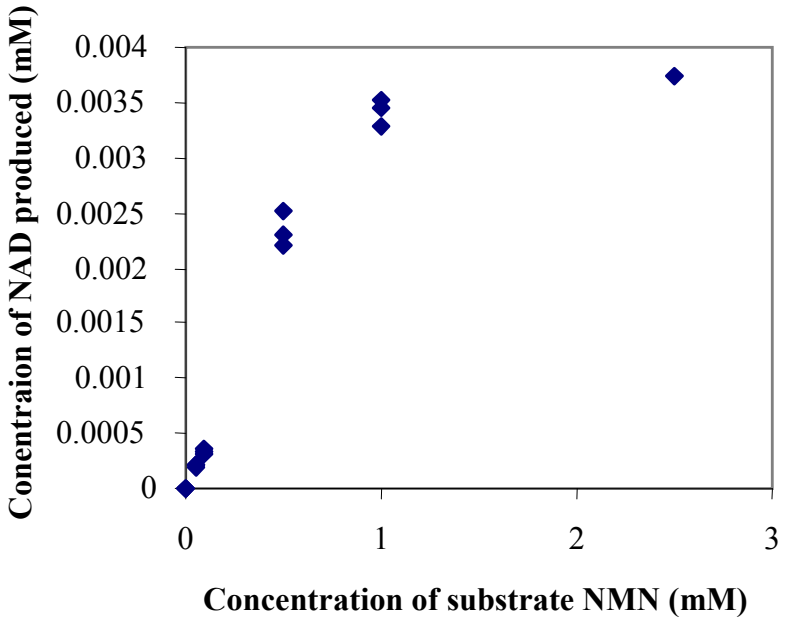

Figure 5.21 Michealis Menton kinetics of NaMNAT At5g55810 activity. Graph shows the increase in production of NAD^+ with increasing concentration of substrate NMN.

The specific activity of this enzyme was calculated to be 3.1 +/- 0.1 nmols/ug/hour with the K_m at 1mM NMN and V_{max} at 0.0041mM NAD^+.

5.4 Discussion

Utilization of NAD as a substrate by sirtuins and PARPs produces nicotinamide and the NAD salvage pathway functions to recycle the nicotinamide back into NAD^+. Nicotinamide is converted to Nicotinic acid by nicotinamidases, which is then converted by NAPRTs and NaMNATs to NaAD. The final step into NAD^+ is completed by NAD synthases. This pathway is present in *E. coli*, yeast, plants, *C. elegans* and *D. melanogaster* but differs in mammals. The mammalian NAD salvage pathway lacks nicotinamidases and nicotinamide is converted to NAD^+ via NMN by the action of NamPRT and NMNAT (see Section 1.5.2 for full description).

5.4.1 Identification NAD salvage pathway genes in A. thaliana

Nicotinamidase enzymes have been identified in *E. coli* (Frothingham et al. 1996), yeast (Hu et al. 2007a), *D. melanogaster* (Balan et al. 2008) and *C. elegans* (van der Horst et al. 2007). Three nicotinamidases were identified in *A. thaliana* through protein BLAST searches using nicotinamidases sequences from other organisms. The *A. thaliana* nicotinamidases showed high similarity in the proposed catalytic regions only, but overall sequence homology to both *E. coli* and yeast nicotinamidase was very low.

Yeast NAPRT structure had been clarified by x-ray crystallography (Chappie et al. 2005) and although Arabidopsis NAPRT At2g23420 contains a homologous region thought to be essential for the functioning of the active site, overall homology to yeast NAPRT is very low at 22% similarity. It is more similar to NAPRTs identified in humans and mice but there is no information on the structure of these proteins.

The sequence for *A. thaliana* NaMNAT contains 2 conserved motifs found in all NaMNAT enzymes although the function of these conserved regions in unknown. Overall the

Arabidopsis NaMNAT has low homology to human NaMNAT which has had its structure elucidated by x-ray crystallography (Schweiger et al. 2001a). For this reason it is difficult to ascertain any similarity in domain structure of the Arabidopsis protein from that of the human sequence.

5.4.2 Expression of *A. thaliana* nicotinamidases genes

The largest difference seen in gene expression for the nicotinamidases is for NAMase2 with plant stress hormone Abscisic acid. NAMase2 also shows an increase in gene expression with phosphate starvation. At2g23230 and NAMase3 are both up regulated by MMS and Bleomycin. All 3 nicotinamidases are down regulated by UV-B exposure.

These results are consistent with the results found in two papers published on nicotinamidases in 2007. The first report showed that seeds of null lines for NAMase1 were hypersensitive to Abscisic acid with reduced germination potential and inhibited growth. These null lines were also more sensitive to DNA damaging agent MMS (Hunt et al 2007). The paper suggests this response in nicotinamidase activity results from changes in PARP activity although no data is provided to support this. However, the RT-PCR and qPCR presented in this chapter shows a dramatic increase in PARP AtPARP3 with Abscisic acid and PARP AtPARP1 and AtPARP2 with MMS. This is not surprising considering the increase in expression of the NAD utilising sirtuin and PARP genes with DNA damaging agents. However, exposure to UV-B also causes an increase in gene expression of sirtuins and PARPs, but this has the opposite effect on nicotinamidase transcript levels where a large decrease is seen.

It is interesting that T-DNA insertion null lines are commercially available for both nicotinamidase genes At2g23230 and NAMase3 but not for At2g23220. This could suggest that an inactivation of At2g23220 may be lethal.

In the second paper published on nicotinamidases in Arabidopsis an extra gene was identified at At2g22570 (Wang and Pichersky 2007). Growth of null mutants for this nicotinamidase was found to be inhibited by Abscisic acid and salt. The Abscisic acid signal transduction pathway mediates the response to conditions of drought and salinity (Finkelstein et al. 2002 Xiong et al. 2002). An increase in Abscisic acid causes the production of cyclic ADP ribose (Wu et al. 2003). This paper also showed an increase in sensitivity of At2g22570 to salt, although the RT-PCR presented here showed no change in the other nicotinamidase gene expression with salt.

Nicotinamide acts as an inhibitor on the activity of both sirtuins and PARPs, and the increase in their activity would produce a rise in the production of nicotinamide. The nicotinamide would have to be converted by nicotinamidases to alleviate the inhibition.

5.4.3 Activity of Nicotinamidase protein.

Purified protein from *A. thaliana* genes NAMase2 and NAMase1 showed nicotinamidase activity by converting nicotinamide to nicotinic acid. Time did not allow for enough samples in triplicate for kinetic analysis to determine the Km and Vmax of the proteins, and the publishing of papers on these genes made any repeat of HPLC unnecessary (Hunt et al 2007). Therefore it is not possible to compare activities of these with nicotinamidases from other sources.

Purified protein of NAMase3 did not show nicotinamidases activity, which was also confirmed by others (Hunt et al 2007). NAMase3 is annotated in both the TAIR and NCBI websites as an isochorismatase, a group of enzymes normally only found in bacteria. It is possible that NAMase3 catalyses different reactions.

An increase in nicotinamidase activity has been shown to increase activity of sirtuins in yeast (Gallo et al. 2004), *E. coli* (Frothingham et al. 1996), *C. elegans* (van der Horst et al. 2007)

and *D. melanogaster* (Balan et al. 2008). Investigations into changes in sirtuin activity in nicotinamidase overexpressing lines may confirm the same in plants. So far there has been little data published on the effect of an increase in nicotinamidase activity on PARPs despite the hypothesis that an increase in NAD recycling confers an increase in cellular energy homeostasis and stress resistance. It would be interesting in future to test this on lines with altered activity of enzymes involved in the NAD salvage pathway.

5.4.4 Activity of NAPRT and NaMNAT

A NAPRT gene was identified in *A. thaliana* by BLAST searches with sequences from NAPRT genes characterised from other organisms. This gene was expressed with a Histidine epitope tag in *E. coli* BL21 cells and the protein purified. The protein was assayed for activity with nicotinic acid as a substrate and products were analysed by HPLC. The formation of nicotinic acid mononucleotide characterises At2g23420 as a NAPRT.

Similarly, a putative NaMNAT sequence was also identified in *A. thaliana* by sequence homology to other NaMNATs. Protein purified from expression of this gene in *E. coli* was assayed with substrates NaMN and NMN and the products analysed by HPLC. The formation of NAD by At5g55810 demonstrated its NaMNAT enzymic activity.

T-DNA insertions in both NaMNAT and NAPRT genes could further reveal the effects of the NAD salvage pathway on cellular NAD levels, particularly in response to stresses that unregulate sirtuins and PARPs.

Chapter 6: Discussion.

6.1 The responses of sirtuins, PARPs and PARGs to DNA damage.

For all of the sirtuins, PARPs and PARGs an increase in gene expression was seen with DNA damaging agents, suggesting a role for the NAD utilizing enzymes and the NAD salvage pathway.

Investigations using null lines for each of the sirtuins, PARPs and PARGs with DNA damaging agents showed an increase in susceptibility to MMS for null AtPARG1. Sirtuin At5g55760 null lines were less tolerant of UV-B exposure.

There are different DNA repair pathways specific to different types of DNA damage. Double strand breaks are particularly hazardous to cells because they can result in genome rearrangements. There are two mechanisms for repair, non-homologous end joining (NHEJ), and homologous recombination. Single strand breaks are repaired by either the Nucleotide Excision Repair (NER) or Base Excision Repair (BER) pathways. Bulky helix distorting changes produced by UV-B exposure is repaired by the NER pathway whilst simpler single strand breaks that arises from oxidation or alkylation (e.g. DNA damaging agent MMS) are repaired by the Base Excision Repair pathway.

6.1.1 PARG AtPARG1 null lines are more sensitive to DNA damaging agents.

AtPARG1 null lines showed increased cell death phenotype with MMS application. Published work on other model organisms with mutant PARG genes also showed accelerated cell death under normal growing conditions without the addition of any DNA damaging agents. Mice lacking PARGs die at embryonic day 3.5 (Koh et al. 2004) and Drosophila PARG null mutants abort and show neural degeneration at the early larval stages (Hanai et al. 2004).

In all model organisms only one PARG gene has been identified except, for *C. elegans,* and as shown here in *A. thaliana*. Drosophila and mice lacking the PARG gene show a cell death phenotype under normal growth conditions without any induced DNA damage. The stronger phenotype in null Drosophila and mice lines compared to *A. thaliana* could be due to Arabidopsis having two PARG genes. However, it is unlikely that functional redundancy exists between the two *A. thaliana* PARG genes as no phenoptype is seen with DAN damaging agents for AtPARG2 null lines. This would suggest that the two AtPARG genes have separate roles.

No phenotype for the three PARP null lines was observed with DNA damage, suggesting that functional redundancy exists between the three PARP genes.

PARG has been shown to control activity of PARP enzymes by the removal of PAR and there are different hypothesis for PARP/PARG involvement in DNA repair as detailed in section 1.3.3.1. Firstly, ADP ribosylation of histones affects chromatin condensation. Secondly, PARP has been shown to recruit DNA repair proteins. Thirdly, ADPribose polymer itself has been indicated as a cell death signal by two possible mechanisms. Firstly, an increase in PARP activity could deplete cellular NAD causing metabolic failure and necrosis (De Block et al. 2005). The second mechanism was proposed after a report showed that ADP ribose polymer acts as a signal for programmed cell death by the induction of Apoptosis Inducing Factor, AIF (Yu et al. 2006) translocation to the nucleus where it causes DNA fragmentation and apoptosis (Susin et al. 1999a). It is interesting that these two mechanisms evoke different modes of cell death, as an increase in ADPribose polymer could lead to necrosis (cell breakdown and failure) or a controlled deliberate apoptosis.

In AtPARG1 null lines there is less reversal of the activity of PARP proteins. Theoretically this would suggest that the accumulation of ADP ribose polymer and the depletion of NAD would lead to an increase in cell death.

6.1.2 The response of Sirtuin At5g55760 null lines to DNA damaging chemicals.

Gene expression of At5g55760 was shown to increase with the DNA damaging agents MMS and Bleomycin although there was no change in transcript level for At5g09230. T-DNA inactivated At5g55760 Arabidopsis plants were more sensitive to DNA damaging agent MMS.

Sirtuin involvement in DNA repair is consistent with previous published data. A paper on 2 sirtuin genes in rice showed that RNAi SRT1 knockdown lines (shows most homology to At5g55760) showed an increase in DNA breaks under normal growing conditions (Huang et al. 2007). Chromatin immunoprecipitation from RNAi knockdown lines showed an increase in acetylation of transposon and retroelements, as well as some programmed cell death genes. Sirt6 knockout mice also display a decrease in DNA repair and genomic instability (Mostoslavsky et al. 2006). These papers suggest that sirtuins have a role in safeguarding the cell against genome instability, which is consistent with the phenotype for At5g55760 null lines with MMS. A weak phenotype was observed with Arabidopsis sirtuin At5g55760 inactivated lines, which were less tolerant of MMS. It is possible that a stronger phenotype for sirtuin in *A. thaliana* would be seen with a double mutant for both sirtuin genes.

Although sirtuins were identified as histone deacetylases, they have been shown to deacetylate and ADP ribosylate other proteins. Proteins identified in mammalian cells as targets for sirtuin deacetylation appear to be involved in cell death mediation. These proteins include tumour suppressor transcription factor p53 (Vaziri et al. 2001), FOXO transcription factors and Ku70 (Cohen et al. 2004a). There are several pathways for apoptosis although in the case of DNA damaged cell, this is preferentially through a p53 dependent pathway. Deacetylation by mammalian SIRT1 of p53 has been shown to repress p53 and DNA damage induced cell death (Luo et al. 2001). FOXO transcription factors have been shown to initiate apoptosis by activating transcription of cell death components FasL and Bim (reviewed in

(Van der Heide et al. 2004). Sirtuin deacetylation of FOXO decreases its DNA binding properties and inhibiting cell death (Yang et al. 2005).

An important mediator of apoptosis, Ku70 initiates Bax induced apoptosis when acetylated. It has been shown that sirtuin deacetylation of Ku70 suppresses Bax induced apoptosis in mouse fibroblast cells (Cohen et al. 2004a)).

The targets for At5g55760 are unknown and in future investigations to identify interactors using yeast 2 hybrid system, or At5g55760 TAP tag fusion proteins may further elucidate this mechanism. Co- immunoprecipitation could also be performed on the 35S:HA:At5g55760 lines identified in this project. This involves using a commercially available antibody to the HA tag to capture the At5g55760 and any interacting target proteins.

6.1.3 Sirtuin At5g09230 involvement in UV-B signalling pathway

Sirtuin At5g09230 shows an increase in gene expression with exposure to UV-B light. At5g09230 null lines identified here showed more susceptibility to the damaging effects of UV-B compared with wild type plants. Components of the UV-B signalling pathway have been characterised as UVR8 and transcription factor Hy5. Prof. Gareth Jenkins (University of Glasgow) supplied T-DNA inactivated lines for both UVR8 and HY5 and At5g09230 transcript levels in these were investigated. At5g09230 was shown to be under transcriptional control of both UVR8 and Hy5.

It is interesting to note that UVR8 contains a sequence and structural similarity to Regulator of Chromatin Condensation (RCC1) protein (Kliebenstein et al. 2002). This RCC1 protein binds to chromatin and acts as a nucleotide exchange factor for the small GTP binding protein Ran. This exchange generates a Ran-GTP/RanGDP gradient across the nuclear envelop required to drive nucleo-cytoplasmic transport (Renault et al. 1998). Although UVR8 has not been shown to act as a chromatin modifier, its homolog RCC1 and sirtuin homologs have been shown in human cells and Drosophila to alter chromatin structure (Barlow et al.

2001;Denu 2003; Li et al. 2003). It would not be unreasonable to suggest a possible role in the UV signalling pathway for At5g09230 in chromatin modification.

It would be interesting to know if decondensed chromatin in a looser structure suffers from more DNA damage on exposure to UV-B compared to condensed chromatin.

6.1.4 Nicotinamidase response to DNA damage.

Nicotinamidases convert nicotinamide produced by sirtuins and PARPs into nicotinic acid. Nicotinamidase activity has been shown in other model organisms to increase the activity of sirtuins and PARPs by removing inhibiting nicotinamide (Balan et al. 2008; Gallo et al. 2004). Nicotinamidases perform the first step for the NAD salvage pathway, which is responsible for converting Nicotinamide back into NAD^+, hence replenishing cellular NAD^+ levels. The activation of nicotinamidases may help prevent against NAD^+ depletion.

Sirtuin gene expression was upregulated with MMS and UV-B. However, although the genes NAMase1 and NAMase3 were shown to be upregulated with DNA damaging agents MMS and Bleomycin, all three nicotinamidases genes were strongly downregulated with UV-B.

6.1.5 Future work on DNA damage

For future work on PARPs, PARGs and sirtuin activity in Arabidopsis, transgenic and null lines could be used to measure cellular NAD^+, cADPr and nicotinamide levels. This may support or contradict some of the hypothesis relating to PARP and PARG activity in DNA repair.

One hypothesis proposes an increase in the activity of PARP depletes cellular NAD^+ to such an extent to cause necrosis and this could be studied by monitoring metabolite concentrations.

The activity of both sirtuin genes has to be verified. Although sirtuins were identified as protein deacetylases the closest mammalian homologs to *A. thaliana* sirtuins are poly ADP ribosylases.

The targets for Arabidopsis PARPs and sirtuins are unknown. PARG null lines accumulate ADPribose polymer for which there is a commercially available antibody. This could be used to isolate poly ADP ribosylated target proteins by immunoprecipitation. Work in other model organisms has identified many transcription factors and histones as acceptor proteins for poly ADP ribosylation although the mechanisms for DNA repair are still very unclear. Identification of acceptor proteins for poly ADP ribosylation in Arabidopsis would help elucidate the response of PARPs to DNA damage.

Future work could include a sirtuin yeast 2 hybrid screen to identify possible interactors of the sirtuins in Arabidopsis.

An antibody has also been raised to At5g09230 for immunoprecipitation studies. Identification of At5g09230 interactors would further reveal the function of At5g09230 in UV-B signalling pathway.

A commercially available antibody to acetylated histones could be used on sirtuin knockout lines in order to verify histone deacetylase activity of sirtuins. It could also be used to investigate the possible role of At5g09230 in chromatin remodelling in the UV-B signalling pathway.

Continuing work could also include localisation studies for Arabidopsis PARG proteins. The longest isoform of mammalian PARG contains a putative regulatory domain with a Nuclear export signal (NES) and nuclear localisation signal (NLS) and has been shown to be translocated from the cytoplasm to the nucleus (Winstall et al. 1999). However, both of the Arabidopsis PARG genes lack the putative regulatory domain.

TUNEL and COMET assays can be used to measure the extent of DNA fragmentation and are also often used as a measure of apoptosis. Since all of the sirtuins, PARPs and PARGs have shown differences in gene expression with DNA damage it would be interesting to test all the knockout lines for a change in genomic instability compared to wild type plants.

One hypothesis suggests that PARPs binds to damaged DNA to recruits repair enzymes. Electrophoretic mobility shift assay (EMSA) can be used to examine whether Arabidopsis PARP and sirtuin proteins bind to damaged DNA substrate. A yeast 2 hybrid assay could be used to investigate interactions between Arabidopsis PARP and homologs of DNA repair proteins that have been shown to interact with PARPs in other organisms e.g. XRCC1.

6.2 Role of poly ADP ribosylation in Abscisic acid signalling

PARP AtPARP3 shows a dramatic increase in gene expression with the addition of plant stress hormone Abscisic acid (ABA), which is known to mediate plant responses to drought, salinity and cold (Abscisic acid signalling reviewed in Leung & Giraudat 1998. Abscisic acid is also the key hormone required for the breaking of seed dormancy in the early stages of germination (Gubler et al. 2005). Under conditions of salt, drought and cold stress there are more metabolic constraints on cellular energy (and ultimately NAD) as plants initiate coping mechanisms, mediated by Abscisic acid.

An additional PARP gene identified here (AtPARP3) shows a dramatic increase in expression with the addition of Abscisic acid. This is different from the published results for the other two Arabidopsis PARP genes (AtPARP1 and AtPARP2) suggesting that AtPARP3 has a very different biological role.

A. thaliana lines with reduced AtPARP1 and AtPARP2 activity showed an increase in plant tolerance to salt and Abscisic acid treatment (De Block et al. 2005). DNA microarray data on *A. thaliana* RNAi AtPARP2 lines showed an upregulation of ABA responsive genes with a decrease in PARP activity (Vanderauwera et al. 2007). The hypothesis suggested for this observation is that with reduced PARP activity plants are more able to maintain proficient energy regulation during stress.

DNA microarray profiling of *A. thaliana* with induced expression of Aplysia ADPR cyclase resulted in an increase of more than 100 Abscisic acid responsive genes (Sanchez et al. 2004). ABA activates ADPR cylases and cADPr induces a subset of ABA-responsive genes in Arabidopsis. However AtPARP3 is not shown to be upregulated, suggesting that AtPARP3 is involved in a cADPr independent ABA signalling pathway.

The addition of ABA also caused an increase in gene expression of nicotinamidase A5g23220. These enzymes are responsible for converting nicotinamide produced by PARPs back to NAD and are the first step in the NAD salvage pathway. Nicotinamide also acts as an inhibitor on the activity of PARPs and it could be that nicotinamidases are upregulated in order remove nicotinamide before inhibition of PARP takes place.

The ABA signalling pathway is well characterised with mutants at key stages of the pathway. Analysis of AtPARP3 and nicotinamidase NAMase2 transcript in these mutants in response to ABA could identify the position of their involvement in the pathway.

The increase in gene expression of AtPARP3 with the addition of Abscisic acid might reduce cellular concentration of NAD by the formation of large ADP ribose polymers. Investigations into the concentration of cellular NAD would help further understand the effect of Abscisic acid treatment.

No knockout lines for NAMase2 were identified, which would suggest inactivation of this nicotinamidase is lethal. In future analysis of NAPRT and NaMNAT transcript levels with

ABA treatment would elucidate if all genes of the NAD salvage pathway were upregulated in order to resynthesise NAD. AtPARP3 knockout lines have been identified here which could be used for germination studies to see if there are any differences in germination rates. Plant responses to salt, mannitol, drought, and high light are all partially controlled by Abscisic acid levels but there may be differences in the signalling pathways to these stress conditions. There are mutants for all of these pathways and transcript analysis could identify the signalling pathway AtPARP3 is involved.

AtPARP3 is upregulated with the addition of auxin which controls cell elongation and phototropism. AtPARP3 null lines could be used to investigate differences in plant growth controlled by auxin such as stems growing towards a light source and roots growing down in response to gravity.

6.3 Effect of PARG AtPARG1 on circadian rhythm.

Under normal growing conditions AtPARG1 knockout lines show an early flowering phenotype. Previous work screening *A. thaliana* for mutants with alterations in the circadian clock had identified the AtPARG1 (referred to as TEJ) gene (Panda et al. 2002). Mutants for AtPARG1 showed an alteration in the transition from vegetative growth to flowering resulting in an early flowering phenotype. The effect of PARG on circadian rhythm could be explained by a link to cyclic ADP ribose (cADPr). cADPr is synthesised from NAD by ADPribose cyclases and plays a major role in initiating calcium ion release (Lee et al. 1989; Lee et al. 1995). Circadian oscillations of cADPr have been shown to correspond to oscillations in cellular calcium ions (Dodd et al. 2007). cADPr is produced from the degradation of NAD so presumably there exists competition between PARPs and ADPribose cyclases for NAD as a substrate.

In AtPARG1 knockout lines there is less control of the activity of PARP proteins leading to the accumulation of ADP ribose polymer and the depletion of NAD. This could affect the production of cADPr and cause the early flowering phenotype observed in this report and in the TEJ mutant (Panda et al. 2002).

6.4 Crosstalk between proteins involved in NAD utilisation.

PARP and sirtuins both utilise NAD as a substrate and a hypothesis proposing crosstalk between PARPs and sirtuins has been suggested whereby NAD/ nicotinamide levels could affect the activity of both PARPs and sirtuins. (Zhang 2003). In response to DNA damage increased PARP activity generates very high local concentration of nicotinamide. This increase in nicotinamide would inhibit sirtuin activity at the site of DNA damage, preventing chromatin condensation by sirtuins so that the DNA repair proteins can gain access to DNA breaks.

DNA microarray data on RNAi PARP2 knockout lines in *A. thaliana* shows an up-regulation of Abscisic acid responsive genes, and suggest Abscisic acid controls NAD concentration by cyclic ADPribose (cADPr). Therefore treatment with Abscisic acid will cause both PARP and ADPribose cyclases to use NAD. This will result in a further decrease in NAD and an increase in competition of for NAD.

DNA microarray profiling of Arabidopsis with induced expression of Aplysia ADPR cyclase resulted in an increase of more than 100 Abscisic acid responsive genes (Sanchez et al. 2004). ABA activates ADPR cylases and cADPr induces a subset of ABA-responsive genes in Arabidopsis. cADPr has also been implicated in circadian rhythms as it shows similar oscillations to circadian calcium ion release. The early flowering phenotype seen for AtPARG1 knockout lines would possibly accumulate more ADPribose polymer and increase competition for NAD between PARPs and ADPribose cyclases. To date although cADPr has

been identified in *A. thaliana* no genes with homology to characterised mammalian ADPribose cyclases have been identified or proteins with the enzyme purified.

Chapter 6 References

References

Ahuja, N., Schwer, B., Carobbio, S., Waltregny, D., North, B. J., Castronovo, V., Maechler, P., & Verdin, E. 2007, "Regulation of Insulin Secretion by SIRT4, a Mitochondrial ADP-ribosyltransferase", *Journal of Biological Chemistry*, vol. 282, no. 46, pp. 33583-33592.

Akiyama, T., Takasawa, S., Nata, K., Kobayashi, S., Abe, M., Shervani, N. J., Ikeda, T., Nakagawa, K., Unno, M., Matsuno, S., & Okamoto, H. 2001, "Activation of Reg gene, a gene for insulin-producing beta -cell regeneration: Poly(ADP-ribose) polymerase binds Reg promoter and regulates the transcription by autopoly(ADP-ribosyl)ation", *Proceedings of the National Academy of Sciences*, vol. 98, no. 1, pp. 48-53.

Allen, G. J., Muir, S., & Sanders, D. 1995, "Release of $Ca2^{+}$ from individual plant vacuoles by both InsP3 and cyclic ADP-ribose", *Science*, vol. 268, no. 5211, pp. 735-737.

Althaus, F. R. 1992, "Poly ADP-ribosylation: a histone shuttle mechanism in DNA excision repair", *Journal of Cell Science*, vol. 102, no. 4, pp. 663-670.

Alvarez-Gonzalez, R. 1988, "3'-Deoxy-NAD+ as a substrate for poly(ADP-ribose)polymerase and the reaction mechanism of poly(ADP-ribose) elongation", *Journal of Biological Chemistry*, vol. 263, no. 33, pp. 17690-17696.

Alvarez-Gonzalez R, Althaus FR (1989) Poly(ADP-ribose) catabolism in mammalian cells exposed to DNA-damaging agents. *Mutational Research* 218; 67-74

Amé, J. C., Jacobson, E. L., Jacobson, E. L., Jacobson, E. L., Jacobson, M. K., & Jacobson, M. K. 1999, "Molecular heterogeneity and regulation of poly(ADP-ribose) glycohydrolase", *Molecular and Cellular Biochemistry*, vol. 193, no. 1, pp. 75-81.

Amé JC, Spenlehauer C, de Murcia G (2004) The PARP superfamily. *Bioessays* 26 (8), 882-893

Amor, Y., Babiychuk, E., Inzθ, D., & Levine, A. 1998, "The involvement of poly(ADP-ribose) polymerase in the oxidative stress responses in plants", *FEBS Letters*, vol. 440, no. 1-2, pp. 1-7.

Anastasiou, D. & Krek, W. 2006, "SIRT1: Linking Adaptive Cellular Responses to Aging-Associated Changes in Organismal Physiology", *Physiology*, vol. 21, no. 6, pp. 404-410.

Anderson, M. G., Scoggin, K. E. S., Simbulan-Rosenthal, C. M., & Steadman, J. A. 2000, "Identification of Poly(ADP-Ribose) Polymerase as a Transcriptional Coactivator of the Human T-Cell Leukemia Virus Type 1 Tax Protein", *The Journal of Virology*, vol. 74, no. 5, pp. 2169-2177.

Anderson, R. M., Bitterman, K. J., Wood, J. G., Medvedik, O., Cohen, H., Lin, S. S., Manchester, J. K., Gordon, J. I., & Sinclair, D. A. 2002, "Manipulation of a Nuclear NAD+ Salvage Pathway Delays Aging without Altering Steady-state NAD^+ Levels", *Journal of Biological Chemistry*, vol. 277, no. 21, pp. 18881-18890.

Anderson, R. M., Bitterman, K. J., Wood, J. G., Medvedik, O., & Sinclair, D. A. 2003, "Nicotinamide and PNC1 govern lifespan extension by calorie restriction in Saccharomyces cerevisiae", *Nature*, vol. 423, no. 6936, pp. 181-185.

Andrabi, S. A., Kim, N. S., Yu, S. W., Wang, H., Koh, D. W., Sasaki, M., Klaus, J. A., Otsuka, T., Zhang, Z., Koehler, R. C., Hurn, P. D., Poirier, G. G., Dawson, V. L., & Dawson, T. M. 2006, "Poly(ADP-ribose) (PAR) polymer is a death signal", *Proceedings of the National Academy of Sciences*, vol. 103, no. 48, pp. 18308-18313.

Anson, R. M., Guo, Z., de Cabo, R., Iyun, T., Rios, M., Hagepanos, A., Ingram, D. K., Lane, M. A., & Mattson, M. P. 2003, "Intermittent fasting dissociates beneficial effects of dietary restriction on glucose metabolism and neuronal resistance to injury from calorie intake", *Proceedings of the National Academy of Sciences of the United States of America*, vol. 100, no. 10, pp. 6216-6220.

Araki, T., Sasaki, Y., & Milbrandt, J. 2004, "Increased Nuclear NAD Biosynthesis and SIRT1 Activation Prevent Axonal Degeneration", *Science*, vol. 305, no. 5686, pp. 1010-1013.

Ashihara, H., Stasolla, C., Yin, Y., Loukanina, N., & Thorpe, T. A. 2005, "De novo and salvage biosynthetic pathways of pyridine nucleotides and nicotinic acid conjugates in cultured plant cells", *Plant Science*, vol. 169, no. 1, pp. 107-114.

Astrom, S. U., Okamura, S. M., & Rine, J. 1999, "Yeast cell-type regulation of DNA repair", *Nature*, vol. 397, no. 6717, p. 310.

Avalos, J. L., Celic, I., Muhammad, S., Cosgrove, M. S., Boeke, J. D., & Wolberger, C. 2002, "Structure of a Sir2 Enzyme Bound to an Acetylated p53 Peptide", *Molecular Cell*, vol. 10, no. 3, pp. 523-535.

Avalos, J. L., Bever, K. M., & Wolberger, C. 2005, "Mechanism of Sirtuin Inhibition by Nicotinamide: Altering the NAD+ Cosubstrate Specificity of a Sir2 Enzyme", *Molecular Cell*, vol. 17, no. 6, pp. 855-868.

Babiychuk E, Cottrill PB, Storozhenko S, Fuangthong M, Chem Y, O'Farrell MK, Van Montagu M, Inzé D, Kushnir S. (2002) Higher plants possess two structurally different poly (ADP-ribose) polymerases. *The Plant Journal.* Vol 15; 5, pp 635-645.

Balan, V., Miller, G. S., Kaplun, L., Balan, K., Chong, Z. Z., Li, F., Kaplun, A., VanBerkum, M. F. A., Arking, R., Freeman, D. C., Maiese, K., & Tzivion, G. 2008, "Lifespan extension and neuronal cell protection by drosophila nicotinamidase", *Journal of Biological Chemistry* p. M804681200.

Barlow, A. L., van Drunen, C. M., Johnson, C. A., Tweedie, S., Bird, A., & Turner, B. M. 2001, "dSIR2 and dHDAC6: Two Novel, Inhibitor-Resistant Deacetylases in Drosophila melanogaster", *Experimental Cell Research*, vol. 265, no. 1, pp. 90-103.

Barnes, D. E. & Lindahl, T. 2004, "Repair and genetic consequences of endogenous DNA base damage in mammalian cells", *Annual Review of Genetics*, vol. 38, no. 1, pp. 445-476.

Baur, J. A., Pearson, K. J., Price, N. L., Jamieson, H. A., Lerin, C., Kalra, A., Prabhu, V. V., Allard, J. S., Lopez-Lluch, G., Lewis, K., Pistell, P. J., Poosala, S., Becker, K. G., Boss, O., Gwinn, D., Wang, M., Ramaswamy, S., Fishbein, K. W., Spencer, R. G., Lakatta, E. G., Le Couteur, D., Shaw, R. J., Navas, P., Puigserver, P., Ingram, D. K., de Cabo, R., & Sinclair, D. A. 2006, "Resveratrol improves health and survival of mice on a high-calorie diet", *Nature*, vol. 444, no. 7117, pp. 337-342.

Berger, F., Lau, C., Dahlmann, M., & Ziegler, M. 2005, "Subcellular Compartmentation and Differential Catalytic Properties of the Three Human Nicotinamide Mononucleotide Adenylyltransferase Isoforms", *Journal of Biological Chemistry*, vol. 280, no. 43, pp. 36334-36341.

Berger NA (1985) Poly(ADP-ribose) in the cellular response to DNA damage. *Radiation Research* 101:4-15.

Bernheim, M. L. C. 1967, "Hydrolysis of nicotinyl hydroxamate by a yeast nicotinamidase", *Archives of Biochemistry and Biophysics*, vol. 120, no. 1, pp. 186-191.

Berridge, M. J. 1993, "Inositol trisphosphate and calcium signalling", *Nature*, vol. 361, no. 6410, pp. 315-325.

Berríos-Rivera SJ, San KY, Bennett GN. (2002) The effect of NAPRTase overexpression on the total levels of NAD, the NADH/NAD^+ ratio, and the distribution of metabolites in Escherichia coli. *Metabolic Engineering.* Jul; 4 (3): 238-47.

Bitterman, K. J., Anderson, R. M., Cohen, H. Y., Latorre-Esteves, M., & Sinclair, D. A. 2002, "Inhibition of Silencing and Accelerated Aging by Nicotinamide, a Putative Negative Regulator of Yeast Sir2 and Human SIRT1", *Journal of Biological Chemistry*, vol. 277, no. 47, pp. 45099-45107.

Block, M. D., Verduyn, C., Brouwer, D. D., & Cornelissen, M. 2005, "Poly(ADP-ribose) polymerase in plants affects energy homeostasis, cell death and stress tolerance", *The Plant Journal*, vol. 41, no. 1, pp. 95-106.

Borra, M. T., Smith, B. C., & Denu, J. M. 2005, "Mechanism of Human SIRT1 Activation by Resveratrol", *Journal of Biological Chemistry*, vol. 280, no. 17, pp. 17187-17195.

Bouchard, V. J., Rouleau, M., & Poirier, G. G. 2003, "PARP-1, a determinant of cell survival in response to DNA damage", *Experimental Hematology*, vol. 31, no. 6, pp. 446-454.

Brachmann, C. B., Sherman, J. M., Devine, S. E., Cameron, E. E., Pillus, L., & Boeke, J. D. 1995, "The SIR2 gene family, conserved from bacteria to humans, functions in silencing, cell cycle progression, and chromosome stability", *Genes and Development*, vol. 9, no. 23, pp. 2888-2902.

Brown, B. A., Cloix, C., Jiang, G. H., Kaiserli, E., Herzyk, P., Kliebenstein, D. J., & Jenkins, G. I. 2005, "A UV-B-specific signaling component orchestrates plant UV

protection", *Proceedings of the National Academy of Sciences of the United States of America*, vol. 102, no. 50, pp. 18225-18230.

Buck, S. W., Gallo, C. M., & Smith, J. S. 2004, "Diversity in the Sir2 family of protein deacetylases", *Journal of Leukocyte Biology*, vol. 75, no. 6, pp. 939-950.

Burgess, G. M., Godfrey, P. P., McKinney, J. S., Berridge, M. J., Irvine, R. F., & Putney, J. W. 1984, "The second messenger linking receptor activation to internal Ca release in liver", *Nature*, vol. 309, no. 5963, pp. 63-66.

Cervellera, M. N. & Sala, A. 2000, "Poly(ADP-ribose) Polymerase Is a B-MYB Coactivator", *Journal of Biological Chemistry*, vol. 275, no. 14, pp. 10692-10696.

Chambon, P., Weill, J. D., & Mandel, P. 1963, "Nicotinamide mononucleotide activation of a new DNA-dependent polyadenylic acid synthesizing nuclear enzyme", *Biochemical and Biophysical Research Communications*, vol. 11, no. 1, pp. 39-43.

Chappie, J. S., Cαnaves, J. M., Han, G. W., Rife, C. L., Xu, Q., & Stevens, R. C. 2005, "The Structure of a Eukaryotic Nicotinic Acid Phosphoribosyltransferase Reveals Structural Heterogeneity among Type II PRTases", *Structure*, vol. 13, no. 9, pp. 1385-1396.

Chen, J., Zhou, Y., Mueller-Steiner, S., Chen, L. F., Kwon, H., Yi, S., Mucke, L., & Gan, L. 2005, "SIRT1 Protects against Microglia-dependent Amyloid-{beta} Toxicity through Inhibiting NF-{kappa}B Signaling", *Journal of Biological Chemistry*, vol. 280, no. 48, pp. 40364-40374.

Christie, J. M. & Jenkins, G. I. 1996, "Distinct UV-B and UV-A/Blue Light Signal Transduction Pathways Induce Chalcone Synthase Gene Expression in Arabidopsis Cells", *THE PLANT CELL*, vol. 8, no. 9, pp. 1555-1567.

Cohen, H. Y., Lavu, S., Bitterman, K. J., Hekking, B., Imahiyerobo, T. A., Miller, C., Frye, R., Ploegh, H., Kessler, B. M., & Sinclair, D. A. 2004a, "Acetylation of the C Terminus of Ku70 by CBP and PCAF Controls Bax-Mediated Apoptosis", *Molecular Cell*, vol. 13, no. 5, pp. 627-638.

Cohen, H. Y., Miller, C., Bitterman, K. J., Wall, N. R., Hekking, B., Kessler, B., Howitz, K. T., Gorospe, M., de Cabo, R., & Sinclair, D. A. 2004b, "Calorie Restriction Promotes Mammalian Cell Survival by Inducing the SIRT1 Deacetylase", *Science*, vol. 305, no. 5682, pp. 390-392.

Collinge, M. A. & Althaus, F. R. 1994, "Expression of human poly(ADP-ribose) polymerase in Saccharomyces cerevisiae", *Molecular and General Genetics MGG*, vol. 245, no. 6, pp. 686-693.

Cortes, U., Tong, W. M., Coyle, D. L., Meyer-Ficca, M. L., Meyer, R. G., Petrilli, V., Herceg, Z., Jacobson, E. L., Jacobson, M. K., & Wang, Z. Q. 2004, "Depletion of the 110-Kilodalton Isoform of Poly(ADP-Ribose) Glycohydrolase Increases Sensitivity to Genotoxic and Endotoxic Stress in Mice", *Molecular and Cellular Biology*, vol. 24, no. 16, pp. 7163-7178.

D'Amours, D., Desnoyers, S., D'Silva, I., & Poirier, G. G. 1999, "Poly(ADP-ribosyl)ation reactions in the regulation of nuclear functions", *Biochemical Journal*, vol. 342, no. 2, pp. 249-268.

de Murcia, G., Huletsky, A., Lamarre, D., Gaudreau, A., Pouyet, J., Daune, M., & Poirier, G. G. 1986, "Modulation of chromatin superstructure induced by poly(ADP-ribose) synthesis and degradation", *Journal of Biological Chemistry*, vol. 261, no. 15, pp. 7011-7017.

de Murcia, J. M., Niedergang, C., Trucco, C., Ricoul, M., Dutrillaux, B., Mark, M., Oliver, F. J., Masson, M., Dierich, A., LeMeur, M., Walztinger, C., Chambon, P., & de Murcia, G. 1997, "Requirement of poly(ADP-ribose) polymerase in recovery from DNA damage in mice and inácells", *Proceedings of the National Academy of Sciences*, vol. 94, no. 14, pp. 7303-7307.

de Murcia G, Jongstra- Bilen J, Ittel ME, Mandel P, Delain E (1983) Poly(ADP-ribose) polymerase auto-modification and interaction with DNA: electron microscopic visualization. *Embo J.* 2(4): 543-548).

Denu, J. M. 2003, "Linking chromatin function with metabolic networks: Sir2 family of NAD+-dependent deacetylases", *Trends in Biochemical Sciences*, vol. 28, no. 1, pp. 41-48.

Denu, J. M. 2005, "The Sir2 family of protein deacetylases", *Current Opinion in Chemical Biology*, vol. 9, no. 5, pp. 431-440.

Dequen, F., Gagnon, S. N., & Desnoyers, S. 2005, "Ionizing radiations in Caenorhabditis elegans induce poly(ADP-ribosyl)ation, a conserved DNA-damage response essential for survival", *DNA Repair*, vol. 4, no. 7, pp. 814-825.

Dodd, A. N., Gardner, M. J., Hotta, C. T., Hubbard, K. E., Dalchau, N., Love, J., Assie, J. M., Robertson, F. C., Jakobsen, M. K., Goncalves, J., Sanders, D., & Webb, A. A. R. 2007, "The Arabidopsis Circadian Clock Incorporates a cADPR-Based Feedback Loop", *Science*, vol. 318, no. 5857, pp. 1789-1792.

Doucet, C., Doucet-Chabeaud, G., Godon, Godon, C., Brutesco, Brutesco, C., de, M., Murcia, G. d., Kazmaier, & Kazmaier, M. 2001, "Ionising radiation induces the expression of PARP-1 and PARP-2 genes in Arabidopsis", *Molecular Genetics and Genomics*, vol. 265, no. 6, pp. 954-963.

Earley KW, Haag JR, Pontes O, Opper K, Juehne T, Song K, Pikaard CS (2006) Gateway-compatible vectors for plant functional genomics and proteomics. *Plant Journal*. Vol 14(4), 616-629

Emanuelli, M., Amici, A., Carnevali, F., Pierella, F., Raffaelli, N., & Magni, G. 2003, "Identification and characterization of a second NMN adenylyltransferase gene in Saccharomyces cerevisiae", *Protein Expression and Purification*, vol. 27, no. 2, pp. 357-364.

Faraone-Mennella, M. R., Gambacorta, A., Nicolaus, B., & Farina, B. 1998, "Purification and biochemical characterization of a poly(ADP-ribose) polymerase-like enzyme from the thermophilic archaeon Sulfolobus solfataricus", *Biochemical Journal*, vol. 335, no. 2, pp. 441-447.

Finkelstein, R. R., Gampala, S. S. L., & Rock, C. D. 2002, "Abscisic Acid Signaling in Seeds and Seedlings", *The Plant Cell*, vol. 14, no. 90001, p. S15-S45.

Finnin, M. S., Donigian, J. R., & Pavletich, N. P. 2001, "Structure of the histone deacetylase SIRT2", *Nat Struct Mol Biol*, vol. 8, no. 7, pp. 621-625.

Flachmann R, Kunz N, Seifert J, Gutlich M, Wientjes FJ, Laufer A, Gassen HG 1988, "Molecular biology of pyridine nucleotide biosynthesis in Escherichia coli. Cloning and characterization of quinolinate synthesis genes nadA and nadB", *European Journal of Biochemistry*, vol. 175, no. 2, pp. 221-228.

Ford, E., Voit, R., Liszt, G., Magin, C., Grummt, I., & Guarente, L. 2006, "Mammalian Sir2 homolog SIRT7 is an activator of RNA polymerase I transcription", *Genes and Development*, vol. 20, no. 9, pp. 1075-1080.

Frescas, D., Valenti, L., & Accili, D. 2005, "Nuclear Trapping of the Forkhead Transcription Factor FoxO1 via Sirt-dependent Deacetylation Promotes Expression of Glucogenetic Genes", *Journal of Biological Chemistry*, vol. 280, no. 21, pp. 20589-20595.

Frohnmeyer, H. & Staiger, D. 2003, "Ultraviolet-B Radiation-Mediated Responses in Plants. Balancing Damage and Protection", *Plant Physiology*, vol. 133, no. 4, pp. 1420-1428.

Frothingham, R., Meeker-O'Connell, W. A., Talbot, E. A., George, J. W., & Kreuzer, K. N. 1996, "Identification, cloning, and expression of the Escherichia coli pyrazinamidase and nicotinamidase gene, pncA", *Antimicrobial Agents and Chemotherapy*, vol. 40, no. 6, pp. 1426-1431.

Frye, R. A. 1999, "Characterization of Five Human cDNAs with Homology to the Yeast SIR2 Gene: Sir2-like Proteins (Sirtuins) Metabolize NAD and May Have Protein ADP-Ribosyltransferase Activity", *Biochemical and Biophysical Research Communications*, vol. 260, no. 1, pp. 273-279.

Frye, R. A. 2000a, "Phylogenetic Classification of Prokaryotic and Eukaryotic Sir2-like Proteins", *Biochemical and Biophysical Research Communications*, vol. 273, no. 2, pp. 793-798.

Frye, R. A. 2000b, "Phylogenetic Classification of Prokaryotic and Eukaryotic Sir2-like Proteins", *Biochemical and Biophysical Research Communications*, vol. 273, no. 2, pp. 793-798.

Gagnon, S. N., Hengartner, M. O., & Desnoyers, S. 2002, "The genes pme-1 and pme-2 encode two poly(ADP-ribose) polymerases in Caenorhabditis elegans", *Biochemical Journal*, vol. 368, no. 1, pp. 263-271.

Gallo, C. M., Smith, D. L., Jr., & Smith, J. S. 2004, "Nicotinamide Clearance by Pnc1 Directly Regulates Sir2-Mediated Silencing and Longevity", *Molecular and Cellular Biology*, vol. 24, no. 3, pp. 1301-1312.

Gorospe, M. & de Cabo, R. 2008, "AsSIRTing the DNA damage response", *Trends in Cell Biology*, vol. 18, no. 2, pp. 77-83.

Gradwohl, G., Murcia, J. M. D., Molinete, M., Simonin, F., Koken, M., Hoeijmakers, J. H. J., & de Murcia, G. 1990, "The Second Zinc-Finger Domain of Poly(ADP-Ribose) Polymerase Determines Specificity for Single-Stranded Breaks in DNA", *Proceedings of the National Academy of Sciences*, vol. 87, no. 8, pp. 2990-2994.

Griesenbeck, J., Ziegler, M., Tomilin, N., Schweiger, M., & Oei, S. L. 1999, "Stimulation of the catalytic activity of poly(ADP-ribosyl) transferase by transcription factor Yin Yang 1", *FEBS Letters*, vol. 443, no. 1, pp. 20-24.

Guarente, L. 2005, "Calorie restriction and SIR2 genes--Towards a mechanism", *Mechanisms of Ageing and Development*, vol. 126, no. 9, pp. 923-928.

Gubler, F., Millar, A. A., & Jacobsen, J. V. 2005, "Dormancy release, ABA and pre-harvest sprouting", *Current Opinion in Plant Biology*, vol. 8, no. 2, pp. 183-187.

Ha, H. C., Hester, L. D., & Snyder, S. H. 2002, "Poly(ADP-ribose) polymerase-1 dependence of stress-induced transcription factors and associated gene expression in glia", *Proceedings of the National Academy of Sciences*, vol. 99, no. 5, pp. 3270-3275.

Ha, H. C. & Snyder, S. H. 1999, "Poly(ADP-ribose) polymerase is a mediator of necrotic cell death by ATP depletion", *Proceedings of the National Academy of Sciences*, vol. 96, no. 24, pp. 13978-13982.

Haigis, M. C. & Guarente, L. P. 2006, "Mammalian sirtuins--emerging roles in physiology, aging, and calorie restriction", *Genes and Development*, vol. 20, no. 21, pp. 2913-2921.

Haigis, M. C., Mostoslavsky, R., Haigis, K. M., Fahie, K., Christodoulou, D. C., Murphy, A. J., Valenzuela, D. M., Yancopoulos, G. D., Karow, M., Blander, G., Wolberger, C., Prolla, T. A., Weindruch, R., Alt, F. W., & Guarente, L. 2006, "SIRT4 Inhibits Glutamate Dehydrogenase and Opposes the Effects of Calorie Restriction in Pancreatic [beta] Cells", *Cell*, vol. 126, no. 5, pp. 941-954.

Hanai, S., Kanai, M., Ohashi, S., Okamoto, K., Yamada, M., Takahashi, H., & Miwa, M. 2004, "Loss of poly(ADP-ribose) glycohydrolase causes progressive neurodegeneration in Drosophila melanogaster", *Proceedings of the National Academy of Sciences*, vol. 101, no. 1, pp. 82-86.

Hara, N., Yamada, K., Shibata, T., Osago, H., Hashimoto, T., & Tsuchiya, M. 2007, "Elevation of Cellular NAD Levels by Nicotinic Acid and Involvement of Nicotinic Acid Phosphoribosyltransferase in Human Cells", *Journal of Biological Chemistry*, vol. 282, no. 34, pp. 24574-24582.

Harden A, Young WJ (1913) The Enzymatic Formation of Polysaccharides by Yeast Preparations *Biochem J.* 1913 Dec; 7(6): 630-636).

Harden A. (1929) The Function of phosphate in alcoholic fermentation. Nobel Lecture December12, 1929.

Harrisingh, M. C. & Nitabach, M. N. 2008, "CIRCADIAN RHYTHMS: Integrating Circadian Timekeeping with Cellular Physiology", *Science*, vol. 320, no. 5878, pp. 879-880.

Hashida SN, Takahashi H, Kawai-Yamada M[1] and Uchimiya H (2007) A. thaliana nicotinate/nicotinamide mononucleotide adenyltransferase (AtNMNAT) is required for pollen tube growth. *Plant Journal* Feb;49(4):694-703.

Hassa, P. O., Haenni, S. S., Elser, M., & Hottiger, M. O. 2006, "Nuclear ADP-Ribosylation Reactions in Mammalian Cells: Where Are We Today and Where Are We Going?", *Microbiology and Molecular Biology Reviews*, vol. 70, no. 3, pp. 789-829.

Hassa P.O, Hottiger M.O. (2002) The functional role of poly (ADP-ribose) polymerase1 as novel coactivator of NF-kappaB in inflammatory diseases. *Cellular and Molecular Life Sciences.* Sep; 59(9): 1535-53.

Hassa HO, Hottiger MO (2008) The diverse biological roles of mammalian PARPS, a small but powerful family of poly-ADP-ribose polymerases. *Frontiers in Bioscience* Jan 1;13:3046-82.

Hatakeyama, K., Nemoto, Y., Ueda, K., & Hayaishi, O. 1986, "Purification and characterization of poly(ADP-ribose) glycohydrolase. Different modes of action on large and small poly(ADP-ribose)", *Journal of Biological Chemistry*, vol. 261, no. 32, pp. 14902-14911.

Hayashi, K., Tanaka, M., Shimada, T., Miwa, M., & Sugimura, T. 1983, "Size and shape of poly(ADP-ribose): Examination by gel filtration, gel electrophoresis and electron microscopy", *Biochemical and Biophysical Research Communications*, vol. 112, no. 1, pp. 102-107.

Heeres, J. T. & Hergenrother, P. J. 2007, "Poly(ADP-ribose) makes a date with death", *Current Opinion in Chemical Biology*, vol. 11, no. 6, pp. 644-653.

Hellmich MR, Strumwasser F 1991. Purification and characterization of a molluscan egg-specific NADase, a second-messenger enzyme.*Cell regul* Mar 2(3);193

Heltweg, B., Gatbonton, T., Schuler, A. D., Posakony, J., Li, H., Goehle, S., Kollipara, R., DePinho, R. A., Gu, Y., Simon, J. A., & Bedalov, A. 2006, "Antitumor Activity of a Small-Molecule Inhibitor of Human Silent Information Regulator 2 Enzymes", *Cancer Research*, vol. 66, no. 8, pp. 4368-4377.

Hiratsuka, M., Inoue, T., Toda, T., Kimura, N., Shirayoshi, Y., Kamitani, H., Watanabe, T., Ohama, E., Tahimic, C. G. T., Kurimasa, A., & Oshimura, M. 2003, "Proteomics-based identification of differentially expressed genes in human gliomas: down-regulation of SIRT2 gene", *Biochemical and Biophysical Research Communications*, vol. 309, no. 3, pp. 558-566.

Hoeijmakers, J. H. J. 2001, "Genome maintenance mechanisms for preventing cancer", *Nature*, vol. 411, no. 6835, pp. 366-374.

Honjo, T., Nishizuka, Y., Hayaishi, O., & Kato, I. 1968, "Diphtheria Toxin-dependent Adenosine Diphosphate Ribosylation of Aminoacyl Transferase II and Inhibition of Protein Synthesis", *Journal of Biological Chemistry*, vol. 243, no. 12, pp. 3553-3555.

Howitz, K. T., Bitterman, K. J., Cohen, H. Y., Lamming, D. W., Lavu, S., Wood, J. G., Zipkin, R. E., Chung, P., Kisielewski, A., Zhang, L. L., Scherer, B., & Sinclair, D. A. 2003, "Small molecule activators of sirtuins extend Saccharomyces cerevisiae lifespan", *Nature*, vol. 425, no. 6954, pp. 191-196.

Hu, G., Taylor, A. B., McAlister-Henn, L., & Hart, P. J. 2007a, "Crystal structure of the yeast nicotinamidase Pnc1p", *Archives of Biochemistry and Biophysics*, vol. 461, no. 1, pp. 66-75.

Hu, G., Taylor, A. B., McAlister-Henn, L., & Hart, P. J. 2007b, "Crystal structure of the yeast nicotinamidase Pnc1p", *Archives of Biochemistry and Biophysics*, vol. 461, no. 1, pp. 66-75.

Huang, L., Sun, Q., Qin, F., Li, C., Zhao, Y., & Zhou, D. X. 2007, "Down-Regulation of a SILENT INFORMATION REGULATOR2-Related Histone Deacetylase Gene, OsSRT1, Induces DNA Fragmentation and Cell Death in Rice", *Plant Physiology*, vol. 144, no. 3, pp. 1508-1519.

Huletsky, A., de Murcia, G., Muller, S., Hengartner, M., Menard, L., Lamarre, D., & Poirier, G. G. 1989, "The effect of poly(ADP-ribosyl)ation on native and H1-depleted chromatin. A role of poly(ADP-ribosyl)ation on core nucleosome structure", *Journal of Biological Chemistry*, vol. 264, no. 15, pp. 8878-8886.

Hunt L, Holdsworth MJ, Gray JE (2007) Nicotinamidase activity is important for germination. *Plant Journal*. Aug;51(3):341-51.

Hunt, L., Lerner, F., & Ziegler, M. 2004, "NAD - new roles in signalling and gene regulation in plants", *New Phytologist*, vol. 163, no. 1, pp. 31-44.

Igamberdiev, A. U. & Gardestr÷m, P. 2003, "Regulation of NAD- and NADP-dependent isocitrate dehydrogenases by reduction levels of pyridine nucleotides in mitochondria and cytosol of pea leaves", *Biochimica et Biophysica Acta (BBA) - Bioenergetics*, vol. 1606, no. 1-3, pp. 117-125.

Ikejima, M., Noguchi, S., Yamashita, R., Ogura, T., Sugimura, T., Gill, D. M., & Miwa, M. 1990, "The zinc fingers of human poly(ADP-ribose) polymerase are differentially required for the recognition of DNA breaks and nicks and the consequent enzyme activation. Other structures recognize intact DNA", *Journal of Biological Chemistry*, vol. 265, no. 35, pp. 21907-21913.

Imai, S. i., Armstrong, C. M., Kaeberlein, M., & Guarente, L. 2000, "Transcriptional silencing and longevity protein Sir2 is an NAD-dependent histone deacetylase", *Nature*, vol. 403, no. 6771, pp. 795-800.

Jackson, M. D., Schmidt, M. T., Oppenheimer, N. J., & Denu, J. M. 2003, "Mechanism of Nicotinamide Inhibition and Transglycosidation by Sir2 Histone/Protein Deacetylases", *Journal of Biological Chemistry*, vol. 278, no. 51, pp. 50985-50998.

Jia, H., Yan, T., Feng, Y., Zeng, C., Shi, X., & Zhai, Q. 2007, "Identification of a critical site in Wlds: Essential for Nmnat enzyme activity and axon-protective function", *Neuroscience Letters*, vol. 413, no. 1, pp. 46-51.

Juarez-Salinas, H., Levi, V., Jacobson, E. L., & Jacobson, M. K. 1982, "Poly(ADP-ribose) has a branched structure in vivo", *Journal of Biological Chemistry*, vol. 257, no. 2, pp. 607-609.

Kaeberlein, M., McDonagh, T., Heltweg, B., Hixon, J., Westman, E. A., Caldwell, S. D., Napper, A., Curtis, R., DiStefano, P. S., Fields, S., Bedalov, A., & Kennedy, B. K. 2005, "Substrate-specific Activation of Sirtuins by Resveratrol", *Journal of Biological Chemistry*, vol. 280, no. 17, pp. 17038-17045.

Kaeberlein, M., McVey, M., & Guarente, L. 1999, "The SIR2/3/4 complex and SIR2 alone promote longevity in Saccharomyces cerevisiae by two different mechanisms", *Genes and Development*, vol. 13, no. 19, pp. 2570-2580.

Kaiser, P., Auer, B., & Schweiger, M. 1992, "Inhibition of cell proliferation in Saccharomyces cerevisiae by expression of human NAD+ ADP-ribosyltransferase requires the DNA binding domain ("zinc fingers")", *Molecular and General Genetics MGG*, vol. 232, no. 2, pp. 231-239.

Kameoka, M., Ota, K., Tetsuka, T., Tanaka, Y., Itaya, A., Okamoto, T., & Yoshihara, K. 2000, "Evidence for regulation of NF-kappaB by poly(ADP-ribose) polymerase", *Biochemical Journal*, vol. 346, no. 3, pp. 641-649.

Kameshita, I., Matsuda, Z., Taniguchi, T., & Shizuta, Y. 1984, "Poly (ADP-Ribose) synthetase. Separation and identification of three proteolytic fragments as the substrate-binding domain, the DNA-binding domain, and the automodification domain", *Journal of Biological Chemistry*, vol. 259, no. 8, pp. 4770-4776.

Katoh, A., Uenohara, K., Akita, M., & Hashimoto, T. 2006, "Early Steps in the Biosynthesis of NAD in Arabidopsis Start with Aspartate and Occur in the Plastid", *PLANT PHYSIOLOGY*, vol. 141, no. 3, pp. 851-857.

Kauppinen, T. M. 2007, "Multiple roles for poly(ADP-ribose)polymerase-1 in neurological disease", *Neurochemistry International*, vol. 50, no. 7-8, pp. 954-958.

Kawaichi, M., Ueda, K., & Hayaishi, O. 1981, "Multiple autopoly(ADP-ribosyl)ation of rat liver poly(ADP-ribose) synthetase. Mode of modification and properties of automodified synthetase", *Journal of Biological Chemistry*, vol. 256, no. 18, pp. 9483-9489.

Kennedy, B. K., Austriaco, N. R., Zhang, J., & Guarente, L. 1995, "Mutation in the silencing gene S/R4 can delay aging in S. cerevisiae", *Cell*, vol. 80, no. 3, pp. 485-496.

Khan, J. A., Forouhar, F., Tao, X., & Tong, L. 2007, "Nicotinamide adenine dinucleotide metabolism as an attractive target for drug discovery", *Expert Opinion on Therapeutic Targets*, vol. 11, no. 5, pp. 695-705.

Kim, H., Jacobson, E. L., & Jacobson, M. K. 1993, "Synthesis and degradation of cyclic ADP-ribose by NAD glycohydrolases", *Science*, vol. 261, no. 5126, pp. 1330-1333.

Kim, M. Y., Mauro, S., Gevry, N., Lis, J. T., & Kraus, W. L. 2004, "NAD+-Dependent Modulation of Chromatin Structure and Transcription by Nucleosome Binding Properties of PARP-1", *Cell*, vol. 119, no. 6, pp. 803-814.

Kim, M. Y., Zhang, T., & Kraus, W. L. 2005, "Poly(ADP-ribosyl)ation by PARP-1: `PAR-laying' NAD+ into a nuclear signal", *Genes and Development*, vol. 19, no. 17, pp. 1951-1967.

Kim, S., Benguria, A., Lai, C. Y., & Jazwinski, S. M. 1999, "Modulation of Life-span by Histone Deacetylase Genes in Saccharomyces cerevisiae", *Molecular Biology of the Cell*, vol. 10, no. 10, pp. 3125-3136.

Kliebenstein, D. J., Lim, J. E., Landry, L. G., & Last, R. L. 2002, "Arabidopsis UVR8 Regulates Ultraviolet-B Signal Transduction and Tolerance and Contains Sequence Similarity to Human Regulator of Chromatin Condensation 1", *Plant Physiology*, vol. 130, no. 1, pp. 234-243.

Koh, D. W., Lawler, A. M., Poitras, M. F., Sasaki, M., Wattler, S., Nehls, M. C., Stöger, T., Poirier, G. G., Dawson, V. L., & Dawson, T. M. 2004, "Failure to degrade poly(ADP-ribose) causes increased sensitivity to cytotoxicity and early embryonic lethality", *Proceedings of the National Academy of Sciences of the United States of America*, vol. 101, no. 51, pp. 17699-17704.

Koh DW, Patel CN, Ramsinghani S, Slama JT, Oliveria MA, Jacobsen MK (2003) *Biochemistry* 6;42(17):4855-63)

Kotaja, N., Karvonen, U., Janne, O. A., & Palvimo, J. J. 2002, "PIAS Proteins Modulate Transcription Factors by Functioning as SUMO-1 Ligases", *Molecular and Cellular Biology*, vol. 22, no. 14, pp. 5222-5234.

Kruszewski, M. & Szumiel, I. 2005, "Sirtuins (histone deacetylases III) in the cellular response to DNA damage--Facts and hypotheses", *DNA Repair*, vol. 4, no. 11, pp. 1306-1313.

Kusama S, Ueda R, Suda T, Nishihara S, Matsuura ET (2008) Involvement of *Drosophila Sir2*-like genes in the regulation of life span. *Genes and Genetic systems.* Vol. 81 (2006), No. 5 p.341-348

Lagouge, M., Argmann, C., Gerhart-Hines, Z., Meziane, H., Lerin, C., Daussin, F., Messadeq, N., Milne, J., Lambert, P., Elliott, P., Geny, B., Laakso, M., Puigserver, P., & Auwerx, J. 2006, "Resveratrol Improves Mitochondrial Function and Protects against Metabolic Disease by Activating SIRT1 and PGC-1[alpha]", *Cell*, vol. 127, no. 6, pp. 1109-1122.

Leckie, C. P., McAinsh, M. R., Allen, G. J., Sanders, D., & Hetherington, A. M. 1998, "Abscisic acid-induced stomatal closure mediated by cyclic ADP-ribose", *Proceedings of the National Academy of Sciences*, vol. 95, no. 26, pp. 15837-15842.

Lee, H. C., Walseth, T. F., Bratt, G. T., Hayes, R. N., & Clapper, D. L. 1989, "Structural determination of a cyclic metabolite of NAD^+ with intracellular $Ca2^+$-mobilizing activity", *Journal of Biological Chemistry*, vol. 264, no. 3, pp. 1608-1615.

Lee, H. C. & Aarhus, R. 1995, "A Derivative of NADP Mobilizes Calcium Stores Insensitive to Inositol Trisphosphate and Cyclic ADP-ribose", *Journal of Biological Chemistry*, vol. 270, no. 5, pp. 2152-2157.

Lee, H. C., Aarhus, R., & Graeff, R. M. 1995, "Sensitization of Calcium-induced Calcium Release by Cyclic ADP-ribose and Calmodulin", *Journal of Biological Chemistry*, vol. 270, no. 16, pp. 9060-9066.

Lepiniec, L. c., Babiychuk, E., Kushnir, S., Van Montagu, M., & Inzé, D. 1995, "Characterization of anA. thaliana cDNA homologue to animal poly(ADP-ribose) polymerase", *FEBS Letters*, vol. 364, no. 2, pp. 103-108.

Leung, J. & Giraudat, J. 1998, "ABSCISIC ACID SIGNAL TRANSDUCTION", *Annual Review of Plant Physiology and Plant Molecular Biology*, vol. 49, no. 1, pp. 199-222.

Li, H. Y., Wirtz, D., & Zheng, Y. 2003, "A mechanism of coupling RCC1 mobility to RanGTP production on the chromatin in vivo", *The Journal of Cell Biology*, vol. 160, no. 5, pp. 635-644.

Li, W., Zhang, B., Tang, J., Cao, Q., Wu, Y., Wu, C., Guo, J., Ling, E. A., & Liang, F. 2007, "Sirtuin 2, a Mammalian Homolog of Yeast Silent Information Regulator-2 Longevity Regulator, Is an Oligodendroglial Protein That Decelerates Cell Differentiation through Deacetylating {alpha}-Tubulin", *Journal of Neuroscience*, vol. 27, no. 10, pp. 2606-2616.

Lieber, C. S., Leo, M. A., Wang, X., & DeCarli, L. M. 2008, "Alcohol alters hepatic FoxO1, p53, and mitochondrial SIRT5 deacetylation function", *Biochemical and Biophysical Research Communications*, vol. 373, no. 2, pp. 246-252.

Lin, S. J., Defossez, P. A., & Guarente, L. 2000, "Requirement of NAD and SIR2 for Life-Span Extension by Calorie Restriction in Saccharomyces cerevisiae", *Science*, vol. 289, no. 5487, pp. 2126-2128.

Lin, W., Ame, J. C., Aboul-Ela, N., Jacobson, E. L., & Jacobson, M. K. 1997a, "Isolation and Characterization of the cDNA Encoding Bovine Poly(ADP-ribose) Glycohydrolase", *Journal of Biological Chemistry*, vol. 272, no. 18, pp. 11895-11901.

Lin, W., Ame, J. C., Aboul-Ela, N., Jacobson, E. L., & Jacobson, M. K. 1997b, "Isolation and Characterization of the cDNA Encoding Bovine Poly(ADP-ribose) Glycohydrolase", *Journal of Biological Chemistry*, vol. 272, no. 18, pp. 11895-11901.

Liszt, G., Ford, E., Kurtev, M., & Guarente, L. 2005, "Mouse Sir2 Homolog SIRT6 Is a Nuclear ADP-ribosyltransferase", *Journal of Biological Chemistry*, vol. 280, no. 22, pp. 21313-21320.

Liu, B., Gross, M., ten Hoeve, J., & Shuai, K. 2001, "A transcriptional corepressor of Stat1 with an essential LXXLL signature motif", *Proceedings of the National Academy of Sciences of the United States of America*, vol. 98, no. 6, pp. 3203-3207.

Lombard, D. B., Schwer, B., Alt, F. W., & Mostoslavsky, R. 2008, "SIRT6 in DNA repair, metabolism and ageing", *Journal of Internal Medicine*, vol. 263, no. 2, pp. 128-141.

Lombard, D. B., Chua, K. F., Mostoslavsky, R., Franco, S., Gostissa, M., & Alt, F. W. 2005, "DNA Repair, Genome Stability, and Aging", *Cell*, vol. 120, no. 4, pp. 497-512.

Love, S., Barber, R., & Wilcock, G. K. 1999, "Increased poly(ADP-ribosyl)ation of nuclear proteins in Alzheimer's disease", *Brain*, vol. 122, no. 2, pp. 247-253.

Luo, J., Nikolaev, A. Y., Imai, S. i., Chen, D., Su, F., Shiloh, A., Guarente, L., & Gu, W. 2001, "Negative Control of p53 by Sir2[alpha] Promotes Cell Survival under Stress", *Cell*, vol. 107, no. 2, pp. 137-148.

Mackerness, S., John, C. F., Jordan, B., & Thomas, B. 2001, "Early signaling components in ultraviolet-B responses: distinct roles for different reactive oxygen species and nitric oxide", *FEBS Letters*, vol. 489, no. 2-3, pp. 237-242.

Malanga, M., Pleschke, J. M., Kleczkowska, H. E., & Althaus, F. R. 1998, "Poly(ADP-ribose) Binds to Specific Domains of p53 and Alters Its DNA Binding Functions", *Journal of Biological Chemistry*, vol. 273, no. 19, pp. 11839-11843.

Marsischky, G. T., Wilson, B. A., & Collier, R. J. 1995, "Role of Glutamic Acid 988 of Human Poly-ADP-ribose Polymerase in Polymer Formation", *Journal of Biological Chemistry*, vol. 270, no. 7, pp. 3247-3254.

Masson, M., Niedergang, C., Schreiber, V., Muller, S., Menissier-de Murcia, J., & de Murcia, G. 1998, "XRCC1 Is Specifically Associated with Poly(ADP-Ribose) Polymerase and Negatively Regulates Its Activity following DNA Damage", *Molecular and Cellular Biology*, vol. 18, no. 6, pp. 3563-3571.

Masutani, M., Nozaki, T., Nakamoto, K., Nakagama, H., Suzuki, H., Kusuoka, O., Tsutsumi, M., & Sugimura, T. 2000, "The response of Parp knockout mice against DNA damaging agents", *Mutation Research/Reviews in Mutation Research*, vol. 462, no. 2-3, pp. 159-166.

Masutani M, Nakagama H, Sugimura T (2003) Poly(ADP-ribose) and carcinogenesis. *Genes chromosomes and cancer* 38: 339-348

Mathis, G. & Althaus, F. R. 1987, "Release of core DNA from nucleosomal core particles following (ADP-ribose)n-modification", *Biochemical and Biophysical Research Communications*, vol. 143, no. 3, pp. 1049-1054.

McCay, C. M., Crowell, M. F., & Maynard, L. A. 1935, "The Effect of Retarded Growth Upon the Length of Life Span and Upon the Ultimate Body Size: One Figure", *Journal of Nutrition*, vol. 10, no. 1, pp. 63-79.

Mehl, R. A., Kinsland, C., & Begley, T. P. 2000, "Identification of the Escherichia coli Nicotinic Acid Mononucleotide Adenylyltransferase Gene", *The Journal of Bacteriology*, vol. 182, no. 15, pp. 4372-4374.

Meyer, R. G., Meyer-Ficca, M. L., Jacobson, E. L., & Jacobson, M. K. 2003, "Human poly(ADP-ribose) glycohydrolase (PARG) gene and the common promoter sequence it shares with inner mitochondrial membrane translocase 23 (TIM23)", *Gene*, vol. 314, pp. 181-190.

Meyer, R. G., Meyer-Ficca, M. L., Whatcott, C. J., Jacobson, E. L., & Jacobson, M. K. 2007, "Two small enzyme isoforms mediate mammalian mitochondrial poly(ADP-ribose) glycohydrolase (PARG) activity", *Experimental Cell Research*, vol. 313, no. 13, pp. 2920-2936.

Meyer-Ficca, M. L., Meyer, R. G., Coyle, D. L., Jacobson, E. L., & Jacobson, M. K. 2004, "Human poly(ADP-ribose) glycohydrolase is expressed in alternative splice variants

yielding isoforms that localize to different cell compartments", *Experimental Cell Research*, vol. 297, no. 2, pp. 521-532.

Michishita, E., Park, J. Y., Burneskis, J. M., Barrett, J. C., & Horikawa, I. 2005, "Evolutionarily Conserved and Nonconserved Cellular Localizations and Functions of Human SIRT Proteins", *Molecular Biology of the Cell*, vol. 16, no. 10, pp. 4623-4635.

Milne, J. C., Lambert, P. D., Schenk, S., Carney, D. P., Smith, J. J., Gagne, D. J., Jin, L., Boss, O., Perni, R. B., Vu, C. B., Bemis, J. E., Xie, R., Disch, J. S., Ng, P. Y., Nunes, J. J., Lynch, A. V., Yang, H., Galonek, H., Israelian, K., Choy, W., Iffland, A., Lavu, S., Medvedik, O., Sinclair, D. A., Olefsky, J. M., Jirousek, M. R., Elliott, P. J., & Westphal, C. H. 2007, "Small molecule activators of SIRT1 as therapeutics for the treatment of type 2 diabetes", *Nature*, vol. 450, no. 7170, pp. 712-716.

Min, J., Landry, J., Sternglanz, R., & Xu, R. M. 2001, "Crystal Structure of a SIR2 Homolog-NAD Complex", *Cell*, vol. 105, no. 2, pp. 269-279.

Mishra, N. S., Tuteja, R., & Tuteja, N. 2006, "Signaling through MAP kinase networks in plants", *Archives of Biochemistry and Biophysics*, vol. 452, no. 1, pp. 55-68.

Miwa, M. & Sugimura, T. 1971, "Splitting of the Ribose-Ribose Linkage of Poly(Adenosine Diphosphate-Ribose) by a Calf Thymus Extract", *Journal of Biological Chemistry*, vol. 246, no. 20, pp. 6362-6364.

Moroni, F. 2008, "Poly(ADP-ribose)polymerase 1 (PARP-1) and postischemic brain damage", *Current Opinion in Pharmacology*, vol. 8, no. 1, pp. 96-103.

Mortimer RK & Johnston JR, 1959, "Life Span of Individual Yeast Cells", *Nature*, vol. 183, no. 4677, pp. 1751-1752.

Mostoslavsky, R., Chua, K. F., Lombard, D. B., Pang, W. W., Fischer, M. R., Gellon, L., Liu, P., Mostoslavsky, G., Franco, S., Murphy, M. M., Mills, K. D., Patel, P., Hsu, J. T., Hong, A. L., Ford, E., Cheng, H. L., Kennedy, C., Nunez, N., Bronson, R., Frendewey, D., Auerbach, W., Valenzuela, D., Karow, M., Hottiger, M. O., Hursting, S., Barrett, J. C., Guarente, L., Mulligan, R., Demple, B., Yancopoulos, G. D., & Alt, F. W. 2006, "Genomic Instability and Aging-like Phenotype in the Absence of Mammalian SIRT6", *Cell*, vol. 124, no. 2, pp. 315-329.

Ménissier-de Murcia, J., Molinete, M., Gradwohl, G., Simonin, F., & de Murcia, G. 1989, "Zinc-binding domain of poly(ADP-ribose)polymerase participates in the recognition of single strand breaks on DNA", *Journal of Molecular Biology*, vol. 210, no. 1, pp. 229-233.

Nakagawa, T., Kurose, T., Hino, T., Tanaka, K., Kawamukai, M., Niwa, Y., Toyooka, K., Matsuoka, K., Jinbo, T., & Kimura, T. 2007, "Development of series of gateway binary vectors, pGWBs, for realizing efficient construction of fusion genes for plant transformation", *Journal of Bioscience and Bioengineering*, vol. 104, no. 1, pp. 34-41.

Nie, J., Sakamoto, S., Song, D., Qu, Z., Ota, K., & Taniguchi, T. 1998, "Interaction of Oct-1 and automodification domain of poly(ADP-ribose) synthetase", *FEBS Letters*, vol. 424, no. 1-2, pp. 27-32.

Noctor, G., Queval, G., & Gakiere, B. 2006, "NAD(P) synthesis and pyridine nucleotide cycling in plants and their potential importance in stress conditions", *Journal of Experimental Botany*, vol. 57, no. 8, pp. 1603-1620.

North, B. J., Marshall, B. L., Borra, M. T., Denu, J. M., & Verdin, E. 2003, "The Human Sir2 Ortholog, SIRT2, Is an NAD^+-Dependent Tubulin Deacetylase", *Molecular Cell*, vol. 11, no. 2, pp. 437-444.

Oei, S. L., Griesenbeck, J., Schweiger, M., Babich, V., Kropotov, A., & Tomilin, N. 1997, "Interaction of the Transcription Factor YY1 with Human Poly(ADP-Ribosyl) Transferase", *Biochemical and Biophysical Research Communications*, vol. 240, no. 1, pp. 108-111.

Oei, S. L., Griesenbeck, J., Schweiger, M., & Ziegler, M. 1998, "Regulation of RNA Polymerase II-dependent Transcription by Poly(ADP-ribosyl)ation of Transcription Factors", *Journal of Biological Chemistry*, vol. 273, no. 48, pp. 31644-31647.

Ogata, N., Ueda, K., Kawaichi, M., & Hayaishi, O. 1981, "Poly(ADP-ribose) synthetase, a main acceptor of poly(ADP-ribose) in isolated nuclei", *Journal of Biological Chemistry*, vol. 256, no. 9, pp. 4135-4137.

Oliver, A. W., Ame, J. C., Roe, S. M., Good, V., de Murcia, G., & Pearl, L. H. 2004, "Crystal structure of the catalytic fragment of murine poly(ADP-ribose) polymerase-2", *Nucleic Acids Research*, vol. 32, no. 2, pp. 456-464.

Panda, S., Poirier, G. G., & Kay, S. A. 2002, "tej Defines a Role for Poly(ADP-Ribosyl)ation in Establishing Period Length of the Arabidopsis Circadian Oscillator", *Developmental Cell*, vol. 3, no. 1, pp. 51-61.

Patel, C. N., Koh, D. W., Jacobson, M. K., & Oliveira, M. A. 2005, "Identification of three critical acidic residues of poly(ADP-ribose) glycohydrolase involved in catalysis: determining the PARG catalytic domain", *Biochemical Journal*, vol. 388, no. 2, pp. 493-500.

Pearson, K. J., Baur, J. A., Lewis, K. N., Peshkin, L., Price, N. L., Labinskyy, N., Swindell, W. R., Kamara, D., Minor, R. K., Perez, E., Jamieson, H. A., Zhang, Y., Dunn, S. R., Sharma, K., Pleshko, N., Woollett, L. A., Csiszar, A., Ikeno, Y., Le Couteur, D., Elliott, P. J., Becker, K. G., Navas, P., Ingram, D. K., Wolf, N. S., Ungvari, Z., Sinclair, D. A., & de Cabo, R. 2008, "Resveratrol Delays Age-Related Deterioration and Mimics Transcriptional Aspects of Dietary Restriction without Extending Life Span", *Cell Metabolism*, vol. 8, no. 2, pp. 157-168.

Perkins, E., Sun, D., Nguyen, A., Tulac, S., Francesco, M., Tavana, H., Nguyen, H., Tugendreich, S., Barthmaier, P., Couto, J., Yeh, E., Thode, S., Jarnagin, K., Jain, A., Morgans, D., & Melese, T. 2001, "Novel Inhibitors of Poly(ADP-ribose) Polymerase/PARP1 and PARP2 Identified Using a Cell-based Screen in Yeast", *Cancer Research*, vol. 61, no. 10, pp. 4175-4183.

Picard, F., Kurtev, M., Chung, N., Topark-Ngarm, A., Senawong, T., Machado de Oliveira, R., Leid, M., McBurney, M. W., & Guarente, L. 2004b, "Sirt1 promotes fat mobilization in white adipocytes by repressing PPAR-[gamma]", *Nature*, vol. 429, no. 6993, pp. 771-776.

Picard, F., Kurtev, M., Chung, N., Topark-Ngarm, A., Senawong, T., Machado de Oliveira, R., Leid, M., McBurney, M. W., & Guarente, L. 2004a, "Sirt1 promotes fat mobilization in white adipocytes by repressing PPAR-[gamma]", *Nature*, vol. 429, no. 6993, pp. 771-776.

Pleschke, J. M., Kleczkowska, H. E., Strohm, M., & Althaus, F. R. 2000, "Poly(ADP-ribose) Binds to Specific Domains in DNA Damage Checkpoint Proteins", *Journal of Biological Chemistry*, vol. 275, no. 52, pp. 40974-40980.

Poirier, G. G., de Murcia, G., Jongstra-Bilen, J., Niedergang, C., & Mandel, P. 1982a, "Poly(ADP-ribosyl)ation of polynucleosomes causes relaxation of chromatin structure", *Proceedings of the National Academy of Sciences of the United States of America*, vol. 79, no. 11, pp. 3423-3427.

Poirier, G. G., Murcia, G. D., Jongstra-Bilen, J., Niedergang, C., & Mandel, P. 1982b, "Poly(ADP-Ribosyl)ation of Polynucleosomes Causes Relaxation of Chromatin Structure", *Proceedings of the National Academy of Sciences*, vol. 79, no. 11, pp. 3423-3427.

Preiss, J. & Handler, P. 1958, "Biosynthesis of Diphosphopyridine Nucleotide. II. ENZYMATIC ASPECTS", *Journal of Biological Chemistry*, vol. 233, no. 2, pp. 493-500.

Realini, C. A. & Althaus, F. R. 1992, "Histone shuttling by poly(ADP-ribosylation)", *Journal of Biological Chemistry*, vol. 267, no. 26, pp. 18858-18865.

Renault, L., Nassar, N., Vetter, I., Becker, J., Klebe, C., Roth, M., & Wittinghofer, A. 1998, "The 1.7[thinsp]A crystal structure of the regulator of chromosome condensation (RCC1) reveals a seven-bladed propeller", *Nature*, vol. 392, no. 6671, pp. 97-101.

Rodgers, J. T., Lerin, C., Haas, W., Gygi, S. P., Spiegelman, B. M., & Puigserver, P. 2005, "Nutrient control of glucose homeostasis through a complex of PGC-1[alpha] and SIRT1", *Nature*, vol. 434, no. 7029, pp. 113-118.

Rogina, B. & Helfand, S. L. 2004, "Sir2 mediates longevity in the fly through a pathway related to calorie restriction", *Proceedings of the National Academy of Sciences*, vol. 101, no. 45, pp. 15998-16003.

Ruf, A., de Murcia, J. M., de Murcia, G. M., & Schulz, G. E. 1996, "Structure of the catalytic fragment of poly(ADP-ribose) polymerase fromáchicken", *Proceedings of the National Academy of Sciences*, vol. 93, no. 15, pp. 7481-7485.

Ruscetti, T., Lehnert, B. E., Halbrook, J., Le Trong, H., Hoekstra, M. F., Chen, D. J., & Peterson, S. R. 1998, "Stimulation of the DNA-dependent Protein Kinase by Poly(ADP-Ribose) Polymerase", *Journal of Biological Chemistry*, vol. 273, no. 23, pp. 14461-14467.

Sanchez JP, Duque P, Chua N-H (2004) ABA activates ADPR cyclase and cADPR induces a subset of ABA-responsive genes in Arabidopsis. *Plant Journal* 38, 381-395

Sandmeier, J. J., Celic, I., Boeke, J. D., & Smith, J. S. 2002, "Telomeric and rDNA Silencing in Saccharomyces cerevisiae Are Dependent on a Nuclear NAD+ Salvage Pathway", *Genetics*, vol. 160, no. 3, pp. 877-889.

Schmid, M., Davison, T. S., Henz, S. R., Pape, U. J., Demar, M., Vingron, M., Scholkopf, B., Weigel, D., & Lohmann, J. U. 2005, "A gene expression map of A. thaliana development", *Nat Genet*, vol. 37, no. 5, pp. 501-506.

Schreiber, V., Dantzer, F., Ame, J. C., & de Murcia, G. 2006, "Poly(ADP-ribose): novel functions for an old molecule", *Nat Rev Mol Cell Biol*, vol. 7, no. 7, pp. 517-528.

Schweiger, M., Hennig, K., Lerner, F., Niere, M., Hirsch-Kauffmann, M., Specht, T., Weise, C., Oei, S. L., & Ziegler, M. 2001b, "Characterization of recombinant human nicotinamide mononucleotide adenylyl transferase (NMNAT), a nuclear enzyme essential for NAD synthesis", *FEBS Letters*, vol. 492, no. 1-2, pp. 95-100.

Schweiger, M., Hennig, K., Lerner, F., Niere, M., Hirsch-Kauffmann, M., Specht, T., Weise, C., Oei, S. L., & Ziegler, M. 2001a, "Characterization of recombinant human nicotinamide mononucleotide adenylyl transferase (NMNAT), a nuclear enzyme essential for NAD synthesis", *FEBS Letters*, vol. 492, no. 1-2, pp. 95-100.

Shall, S. & de Murcia, G. 2000, "Poly(ADP-ribose) polymerase-1: what have we learned from the deficient mouse model?", *Mutation Research/DNA Repair*, vol. 460, no. 1, pp. 1-15.

Sherman, J. M., Stone, E. M., Freeman-Cook, L. L., Brachmann, C. B., Boeke, J. D., & Pillus, L. 1999, "The Conserved Core of a Human SIR2 Homologue Functions in Yeast Silencing", *Molecular Biology of the Cell*, vol. 10, no. 9, pp. 3045-3059.

Shi, T., Wang, F., Stieren, E., & Tong, Q. 2005, "SIRT3, a Mitochondrial Sirtuin Deacetylase, Regulates Mitochondrial Function and Thermogenesis in Brown Adipocytes", *Journal of Biological Chemistry*, vol. 280, no. 14, pp. 13560-13567.

Shimokawa, T., Masutani, M., Nagasawa, S., Nozaki, T., Ikota, N., Aoki, Y., Nakagama, H., & Sugimura, T. 1999, "Isolation and Cloning of Rat Poly(ADP-Ribose) Glycohydrolase: Presence of a Potential Nuclear Export Signal Conserved in Mammalian Orthologs", *Journal of Biochemistry*, vol. 126, no. 4, pp. 748-755.

Shin, D. H., Oganesyan, N., Jancarik, J., Yokota, H., Kim, R., & Kim, S. H. 2005, "Crystal Structure of a Nicotinate Phosphoribosyltransferase from Thermoplasma acidophilum", *Journal of Biological Chemistry*, vol. 280, no. 18, pp. 18326-18335.

Sims, J. L., Berger, S. J., & Berger, N. A. 1983, "Poly(ADP-ribose) polymerase inhibitors preserve oxidized nicotinamide adenine dinucleotide and adenosine 5'-triphosphate pools in DNA-damaged cells: mechanism of stimulation of unscheduled DNA synthesis", *Biochemistry*, vol. 22, no. 22, pp. 5188-5194.

Sinclair, D. 2005a, "Sirtuins for healthy neurons", *Nat Genet*, vol. 37, no. 4, pp. 339-340.

Sinclair, D. A. 2005b, "Toward a unified theory of caloric restriction and longevity regulation", *Mechanisms of Ageing and Development*, vol. 126, no. 9, pp. 987-1002.

Smith, H. M. & Grosovsky, A. J. 1999, "PolyADP-ribose-mediated regulation of p53 complexed with topoisomerase I following ionizing radiation", *Carcinogenesis*, vol. 20, no. 8, pp. 1439-1444.

Sorci, L., Cimadamore, F., Scotti, S., Petrelli, R., Cappellacci, L., Franchetti, P., Orsomando, G., & Magni, G. 2007, "Initial-Rate Kinetics of Human NMN-Adenylyltransferases: Substrate and Metal Ion Specificity, Inhibition by Products and Multisubstrate Analogues, and Isozyme Contributions to NAD+ Biosynthesis", *Biochemistry*, vol. 46, no. 16, pp. 4912-4922.

St Laurent, J. F., Gagnon, S. N., Dequen, F., Hardy, I., & Desnoyers, S. 2007, "Altered DNA damage response in Caenorhabditis elegans with impaired poly(ADP-ribose) glycohydrolases genes expression", *DNA Repair*, vol. 6, no. 3, pp. 329-343.

Susin, S. A., Lorenzo, H. K., Zamzami, N., Marzo, I., Snow, B. E., Brothers, G. M., Mangion, J., Jacotot, E., Costantini, P., Loeffler, M., Larochette, N., Goodlett, D. R., Aebersold, R., Siderovski, D. P., Penninger, J. M., & Kroemer, G. 1999b, "Molecular characterization of mitochondrial apoptosis-inducing factor", *Nature*, vol. 397, no. 6718, pp. 441-446.

Susin, S. A., Lorenzo, H. K., Zamzami, N., Marzo, I., Snow, B. E., Brothers, G. M., Mangion, J., Jacotot, E., Costantini, P., Loeffler, M., Larochette, N., Goodlett, D. R., Aebersold, R., Siderovski, D. P., Penninger, J. M., & Kroemer, G. 1999a, "Molecular characterization of mitochondrial apoptosis-inducing factor", *Nature*, vol. 397, no. 6718, pp. 441-446.

Tanaka, T. & Knox, W. E. 1959, "The Nature and Mechanism of the Tryptophan Pyrrolase (Peroxidase-Oxidase) Reaction of Pseudomonas and of Rat Liver", *Journal of Biological Chemistry*, vol. 234, no. 5, pp. 1162-1170.

Tanner, K. G., Landry, J., Sternglanz, R., & Denu, J. M. 2000, "Silent information regulator 2 family of NAD- dependent histone/protein deacetylases generates a unique product, 1-O-acetyl-ADP-ribose", *Proceedings of the National Academy of Sciences*, vol. 97, no. 26, pp. 14178-14182.

Tissenbaum, H. A. & Guarente, L. 2001, "Increased dosage of a sir-2 gene extends lifespan in Caenorhabditis elegans", *Nature*, vol. 410, no. 6825, pp. 227-230.

Tsukamoto, Y., Kato, J. i., & Ikeda, H. 1997, "Silencing factors participate in DNA repair and recombination in Saccharomyces cerevisiae", *Nature*, vol. 388, no. 6645, pp. 900-903.

Tulin, A. & Spradling, A. 2003, "Chromatin Loosening by Poly(ADP)-Ribose Polymerase (PARP) at Drosophila Puff Loci", *Science*, vol. 299, no. 5606, pp. 560-562.

Uchida, K., Hanai, S., Ishikawa, K., Ozawa, Y., Uchida, M., Sugimura, T., & Miwa, M. 1993, "Cloning of cDNA Encoding Drosophila Poly(ADP-Ribose) Polymerase: Leucine Zipper in the Auto-Modification Domain", *Proceedings of the National Academy of Sciences*, vol. 90, no. 8, pp. 3481-3485.

Vakhrusheva, O., Smolka, C., Gajawada, P., Kostin, S., Boettger, T., Kubin, T., Braun, T., & Bober, E. 2008, "Sirt7 Increases Stress Resistance of Cardiomyocytes and Prevents Apoptosis and Inflammatory Cardiomyopathy in Mice", *Circulation Research*, vol. 102, no. 6, pp. 703-710.

Valenzano, D. R., Terzibasi, E., Genade, T., Cattaneo, A., Domenici, L., & Cellerino, A. 2006, "Resveratrol Prolongs Lifespan and Retards the Onset of Age-Related Markers in a Short-Lived Vertebrate", *Current Biology*, vol. 16, no. 3, pp. 296-300.

Van Der Heide, L. P., Hoekman, M. F. M., & Smidt, M. P. 2004, "The ins and outs of FoxO shuttling: mechanisms of FoxO translocation and transcriptional regulation", *Biochemical Journal*, vol. 380, no. 2, pp. 297-309.

van der Horst, A., Schavemaker, J. M., Pellis-van Berkel, W., & Burgering, B. M. T. 2007, "The Caenorhabditis elegans nicotinamidase PNC-1 enhances survival", *Mechanisms of Ageing and Development*, vol. 128, no. 4, pp. 346-349.

Vanderauwera, S., De Block, M., Van de Steene, N., van de Cotte, B., Metzlaff, M., & Van Breusegem, F. 2007, "Silencing of poly(ADP-ribose) polymerase in plants alters abiotic stress signal transduction", *Proceedings of the National Academy of Sciences*, vol. 104, no. 38, pp. 15150-15155.

Vaziri, H., Dessain, S. K., Eaton, E. N., Imai, S. i., Frye, R. A., Pandita, T. K., Guarente, L., & Weinberg, R. A. 2001, "hSIR2SIRT1 Functions as an NAD-Dependent p53 Deacetylase", *Cell*, vol. 107, no. 2, pp. 149-159.

Virag, L. & Szabo, C. 2002, "The Therapeutic Potential of Poly(ADP-Ribose) Polymerase Inhibitors", *Pharmacological Reviews*, vol. 54, no. 3, pp. 375-429.

Wang, Z. Q., Stingl, L., Morrison, C., Jantsch, M., Los, M., Schulze-Osthoff, K., & Wagner, E. F. 1997, "PARP is important for genomic stability but dispensable ináapoptosis", *Genes and Development*, vol. 11, no. 18, pp. 2347-2358.

Wang G, Pichersky E (2007) Nicotinamidase participates in the salvage pathway of NAD biosynthesis in *Arabidopsis. Plant Journal*. Mar;49(6):1020-9.

Werner, E., Ziegler, M., Lerner, F., Schweiger, M., & Heinemann, U. 2002, "Crystal structure of human nicotinamide mononucleotide adenylyltransferase in complex with NMN", *FEBS Letters*, vol. 516, no. 1-3, pp. 239-244.

Whittle, C. A., Beardmore, T., & Johnston, M. O. 2001, "Is G1 arrest in plant seeds induced by a p53-related pathway?", *Trends in Plant Science*, vol. 6, no. 6, pp. 248-251.

Wielckens, K., Schmidt, A., George, E., Bredehorst, R., & Hilz, H. 1982, "DNA fragmentation and NAD depletion. Their relation to the turnover of endogenous mono(ADP-ribosyl) and poly(ADP-ribosyl) proteins", *Journal of Biological Chemistry*, vol. 257, no. 21, pp. 12872-12877.

Williams, R. S., Chasman, D. I., Hau, D. D., Hui, B., Lau, A. Y., & Glover, J. N. M. 2003, "Detection of Protein Folding Defects Caused by BRCA1-BRCT Truncation and Missense Mutations", *Journal of Biological Chemistry*, vol. 278, no. 52, pp. 53007-53016.

Winstall, E., Affar, E. B., Shah, R., Bourassa, S., Scovassi, I. A., & Poirier, G. G. 1999, "Preferential Perinuclear Localization of Poly(ADP-ribose) Glycohydrolase", *Experimental Cell Research*, vol. 251, no. 2, pp. 372-378.

Wood, J. G., Rogina, B., Lavu, S., Howitz, K., Helfand, S. L., Tatar, M., & Sinclair, D. 2004b, "Sirtuin activators mimic caloric restriction and delay ageing in metazoans", *Nature*, vol. 430, no. 7000, pp. 686-689.

Wood, J. G., Rogina, B., Lavu, S., Howitz, K., Helfand, S. L., Tatar, M., & Sinclair, D. 2004a, "Sirtuin activators mimic caloric restriction and delay ageing in metazoans", *Nature*, vol. 430, no. 7000, pp. 686-689.

Wu, Y., Sanchez, J. P., Lopez-Molina, L., Himmelbach, A., Grill, E., & Chua, N. H. 2003, "The abi1-1 mutation blocks ABA signaling downstream of cADPR action", *The Plant Journal*, vol. 34, no. 3, pp. 307-315.

Xiong, L., Schumaker, K. S., & Zhu, J. K. 2002, "Cell Signaling during Cold, Drought, and Salt Stress", *The Plant Cell*, vol. 14, no. 90001, p. S165-S183.

Yang, T. & Sauve, A. 2006, "NAD metabolism and sirtuins: Metabolic regulation of protein deacetylation in stress and toxicity", *The AAPS Journal*, vol. 8, no. 4, p. E632-E643.

Yang Y, et al (2005) Suppression of FOXO1 activity by FHL2 through SIRT1-mediated deacetylation. *EMBO J* Mar 9;24(5):1021-32

Yu, S. W., Andrabi, S. A., Wang, H., Kim, N. S., Poirier, G. G., Dawson, T. M., & Dawson, V. L. 2006, "Apoptosis-inducing factor mediates poly(ADP-ribose) (PAR) polymer-induced cell death", *Proceedings of the National Academy of Sciences*, vol. 103, no. 48, pp. 18314-18319.

Yu, S. W., Wang, H., Poitras, M. F., Coombs, C., Bowers, W. J., Federoff, H. J., Poirier, G. G., Dawson, T. M., & Dawson, V. L. 2002, "Mediation of Poly(ADP-Ribose) Polymerase-1-Dependent Cell Death by Apoptosis-Inducing Factor", *Science*, vol. 297, no. 5579, pp. 259-263.

Yuan, Z., Zhang, X., Sengupta, N., Lane, W. S., & Seto, E. 2007, "SIRT1 Regulates the Function of the Nijmegen Breakage Syndrome Protein", *Molecular Cell*, vol. 27, no. 1, pp. 149-162.

Zielger M, Oei SL (2001) A cellular survival switch: poly(ADP-ribosyl)ation stimulates DNA repair and silences transcription. *BioEssays*. 2001 Jun;23(6):543-8.

Zhai, R. G., Zhang, F., Hiesinger, P. R., Cao, Y., Haueter, C. M., & Bellen, H. J. 2008, "NAD synthase NMNAT acts as a chaperone to protect against neurodegeneration", *Nature*, vol. 452, no. 7189, pp. 887-891.

Zhao, K., Chai, X., Clements, A., & Marmorstein, R. 2003, "Structure and autoregulation of the yeast Hst2 homolog of Sir2", *Nat Struct Mol Biol*, vol. 10, no. 10, pp. 864-871.

Zhang J (2003) Are poly(ADP-ribosyl)ation by PARP-1 and deacetylation by Sir2 linked? *Bioessays* Aug;25(8):808-14

Zhou, T., Kurnasov, O., Tomchick, D. R., Binns, D. D., Grishin, N. V., Marquez, V. E., Osterman, A. L., & Zhang, H. 2002, "Structure of Human Nicotinamide/Nicotinic Acid Mononucleotide Adenylyltransferase. Basis for the dual substrate specificity and activation of

the oncolytic agent tiazofurin", *Journal of Biological Chemistry*, vol. 277, no. 15, pp. 13148-13154.

[Reference to de Gruijl] 1999, "Skin cancer and solar UV radiation", *European Journal of Cancer*, vol. 35, no. 14, pp. 2003-2009.